

Development of novel antibody-based diagnostics for the early and rapid detection of cardiac markers

Barry Mc Donnell

Ph.D. Thesis

**Based on research carried out for the Biomedical Diagnostic Institute (BDI)
in the School of Biotechnology (BDI), Dublin City University (DCU).**

Supervisor: Professor Richard O’Kennedy.

Date: September, 2010.

I hereby certify that this material, which I now submit for assessment on the programme of study leading to the award of PhD is entirely my own work, that I have exercised reasonable care to ensure that the work is original, and does not to the best of my knowledge breach any law of copyright, and has not been taken from the work of others save and to the extent that such work has been cited and acknowledged within the text of my work.

Signed:

ID No.: 51418394

Date:

Table of contents

Acknowledgements	i
Figure Legends	ii-xiii
Abbreviations	1-5
Abstract	6
Aims and objectives	7-8
1.0 Introduction	
1.1 Prevalence of cardiovascular disease	10
1.2 Pathophysiology of acute coronary syndromes	10
1.3 The first use of cardiac markers	11
1.4 The ideal characteristics of a cardiac marker	11-12
1.5 Markers of inflammation	12
1.6 C-reactive protein (CRP)	12-14
1.7 Myeloperoxidase (MPO)	14-16
1.8 Antibody production	16-18
2.0 Materials and Methods	
2.1 Equipment	20-21
2.2 Bacterial culture compositions	22
2.3 Bacterial cells for cloning and expression	22
2.4 Buffer compositions	23
2.5 SDS-PAGE and Western Blotting	24-25
2.6 Commercial kits for processing of DNA and protein	26
2.7 Commercial antibodies	27
2.8 Generation and characterisation of rabbit anti-CRP polyclonal antibodies	
2.8.1 Immunisation of New Zealand White rabbits and antibody titre determination	28
2.8.2 Protein A purification of anti-CRP polyclonal antibody from rabbit serum	28

2.8.3 SDS-PAGE of anti-CRP polyclonal antibody (pAb) protein G purification	29
2.8.4 Checkerboard ELISA of purified anti-CRP polyclonal antibody	29-30
2.8.5 Fluorescent labelling of purified rabbit anti-CRP pAb with commercial DyLight 647™ kit	30
2.8.6 Fluorescent sandwich ELISA of purified rabbit pAb labelled with DyLight 647™	30-32
2.8.7 Preconcentration study of rabbit anti-CRP polyclonal antibody onto CM5 sensorchip	32
2.8.8 Immobilisation of rabbit anti-CRP polyclonal antibody onto CM5 sensorchip	32

2.9 Generation and characterisation of a mouse anti-CRP scFv library

2.9.1 Immunisation of Balb/c mice and antibody titre determination	33
2.9.2 Extraction and isolation of total RNA from immunised mice	33-34
2.9.3 Reverse transcription of total RNA to cDNA	34
2.9.4 PCR primers for amplification of mouse scFv (pAK series)	35-36
2.9.5 Amplification of antibody variable domain genes using pAK series primers	37
2.9.6 Purification of V_H and V_L variable gene fragments using the Promega clean-up Kit	38
2.9.7 Splice by Overlap extension (SOE) PCR	38-39
2.9.8 <i>Sfi</i> I restriction digest of purified SOE-PCR fragment and ligation into pAK 100 vector	39-40
2.9.9 Electro-transformation of scFv-containing plasmid into XL-1 Blue <i>E.coli</i> cells	41
2.9.10 Rescue and subsequent precipitation of scFv-displaying phage	41-42
2.9.11 Enrichment of a murine phage library via biopanning against immobilized antigens	42-43
2.9.12 Polyclonal phage ELISA and scFv check via 'colony-pick' PCR	43-44
2.9.13 Subcloning of pan 4 output scFv fragments into pAK 400 vector for soluble Expression	44-47
2.9.14 Direct and inhibition ELISA of scFv fragments in pAK 400 expression vector	47-48
2.9.15 Production of C11-2 scFv template for sub-cloning into pComb3X vector	48
2.9.16 PCR primers for sub-cloning of mouse scFv from pAK400 to pComb3X vector	49
2.9.17 Nested PCR for conversion of mouse scFv from pAK400 to pComb3X format	49-50
2.9.18 <i>Sfi</i> I restriction digest of nested PCR product and ligation into pComb3X vector	50-52
2.9.19 Optimisation of scFv expression in Terrific Broth (TB) medium	52

<i>2.10 Generation and characterisation of a chicken anti-CRP scFv library</i>	
2.10.1 Construction, screening and selection of avian anti-CRP scFv library	52-53
2.10.2 Cross reactivity analysis of avian scFv clones using a capture ELISA method	53-54
2.10.3 Large-scale protein expression and extraction from bacterial cultures	54-55
2.10.4 Purification of scFv fragments using immobilised metal affinity chromatography (IMAC)	55
2.10.5 Preparation of monomeric CRP (mCRP)	55
2.10.6 Amplification of C λ cys chain from isolated chicken cDNA	56
2.10.7 Replacement of the existing C κ chain of the pMoPAC 16 vector with a C λ cys chain	56-57
2.10.8 Analysis of C λ -scFv (scAb) transformants clones via direct ELISA	57-58
2.10.9 Nested PCR for cloning of H2 scFv gene into the pMoPac 16 vector	58-60
2.10.10 SfiI restriction digest of nested PCR product and ligation into pMoPac 16 vector	60
2.10.11 Transfer of purified D9 scAb to nitrocellulose membrane and western blot analysis	60-61
<i>2.11 Generation and characterisation of a chicken anti-MPO scFv library</i>	
2.11.1 Immunisation and serum titre of MPO-immunised chicken	61-62
2.11.2 Extraction and isolation of RNA from immunised chicken	62
2.11.3 Reverse transcription of total RNA to cDNA	62
2.11.4 PCR primers for amplification of chicken scFv (pComb series)	63
2.11.5 Construction of chicken anti-MPO scFv library	63
2.11.6 Electro-transformation of scFv containing plasmid into XLI-Blue <i>E.coli</i> cells	64
2.11.7 Rescue of chicken anti-MPO scFv-displaying phage	64
2.11.8 Enrichment of library via biopanning against immobilised antigen	65-66
2.11.9 Polyclonal phage ELISA	67
2.11.10 Infection of enriched phage pool into <i>E. coli</i> Top 10 F' (non-suppressor strain) for soluble expression	67
2.11.11 Direct and inhibition ELISA of soluble expressed scFv fragments	67-68
2.11.12 Immobilisation and reference cell surface capping for anti-MPO scFv analysis	68-69
2.11.13 'Off-rate' analysis of anti-MPO scFv clones	69
2.11.14 Titration ELISA of purified avian anti-MPO B10B scFv	69
2.11.15 Novel assay for direct detection of captured MPO	70
2.11.16 Preliminary hybrid lateral flow/western blot assay for detection of MPO	70

<i>2.12 Immunoassays using novel platforms</i>	
<i>2.12.1 Lateral flow assay using purified avian B10B anti-MPO scFv</i>	71
<i>2.12.2 Fluorescent competition assay using the Åmic Open Lateral Flow (OLF) platform</i>	71-72
<i>2.12.3 Fluorescent sandwich-based assay on novel supercritical angular fluorescence (SAF) enhanced parabolic chip platform</i>	72
<i>2.12.4 Analysis of the CRP-specific D9 scAb using the SPR-based Spectral platform</i>	73

3.0 Results & Discussion

<i>3.1 Generation and characterisation of rabbit anti-CRP polyclonal antibodies</i>	
<i>3.1.1 Rabbit immune system</i>	76
<i>3.1.2 CRP as a target analyte</i>	76-78
<i>3.1.3 New Zealand white rabbits (XZB5 and XZCG) serum titres</i>	78
<i>3.1.4 Protein A purification of rabbit anti-CRP polyclonal antibody</i>	79
<i>3.1.5 Checkerboard ELISA to determine titre of purified rabbit anti-CRP polyclonal antibody</i>	80-81
<i>3.1.6 Fluorescent sandwich ELISA of purified rabbit pAb labelled with DyLight 647</i>	81-83
<i>3.1.7 'Real-time' characterisation of rabbit anti-CRP polyclonal antibody using Biacore™</i>	84-87
<i>3.1.8 Discussion of results</i>	88-89
<i>3.2 Generation and characterisation of a mouse anti-CRP scFv library</i>	
<i>3.2.1 Murine immune system</i>	91
<i>3.2.2 Mouse serum titre</i>	91
<i>3.2.3 Mouse variable heavy and light chain optimisation in various buffer compositions</i>	92
<i>3.2.4 Mouse SOE-PCR of variable heavy and light chain</i>	93
<i>3.2.5 Library construction and subsequent enrichment via biopanning</i>	94-95
<i>3.2.6 Mouse polyclonal phage ELISA</i>	96-97
<i>3.2.7 Identification of scFv gene insert in panned murine scFv library</i>	97
<i>3.2.8 Soluble expression and direct ELISA of mouse anti-CRP scFv clones</i>	98-99
<i>3.2.9 Soluble inhibition ELISA of mouse anti-CRP scFv clones</i>	99-100
<i>3.2.10 Sequencing of 10 best mouse anti-CRP scFv clones</i>	101-102
<i>3.2.11 Biacore analysis of mouse anti-CRP scFv C11-2 in pAK400 format</i>	102-104

3.2.12 Primer design and subcloning of C11-2 scFv via 'nested' PCR	105-107
3.2.13 Identification of successfully subcloned scFv fragments via direct and inhibition ELISA	107-109
3.2.14 Sequence analysis of mouse anti-CRP scFv C11-2 subclone	109-111
3.2.15 Cross-reactivity analysis of mouse anti-CRP scFv C11-2 subclone by ELISA	111-113
3.2.16 Kinetic analysis of C11-2 scFv subclone using the Biacore 3000 system	113-116
3.2.17 Discussion of results	116-118
3.3 Generation and characterisation of a chicken anti-CRP scFv library	
3.3.1 Avian immune system	120
3.3.2 Construction, screening and selection of avian anti-CRP scFv library	121
3.3.3 Cross-reactivity analysis of avian anti-CRP scFv clones	121-123
3.3.4 Kinetic analysis of avian anti-CRP scFv clones using the Biacore A100 system	124-126
3.3.5 Large-scale IMAC purification of anti-CRP scFvs	126-127
3.3.6 Engineering of avian CRP-specific H2 scFv for direct conjugation on the SPRSpectral® platform	127-133
3.3.7 Large-scale expression and purification of the CRP-specific scAb fragment	133-134
3.3.8 Western blot analysis of the CRP-specific D9 scAb purified via IMAC	135-137
3.3.9 Discussion of results	137-138
3.4 Generation and characterisation of a chicken anti-MPO scFv library	
3.4.1 Multimarker detection	140
3.4.2 MPO as a target analyte	140-141
3.4.3 Serum titre of MPO-immunised chickens	141-142
3.4.4 RNA extraction and cDNA synthesis	142
3.4.5 Library construction and subsequent enrichment via biopanning	143
3.4.6 Polyclonal phage ELISA	144-145
3.4.7 Soluble expression and direct ELISA of chicken anti-MPO scFv clones	145-146
3.4.8 Preliminary Biacore analysis	146-147
3.4.9 'Off-rate' analysis of avian anti-MPO scFv clones	147-148
3.4.10 Sequence analysis of Avian B10B anti-MPO scFv clone	148-149
3.4.11 Large-scale IMAC purification of B10B anti-MPO scFv	149-150
3.4.12 Titration and inhibition of B10B anti-MPO scFv	150-153
3.4.13 Kinetic analysis of B10B anti-MPO scFv clone	153-155

3.4.14 <i>Direct detection of MPO with TMB/OPD</i>	155-157
3.4.15 <i>Lateral flow assay development</i>	157-160
3.4.16 <i>Discussion of results</i>	160-162
3.5 <i>Point-of-care platforms for detection of CRP and MPO</i>	
3.5.1 <i>Point-of-care technology</i>	164-165
3.5.2 <i>Lateral flow immunoassay (LFIA)</i>	165-167
3.5.3 <i>Amic Open Lateral Flow (OLF) platform</i>	168-171
3.5.4 <i>Parabolic chip platform</i>	171-177
3.5.5 <i>SPRSpectral® platform</i>	177-181
3.5.6 <i>Discussion of results</i>	181-182
4.0 Conclusions	184-187
5.0 Publications	189-190
6.0 Bibliography	192-211
7.0 Appendix	213-215

Acknowledgments

I would like to dedicate this thesis to both my parents and my two brothers and thank them for their constant support throughout my PhD.

It has been a long journey and would have been a lot longer but for the help of some terrific colleagues. So, firstly, I would like to thank each member of the Applied Biochemistry Group (ABG), who I worked with over the four years. No matter how little or large the level of help you gave me, it was much appreciated. Not only were you all great colleagues to work with but great friends too. I am sure ye will all agree that we had some crazy nights out on the town, some of which, a lot of us would find it pretty tough to remember (myself included). It is nights like these that give us that much needed distraction from our research, which I know everybody needs. So I would also like to wish each and every one of you, the very best of luck with your research. There is not a doubt in my mind that all of you will accomplish great things in your future or else end up on the dole! Only messing!

Speaking of crazy nights, my mates from college, ye know who ye are. What a shower of lunatics but also what a shower of legends! You could not write the script for some of the antics we got up to both in college and during my PhD. We had some legendary nights out and even holidays, ah lahinch, what a mess, ha! Anyway, I don't know why I am talking like that's the end of them because it has only just begun. So guys (ye know who ye are) if your heading out 'lettuce snow'. To all the lads from home and Deco's, we had some good times, 'the bell' and of course who could forget 'the big V'. Sneaky pint? Many more to come! In the timeless words of 'Noonan' – "Get up ya daisy rooster".

I would also like to thank Professor Richard O'Kennedy for allowing me the privilege to work for his esteemed research group and for providing me with such great guidance over the years. Finally, the person who I would most like to thank is Dr. Stephen Hearty. What can I say? In my opinion, the entire group and all its success would be non-existent without Steve. I am sure that everyone who has worked with Steve will agree that he is an exceptional scientist and a great friend too. The guidance which Steve has provided me with over the years was unparalleled and I always knew that every piece of advice he gave me, was for my benefit and mine alone, a very rare trait these days.

Figure legends

Figure 1.8 Immunoglobulin G (IgG) antibodies, the most abundant of the immunoglobulins, are large molecules of about 150 kDa composed of 4 peptide chains.

Figure 3.1.2 Cartoon models of CRP (ZD Net Healthcare, Accessed 18 January, 2009) and its homologous Serum Amyloid P (SAP) protein.

Figure 3.1.4 SDS-PAGE gel of fractions from Protein A purification of rabbit anti-CRP pAb.

Figure 3.1.5 (a) Checkerboard ELISA using purified rabbit anti-CRP polyclonal antibody (pAb).

Figure 3.1.5 (b) Assay format used for checkerboard ELISA.

Figure 3.1.6 (a) Assay format used for both fluorescent sandwich ELISA.

Figure 3.1.6 (b) Fluorescent sandwich ELISA using purified unlabelled rabbit anti-CRP pAb as capture antibody and fluorescently-labelled rabbit anti-CRP pAb as detection antibody.

Figure 3.1.6 (c) shows the plotted averaged data from part two of the fluorescent sandwich ELISA optimization, performed in triplicate.

Figure 3.1.7 (a) shows a plot of the average CRP-binding response measured in response units (RU) on the Biacore 3000 system.

Figure 3.1.7 (b) shows a 4-parameter calibration curve of inter-assay Biacore 3000 analysis of a direct capture assay, involving purified rabbit anti-CRP pAb.

Figure 3.2.3 The optimisation of the variable heavy (VH) and variable light (VL) chain amplifications using the cDNA from a CRP-immunised Balb/c mouse.

Figure 3.2.4 SOE-PCR using different DMSO concentrations to optimise the product yield.

Figure 3.2.6 Polyclonal phage ELISA involving the phage pools of the unpanned library and the phage outputs from each of the successive rounds of panning.

Figure 3.2.7 ‘Colony-pick’ PCR showing amplification of scFv gene inserts from 10 randomly selected clones from the murine library subjected to 4 rounds of bio-enrichment against CRP.

Figure 3.2.8 Direct ELISA using scFv-enriched lysate of 96 murine anti-CRP scFv clones.

Figure 3.2.9 (a) An inhibition ELISA using the scFv-enriched lysate expressed from the murine anti-CRP scFv clone C11(2).

Figure 3.2.9 (b) Assay format used for inhibition ELISA.

Figure 3.2.10 Sequence alignment of functional variable domains of 10 murine anti-CRP scFv fragments.

Figure 3.2.11 (a) Sensogram of C11-2 lysate (pAK 400 format) following passage across a CM5 chip immobilized with an anti-FLAG M1 mAb.

Figure 3.2.11 (b) Sensogram of C11-2 lysate (pAK 400 format) being passed across CM5 chip immobilized mCRP.

Figure 3.2.12 Optimisation of part 1 of the ‘nested’ PCR using various annealing temperatures.

Figure 3.2.13 (a) Direct ELISA using scFv-enriched lysate from 20 candidate scFv clones.

Figure 3.2.13 (b) An inhibition ELISA using the scFv-enriched lysate expressed from the murine anti-CRP scFv C11(2) subcloned into the pComb3X vector.

Figure 3.2.14 Sequences of the mouse anti-CRP C11-2 scFv clone in its original pAK format and its engineered pComb format.

Figure 3.2.15 (a) Cross reactivity analysis of mouse C11-2 scFv subclone, avian H2 scFv and rabbit pAb via direct ELISA.

Figure 3.2.15 (b) Cross reactivity analysis of C11-2 scFv subclone lysate using an anti-HA capture method on the Biacore 3000.

Figure 3.2.16 (a) Analysis of reactivity of the C11-2 scFv subclone with mCRP using an anti-HA capture method on the Biacore 3000.

Figure 3.2.16 (b) Kinetic analysis fit of the mouse C11-2 scFv subclone using the Biacore 3000 system.

Figure 3.3.3 (a) Cross reactivity analysis of 4 avian scFv's and commercial mAb using direct ELISA.

Figure 3.3.3 (b) Cross reactivity analysis of scFv-enriched H2 clone lysate using an anti-HA capture method on the Biacore 3000.

Figure 3.3.4 (a) Capture assay format used on the Biacore A100 instrument. Biotinylated anti-HA antibody was immobilised on spots 1, 2, 4 and 5 of a series S SAchip.

Figure 3.3.4 (b) Typical kinetic analysis fit of avian anti-CRP scFv clone (F8) using the Biacore A100 system.

Figure 3.3.5 Crude scFv-enriched lysate (L) and purified scFv (S) for all 4 avian anti-CRP scFv antibodies.

Figure 3.3.6 (a) Illustration of a scAb fragment, composed of an scFv fused to a constant chain (kappa or lambda).

Figure 3.3.6 (b) PCR amplification of the C λ cys chain from chicken cDNA using 'in-house' designed primers (Lane 2).

Figure 3.3.6 (c) Schematic diagram of the expression cassettes employed by the pMoPac series of vectors (Hayhurst *et al.*, 2003), a modification of the pAK series (see section 3.2.17).

Figure 3.3.6 (d) Direct ELISA using scAb-enriched lysate from 60 PSA-specific scAb clones.

Figure 3.3.6 (e) PCR amplification of the H2 scFv gene using ‘in-house’ designed primers for incorporation of pAK format *Sfi*I sites.

Figure 3.3.6 (f) Direct ELISA using scAb-enriched lysate from 60 CRP-specific scAb clones.

Figure 3.3.7 SDS-PAGE gel of each fractions of the IMAC purification of the CRP-specific D9 scAb fragment.

Figure 3.3.8 (a) Left - SDS-PAGE gel containing protein marker ladder (Fermentas) in lane 1 and purified D9 scAb in lane 2. Right - A developed nitrocellulose membrane of an identical gel showing protein marker ladder (Lane 1) and CRP-reacting bands of purified D9 scAb (Lane 2).

Figure 3.3.8 (b) Left - SDS-PAGE gel containing purified D9 scAb (Lane 1), protein marker ladder (Lane 2) and purified H2 scFv (Lane 3). Right – The corresponding nitrocellulose membrane probed with the HRP labeled HA-specific mAb.

Figure 3.4.2 Ribbon representation of the MPO dimer structure (left) (Anonymous Last Accessed January, 2009).

Figure 3.4.3 Titration curve illustrating the MPO-specific response of serum taken from the final bleeds (red and blue) for chickens A and B, respectively.

Figure 3.4.6 Polyclonal phage ELISA involving both the pre-panned and pan 4 phage pools from panning of the chicken scFv library.

Figure 3.4.7 Direct soluble ELISA involving scFv-enriched lysate expressed from 120 chicken anti-MPO scFv clones from pan 4.

Figure 3.4.8 Capture assay format used on the Biacore 3000 instrument.

Figure 3.4.9 Analysis of the percentage antibody/antigen complex remaining after 5 min dissociation in buffer for 25 of the MPO-specific scFv clones.

Figure 3.4.10 Sequence of the selected avian anti-MPO scFv clone.

Figure 3.4.11 SDS-PAGE analysis of the various fractions of an IMAC purification of a MPO-specific scFv fragment.

Figure 3.4.12 (a) Titration curve of purified avian anti-MPO B10B scFv against MPO in a direct ELISA format.

Figure 3.4.12 (b) Assay format used for inhibition ELISA.

Figure 3.4.12 (c) Inhibition curve of purified avian anti-MPO scFv against several selected concentrations of MPO.

Figure 3.4.13 Kinetic analysis fit of the avian B10B anti-MPO scFv using the Biacore 3000 system.

Figure 3.4.14 (a) Assay format used for direct detection of MPO with TMB/OPD.

Figure 3.4.14 (b) Use of reactive substrates TMB and OPD as direct detection agents of MPO in an ELISA-based assay.

Figure 3.4.15 (a) Developed nitrocellulose membrane strips from the hybrid LFIA-western blot assay.

Figure 3.4.15 (b) Developed nitrocellulose membrane strips from LFIA optimisation experiments.

Figure 3.4.15 (c) Developed nitrocellulose membrane strips from LFIA optimisation experiments.

Figure 3.5.2 Developed LFIA strips from the fully optimized assay, performed in both MPO-depleted human serum (A) and 50 mM sodium phosphate, pH 7.5, containing 0.05% (v/v) Tween (B).

Figure 3.5.3 (a) The Open lateral flow 4 castchip™ (left) and a magnified image of the micro-pillar structures (right).

Figure 3.5.3 (b) Assay format for competitive CRP assay on Open lateral flow 4castchip™ chip.

Figure 3.5.3 (c) Plotted competition ELISA data for all four purified avian anti-CRP scFv clones and two commercial CRP specific mAb's (Fitzgerald).

Figure 3.5.4 (a) Parabolic array format of biochip together with microfluidic channel for sample delivery (left).

Figure 3.5.4 (b) Optically engineered biosensor platform (left) that focuses collimated light onto surface above critical angle to produce surface-confined TIRF excitation and the same platform exclusively collects SAF fluorescence above the critical angle (right).

Figure 3.5.4 (c) Calibration curve for the determination of CRP levels from depleted human serum using a sandwich-based assay on a paraboloid chip.

Figure 3.5.4 (d) Calibration curve for determination of CRP levels using a sandwich-based assay on the parabolic chip.

Figure 3.5.5 (a) Most widely used configurations of SPR sensors: (a) prism coupler-based SPR system - Attenuated Total Reflection (ATR) method; (b) grating coupler-based SPR system and (c) optical waveguide-based SPR system.

Figure 3.3.5 (b) Plotted data for a direct binding assay using a novel CRP-specific scAb fragment on the SPRSpectral® platform.

Abbreviations

Ab	-	antibody
Abs	-	absorbance
ACS	-	acute coronary syndrome
AHA	-	American Heart Association
AMI	-	acute myocardial infarction
AP	-	alkaline phosphatase
APS	-	ammonium persulfate
ATR	-	attenuated total reflection
BDI	-	Biomedical Diagnostic Institute
BM	-	bone marrow
BNP	-	Brain natriuretic peptide
BRECS	-	B cell recombination excision circles
BSA	-	bovine serum albumin
CAPTURE	-	Chimeric c7E3 Antiplatelet Therapy in Unstable angina Refractory
cCRP	-	cardiac C-reactive protein
CCU	-	cardiac care unit
CDC	-	Centre for Disease Control and Prevention
cDNA	-	complementary deoxyribonucleic acid
CDR	-	complementarity determining region
Cfu	-	colony forming units
CK	-	constant kappa
CK-MB	-	Creatine Kinase-MB
CLT	-	central lab testing
CM	-	carboxymethyl
CRP	-	C-reactive protein
cTnI	-	cardiac troponin I
cTnT	-	cardiac troponin T
C κ	-	constant kappa
C λ	-	constant lambda
CVD	-	cardiovascular disease
Cys	-	cysteine
DCU	-	Dublin City University

dH ₂ O	-	distilled water
DMF	-	dimethylformamide
DMSO	-	dimethyl sulfoxide
DNA	-	deoxyribonucleic acid
dNTP	-	deoxyribonucleotide triphosphate
DTT	-	di-thiotheritol
<i>E. coli</i>	-	Escherichia coli
ECG	-	electrocardiogram
ED	-	emergency department
EDC	-	N-ethyl-N'-(3-dimethylaminopropyl) carbodiimide hydrochloride
EDTA	-	ethylenediaminetetraacetic acid
ELISA	-	enzyme-linked immunosorbent assay
EU	-	European Union
Fab	-	antigen binding fragment
FABP	-	fatty acid binding protein
FC	-	flow cell
FCA	-	Freund's complete adjuvant
FDA	-	Food and Drug Administration
FICA	-	Freund's incomplete adjuvant
FRISC	-	Fragmin during Instability in Coronary Artery Disease
GALT	-	gut-associated lymphoid tissues
GP	-	general practitioner
HA	-	haemagglutinin
HAMA	-	human anti-mouse antibody
HAT	-	hypoxanthine aminopterin thymidine
HBS	-	hepes buffered saline
HF	-	heart failure
H-FABP	-	heart-type fatty acid binding protein
HGPRT	-	hypoxanthine-guanine phosphoribosyltransferase
HIFI	-	high fidelity
His	-	histidine
HRP	-	horse radish peroxidase
hs-CRP	-	high sensitivity C-reactive protein
HTS	-	high-throughput screening

IgG	-	immunoglobulin G
IgM	-	immunoglobulin M
IL	-	interleukin
IMAC	-	immobilised metal affinity chromatography
IMS	-	industrial methylated spirits
IPTG	-	isopropyl- β -D-1-thiogalactopyranoside
IUPAC	-	International Union of Pure and Applied Chemistry
K_D	-	dissociation constant (units = M)
kDa	-	kilo dalton
LFIA	-	lateral flow immunoassay
LFT	-	lateral flow technology
LOD	-	limit of detection
LOQ	-	limit of quantitation
mAb	-	monoclonal antibody
mCRP	-	monomeric CRP
MI	-	myocardial infarction
mL	-	millilitre
MPBST	-	phosphate buffered saline with 1% (w/v) milk and 0.05% (v/v) Tween
MPO	-	myeloperoxidase
mRNA	-	messenger RNA
MWCO	-	molecular weight cut-off
N/A	-	not applicable
NHS	-	N-hydroxysuccinimide
NSTEACS	-	non-ST-segment elevation myocardial infarction
O/N	-	overnight
OD	-	optical density
OLF	-	open lateral flow
OPD	-	o-phenylenediamine dihydrochloride
pAb	-	polyclonal antibody
PAGE	-	polyacrylamide gel electrophoresis
PBS	-	phosphate buffered saline
PBST	-	phosphate buffered saline with 0.05% (v/v) Tween
PC	-	phosphocholine
PCR	-	polymerase chain reaction

PEG	-	polyethylene glycol
pfu	-	phage forming units
pI	-	isoelectric point
PMMA	-	poly(methyl methacrylate)
PNPP	-	p-nitrophenyl phosphate
RAP	-	resonant acoustic profiling
RNA	-	ribonucleic acid
RT	-	reverse transcriptase
RU	-	response unit
POC	-	point-of-care
POCT	-	point-of-care testing
PSA	-	prostate specific antigen
RNA	-	ribonucleic acid
rpm	-	revolutions per minute
RT	-	reverse transcriptase
r.t.	-	room temperature
RU	-	response unit
SA	-	streptavidin
SAF	-	supercritical angular fluorescence
SAP	-	serum amyloid P protein
SB	-	super broth
scAb	-	single chain antibody
scback	-	single chain back
sCD40L	-	soluble CD40 ligand
scFor	-	single chain forward
scFv	-	single chain fragment variable
SD	-	standard deviation
SDS	-	sodium dodecyl sulfate
SOC	-	super optimal catabolite
SOE	-	splice-overlap-extension
SP	-	spleen
SPR	-	surface plasmon resonance
STEMI	-	ST-segment elevation myocardial infarction
TAE	-	Tris-acetate-EDTA

TAT	-	turn-around-time
TB	-	terrific broth
TEMED	-	tetramethylethylenediamine
TIMI	-	Thrombolysis in Myocardial Infarction
TIRF	-	total internal reflection fluorescence
TMB	-	tetramethylbenzidine dihydrochloride
TRI	-	trizol
VH	-	variable heavy
VK	-	variable kappa
VL	-	variable light
v/v	-	volume per volume
w/v	-	weight per volume

Abstract

The principal objective of this research was the production, characterisation and application of antibodies for the detection of both C-reactive protein (CRP) and Myeloperoxidase (MPO), two promising candidates in the field of cardiac diagnostics. CRP is a highly stable acute phase reactant, produced in the liver in response to interleukin (IL)-6. In January 2003 both the Centres for Disease Control and Prevention (CDC) and the American Heart Association (AHA) recommended CRP as the inflammatory marker of choice for assessment of cardiovascular risk. The other biomarker under investigation was MPO, a mediator enzyme secreted by inflammatory cells such as activated neutrophils and monocytes. High levels of MPO have been reported in atherosclerotic plaques and accumulating evidence indicates that MPO may have a causative role in plaque vulnerability. It has been suggested that these markers may even be complementary in the assessment of patient cardiac risk. As a marker of disease activity and vascular inflammation, CRP detection is associated with long-term risk stratification while MPO, being a marker of plaque instability and neutrophil activation, may be prove to be a key marker for short term stratification.

A key feature of this work was to ensure the isolated antibodies had a sufficient level of both functional affinity and specificity for the development of novel diagnostic formats and assay platforms. Both classic polyclonal antibody generation and 'state-of-the-art' phage display technology were employed for the generation of CRP- and MPO-specific antibodies and recombinant fragments. The immune systems of mice, rabbits and chickens were investigated in this work, which allowed for the identification of the main advantages and disadvantages associated with each of the host immune systems and their capacity for generating specific and sensitive antibodies. It was observed that the avian immune system was found to be the most effective system for the generation of functional and soluble antibodies.

The CRP-specific antibodies were incorporated into three novel biosensor platforms for their final characterisation. In addition, a novel lateral flow immunoassay (LFIA) for the rapid detection of MPO was developed, using a recombinant antibody isolated from a MPO-immune library. Spiked samples of depleted human serum were employed in both the biosensor and LFIA systems, thus validating the detection of the analytes in a realistic sample matrix.

Aims and objectives:

The primary goal of this work was the generation of both highly sensitive and specific recombinant antibodies towards the cardiac markers CRP and MPO. CRP has been consistently flagged as having great potential, particularly in the field of cardiac risk assessment. However, as a marker of disease activity and vascular inflammation, CRP detection has been associated with long-term risk stratification. Therefore, the implementation of a more comprehensive risk assessment strategy should also include a cardiac marker capable of identifying short-term risk cardiac patients. As an indicator of plaque instability and neutrophil activation, MPO, may prove to be a key marker for short-term stratification. It was also suggested that both markers may even be complementary in the assessment of patient cardiac risk (Loria *et al.*, 2008). This formed the basis for selection of both of these markers as targets for antibody production in this research.

Initially, polyclonal antibody was generated from rabbits immunised with the chosen targets. The heterogenous nature of polyclonal antibody pools can restrict their use as target-specific reagents. However, polyclonal antibody is a relatively cheap and robust source of control antibody and, furthermore, can provide a highly sensitive capture reagent when combined with a target specific monoclonal antibody in a sandwich-based format. For the generation of the target-specific monoclonal antibodies, phage display-based recombinant antibody technology was employed. Although, hybridoma technology can also be used for monoclonal antibody generation, the direct link of phenotype to genotype in recombinant antibody technology, provides a key attribute for downstream manipulation or re-engineering of isolated antibodies.

Combining an immunised host with phage display technology for the production of recombinant antibodies is well-documented (Berry and Popkov, 2005) and has provided significant breakthroughs in the fields of both diagnostics and therapeutics. However, conflicting opinions persist regarding the choice of immune host used (Andris-Widhopf *et al.*, 2000; O'Brien and Aitken, 2002; Finlay *et al.*, 2005,). Consequently, this work will also investigate this issue by comparatively examining the use of several species in the production of recombinant antibodies against a select antigen, namely CRP. Mice, rabbits and chickens were chosen as the immune hosts for the study, with each species bringing its own unique characteristics and advantages to the antibody production process. Each of the immune host systems will be thoroughly discussed in the introduction of each of their respective sections and also the selection of each of the systems will be validated. It is envisaged this study will

shed some light on the issue of immune host selection and hopefully present some useful findings.

In each case, optimised 'state-of-the-art' phage display systems combined with high-throughput screening and characterisation platforms such as Biacore were employed. These systems will hopefully ensure that the full capacity of the immune systems of each of the species under investigation will be achieved. The ease of construction of the libraries, their characterisation and the final outputs from each of the species will be critically examined. Finally, the developed CRP - and MPO - specific antibodies will be used to validate novel point-of-care (POC) diagnostic platforms. A diverse range of platform technologies will be employed for the final application of the isolated antibodies from this research, ranging from basic yet robust technologies such as standard lateral flow to complex microfluidic chip-based platforms. In each case, the reasoning behind each of the selected platforms will be discussed in the introduction section for each of the respective platforms. In addition, some of the limitations of existing antibody technologies are highlighted and how these may be overcome by employing some of the assay platforms investigated in this research. The performance of these platforms will be analysed using data evaluation packages to identify their ability in providing potential life-saving information in the fight against cardiovascular disease.

Chapter 1

Introduction

1. Introduction:

1.1. Prevalence of cardiovascular disease

Cardiovascular disease (CVD) is the cause of nearly half of all deaths in the western world (49%) (Allender *et al.*, 2008). In addition, up to 50% of patients referred to cardiologists from primary care physicians have been originally misdiagnosed with conditions other than heart failure (HF). Thus, more accurate diagnosis is of paramount importance for improvements in clinical assessments. Furthermore, in the region of 5% of myocardial infarction (MI) patients are discharged from emergency departments (ED) without adequate treatment, as approximately one quarter of these patients present with atypical symptoms and about one third have non-diagnostic electrocardiogram (ECG) changes (Char, Israel and Ladenson, 1998). Failure to diagnose MI in the ED is also a significant contributor towards payments of malpractice for ED physicians (Vukmir, 2004; White *et al.*, 2004; Schull *et al.*, 2006). In addition, the overall financial burden of CVD in the EU is believed to be 192 billion euro per year (Allender *et al.*, 2008).

1.2. Pathophysiology of acute coronary syndromes (ACS)

The vast array of clinical symptoms evident after coronary plaque disruption are often cumulatively referred to as ACS (Braunwald *et al.*, 2002). Initially, rupture of unstable coronary plaques results in intracoronary thrombosis, where the thrombus (bloodclot) leads to a reduction in blood flow (cardiac ischemia), thereby restricting the supply of oxygen to the myocardium. The continuum of this myocardial ischemia is ‘acute coronary syndrome’, which ranges from unstable angina (associated with reversible myocardial injury) to MI with large areas of irreversible damage (cardiac necrosis). Acute coronary syndromes are mainly separated into two categories based on changes seen in the electrocardiograms at presentation: ‘ST-segment elevation myocardial infarction’ (STEMI) and ‘non-ST-segment elevation ACS’ (NSTEMI). The therapeutic approach associated with each of these categories varies substantially. Consequently, it is essential to accurately categorise patients prior to treatment. NSTEMI are also further sub-categorised into unstable angina and non-STEMI. A common pathogenesis is shared by both of these subgroups, as well as similar clinical presentation. However, ischemia in non-STEMI is more severe in intensity and duration and causes irreversible myocardial damage.

1.3. *The first use of cardiac markers*

The earliest documented use of biochemical markers in the study of myocardial infarction was in 1954, which reported that glutamate oxaloacetic transaminase activity in serum increased above the reference range a few hours after acute myocardial infarction (AMI), reaching a peak after 2 to 3 days (Ladue *et al.*, 1954). Biochemical markers now play a fundamental role in the diagnosis, prognosis, monitoring and risk stratification of patients with acute coronary syndromes (ACS) and the redefinition of myocardial infarction is dependent on markers such as cardiac troponin (Alpert *et al.*, 2000; Apple *et al.*, 2007; Morrow and de Lemos, 2007,).

1.4. *The ideal characteristics of a cardiac marker*

To obtain a high diagnostic sensitivity, cardiac biomarkers need to be easily accessible. Hence, smaller soluble molecules with faster release kinetics and rapid clearance from injured tissue are regarded as the most suitable markers for early diagnosis. However, in the case of late diagnosis a highly stable marker with a long plasma half-life is essential. Consequently, peak levels should be reached relatively quickly and persist in circulation for a few hours, as is the case with the cardiac troponins. Conversely, a rapid clearance of the marker from plasma is a crucial feature of markers of recurrent injury. The kinetics of release exhibited by the markers should have a clear relationship with the extent of the injury i.e. infarct sizing. The cardiac marker ideally should be highly specific for cardiac tissue and absent from non-myocardial tissue. It should also have the ability to differentiate between reversible (ischemia) and irreversible (necrosis) damage. The marker has to be thoroughly evaluated by large statistically designed clinical studies before its acceptance into routine clinical use. Finally, it must have the ability to influence therapy, such as providing additional information for existing risk scores or being one of the parameters of a new risk score. Despite the hugely significant developments in the field, there still is considerable controversy surrounding the use of cardiac biomarkers, as no single biomarker fulfils all the criteria of an 'ideal' cardiac biomarker. Presently, the cardiac troponins appear to be the most sensitive and specific biomarkers among all other diagnostic biomarkers for ACS. However, there is a consensus that a single measurement of the cardiac troponins at patient admission is insufficient because a single measurement will not detect 10% to 15% of at-risk patients (Hamm, 2001). Table 7.3.1 (Appendix section) shows some of the existing cardiac markers

currently used and their primary utility in the clinical setting. The two markers focused on in this research thesis were CRP and MPO, both inflammatory markers.

1.5. *Markers of inflammation*

Up to half of the events associated with cardiovascular disease (CVD) occur in asymptomatic individuals (Ridker *et al.*, 2005), thus, emphasising the need for true ‘early’ biomarkers. Consequently, intense research has focused on markers of inflammation (Ross, 1999). Inflammatory processes play a prominent role in the development of both the intermediate and mature atheromatous plaque and also contribute to the destabilisation of vulnerable plaques resulting in ACS (Libby, 2002). Established and novel inflammatory markers such as C-reactive protein (CRP) and myeloperoxidase (MPO) may be elevated before the onset of irreversible damage. Accordingly, several inflammatory mediators have been evaluated as prognostic indicators of the risk of initial ACS, adverse sequelae and recurrent complications.

1.6. *C-reactive protein*

CRP is an acute phase reactant, produced in the liver in response to interleukin (IL)-6. CRP is a pattern recognition molecule made up of five identical subunits (Shrive *et al.*, 1996). Its normal physiological role involves binding to phosphocholine expressed on the surface of dead or dying cells (and some types of bacteria) in order to activate the complement system via the C1q complex (Thompson *et al.*, 1999). In the presence of Ca^{2+} , each subunit binds with high affinity to phosphocholine (PC) (Anderson *et al.*, 1978). As the five ligand-binding sites are all on the same face of the pentamer (Shrive *et al.*, 1996), CRP binds with high avidity to ligand-decorated targets such as bacteria. On the opposite side of each subunit is an effector molecule-binding site that mediates the protein's interaction with C1q, (Agrawal and Volanakis, 1994), Fc γ RI (Marnell *et al.*, 1995) and Fc γ RII (Bharadwaj *et al.*, 1999).

It is a highly stable pentameric protein and its serum concentration can increase 10,000-fold during the acute phase response (Pepys and Berger, 2001; Black *et al.*, 2004; Labarrere and Zaloga, 2004). Investigative data suggests that CRP may play an active role in atherogenesis. It has been shown that CRP co-localises with the membrane attack complex in early atheromatous lesions (Yasojima *et al.*, 2001). Two more recent studies reported the detection of CRP in the early stages of plaque development and also stated a possible involvement in facilitating processes ranging from the initial recruitment of leukocytes to the arterial wall to

the eventual rupture of the plaque itself (Blake and Ridker, 2003; Azzazy *et al.*, 2006). Another interesting study observed the loss of the pentameric symmetry of CRP resulting in a modified or monomeric CRP form (mCRP), which may be the major CRP isoform promoting the proinflammatory response in coronary arteries (Khreiss *et al.*, 2004a).

In January 2003 both the Centres for Disease Control and Prevention (CDC) and the American Heart Association (AHA) recommended CRP as the inflammatory marker of choice for assessment of cardiovascular risk (Pearson *et al.*, 2004). The high sensitivity CRP assay (hs-CRP) was originally developed to aid evaluation of conditions associated with inflammation, in otherwise healthy individuals. Cardiac CRP (cCRP) assays are indicated for use in the clinical identification and stratification of patients at risk of future CVD-associated events. The hs-CRP assay is frequently quoted in a cardiac context and indeed both hs-CRP and cCRP assays have equivalent clinical cut-off and measuring ranges. Nonetheless, the additional performance validation demanded to support the expanded intended use of CRP in indications related to CVD dictates that a clear distinction be made (U.S. Department of Health and Human Services, Food and Drug Administration, Center for Devices and Radiological Health, Office of In Vitro Diagnostic Device Evaluation and Safety, Division of Chemistry and Toxicology Devices, 2005). The recommended guidelines for primary prevention set cut-off points according to relative risk categories: low risk (<1 mg/L), average risk (1-3 mg/L) and high risk (>3 mg/L) for patients with an intermediate 10-year CVD risk (10% to 20% Framingham Risk Score/ATP III guidelines). Recently, hs-CRP has also been incorporated into a cardiac risk score for women, the 'Reynolds risk score', based on a comprehensive study involving nearly 25,000 women over 10 years (Ridker *et al.*, 2007), thus fulfilling one of the key criteria of an 'ideal' marker.

Several large-scale epidemiological studies examining apparently healthy populations have found CRP to be a strong independent predictor of future cardiovascular events, including myocardial infarction, ischemic stroke, peripheral vascular disease and sudden cardiac death (Ross, 1999; Blake and Ridker, 2003; Calabro *et al.*, 2003; Ridker, 2003; Ridker *et al.*, 2005;) and this is evident in the growing number of commercially available hs-CRP tests, one example being the Pathfast® POC test supplied by Mitsubishi Chemical Europe GmbH. The emerging consensus is that subjects in the top quartile of hs-CRP levels are at 2-3 times greater risk of future coronary events than those in the bottom quartile. cCRP levels have been shown to be associated with coronary events as early as 5 years and as late as 15 years into follow up (Sakkinen *et al.*, 2002). Numerous studies like TIMI, CAPTURE and FRISC (Morrow *et al.*, 1998; Heeschen *et al.*, 2000; Lindahl *et al.*, 2000) have examined the

predictive value of CRP and have found it to contribute both independent and additive value to cardiac troponin levels. Furthermore, hs-CRP has been found to have prognostic value among patients without evidence of myocyte necrosis, notably even among patients with normal levels of troponin T (Morrow *et al.*, 1998; Heeschen *et al.*, 2000; Lindahl *et al.*, 2000). The optimal cut-off point for defining 'high' c-CRP levels among patients remains contentious, possibly due to heightened vascular inflammation or subtle undiagnosed inflammatory state at the time of presentation with ACS. For example, the CAPTURE study (Heeschen *et al.*, 2000) found a threshold of 10 mg/L maximised the predictive value of hs-CRP, whereas numerous other studies (Ridker *et al.*, 1997; Ridker *et al.*, 2000; Ridker *et al.*, 2001) have proposed a cut-off point of 3 mg/L to be most suitable. However, a clinical cut-off concentration of ≤ 1.0 mg/mL has been recommended by the 2005 'Industry and FDA staff guidelines' (U.S. Department of Health and Human Services, Food and Drug Administration, Center for Devices and Radiological Health, Office of In Vitro Diagnostic Device Evaluation and Safety, Division of Chemistry and Toxicology Devices, 2005). To date, there is insufficient evidence to substantiate the ability of hs-CRP to identify ACS patients who will benefit from a particular treatment (Heeschen *et al.*, 2000; Solomon *et al.*, 2001). This is further confounded by estimates that more than 30% of patients with severe unstable angina do not present with elevated hs-CRP levels (Ridker and Cook, 2004). Notwithstanding the fact that CRP is the most extensively studied inflammatory marker, several other markers of inflammation exist with particular promise in the field of cardiac risk assessment.

1.7. Myeloperoxidase

MPO is a mediator enzyme secreted by inflammatory cells e.g. activated neutrophils and monocytes. MPO produces hypochlorous acid (HOCl) from hydrogen peroxide (H₂O₂) and chloride anion (Cl⁻) (or the equivalent from a non-chlorine halide) during the neutrophil's respiratory burst, requiring heme as a cofactor. Furthermore, it oxidizes tyrosine to tyrosyl radical using hydrogen peroxide as an oxidizing agent (Heinecke *et al.*, 1993). Both hypochlorous acid and tyrosyl radical are cytotoxic and are used by neutrophils to kill bacteria and other pathogens. High levels of MPO have been reported in atherosclerotic plaques (Blake and Ridker, 2003) and accumulating evidence indicates that MPO may also have a causative role in plaque vulnerability (Hazen, 2004). MPO can generate several reactive oxidised intermediates, concomitantly inducing oxidative damage of cells and tissues

(Brennan *et al.*, 2003). Such reactive intermediates have been found at increased levels in low density lipoprotein (LDL) isolated from atherosclerotic lesions (Hazen and Heinecke, 1997). Moreover, high MPO expression levels have been reported in patients with sudden cardiac death, at sites of plaque rupture, superficial erosions and in the lipid core, whereas less harmful fatty streaks were observed to exhibit little MPO expression (Sugiyama *et al.*, 2001). Several recent clinical studies have suggested that MPO levels may play a potentially important diagnostic and prognostic role in endothelial function, CAD and ACS. The role of MPO as an independent predictor of endothelial dysfunction has been demonstrated (Vita *et al.*, 2004) and further studies have underlined the value of MPO as a predictor of cardiac risk in populations with different incidences of ACS (Baldus *et al.*, 2003; Brennan *et al.*, 2003). Both studies concluded that a single measurement of plasma MPO at hospital admission predicted the risk of major adverse cardiac events for both a 30-day and six month period. Baseline levels of MPO were determinants of patient risk stratification, even in patients with consistently negative cTnT levels. The predictive power of MPO was also found to be independent of soluble fragment CD40 ligand (sCD40L), CRP and BNP in ACS patients with undetectable cTnT concentrations and sCD40L concentrations below their threshold values. MPO levels, in contrast to cTnT, CK-MB and CRP levels, identified patients at risk for cardiac events in the absence of myocardial necrosis. It has subsequently been suggested that MPO may play an important role in identifying short-term risk of recurrent ischemic events, again, independent of clinical risk factors like cTnI and other novel biomarkers (Morrow *et al.*, 2008). A case control study highlighted that increasing levels of leukocyte-MPO and blood-MPO were significant predictors of CAD (Zhang *et al.*, 2001). Individuals in the highest quartile of blood-MPO had a 20-fold higher risk of CAD than individuals in the lowest quartile, following adjustment for white blood cell count and Framingham risk score. In August 2005, the FDA approved the first MPO assay, CardioMPO™, developed by PrognostiX, Inc. The test is a sandwich enzyme immunoassay cleared for use in conjunction with clinical history, ECG and other cardiac biomarkers to evaluate patients with chest pain at risk of major adverse cardiac events.

MPO appears to be one of the most promising contemporary candidates, yet due to its relatively recent emergence, there is still uncertainty about the additional benefits of MPO over standard ischemic biomarkers. Therefore, further supporting evidence is required to clarify this issue before it achieves widespread clinical acceptance. Moreover, almost all data for MPO is in the setting of ACS or established CAD and, thus, it remains unclear whether

MPO can provide additional information to conventional atherothrombotic risk factors used in the Framingham Risk Score.

1.8. Antibody production

The traditional approach for the production of monoclonal antibodies (mAbs) was dominated by the use of hybridoma fusion techniques, first introduced by Kohler and Milstein in 1975 (Köhler and Milstein, 1975). This technique commences with the immunisation of a relevant animal host (e.g. mouse) with a specific immunogen (the antigen against which antibodies are required). An adjuvant such as Freund's complete adjuvant is commonly administered in combination with the immunogen so as to augment a desired immune response (i.e. production of antibodies). The level of antibody, specific for the immunised antigen, is periodically calculated using a serum titre from the immunised animal. When a sufficient serum antibody titer is achieved (1/100,000 or higher), the immunised animal is sacrificed and its spleen removed. The spleen provides a rich source of antibody-producing B cells, which possess a hypoxanthine guanine phosphoribosyl transferase (HGPRT) gene, a crucial gene in the hybridoma process. These B cells are isolated and fused with myeloma cells (lack HGPRT), resulting in their immortalisation as hybridoma cells. A commonly used agent in the fusion process is polyethylene glycol (PEG), which promotes cell permeability and exchange of nuclei. The resultant hybridomas are cultured in Hypoxanthine Aminopterin Thymidine (HAT) medium, a selective medium in which only the fused hybrid cells may survive. Its selectivity is achieved via the presence of aminopterin in the medium, which blocks the pathway that allows for nucleotide synthesis. Hence, unfused myeloma cells die due to their inability to produce nucleotides by the *de novo* or salvage pathways (lack the HGPRT gene). In addition, unfused B cells die due to their limited life-span. Therefore, the only-surviving cells are the B cell-myeloma hybrids, as a consequence of their immortality combined with the possession of the essential HGPRT gene. Hybridoma cells secreting the antigen-specific monoclonal antibodies are then identified via screening of the cells media supernatant by techniques such as enzyme-linked immunosorbent assay (ELISA). Enrichment of these positively identified hybridomas is achieved by limiting dilution, to obtain a homogeneous cell clone secreting the desired mAb (Little *et al.*, 2000).

Since the culmination of hybridoma technology, the production of antibodies was revolutionised by the development of modern molecular biology methods for the expression of recombinant DNA. Among the various strategies developed for the *in vitro* production and

selection of recombinant antibodies, phage display has proven to be a robust and versatile technology. Phage display allows for the generation of billions of phage particles expressing an antibody fragment at their surface that has the potential to bind to the desired antigen. Phage display encompasses the four key components of selection platforms: genotypic diversity, genotype/phenotype coupling, selection pressure and amplification (Bradbury and Marks, 2004). A schematic representation of the phage selection cycle can be found in section 7.2.1 (Appendix section) has led to the ability to produce antibodies with affinities unobtainable in the immune system. A crucial advantage of this technology is the direct link that exists between the experimental phenotype and its encapsulated genotype, which allows the evolution of the selected binders into optimised molecules.

The enrichment of phage presenting the desired binding protein (or peptide) is achieved by affinity selection of a phage library against a specific target molecule. In this “panning” process, binding phage are captured whereas non-binding phage are washed off. The bound phage are eluted (usually low pH or trypsin elution) and amplified by reinfection into *E. coli* cells. Put simply, the selection from phage display libraries is a cyclic process of selective enrichment and amplification. Typically, affinity is enriched (matured) through multiple rounds of biopanning, a process that involves binding to reducing concentrations of the ligand of interest. Four to six rounds of this process is usually sufficient to select for phage displaying high-affinity antibody fragments.

Phage display systems can be grouped into two classes on the basis of the vector system used for the production of phages:

1. True phage vectors – directly derived from the genome of filamentous phage (M13, f1, or fd) and encode all the proteins needed for the replication and assembly of the filamentous phage.
2. Phagemid vectors – produce the fusion coat protein. A phagemid is a plasmid that bears a phage-derived origin of replication in addition to its plasmid origin of replication. The phage-derived origin of replication is also known as the intergenic region.

In general, the two kinds of libraries that can be used are either naïve or immune libraries. Naive or semi-synthetic established libraries possessing greater than 10^{10} individual clones offer the possibility of selection of antibodies of any desired specificity without the need for immunisation. Nevertheless, the combination of an immunised host with phage display technology was shown to produce superior antibodies with both high affinity and specificity

towards cognate antigens (Krebber *et al.*, 1997; Barbas *et al.*, 2001). In addition to the vast array of potential library sources, huge advances in molecular biology have led to the ability to construct custom recombinant antibody formats (Figure 1.8). The two predominant formats chosen are either the single chain Fv (scFv) or Fab antibody fragment format.

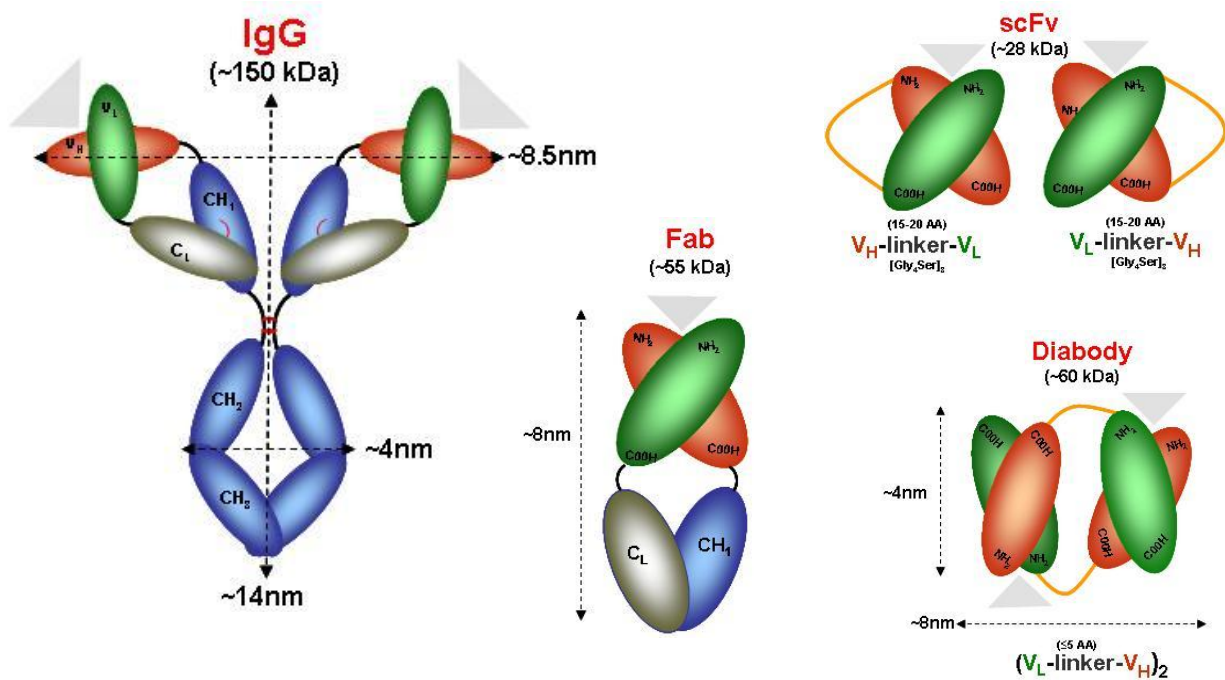


Figure 1.8 Immunoglobulin G (IgG) antibodies, the most abundant of the immunoglobulins, are large molecules of about 150 kDa composed of 4 peptide chains. It contains 2 identical heavy chains (blue and red) of about 50 kDa and 2 identical light chains (green and grey) of about 25 kDa in molecular weight. The two heavy chains are linked to each other and to a light chain each by disulphide bonds. The building block that is most frequently used to create novel antibody formats is the single-chain variable (V)-domain antibody fragment (scFv), which comprises V domains from the heavy and light chain (V_H and V_L domain) joined by a peptide linker of up to 15 amino-acid residues. The Fab fragment is a modification of this format, which also contains a constant heavy and light chain for increased stability. The diabody format is comprised of the heavy and light-chain variable regions joined by a flexible peptide linker. The linker is long enough to allow separation of the domains so that two of the polypeptides can assemble into a dimer, making the antibody divalent.

Chapter 2

Materials and Methods

2.0 Materials and Methods

2.1 Equipment

Biometra T _{GRADIENT} PCR machine	-	LABREPCO, 101 Witmer Road, Suite 700, Horsham, PA19044, USA.
Nanodrop™ ND-1000	-	NanoDrop Technologies, Inc., 3411 Silverside Rd 100BC, Wilmington, DE19810-4803, USA.
Gene Pulser Xcell™ electroporation system	-	Bio-Rad Laboratories, Inc., 2000 Alfred Nobel Drive, Hercules, California 94547, USA.
ORBI-safe TS Netwise orbital shaking incubator	-	Sanyo Europe Ltd., 18 Colonial Way, Watford, WD24 4PT, United Kingdom.
Trans-Blot® Semi-dry Transfer cell	-	Bio-Rad Laboratories, Inc., 2000 Alfred Nobel Drive, Hercules, California 94547, USA.
Roller mixer SRT1	-	Sciencelab, Inc., 14025 Smith Rd. Houston, Texas 77396, USA.

Safire 2 plate reader	- Tecan Group Ltd., Seestrasse 103, CH-8708 Männedorf, Switzerland.
PX2 thermal cycler	- Thermo Electron Corporation, 81 Wyman Street, Waltham, Massachusetts (MA), 02454, USA.
Biacore 3000 and A100	- GE Healthcare Bio-Sciences AB, SE-751 84 Uppsala Sweden.
Vibra Cell™ sonicator	- Sonics and Materials Inc., 53 Church Hill Road, Newtown, CT 06470-1614, USA.
sciFLEXARRAYER™ S3	- Scienion AG, Otto-Hahn-Straße 15, D-44227 Dortmund, Germany.
Linomat 5	- CAMAG, Sonnenmattstrasse 11, P.O. Box 216, CH-4132 Muttenz 1, Switzerland.

2.2 Bacterial culture compositions

2 x TY Media	Tryptone	16 g/L
	Yeast Extract	10 g/L
	NaCl	5 g/L
Super Broth (SB) Media	MOPS	10 g/L
	Yeast Extract	30 g/L
	Yeast Extract	20 g/L
Terrific Broth (TB)	Tryptone	12 g/L
	Yeast Extract	24 g/L
	Glycerol	4 mL/L
	KH ₂ PO ₄	2.31 g/L
	K ₂ HPO ₄	12.54 g/L
Super Optimal Catabolite (SOC) Media	Tryptone	20 g/L
	Yeast Extract	5 g/L
	NaCl	0.5 g/L
	KCl	2.5 mM
	MgCl ₂	20 mM
	Glucose	20 mM

2.3 Bacterial cells for cloning and expression

E. coli TOP10 F' strain: {*lacI*^q, Tn10(Tet^R)} *mcrA* Δ (*mrr-hsdRMS-mcrBC*) ϕ 80*lacZ* Δ M15 Δ *lacX74* *recA1* *araD139* Δ (*ara-leu*)7697 *galU* *galK* *rpsL* (Str^R) *endA1* *nupG*

E. coli XL1-Blue strain: *recA1* *endA1* *gyrA96* *thi-1* *hsdR17* *supE44* *relA1* *lac* [F' *proAB* *lacI*^q Δ M15 Tn10 (Tet^R)].

2.4 Buffer Composition

Phosphate buffered saline (PBS)	0.15 M NaCl	
	2.5 mM KCl	
	10 mM Na ₂ HPO ₄	
	18 mM KH ₂ PO ₄	
	pH 7.4	
PBS-Tween 20 (0.05% (v/v) PBST)	0.15 M NaCl	
	2.5 mM KCl	
	10 mM Na ₂ HPO ₄	
	18 mM KH ₂ PO ₄	
	0.05% (v/v) Tween 20	
	pH 7.4	
Milk-PBST (MPBST)	0.15 M NaCl	
	2.5 mM KCl	
	10 mM Na ₂ HPO ₄	
	18 mM KH ₂ PO ₄	
	0.05% (v/v) Tween 20	
	Specified % (w/v) milk marvel powder	
pH 7.4		
Hepes buffered saline (HBS)	HEPES	2.38 g/L
	NaCl	8.77 g/L
	EDTA	1.27 g/L
	Tween	0.5 mL/L
	pH 7.4	

2.5 SDS PAGE and Western Blotting

<u>12.5% Separation gel</u>	<u>1gel (6mL)</u>
1 M TrisHCl, pH 8.8	1.5 mL
30% (w/v) acrylamide (Acrylagel)	2.5 mL
2% (w/v) methylamine bisacrylamide (Bis-Acrylagel)	1.0 mL
Distilled water	934 μ L
10% (w/v) sodium dodecyl sulfate (SDS)	30 μ L
10% (w/v) APS	30 μ L
TEMED	6 μ L

<u>4.5% Stacking gel</u>	<u>1gel (2.5mL)</u>
1 M TrisHCl, pH 6.8	300 μ L
30% (w/v) acrylamide (Acrylagel)	375 μ L
2% (w/v) methylamine bisacrylamide (Bis-Acrylagel)	150 μ L
Distilled water	1.74 mL
10% (w/v) SDS	24 μ L
10% (w/v) APS	24 μ L
TEMED	2.5 μ L

<u>10 X electrophoresis buffer</u>	
50mM Tris, pH 8.3	30 g
196mM Glycine	144 g
0.1% (w/v) SDS	10 g
Distilled water to 1 L	

Loading buffer (4 X)

Tris 0.5M, pH 6.8	2.5 mL
Glycerol	2.0 mL
2 mercaptoethanol	0.5 mL
20% SDS (w/v)	2.5 mL
Bromophenol blue	20 ppm
Distilled water	2.5 mL

Coomassie stain dye/ 500mL

Coomassie blue R-250	1 g
Methanol	225 mL
Distilled water	225 mL
Acetic acid	50 mL

Coomassie destain/L

Acetic acid	250 mL
Methanol	250 mL
Distilled water	650 mL

Transfer Buffer/L

1 X SDS electrophoresis buffer	800 mL
Methanol	200 mL

2.6 Commercial kits

- | | | |
|---|---|--|
| Superscript III reverse transcriptase kit | - | Invitrogen Corporation,
5791 Van Allen Way,
Carlsbad, CA 92008, USA . |
| Perfectprep Gel Cleanup Kit | - | Eppendorf AG,
Barkhausenweg 1,
Hamburg 22339,
Germany. |
| Wizard Plus SV Miniprep™ kit | - | Promega,
2800 Woods Hollow Road,
Madison, WI 53711,
United States. |
| Commercial DyLight 647™ kit | - | Fisher Thermo Scientific,
47341 Bayside Pkwy.,
Fremont, CA 94538, USA. |
| QIAquick™ gel extraction Kit | - | Qiagen,
28159 Avenue Stanford,
Valencia, CA 91355, USA. |

2.7 Commercial antibodies

Anti-M13 antibody (HRP-labelled)	-	GE Healthcare Bio-Sciences AB, SE-751 84 Uppsala, Sweden.
Mouse anti-HA (HRP-labelled) mAb	-	Roche Diagnostics, Grenzacherstrasse 124, Basel 4070, Switzerland.
CRP-specific mAb (section 3.3.3)	-	HyTest, Joukahaisenkatu 6, 20520, Turku, Finland.
CRP-specific mAb (section 3.5.3)	-	Fitzgerald Industries International, 30 Sudbury Road, Suite 1A North, Acton, MA, 01720, USA.
Anti-histidine (HRP-labelled) mAb	-	Sigma Aldrich, 3050 Spruce Street, St. Louis, MO 63103, USA.
Anti-rabbit (HRP-labelled) pAb	-	Sigma Aldrich
Anti-mouse (HRP-labelled) pAb	-	Sigma Aldrich
Anti-FLAG tag M1 mAb	-	Sigma Aldrich
Anti-FLAG tag M2 mAb	-	Sigma Aldrich

2.8 Generation and characterisation of rabbit anti-CRP polyclonal antibodies

2.8.1 Immunisation of New Zealand White rabbits and antibody titre determination.

CRP immunisations were administered by 1 mL sub-cutaneous injections with antigen-grade CRP (HyTest). On day 1, the rabbits were immunised with 200 µg of antigen grade CRP in PBS, mixed in a 1:1 ratio with Freund's complete adjuvant (FCA). Freund's complete adjuvant is an emulsified mineral oil antigen solution used as an immunopotentiator. The first boost (day 14) was then administered using 100 µg of CRP in PBS, mixed in a 1:1 ratio with Freund's incomplete adjuvant (FICA). The final 3 boosts that followed (days 35, 49 and 70) all contained 50 µg of CRP and were administered in the same manner as the first boost. Finally, on day 75, the rabbits were sacrificed and both their spleens and bone marrow removed.

2.8.2 Protein A purification of anti-CRP polyclonal antibody from rabbit serum.

A 1 mL suspension of immobilised protein A (immobilised on Sepharose 4B, stored in sterile-filtered PBS containing 20% (v/v) ethanol) was equilibrated in a column with 30 mL of sterile-filtered PBS. Two vials of serum from the sacrificed rabbit were pooled and made up to a final volume of 10 mL with sterile-filtered 1 x PBS (pH 7.4). The 10 mL mixture of diluted pAb-rich serum was then passed through the column and the eluant collected and passed through the column a second time. A total of 30 mL of wash buffer (sterile-filtered PBS) was passed through the column and, subsequently, the retained protein was eluted with 0.1 M glycine-HCl buffer (pH 2.5). Fractions of eluate were collected in micro-centrifuge tubes containing 150 µL of neutralisation buffer (2 M Tris-HCl, pH 8.5). This served to rapidly neutralise the highly acidic environment of the elution buffer, thereby, preventing denaturation of the eluted IgG fraction. The protein in each of the fractions was quantified using the NanoDrop™ ND-1000 using the pre-programmed 'IgG' option (mass extinction coefficient of 13.7 at 280 nm). The fractions containing high concentrations of IgG were pooled, desalted on a PD10™ size exclusion column against PBS and stored at -20°C until required for further use. All purification and desalting procedures were conducted at 4°C.

2.8.3 SDS-PAGE of anti-CRP pAb protein G purification.

Proteins were separated using 10% (w/v) SDS-PAGE gels (20 µg/lane) to analyse purity and to determine the apparent molecular weight. The gel consisted of a resolving gel and a stacking gel. The resolving gel contained H₂O, 30% (w/v) acrylamide (Ultrapure Acrylagel, National Diagnostics), 2% (w/v) methylamine bisacrylamide (Bis-Acrylagel), 1.5 M Tris pH 8.8, 10% (w/v) SDS, 10% (w/v) ammonium persulfate (APS) and TEMED. The stacking gel contained H₂O, 30% (w/v) acrylamide, 2% (w/v) methylamine bisacrylamide (Bis-acrylagel), 1M Tris pH 6.8, 10% (w/v) SDS, 10% (w/v) ammonium persulfate and TEMED. These gels are left to polymerise between two clean glass plates. After the stacking gel was poured, a comb is inserted to make wells in preparation for loading of the protein samples. The samples were prepared by adding appropriate volumes of 4x gel loading buffer and deionised water. The gel loading buffer was prepared using Tris 0.5 M (pH 6.8), 20% (w/v) SDS, 15% (v/v) glycerol, bromophenol blue, 2-β-mercaptoethanol and deionised water. A 20 µg quantity of each protein sample was added into each well in a total volume of 20 µL. The gels were placed in an electrophoresis apparatus and submerged in electrophoresis buffer. The electrophoresis buffer was prepared using 50 mM Tris pH 8.3, 196 mM glycine and 0.1% (w/v) SDS. The apparatus is attached to a power supply and a voltage of 200 V is applied to the gel. The gels were allowed to run until the tracker dye had reached the bottom of the gel, taking approximately 30 - 45 minutes. The gels were taken out and stained using Coomassie stain (0.2% (w/v) Coomassie blue R-25, 45% (v/v) methanol, 45% water, 10% (v/v) acetic acid) for 3-4 h. Finally, the stained gels were destained overnight using Coomassie destain (10% (v/v) acetic acid, 25% (v/v) methanol, 65% (v/v) water). The destain solution was changed 2-3 times (until the background non-specific staining was removed).

2.8.4 Checkerboard ELISA of purified anti-CRP polyclonal antibody.

A 96 well plate (Maxisorp™, Nunc) was coated with varying concentrations of CRP antigen in 1 x PBS (pH 7.4) and left O/N at 4°C. The following day, the antigen-coated plate was then blocked with a 3% (w/v) BSA -PBS solution (200 µL per well) for 1 h at 37°C. A vial of purified rabbit anti-CRP polyclonal antibody (pAb) (section 2.8.2) was removed from -20°C and thawed. Serial dilutions of the purified pAb were made in 1% (w/v) BSA in PBST, added (100 µL per well) to the corresponding coated/blocked well and incubated at 37°C for 1 h.

Following incubation, the plates were washed using PBST (x3) and PBS (x3) to remove any unbound pAb. The CRP-pAb complex was detected using 100 μ L per well of a 1/2000 dilution of an anti-rabbit (HRP-labelled) secondary pAb produced in a goat (Sigma #A6154). After a 1 h incubation at 37°C with the secondary mAb, the plate was washed again with PBST (x3) and PBS (x3) to remove any unbound detection antibody. TMB substrate was then added (100 μ L per well) and left to react for 20 min at 37°C. The reaction was quenched by the addition of 100 μ L per well of 10% (v/v) HCl, after which the absorbance was determined at 450 nm on a Safire 2 plate reader (Tecan).

2.8.5 Fluorescent labelling of purified rabbit anti-CRP pAb with commercial DyLight 647™ kit.

Purified rabbit pAb (section 2.8.2) was diluted in sterile-filtered PBS to a concentration of 1 mg/mL in a final volume of 100 μ L. A 10 μ L volume of borate buffer (0.67 M) was added to the diluted pAb. The lyophilised DyLight™ reagent was reconstituted with 20 μ L of dimethylformamide (DMF) and then 5 μ L added to the pAb in borate buffer. The mixture was inverted several times to ensure thorough mixing and then incubated for 45 min at room temperature (tube was wrapped in tin foil to protect from light). The caps of two Zeba™ columns (AGB) were loosened and the bottom plugs twisted off. Each column was placed into a 1.5 mL tube and centrifuged for 1 min at 1,750 x g to remove the storage solution. Following this centrifugation step, the columns were blotted against filter paper to remove any residual ethanol and then placed into clean 1.5 mL tubes. The caps were removed from the columns and 55 μ L of the incubated reaction was directly applied to the centre of the compacted resin bed of each column. The labelled pAb was collected into the 1.5 mL tubes by centrifugation for 2 min at 1,750 x g and then stored at -20°C in 10 μ L aliquots.

2.8.6 Fluorescent sandwich ELISA of purified rabbit pAb labelled with DyLight 647™.

Part 1 - Determination of the optimal rabbit anti-CRP pAb coating concentration:

A black 96 well fluorescence plate (Greiner®) was coated with 6 different concentrations (10, 7.5, 5.0, 2.5, 1.0, 0.5 μ g/mL) of purified anti-CRP pAb (section 2.8.2) incubated O/N at 4°C (The primary difference between white and black plates is their reflective properties. White plates reflect light and will maximize light output signal, whereas black plates absorb light and reduce background). The following day, the coated plate was then blocked with a

3% (w/v) BSA-PBS solution (200 μ L per well) for 1 h at 37°C. Next, CRP antigen was diluted in 1% (w/v) BSA-PBST to a final concentration of 1 μ g/mL and 100 μ L was added to each well of the coated/blocked well and incubated at 37°C for 1 h. The plate was then washed using PBST (x3) and PBS (x3) to remove any unbound CRP antigen. A vial of the DyLight 647 TM - labelled rabbit anti-CRP pAb (section 2.8.5) was removed from -20°C and thawed. Serial doubling dilutions from 1/250 to 1/128000 of the fluorescently labelled pAb were made in 1% (w/v) BSA-PBST and then added to wells of a 96 well plate for a 1 h incubation at 37°C. Following incubation, the plates were washed using PBST (x3) and PBS (x3) to remove any unbound labelled pAb. The absorbance was then read on a Safire 2 plate reader (Tecan) using the conditions below:

<u>Measurement mode:</u>	<u>Fluorescence</u>
Excitation wavelength:	652 nm
Emission wavelength:	673 nm
Excitation bandwidth:	9 nm
Emission bandwidth:	9 nm
Gain (Manual):	140
Number of reads:	10
FlashMode:	High sensitivity
Integration time:	40 μ s
Lag time:	0 μ s
Plate definition file:	GRE96fb.pdf
Z-Position (Calc. from Well B2):	4800 μ m
Shake duration (Orbital Medium):	5 s
Target Temperature:	37°C
Current Temperature:	27°C

Part 2 – Titration of CRP antigen:

A black 96 well plate (Greiner®) was coated with a set optimal concentration (determined in Part 1 of assay) of purified anti-CRP pAb and left O/N at 4°C. The following day, the coated plate was then blocked with a 3% (w/v) BSA-PBS solution (200 μ L per well) for 1 h at 37°C. Next, serial doubling dilutions from 1000 ng/mL to 3.9 ng/mL of CRP antigen were made in 1% (w/v) BSA-PBST and each concentration added to designated wells (100 μ L per well) of the coated/blocked plate for a 1 h incubation at 37°C. The plate was then washed using PBST

(x3) and PBS (x3) to remove any unbound CRP antigen. A vial of DyLight 647TM-labelled rabbit anti-CRP pAb (section 2.8.5) was removed from -20°C and thawed. The fluorescently labelled pAb was diluted in 1% (w/v) BSA-PBST to an optimised dilution of 1/500 and then added wells of a 96 well plate for a 1 h incubation at 37°C. Following incubation, the plates were washed using PBST (x3) and PBS (x3) to remove any unbound labelled pAb. The absorbance was then read on a Safire 2 plate reader (Tecan) using the same conditions described in part 1.

2.8.7 Preconcentration study of rabbit anti-CRP polyclonal antibody onto a CM5 sensorchip.

Purified rabbit anti-CRP polyclonal antibody (pAb) was diluted in sterile-filtered 10 mM sodium acetate buffers that had been adjusted with 10% (v/v) acetic acid to pH values 3.8, 4.0, 4.2, 4.4, 4.6, 4.8, 5.0 and 5.2. The pAb was diluted at each respective pH to a final concentration of 25 µg/mL and sequentially passed over an un-activated carboxymethylated dextran sensor chip surface at a flow rate of 10 µL/min. The pH showing the greatest degree of pre-concentration, reflected by the highest response unit (RU) value and the sharpest slope, was chosen as the carrier buffer for immobilisation. The optimal conditions for EDC/NHS chemistry to take place, is at a pH of approximately 5.0.

2.8.8 Immobilisation of rabbit anti-CRP polyclonal antibody onto CM5 sensorchip.

The carboxymethylated dextran matrix on the sensor chip was activated by mixing equal volumes of 100 mM NHS (N-hydroxysuccinimide) and 400 mM EDC (N-ethyl-N-(dimethylaminopropyl) carbodiimide hydrochloride) and injecting the mixture over the sensor chip surface for 10 min at a flowrate of 5 µL/min. The purified rabbit anti-CRP pAb was diluted in 10 mM sodium acetate, pH 4.0, to a concentration of 25 µg/mL. This solution was then injected over the activated chip surface for 20 min at a flowrate of 5 µL/min. A 1 M ethanolamine hydrochloride solution (pH 8.5) was injected for 8 min, resulting in both capping of any unreacted active groups and removal of loose non-covalently attached proteins. Finally, loosely bound material was further removed using two 30 s pulses of 5 mM NaOH.

2.9 Generation and characterisation of mouse anti-CRP scFv library

2.9.1 Immunisation of BALB/c mice and antibody titre determination.

All procedures involving animals were approved and licensed by the Department of Health and Children under license number B100/3816. Every precaution was taken to ensure the minimum distress to the animals.

BALB/c mice aged 5-8 weeks were initially immunised with a final concentration of 50 µg/mL CRP, mixed in a 1:1 ratio with Freund's complete adjuvant. The mixture was vigorously shaken to ensure formation of a completely homogenous solution. A volume of 200 µL was injected into the peritoneal cavity of the BALB/c mice for immunisation. Subsequent injections (200 µL) were performed with 25 µg/ml CRP mixed in a 1:1 ratio with Freund's incomplete adjuvant. A tail bleed was taken from the mice 7 days after injection and the antibody titre against CRP determined. Once a high titre response to the CRP antigen was reached, the mice were given a final boost into the peritoneal cavity and then sacrificed 7 days later.

2.9.2 Extraction and isolation of total RNA from immunised mice.

To ensure an uncontaminated environment (free from contaminant RNA) a Gelaire BSB 4 laminar unit was sprayed with both IMS and RNase™ ZAP. The mice were sacrificed by cervical dislocation and their spleens removed using sterile surgical tools. All excess fat was trimmed from the spleen before being transferred into a 50 mL 'RNase-free' tube containing 10 mL of TRI™ reagent (MRC Ltd.). A homogenizer, previously autoclaved at 120°C for 15 min and baked overnight (O/N) at 180°C, was used to homogenize the spleen. The homogenized spleen was incubated for 5 min at room temperature to allow for the total dissociation of nucleoprotein complexes while maintaining the integrity of the RNA. The homogenized spleen was then centrifuged at 2,465 x g (Eppendorf centrifuge 5810R) for 10 min at 4°C to pellet any excess cell debris and the supernatant transferred into a 50 mL polypropylene Oakridge tube. Chloroform (2 mL) was then added to the tube containing the supernatant and then thoroughly mixed and incubated for 15 min at room temperature. Chloroform leads to the separation of the homogenized spleen into an upper aqueous phase (containing RNA) and a lower organic phase (containing DNA and protein). The resultant

mixture was then centrifuged at 17,500 x g (Eppendorf centrifuge 5810R) for 15 min at 4°C. The centrifugation produced 3 layers, consisting of a lower red phenol/chloroform phase, a protein interphase and a colourless liquid upper phase with the RNA. The upper aqueous phase was carefully transferred (ensuring no lower layer contamination) into an 85 mL polycarbonate Oakridge tube and subjected to RNA precipitation by addition of 5 mL of isopropanol. The RNA was allowed precipitate for 10 min at room temperature and then centrifuged at 17,500 x g (Eppendorf centrifuge 5810R) for 25 min at 4°C, resulting in a white RNA pellet. The isopropanol supernatant was carefully decanted and the pellet washed with 2 mL of 75% (v/v) ethanol by centrifugation at 17,500 x g for 10 min at 4°C. Finally, the pellet was allowed to air dry in the laminar hood and then resuspended in 250 µL of molecular grade water.

2.9.3 Reverse transcription of total RNA to cDNA.

<u>Mixture 1 Component</u>	<u>10 µL Volume</u>	<u>Conc. in 10 µL reaction</u>
Total RNA	1.85 µL	5 µg/rxn
Oligo (dT) primer	1 µL	0.5 µg/rxn
dNTP mix	1 µL	1 mM
Molecular grade H ₂ O	6.15 µL	N/A

<u>Mixture 2 Component</u>	<u>10 µL Volume</u>	<u>Conc. in 10 µL reaction</u>
10 X RT Buffer	2 µL	2 X
MgCl ₂	4 µL	2.5 mM
DTT	2 µL	20 mM
RNase Out	1 µL	1 U/µL
Superscript III enzyme	1 µL	200 U/µL

A 20 X reaction for mixture 1 was set up on ice and then split up into 8 x 25 µL aliquots in sterile PCR tubes. The 8 PCR tubes were incubated at 65°C for 5 min and then placed on ice, while a 20 X reaction for mixture 2 was set up. Next, 25 µL of the incubated mixture 2 was added to all 8 of the 25 µL aliquots of mixture 1 and left to incubate at 50°C for 50 min, followed by 85°C for 5 min. Finally, 5 µL of RNase[™] H was added to each of the 8 x 50 µL reactions and incubated at 37°C for 20 min.

2.9.4 PCR primers for amplification of mouse scFv (pAK series)

The primers listed below were obtained from Eurofins-MWG-Operon (318 Worple Road, Raynes Park, London, SW20 8QU) and are compatible with the primers set described by Krebber and co-workers (Krebber *et al.*, 1997) for the pAK vector system. The sequences are given using the IUPAC nomenclature of mixed bases shown in underlined capital letters, R = A or G; Y = C or T; M = A or C; K = G or T; S = C or G; W = A or T; H = A or C or T; B = C or G or T; V = A or C or G; D = A or G or T.

Variable light chain back primers

- LB1 5'gcatggcggactacaaaGAYATCCAGCTGACTCAGCC3'
LB2 5'gcatggcggactacaaaGAYATTGTTCTCWCCCAGTC3'
LB3 5'gcatggcggactacaaaGAYATTGTGMTMACTCAGTC3'
LB4 5'gcatggcggactacaaaGAYATTGTGYTRACACAGTC3'
LB5 5'gcatggcggactacaaaGAYATTGTRATGACMCAGTC3'
LB6 5'gcatggcggactacaaaGAYATTMAGATRAMCCAGTC3'
LB7 5'gcatggcggactacaaaGAYATTCAGATGAYDCAGTC3'
LB8 5'gcatggcggactacaaaGAYATYCAGATGACACAGAC3'
LB9 5'gcatggcggactacaaaGAYATTGTTCTCAWCCAGTC3'
LB10 5'gcatggcggactacaaaGAYATTGWGCTSACCCAATC3'
LB11 5'gcatggcggactacaaaGAYATTSTRATGACCCRTC3'
LB12 5'gcatggcggactacaaaGAYRTTKTGATGACCCRAC3'
LB13 5'gcatggcggactacaaaGAYATTGTGATGACBCAGKC3'
LB14 5'gcatggcggactacaaaGAYATTGTGATAACYCAGGA3'
LB15 5'gcatggcggactacaaaGAYATTGTGATGACCCAGWT3'
LB16 5'gcatggcggactacaaaGAYATTGTGATGACACAACC3'
LB17 5'gcatggcggactacaaaGAYATTTTGCTGACTCAGTC3'
LB λ 5'gcatggcggactacaaaGATGCTGTTGTGACTCAGGAATC3'

Variable light chain forward primers

- LF1 5'ggagccgccgcc(agaaccaccacc)₂ACGTTTGATTTCCAGCTTGG3'

LF2 5'ggagccgccgcc(agaaccaccacc)₂ACGTTTTATTTCCAGCTTGG3'
 LF4 5'ggagccgccgcc(agaaccaccacc)₂ACGTTTTATTTCCAACCTTG3'
 LF5 5'ggagccgccgcc(agaaccaccacc)₂ACGTTTCAGCTCCAGCTTGG3'
 LFλ 5'ggagccgccgcc(agaaccaccacc)₂ACCTAGGACAGTCAGTTTGG3'

Variable heavy chain back primers

HB1 5'ggcggcggcggtccggtggtggtgatccGAKGTRMAGCTTCAGGAGTTC3'
 HB2 5'ggcggcggcggtccggtggtggtgatccGAGGTBCAGCTBCAGCAGTC3'
 HB3 5'ggcggcggcggtccggtggtggtgatccCAGGTGCAGCTGAAGSASTC3'
 HB4 5'ggcggcggcggtccggtggtggtgatccGAGGTCCARCTGCAACARTC3'
 HB5 5'ggcggcggcggtccggtggtggtgatccCAGGTYCAGCTBCAGCARTC3'
 HB6 5'ggcggcggcggtccggtggtggtgatccCAGGTYCARCTGCAGCAGTC3'
 HB7 5'ggcggcggcggtccggtggtggtgatccCAGGTCCACGTGAAGCAGTC3'
 HB8 5'ggcggcggcggtccggtggtggtgatccGAGGTGAASSTGGTGAATC3'
 HB9 5'ggcggcggcggtccggtggtggtgatccGAVGTGAWGYTGGTGGAGTC3'
 HB10 5'ggcggcggcggtccggtggtggtgatccGAGGTGCAGSKGGTGGAGTC3'
 HB11 5'ggcggcggcggtccggtggtggtgatccGAKGTGCAMCTGGTGGAGTC3'
 HB12 5'ggcggcggcggtccggtggtggtgatccGAGGTGAAGCTGATGGARTC3'
 HB13 5'ggcggcggcggtccggtggtggtgatccGAGGTGCARCTTGTTGAGTC3'
 HB14 5'ggcggcggcggtccggtggtggtgatccGARGTRAAGCTTCTCGAGTC3'
 HB15 5'ggcggcggcggtccggtggtggtgatccGAAGTGAARSTTGAGGAGTC3'
 HB16 5'ggcggcggcggtccggtggtggtgatccCAGGTTACTCTRAAAGWGTSTG3'
 HB17 5'ggcggcggcggtccggtggtggtgatccCAGGTCCAACVTCAGCARCC3'
 HB18 5'ggcggcggcggtccggtggtggtgatccGATGTGAACTTGAAGTGTC3'
 HB19 5'ggcggcggcggtccggtggtggtgatccGAGGTGAAGGTCATCGAGTC3'

Variable heavy chain forward primers

HF1 5'ggaattcggccccgagggcCGAGGAAACGGTGACCGTGGT3'
 HF2 5'ggaattcggccccgagggcCGAGGAGACTGTGAGAGTGGT3'
 HF3 5'ggaattcggccccgagggcCGCAGAGACAGTGACCAGAGT3'
 HF4 5'ggaattcggccccgagggcCGAGGAGACGGTGACTGAGGT3'

2.9.5 Amplification of antibody variable domain genes using pAK series primers.

The components for a 1 X reaction were as follows:

<u>Component</u>	<u>20 μL Volume</u>	<u>Conc. in 20 μL reaction</u>
5 X Buffers (A,B,D,G)	4.0 μ L	1 X
V _L /V _H Forward Primer	0.4 μ L	40 pM
V _H /V _L Back Primer	0.4 μ L	40 pM
cDNA	0.4 μ L	0.5 μ g
dNTP	0.4 μ L	0.2 mM
H ₂ O	13.6 μ L	N/A
REDTaq® Polymerase	0.8 μ L	1 U/ μ L

PCR buffer compositions: buffer A (7.5 mM MgCl₂, pH 8.5); buffer B (10 mM MgCl₂, pH 8.5); buffer D (17.5 mM MgCl₂, pH 8.5); buffer G (12.5 mM MgCl₂, pH 9.0).

The PCR for the amplification of the mouse antibody variable domain genes was performed in the Biometra T_{GRADIENT} PCR machine under the following conditions:

<u>Stage</u>	<u>Temperature (°C)</u>	<u>Time (s)</u>
1 (1 cycle)	94	300
2 (7 cycles)	94	60
	68	30
	72	60
3 (24 cycles)	94	60
	68	30
	72	60
4 (1 cycle)	72	600
	4	pause

2.9.6 Purification of V_H and V_L variable gene fragments using the Promega clean up Kit.

The V_H and V_L amplifications were resolved on a 1% (w/v) agarose gel until single bands for both the variable heavy and variable light chains were observed. Both bands were then excised separately using sterile scalpels and transferred into separate clean 1.5 mL micro-centrifuge tubes. Next, 3 volumes of binding buffer was added to every 1 volume of gel slice and then incubated at 50°C until the gel had completely dissolved (approximately 10 min). The guanidine isothiocyanate component of the binding buffer allows for sufficient binding of the DNA to the silica membrane columns. One volume of isopropanol, equal to the original weight of the gel slice, was then added and mixed to allow for precipitation of the DNA. The mixture was then transferred to a clean collection tube and centrifuged at 20,817 x g (Eppendorf centrifuge 5810R) for 1 min to remove any residual buffer. The flow-through was discarded and the column was washed by centrifugation with 750 μ L wash buffer and again with 250 μ L wash buffer. The column was centrifuged at 20,817 x g (Eppendorf centrifuge 5810R) for 2 min to ensure all residual ethanol was removed and the DNA was eluted from the column using 30 μ L molecular grade H₂O. The purified DNA was quantified using the Nanodrop™ ND-1000.

2.9.7 Splice by Overlap extension (SOE) PCR.

The V_H and V_L purified fragments were joined using an SOE-PCR via a glycine-serine linker (G₄S)₄, producing a fragment of approximately 800 bp. The following primers were utilised:

Single chain forward (scFor)	5'ggaattcggcccccag3'
Single chain back (scback)	5'ttactcgcggccagccggccatggcggactacccc3'

<u>Component</u>	<u>50 μL Volume</u>	<u>Conc. in 50 μL reaction</u>
5 X Buffer D	10 μ L	1 X
Sc Forward Primer	1 μ L	50 pM
Sc Back Primer	1 μ L	50 pM
V _H chain	1 μ L	25 ng/rxn
V _L chain	1 μ L	25 ng/rxn
dNTP	1 μ L	0.2 mM
H ₂ O	33 μ L	N/A
REDTaq® Polymerase	2 μ L	0.05 U/ μ L

The SOE-PCR was performed in the Biometra T_{GRADIENT} PCR machine under the following conditions:

<u>Stage</u>	<u>Temperature (°C)</u>	<u>Time (s)</u>
1 (30 cycle)	94	60
	69	30*
	72	60
2 (1 cycle)	72	600
	4	pause

* A gradient was incorporated into the annealing step whereby a 0.5°C decrease was introduced in each successive cycle.

2.9.8 SfiI restriction digest of purified SOE-PCR fragment and ligation into pAK 100 vector.

The scFv fragment and pAK 100 vector (Krebber *et al.*, 1997) for phage selection were cut using *SfiI* restriction enzyme. The *SfiI* enzyme allows for the unidirectional cloning of scFv fragment into the pAK 100 phage display vector. The enzyme recognises 8 bases which are interrupted by 5 non-recognised nucleotides (5'ggccnnnnnggcc3'), thus virtually eliminating internal digestion in antibody sequences. Both digestions (outlined below) were carried out for 5 h at 50°C.

SOE-PCR product SfiI digest

<u>Component</u>	<u>50 μL Volume</u>
SOE product	2.28 μ L
10 X Buffer 2	5 μ L
10 X BSA	5 μ L
H ₂ O	31.72 μ L
<i>Sfi</i> I	6 μ L

pAK 100 vector SfiI digest

<u>Component</u>	<u>150 μL Volume</u>
pAK 100 vector	100 μ L
10 X Buffer 2	15 μ L
10 X BSA	15 μ L
H ₂ O	8 μ L
<i>Sfi</i> I	12 μ L

Both digests were resolved via electrophoresis on a 1% (w/v) agarose gel and then gel purified, as described in section 2.9.6. The restricted scFv gene was then ligated into the pAK 100 vector in a 3:1 (insert:vector) ratio under the conditions below and left at 15°C O/N.

<u>Component</u>	<u>60 μL Volume</u>	<u>Conc. in 60 μL reaction</u>
5 X Ligase buffer	12 μ L	1 X
Digested pAK 100 vector	26.67 μ L	1.2 μ g/rxn
Digested scFv gene	8.74 μ L	0.7 μ g/rxn
H ₂ O	0.59 μ L	N/A
T ₄ DNA Ligase	12 μ L	400 U/ μ L

The ligation was then subjected to an ethanol precipitation under the following conditions:

<u>Component</u>	<u>Volume</u>
Ligation mixture	120 μ L
3M NaAc, pH 5.2	12 μ L
Novagen pellet paint	2 μ L
100% (v/v) ethanol	264 μ L

The precipitation was left O/N at -20°C and then the DNA was harvested by centrifuging at 20,817 x g (Eppendorf centrifuge 5810R) for 20 min at 4°C. The ethanol supernatant was decanted and the pellet was washed by addition of 120 μ L 70% (v/v) ethanol and centrifuging at 20,817 x g (Eppendorf centrifuge 5810R) for 10 min at 4°C. The pellet was allowed to air-dry briefly and then gently dissolved in 5 μ L of molecular grade H₂O.

2.9.9 Electro-transformation of scFv-containing plasmid into XL-1 Blue E. coli cells.

Transformation of the ligated product was performed by electroporation into a commercially available strain of XL-1 Blue *E. coli* cells (Stratagene). The apparatus used was a Gene Pulser Xcell™ electroporation system with the parameters set to 25 μ F, 1.25 kV and gene pulse controller at 200 Ω . After thawing on ice, 50 μ L of the *E. coli* cells were added to the 5 μ L of ligation product, mixed by one gentle pipette action up and down and then left on ice for a 30 s incubation. The mixture was then transferred to a chilled 0.2 cm electroporation cuvette, ensuring all the mixture settled on the bottom and then placed securely in the 'Shockpod'. A pulse was then passed through the cuvette, which was then immediately flushed with 1 mL of pre-warmed SOC medium using a sterile tip. The time lapse between applying the pulse and transferring the cells to the growth media was kept to an absolute minimum for optimal recovery of *E. coli* transformants. A transfer delay of even 1 min has been reported to cause as much as a 3-fold drop in transformation efficiency. The 1 mL of rescued ligation was then transferred into a sterile 20 mL universal tube containing a further 2 mL of pre-warmed SOC medium. The 3 mL of transformant suspension was then incubated for 1 h at 250 rpm at 37°C and then plated out on 2 x TY agar plates supplemented with 25 μ g/mL chloramphenicol and 1% (w/v) glucose. A negative control was also incorporated into the experiment by plating the XL-1 Blue cells containing no plasmid onto an identical chloramphenicol/glucose agar plates. All agar plates were incubated O/N at 37°C and then scraped into 2 x TY medium containing 20% (v/v) glycerol for long term storage at -80°C.

2.9.10 Rescue and subsequent precipitation of scFv-displaying phage.

A conical flask containing 200 mL sterile 2 x TY medium (2% (w/v) glucose and 25 μ g/mL chloramphenicol) was inoculated with 200 μ L of the transformed library glycerol stocks and incubated at 200 rpm and 37°C until mid-exponential phase of growth (OD~ 0.400 @ 600 nm) was achieved. The culture was then pelleted by centrifugation at 3,200 x g at room temperature for 15 min and then resuspended in 200 mL of fresh 2 x TY media containing 25 μ g/mL chloramphenicol and 2 x 10¹¹ pfu/mL helper phage. For subsequent F pilus conjugation to occur (an essential part of infection process) the culture was left static at 37°C for 30 min and then transferred into a 37°C shaking incubator (for 2 h at 250 rpm. Next, kanamycin was added to a final concentration of 50 μ g/mL, before leaving the culture O/N at 30°C and 250 rpm. The O/N culture was then centrifuged at 3,220 x g (Eppendorf centrifuge

5810R) for 15 min at 4°C and the phage supernatant transferred into a sterile 250 mL Sorval™ centrifuge tube containing 8 g of PEG 8000 and 6 g of sodium chloride. The Sorval™ was agitated at 250 rpm until both additives were dissolved and the phage then left precipitate for 1 h at 4°C. The phage was harvested by centrifugation at 6,440 x g for 25 min at 4°C and then resuspended in 2 mL of 2% (w/v) BSA-PBS buffer solution. The resuspended phage pellet was then added to a clean 1.5 mL micro-centrifuge tube and centrifuged at 20,817 x g for 5 min at 4°C to remove any bacterial debris. Lastly, the phage supernatant was transferred to a fresh micro-centrifuge tube and stored on ice at 4°C.

2.9.11 Enrichment of a murine phage library via biopanning against immobilised antigens.

An Immunotube (Maxisorp™, Nunc), previously coated O/N at 4°C with 500 µL of 50 µg/mL CRP in PBS solution, was blocked for 2 h at room temperature with 3% (w/v) BSA in PBS. Following one wash with both PBST and PBS, 500 µL of rescued phage was then added to the immunotube and incubated on a roller mixer ‘SRT1’ for 2 h at room temperature. The immunotube was then washed with PBST (x 3) and PBS (x 3) to remove non-specific phage. Specific phage were then eluted by incubation with 500 µL of 100 mM glycine-HCl, pH 2.2, for 10 min, followed by immediate neutralisation with 30 µL of 2 M Tris-HCl, pH 8.0. Half of the eluted phage (265 µL) was added to mid-exponential phase XL-1 Blue cells, allowed to infect for 30 min static at 37°C and then incubated at 37°C for 1 h at 200 rpm. The culture was then harvested by centrifuging at 3,220 x g (Eppendorf centrifuge 5810R) for 15 min at room temperature after which the pellet was resuspended in 600 µL fresh 2 x TY media. An input titre was performed by making serial dilutions (10^{-1} - 10^{-12}) of the PEG-precipitated phage in exponential growth phase XL-1 Blue cells. Following a 15 min infection at 37°C, the 10^8 - 10^{12} serial dilutions were plated on 2 x TY agar plates containing 25 µg/mL chloramphenicol and incubated O/N at 37°C. All of the subsequent rounds of panning were performed as described above, with the following amendments shown in Table 3.2.11. Also, in the 4th round of panning an antigen challenge was incorporated into the protocol, which meant two separate phage outputs were produced. The antigen challenge involved incubating 5 µg of CRP on the washed immunotube for 10 min to remove any weakly binding phage-scFv fragments, which were infected as usual into mid-exponential phase XL-1 Blue cells. The remaining phage-scFv binding to the immunotube were then eluted as before, with glycine-HCl, and also infected into mid-exponential phase *E. coli* cells.

Table 2.9.11 Parameters varied in panning of murine anti-CRP scFv library

	PAN 1	PAN 2	PAN 3	PAN 4
Culture vol. (mL)	200	200	100	100
CRP-coated	25 µg	25 µg	5 µg	1 µg
Washes	3 x PBST	5 x PBST	10 x PBST	13 x PBST
	3 x PBS	5 x PBS	10 x PBS	13 x PBS
Antigen challenge	No	No	No	Yes

2.9.12 Polyclonal phage ELISA and scFv check via 'colony-pick' PCR.

A 96 well plate ELISA plate (Maxisorp™, Nunc) coated with 100 µL per well of 2 µg/mL CRP was incubated O/N at 4°C. The CRP solution was decanted and the plate was blocked with 3% (w/v) BSA in PBS for 1 h at 37°C. The phage outputs in XL-1 Blue cells from each round were then grown in 10 mL 2 x TY media. When mid-exponential phase of growth was achieved, the cells were rescued with helper phage and shaken O/N at 30°C following the addition of 50 µg/mL kanamycin. The culture was then centrifuged at 3,220 x g (Eppendorf centrifuge 5810R) for 10 min at room temperature and the phage supernatant diluted 10 fold in 1% (w/v) BSA in PBST. A 100 µL volume of each of the diluted phage supernatants were added in duplicate to the ELISA plate and incubated for 1 h at 37°C. Following the incubation of the phage, the plate was washed 3 times with both PBST and PBS. Next, 100 µL of 1/5000 dilution of a HRP-conjugated anti-M13 antibody (GE Healthcare Life Sciences) in 1% (w/v) BSA-PBST was added to each well and incubated for 1 h at 37°C. The specific complex was then detected by the addition of 100 µL of TMB substrate and allowed to develop for 20 min at 37°C. Finally, the reaction was quenched using 100 µL of 1 M HCl and the absorbance values read at 450 nm on a Safire 2 plate reader (Tecan).

Twenty single colonies were randomly picked from the 4th round of panning and incorporated into a 'colony-pick' PCR to ensure the vector was harbouring the scFv fragment. A sterile tip was used to pick a single colony into the following mixture, which was

then placed in a Biometra T_{GRADIENT} PCR machine. The amplified scFv fragments were then analysed via gel electrophoresis on a 1% (w/v) agarose gel.

<u>Component</u>	<u>50 μL Volume</u>	<u>Conc. in 50 μL reaction</u>
5 X Buffer D	10 μ L	1 X
Sc Forward Primer	1 μ L	50 pM
Sc Back Primer	1 μ L	50 pM
dNTP	1 μ L	0.2 mM
H ₂ O	35 μ L	N/A
REDTaq® Polymerase	2 μ L	0.05 U/ μ L

The SOE-PCR was performed in the Biometra T_{GRADIENT} PCR machine under the following conditions:

<u>Stage</u>	<u>Temperature ($^{\circ}$C)</u>	<u>Time (s)</u>
1 (30 cycle)	94	60
	69	30*
	72	60
2 (1 cycle)	72	600
	4	pause

* A gradient was incorporated into the annealing step whereby a 0.5 $^{\circ}$ C decrease was introduced during each successive cycle i.e. annealing temperature of 54 $^{\circ}$ C for final cycle.

2.9.13 Subcloning of pan 4 output scFv fragments into pAK 400 vector for soluble expression.

A culture of both the pan 4 output (XL1-Blue cells) and the pAK 400 vector (Krebber *et al.*, 1997) (XL1-Blue cells) were incubated O/N at 37 $^{\circ}$ C and 250 rpm. Both cultures were then subjected to a plasmid purification using the Promega SV Miniprep™ kit. The cells harbouring the plasmids were harvested by centrifugation at 3,220 x g (Eppendorf centrifuge 5810R) for 15 min. The media supernatant was then decanted and the cell pellets resuspended in 250 μ L cell resuspension solution. The resuspended pellets were then transferred to a 1.5 mL sterile micro-centrifuge tube and 250 μ L cell lysis solution was added, the tube inverted 4

times and incubated at room temperature for 5 min. A 10 μL aliquot of alkaline protease was then added to the lysed cells, mixed by inversion and then incubated for 5 min at room temperature. The addition of alkaline protease results in the inhibition of proteases released during the lysis step. The mixture was then neutralised using 350 μL of a solution containing guanidine hydrochloride, potassium acetate and glacial acetic acid and again mixed by inverting the tube several times. This neutralisation solution causes the genomic DNA and proteins present in the solution to precipitate. The lysed cells were then pelleted by centrifugation at 20,817 x g (Eppendorf centrifuge 5810R) for 10 min and the supernatant containing the plasmid DNA transferred to a spin column supplied with the kit. The spin column was placed in a clean collection tube and centrifuged at 20,817 x g (Eppendorf centrifuge 5810R) at room temperature for 1 min causing the plasmid DNA to bind to the spin column membrane. The membrane-bound DNA was then washed via a 1 min centrifugation with 750 μL of wash solution at 20,817 x g (Eppendorf centrifuge 5810R), followed by a 2 min spin with 250 μL of wash solution at 20,817 x g (Eppendorf centrifuge 5810R). The washed spin column was then transferred to a new sterile 1.5 mL micro-centrifuge tube and the plasmid DNA eluted with 100 μL of molecular grade H_2O .

The scFv fragments were then PCR-amplified from the pan 4 plasmid DNA using the following components and conditions:

<u>Component</u>	<u>50 μL Volume</u>	<u>Conc. in 50 μL reaction</u>
5 X Buffer D	10 μ L	1 X
Sc Forward Primer	1 μ L	50 pM
Sc Back Primer	1 μ L	50 pM
Plasmid DNA	20 μ L	10 μ g
dNTP	1 μ L	0.2 mM
H ₂ O	15 μ L	N/A
REDTaq® Polymerase	2 μ L	0.05 U/ μ L

The PCR was performed in the Biometra T_{GRADIENT} PCR machine under the following conditions:

<u>Stage</u>	<u>Temperature (°C)</u>	<u>Time (s)</u>
1 (30 cycle)	94	60
	69	30*
	72	60
2 (1 cycle)	72	600
	4	pause

* A gradient was incorporated into the annealing step whereby a 0.5°C decrease was introduced during each successive cycle.

Next the pAK 400 vector and the amplified scFv fragments, respectively, were digested using the restriction enzyme *Sfi*I for 5 h at 50°C using the components outlined below:

<u>Components</u>	<u>250 μL Volume</u>	<u>Components</u>	<u>50 μL Volume</u>
pAK 400 Vector	196 μ L	pan 4 plasmid prep	22.2 μ L
10 X buffer 2	25 μ L	10 X buffer 2	5 μ L
100 X BSA	2.5 μ L	10 X BSA	5 μ L
H ₂ O	10.5 μ L	H ₂ O	12.8 μ L
<i>Sfi</i> I restriction enzyme	16 μ L	<i>Sfi</i> I restriction enzyme	5 μ L

The restricted scFv inserts and pAK 400 vector were then purified using the same procedure, as outlined in section 2.9.6, and ligated in a 3:1 (insert:vector) ratio at 15°C O/N under the following conditions.

<u>Component</u>	<u>130 μL Volume</u>	<u>Conc. in 130 μL reaction</u>
5 X Ligase buffer	26 μ L	1 X
Digested pAK 400 vector	34.7 μ L	1.2 μ g/rxn
Digested scFv gene	57.7 μ L	0.7 μ g/rxn
H ₂ O	5.1 μ L	N/A
T ₄ DNA ligase	6.5 μ L	400 U/ μ L

The ligation was then subject to an ethanol precipitation under the following conditions:

<u>Component</u>	<u>Volume</u>
Ligation mixture	130 μ L
3M NaAc, pH 5.2	15 μ L
Novagen pellet paint	2 μ L
100% (v/v) ethanol	325 μ L

Transformation of the ligated product into Top 10 F' *E. coli* cells was performed, as described in section 2.9.9.

2.9.14 Direct and inhibition ELISA of scFv fragments in pAK 400 expression vector.

Individual colonies (384 in total) were picked and grown O/N at 200 rpm and 37°C in single wells containing 100 μ L 2 x TY media with 25 μ g/mL chloramphenicol (stock plates). The 4 x 96 well stock plates were then subcultured into fresh 2 x TY media (180 μ L) containing 1 x 505 (Studier, 2005) (0.5% (v/v) glycerol, 0.05% (v/v) glucose final concentration), 1mM MgSO₄ and 25 μ g/mL chloramphenicol (subcultured plates). Glycerol was then added to the O/N stock plates to a final concentration of 15% (v/v) and then transferred to a -80°C freezer for long-term storage. Meanwhile, the subcultured plates were incubated at 37°C at 200 rpm until cells appeared turbid i.e. an optical density at 600 nm (OD_{600 nm}) of ~0.6 was achieved. Expression was then induced by adding IPTG to a final concentration of 1mM and incubating at 30°C (180 rpm) O/N. Also, for each plate of clones, a 96 well plate

(Maxisorp™, Nunc) was coated with 1 µg/mL CRP in PBS solution (100 µL per well) and left O/N at 4°C. The following day, the antigen coated plate was then blocked with a 3% (w/v) BSA-PBS solution (200 µL per well) for 1 h at 37°C. Meanwhile, the O/N plates of expressed clones were removed from 30°C and subject to a freeze-thaw protocol for the production of scFv-enriched lysate. In this protocol the plates are placed at -80°C until frozen and then thawed at 37°C (this step was repeated a total of 3 times). The plates were then centrifuged at 3,220 x g (Eppendorf centrifuge 5810R) for 15 min to obtain the scFv-enriched lysate supernatant. Each lysate supernatant was then added (100 µL per well) to its corresponding coated/blocked well and incubated at 37°C for 1 h. (Alternatively, an inhibition ELISA was performed, whereby the lysate was pre-incubated with several concentrations of the free antigen and then added to the corresponding coated/blocked well). Following incubation, the plates were washed using PBST (x3) and PBS (x3) to remove any unbound scFv. The CRP-scFv complex was detected with 100 µL per well of 1/2000 dilution of an anti-histidine (HRP-labelled) secondary mAb (Sigma). After a 1 h 37°C incubation with the secondary mAb, TMB was added (100 µL per well) and left react for 20 min at 37°C. The reaction was quenched by the addition of 100 µL per well of 10% (v/v) HCl, after which the absorbance was read at 450 nm on a Safire 2 plate reader (Tecan).

2.9.15 Production of C11-2 scFv template for sub-cloning into pComb3X vector.

An aliquot of a glycerol stock of the selected mouse anti-CRP scFv clones (C11-2 scFv contained in pAK 400 vector in Top 10 F' cells) was inoculated into 10 mL of SB medium (25 µg/mL chloramphenicol) and grown O/N at 37°C at 250 rpm. The O/N culture was then subjected to a plasmid purification using the Promega SV Miniprep™ kit as described in section 2.9.13. Next, a *Sfi*I restriction digest was performed on the plasmid preparation at 50°C for 5 h using the following conditions:

<u>Components</u>	<u>200 µL Volume</u>
pAK 400 Vector	89 µL
10 X buffer 2	20 µL
10 X BSA	20 µL
H ₂ O	64 µL
<i>Sfi</i> I restriction enzyme	7 µL

2.9.16 PCR primers for sub-cloning of mouse scFv from pAK400 to pComb3X vector.

Vκ 5' Sense Primer

MSCVK5

5' GGG CCC AGG CGG CCG AGC TCG AYA TTG TRA TGA CMC AGT C 3'

VH 3' Reverse Primer

SubRev

5' CCT GGC CGG CCT GGC CAC TAG TGA GAG GAG ACT GTG AGA GTG GTG
CCT TC 3'

2.9.17 Nested PCR for conversion of mouse scFv from pAK400 to pComb3X format.

2.9.17 (a) Nested PCR (Part 1) - The components for a 1 X reaction were as follows:

<u>Component</u>	<u>50 μL Volume</u>	<u>Conc. in 50 μL reaction</u>
HIFI buffer (10x)	5 μL	1 X
MSCVK5	1.67 μL	83 pM
SubRev	0.5 μL	83 pM
scFv template	1 μL	27 ng/rxn
dNTP	1 μL	0.2 mM
MgSO ₄	2 μL	2 mM
H ₂ O	38.63 μL	N/A
Platinum HIFI™ Taq	0.2 μL	5 U/ μL

The SOE-PCR was performed in the PX2 thermal cycler (thermo electron corporation) under the following conditions:

<u>Stage</u>	<u>Temperature (°C)</u>	<u>Time (s)</u>
1 (1 cycle)	94	30
2 (30 cycles)	94	30
	60*	30
	68	120
3 (1 cycle)	68	600
	4	pause

*An annealing temperature gradient ranging from 50 - 60°C was incorporated into the PCR.

2.9.17 (b) Nested PCR (Part 2) - The components for a 1 X reaction were as follows:

<u>Component</u>	<u>50 µL Volume</u>	<u>Conc. in 50 µL reaction</u>
HIFI buffer (10x)	5 µL	1 X
MSCVK5	1.67 µL	83 pM
SubRev	0.5 µL	83 pM
New scFv template	1 µL	21.5 ng/rxn
dNTP	1 µL	0.2 mM
MgSO ₄	2 µL	2 mM
H ₂ O	38.63 µL	N/A
Platinum HIFI™ Taq	0.2 µL	5 U/ µL

The PCR conditions employed for part 2 were the same as shown for part 1 except that only the most optimal annealing temperature (60°C) was used.

2.9.18 *SfiI* restriction digest of nested PCR product and ligation into pComb3X vector.

Both the purified nested PCR product (modified scFv gene) and purified pComb3X vector were digested using the restriction enzyme *SfiI* for 5 h at 50°C using the components outlined below:

<u>Components</u>	<u>100 μL Volume</u>	<u>Components</u>	<u>100 μL Volume</u>
Modified scFv insert (25 μ g)	20.3 μ L	pComb3X vector (30 μ g)	40.7 μ L
10 X buffer 2	10 μ L	10 X buffer 2	10 μ L
10 X BSA	10 μ L	10 X BSA	10 μ L
H ₂ O	39.7 μ L	H ₂ O	30.3 μ L
<i>Sfi</i> I restriction enzyme	20 μ L	<i>Sfi</i> I restriction enzyme	9 μ L

Following a 5 h incubation at 50°C, the digested pComb3XSS vector (see section 7.1.1 for vector map) was treated with Antarctic Phosphatase™ enzyme to prevent self-ligation. This enzyme catalyzes the removal of 5' phosphate groups from DNA. The loss of the 5' phosphoryl termini, therefore, prevents the ligase enzyme from working.

Antarctic phosphatase treatment of digested pComb3XSS vector

<u>Component</u>	<u>Volume</u>
pComb3X vector (5 μ g)	50 μ L
Antarctic phosphatase buffer (10x)	5 μ L
Antarctic phosphatase enzyme	2 μ L

The above reaction mixture was incubated for 1 h at 37°C and then the enzyme was heat inactivated at 65°C for 5 min. The restricted products were then purified using the same procedure, as outlined in section 2.9.6, and ligated in a 3:1 (insert:vector) ratio at 15°C O/N under the following conditions:

<u>Component</u>	<u>Volume</u>
Ligase buffer (10x)	20 μ L
Digested pComb3X vector (1.4 μ g)	80 μ L
Digested scFv gene (700 ng)	7.8 μ L
H ₂ O	82.2 μ L
T ₄ DNA ligase	<u>10 μL</u>
Total Volume	200 μ L

The ligation was subjected to an ethanol precipitation, harvested and then transformed into electro-competent Top 10 F' cells (general method described in section 2.9.9). Individual

transformed colonies were cultured and their lysates analysed via direct ELISA using the method described in section 2.9.14.

2.9.19 Optimisation of scFv expression in Terrific Broth (TB) medium.

An aliquot of a glycerol stock of the selected mouse anti-CRP scFv clone (C11-2 scFv contained in pAK 400 vector in Top 10 F' cells) was inoculated into 10 mL of SB medium (25 µg/mL chloramphenicol) and grown O/N at 37°C at 250 rpm. An aliquot of the O/N culture was then subcultured into 20 mL of TB media containing 1 x 505 (0.5% (v/v) glycerol, 0.05% (v/v) glucose final concentration), 1mM MgSO₄ and 25 µg/mL chloramphenicol. The culture was incubated at 37°C at 200 rpm until cells appeared turbid i.e. an optical density at 600 nm (OD 600 nm) of ~0.6 was achieved. Expression was then induced by adding IPTG to a final concentration of 1mM and incubating at 30°C (180 rpm) O/N. The expressed culture was then harvested by centrifuging at 3,220 x g (Eppendorf centrifuge 5810R) for 20 min at 4°C after which the pellet was resuspended in 500 µL of either PBS (ELISA analysis) or HBS buffer (Biacore analysis). Next, the resuspended pellet was subjected to a freeze-thaw protocol to extract the scFv from the cells. The freeze-thaw protocol involved incubating the resuspended cells at -80°C for 15 min, followed by incubation at 37°C for 10 min. This process was repeated 3 times after which the lysed cells were centrifuged at 20,817 x g (Eppendorf centrifuge 5810R) for 15 min at 4°C to obtain the clear lysate supernatant. This scFv-rich lysate was transferred to a clean 1.5 mL micro-centrifuge tube and stored for short-term at 4°C or long-term at -20°C.

2.10 Generation and characterisation of a chicken anti-CRP scFv library

2.10.1 Construction, screening and selection of avian anti-CRP scFv library.

Antibody production and selection was performed as outlined by Leonard *et al.*, (2007), following the methods described by Andris-Widhopf *et al.*, (2000). RNA was extracted from the spleens and bone marrow of two chickens immunised with C-reactive protein and first-strand cDNA synthesis performed using the Superscript III™ kit (see section 2.9.3). The primer sets listed by Andris-Widhopf *et al.*, (2000) were used for the amplification of the

antibody variable heavy and light chain genes from the synthesized cDNA template. SOE-PCR (see section 2.9.7) was employed to join the amplified variable heavy and light chains via an 18 amino acid serine-glycine linker, which was subsequently cloned into the pComb3X vector (see section 7.1.1 for vector map) in a VL-VH scFv format. The cloned scFv library was then electroporated into *E. coli* XL-1 blue (see section 2.11.6) cells generating an antibody library of 3×10^7 clones. The scFv fragments were packaged on the surface of M13K07 phage and subjected to four rounds of panning against microtitre plate wells coated with CRP, whereby the level of stringency throughout the four rounds was gradually increased. Following enrichment of the library, the eluted phage were re-infected into *E. coli* TOP10F' cells for soluble expression. Single colonies were selected, cultured and expressed for incorporation into a monoclonal ELISA to identify binding to CRP. Ninety-six CRP-specific clones were then evaluated via a high-throughput screening strategy using the Biacore A100 protein interaction array system. Crude bacterial extracts of these clones were ranked based on the percentage of the complex left (% left) after dissociation in buffer. Finally, kinetic rate constants (k_a and k_d) and affinity (KD) data were obtained on the final pool of best-performing clones.

2.10.2 Cross reactivity analysis of avian scFv clones using capture ELISA method.

A glycerol stock of the selected clone was inoculated into SB media with 100 µg/mL carbenicillin and grown O/N at 200 rpm at 37°C. The O/N culture was then subcultured into 20 mL of fresh SB media containing 1 x 505 supplement (0.5% (v/v) glycerol, 0.05% (w/v) glucose final concentration), 1mM MgSO₄ and 100 µg/mL carbenicillin. These cultures were incubated at 37°C and 200 rpm until the cells appeared turbid at ~0.600 (OD 600 nm) was achieved. Expression was then induced by adding IPTG to a final concentration of 1mM and transferring to 30°C while shaking (180 rpm) O/N. Also, for each plate of clones, a 96 well plate (Maxisorp™, Nunc) was coated with 5 µg/mL of purified rabbit anti-CRP pAb in PBS solution (100 µL per well) and incubated O/N at 4°C. The following day, the pAb-coated plate was then blocked with a 3% (w/v) BSA-PBS solution (200 µL per well) for 1 h at 37°C. A 2 µg/mL solution of both CRP and SAP in PBST was then added the coated/blocked plate (3 rows with CRP and 3 rows with SAP) and incubated for 1 h at 37°C. Following incubation, the plates were washed using PBST (x3) and PBS (x3) to remove any unbound CRP and SAP. Meanwhile, the O/N cultures of expressed clones were removed from incubation at 30°C and centrifuged at 3,220 x g for 20 min to pellet cells. The cell pellet was

resuspended in 2 mL of PBST and subjected to the same freeze-thaw protocol as described in section 3.3.13. In this protocol, the plates were placed at -80°C until frozen and then thawed at 37°C , which was repeated a total of 3 times. The lysed cells were then centrifuged at $20,817 \times g$ for 5 min to obtain the scFv-containing lysate supernatant. Each lysate supernatant was diluted in PBST and then added in duplicate (100 μL per well) to both the rows with captured CRP and also the rows with captured SAP. A positive control was also incorporated into the ELISA. This consisted of a 1/2000 dilution of a commercially available CRP-specific mAb (HyTest). Following incubation at 37°C for 1 h, the plate was then washed using PBST (x3) and PBS (x3) to remove any unbound scFv and mAb. The scFv bound complexes were detected using a 1/2000 dilution of a mouse anti-HA (HRP-labelled) secondary mAb (Roche Applied Science) and the HyTest mouse anti-CRP mAb bound complex (positive control) was detected using a 1/2000 dilution of an anti-mouse (HRP-labelled) secondary pAb (Sigma). After a 1 h 37°C incubation with the secondary mAb's, 100 μL per well of TMB was added and incubated for 20 min at 37°C . The reaction was quenched by the addition of 100 μL per well of 10% (v/v) HCl, after which the absorbance was read at 450 nm on a Safire 2 plate reader (Tecan).

2.10.3 Large-scale protein expression and extraction from bacterial cultures.

Approximately 5 mL of SB media, containing 100 $\mu\text{g}/\text{mL}$ carbenicillin, was inoculated with 100 μL of stock transformant and grown O/N at 37°C . A 5 mL volume of this culture was then inoculated into 500 mL TB media containing 100 $\mu\text{g}/\text{mL}$ carbenicillin, 1 mM MgSO_4 , 0.5% (v/v) glycerol and 0.05% (w/v) glucose. The subcultured clone was incubated at 37°C at 250 rpm until the cells appeared turbid at ~ 0.600 (OD 600 nm) was achieved. Expression was then induced by adding IPTG to a final concentration of 1mM and transferring to 30°C (250 rpm) O/N.

The O/N expressed culture was then transferred to two 250 mL sorvals tubes and centrifuged at $15,000 \times g$ in a GSM rotor for 20 min ('brake on') to pellet the bacterial cells. The media supernatant was discarded into a bucket of VirkonTM and the excess media removed by inversion of the sorval tube onto a paper towel. The cell pellet was thoroughly resuspended in 30 mL of sonication buffer (1 x PBS, pH 7.4, 0.5 M NaCl and 20 mM imidazole) and aliquoted into 1 mL volumes in 2 mL micro-centrifuge tubes. Each aliquot was sonicated on ice for 45 s (3 s intervals) at an amplitude of 40, using a microtip Vibra CellTM sonicator and

the cell debris removed by centrifuging at 20,817 x g for 10 min at 4°C. The lysate supernatant was then passed through a 0.2 µm filter to remove any residual cell debris.

2.10.4 Purification of scFv fragments using immobilised metal affinity chromatography (IMAC).

A 3 mL aliquot of Ni⁺-NTA agarose resin (QIAGEN) was added to a 20 mL column and equilibrated with 20 mL of running buffer (1 x PBS, 0.5 M NaCl, 20 mM imidazole and 1% (v/v) Tween-20). The filtered lysate was then applied to the equilibrated column and the flow-through collected in a 50 mL tube. The column was then washed with 30 mL of running buffer to remove any loosely bound non-specific proteins, again collecting the flow-through in a 50 mL tube. The scFv fragment was eluted using 100 mM NaAc, pH 4.4, and collected in 24 x 400 µL aliquots in 1.5 mL micro-centrifuge tubes containing 100 µL of filtered neutralisation buffer (50 µL 100 mM NaOH and 50 µL of 10 x PBS). The 12 mL of neutralised scFv was then thoroughly buffer exchanged against filtered PBS (1 x) using a 5 kDa cut-off Vivaspin™ 6 column (AGB, VS0611). The buffer-exchanged scFv was then quantified using the Nanodrop™ ND-1000 and aliquoted into clean PCR tubes and stored at -20°C.

2.10.5 Preparation of monomeric CRP (mCRP).

Modified monomeric CRP was produced according to the methods described by Kresl *et al.*, (Kresl, Potempa and Anderson, 1998) (see section 2.10.5). In this procedure, 2 mg of pentameric CRP was chelated with 10 mM EDTA and incubated in 8.0 M urea for 2 h at 37 °C. Urea was removed by passing the CRP through a PD-10 Sephadex G-25 column equilibrated in PBS (0.15 M NaCl, 2.5 mM potassium chloride, 10 mM disodium hydrogen phosphate and 18 mM sodium dihydrogen phosphate, pH 7.4). The modified CRP protein was quantified by determining absorbance at 280 nm using the Nanodrop™ ND-1000 instrument and stored at 4 °C.

2.10.6 Amplification of C λ cys chain from isolated chicken cDNA.

The components for a 1 X reaction were as follows:

<u>Component</u>	<u>50 μL Volume</u>	<u>Conc. in 50 μL reaction</u>
GoTaq Buffer (5x)	10 μ L	1 X
C λ cys For	0.5 μ L	83 pM
C λ cys Rev	0.5 μ L	83 pM
MgCl ₂	2 μ L	1.5 mM
cDNA	0.5 μ L	0.5 μ g
dNTP	1 μ L	0.2 mM
H ₂ O	35.25 μ L	N/A
Go Taq™ Polymerase	0.25 μ L	5 U/ μ L

The PCR for the amplification of the constant lambda chain containing a terminal cysteine (C λ cys chain) was performed in the PX2 thermal cycler (thermo electron corporation) under the following conditions:

<u>Stage</u>	<u>Temperature (°C)</u>	<u>Time (s)</u>
1 (1 cycle)	94	180
2 (30 cycles)	94	15
	56	30
	72	60
3 (1 cycle)	72	600
	4	pause

2.10.7 Replacement of the existing C κ chain of the pMoPAC 16 vector with a C λ cys chain.

A large-scale plasmid prep of the pMoPac 16 vector (Hayhurst *et al.*, 2003) from ER2925 cells was performed, using a commercially-available plasmid Midi kit (Qiagen). Next, the existing constant kappa (C κ) chain was removed from the purified pMoPac 16 plasmid via digestion with both *Not*1 and *Sal*1 restriction enzymes. Additionally, the amplified C λ cys

chain was purified using the QIAquick™ gel extraction kit and also subjected to digestion with the same restriction enzymes.

pMoPac NotI-SalI digest

<u>Component</u>	<u>Volume</u>
pMoPac vector (10 µg)	15 µL
10 X buffer 3	10 µL
10 X BSA	10 µL
H ₂ O	49 µL
<i>Not</i> I	6 µL
<i>Sal</i> I	<u>10 µL</u>
Total volume	100 µL

Cλcys chain NotI-SalI digest

<u>Component</u>	<u>Volume</u>
Cλcys chain (2 µg)	20 µL
10 X Buffer 3	5 µL
10 X BSA	5 µL
H ₂ O	10 µL
<i>Not</i> I	5 µL
<i>Sal</i> I	<u>5 µL</u>
Total volume	50 µL

Following an incubation O/N at 37°C, the digested products were incubated at 65°C for 20 min for deactivation of both the *Not* I and *Sal* I enzymes. Finally, the deactivated digests were both resolved via agarose gel electrophoresis, gel extracted and then ligated using the following conditions:

<u>Component</u>	<u>Volume</u>
Ligase buffer (10x)	2 µL
Digested pMoPac vector (200 ng)	1.42 µL
Digested Cλcys chain (100 ng)	0.71 µL
H ₂ O	14.87 µL
T ₄ DNA ligase	<u>1 µL</u>
Total Volume	20 µL

2.10.8 Analysis of Cλ-scFv (scAb) transformants clones via direct ELISA.

Individual colonies (60 in total) were picked and inoculated into the inner 60 wells of sterile 96 well plates containing 100 µL SB media with 100 µg/mL carbenicillin and grown O/N at 200 rpm at 37°C (stock plates). The stock plates were then subcultured into fresh SB media (180 µL) containing 1 x 505 supplement (0.5% (v/v) glycerol, 0.05% (w/v) glucose final concentration), 1mM MgSO₄ and 100 µg/mL carbenicillin (subcultured plates). Glycerol was then added to the stock plates to a final concentration of 15% (v/v), which were then

transferred to a -80°C freezer for long term storage. Meanwhile, the subcultured plates were incubated at 37°C and 200 rpm until cells appeared turbid (OD600 nm of ~0.6). Expression was then induced by adding IPTG to a final concentration of 1mM and transferring to 30°C (180 rpm) O/N. Also, for each plate of clones, a 96 well plate (Maxisorp™, Nunc) was coated with 1 µg/mL PSA-PBS solution (100 µL per well) and incubated O/N at 4°C. The following day, the antigen-coated plate was then blocked with 200 µL per well of PBS (containing 2.5% (w/v) milk and 2.5% (w/v) BSA) and incubated for 1 h at 37°C. Meanwhile, the O/N plates of expressed clones were removed from 30°C and subjected to a freeze thaw protocol for the production of scAb-containing lysate. The protocol consisted of the plates being placed at -80°C until frozen and then thawing at 37°C, which was performed a total of 3 times. The plates were then centrifuged at 3,220 x g for 15 min to obtain the scAb-containing lysate supernatant. Each lysate supernatant was then added (100 µL per well) to its corresponding coated/blocked well and incubated at 37°C for 1 h. Following incubation, the plates were washed using PBST (x3) and PBS (x3) to remove any unbound scAb. Next, 100 µL of a 1/2000 dilution of Cλ-specific rabbit serum in PBST (containing 0.5 % (w/v) milk and 0.5 % (w/v) BSA) was added to each well and incubated for 1 h at 37°C. The PSA-bound complex was then detected using a 100 µL per well of a 1/2000 dilution of a HRP-labelled anti-rabbit secondary mAb (Sigma). After a 1 h 37°C incubation with the secondary mAb, 100 µL per well of TMB was added and incubated for 20 min at 37°C. The reaction was quenched by the addition of 100 µL per well of 10% (v/v) HCl, after which the absorbance was read at 450 nm on a Safire 2 plate reader (Tecan).

2.10.9 Nested PCR for cloning of H2 scFv gene into the pMoPac 16 vector.

The H2 scFv gene template for the PCR was prepared by purifying the pComb3X plasmid containing the H2 scFv gene and digesting it with *Sfi*1 enzyme. The resultant H2 scFv gene digest was then purified via gel extraction using a QIAquick™ gel extraction kit.

2.10.9 (a) Nested PCR (Part 1) - The components for a 1 X reaction were as follows:

<u>Component</u>	<u>50 μL Volume</u>	<u>Conc. in 50 μL reaction</u>
HIFI buffer (10x)	5 μ L	1 X
CSCpAK-For	1.58 μ L	83 pM
CSCpAK-Rev	1.25 μ L	83 pM
H2 scFv (<i>Sfi</i> I digested)	1 μ L	6 ng/rxn
dNTP	1 μ L	0.2 mM
MgSO ₄	2 μ L	2 mM
H ₂ O	37.97 μ L	N/A
Platinum HIFI™ Taq	0.2 μ L	5 U/ μ L

The SOE-PCR was performed in the PX2 thermal cycler (Thermo electron corporation) under the following conditions:

<u>Stage</u>	<u>Temperature (°C)</u>	<u>Time (s)</u>
1 (1 cycle)	94	120
2 (30 cycles)	94	30
	56	30
	72	120
3 (1 cycle)	72	600
	4	pause

2.10.9 (b) Nested PCR (Part 2) - The components for a 1 X reaction were as follows:

<u>Component</u>	<u>50 μL Volume</u>	<u>Conc. in 50 μL reaction</u>
HIFI buffer (10x)	5 μ L	1 X
CSCpAK-For	1.58 μ L	83 pM
CSCpAK-Rev	1.25 μ L	83 pM
PCR product from part 1	0.2 μ L	2 ng/rxn
dNTP	1 μ L	0.2 mM
MgSO ₄	2 μ L	2 mM
H ₂ O	38.77 μ L	N/A
Platinum HIFI™ Taq	0.2 μ L	5 U/ μ L

The PCR conditions employed for part 2 of the ‘nested-type’ PCR were identical to those shown for part 1.

2.10.10 SfiI restriction digest of nested PCR product and ligation into pMoPac 16 vector.

Both the purified nested PCR product and purified pMoPac vector were digested using the restriction enzyme *SfiI* for 5 h at 50°C using the components outlined below:

<u>Components</u>	<u>50 µL Volume</u>	<u>Components</u>	<u>100 µL Volume</u>
H2-pAk scFv gene (5 µg)	16.7 µL	E3 pMoPac vector (10 µg)	50 µL
10 X buffer 2	5 µL	10 X buffer 2	10 µL
10 X BSA	5 µL	10 X BSA	10 µL
H ₂ O	19.3 µL	H ₂ O	23 µL
<i>SfiI</i> restriction enzyme	4 µL	<i>SfiI</i> restriction enzyme	7 µL

The restricted products were then gel purified and ligated in a 3:1 (insert:vector) ratio at 15°C O/N under the following conditions:

<u>Component</u>	<u>Volume</u>
Ligase buffer (10x)	2 µL
Digested E3 pMoPac vector (200 µg)	2.8 µL
Digested H2-pAK scFv gene (100 ng)	1.56 µL
H ₂ O	12.64 µL
T ₄ DNA ligase	<u>1 µL</u>
Total Volume	20 µL

The ligation was subjected to an ethanol precipitation, harvested and then transformed into electro-competent Top 10 F' cells (method described in section 2.9.9).

2.10.11 Transfer of purified D9 scAb to nitrocellulose membrane and western blot analysis.

Six sheets of Whatmann filter paper and one sheet of 3 mm nitocellulose (per gel) were cut to the same dimensions of the SDS gel. Each of the layers of filter paper, the nitocellulose membrane and the SDS gel were soaked in transfer buffer for 15 – 30 min. A three layer

sandwich consisting of 3 sheets of filter paper, followed by the SDS Gel, nitrocellulose membrane and filter paper was assembled. All air bubbles were removed by carefully rolling each of the layers with a disposable 10 ml serological pipette. Proteins were transferred from the acrylamide gel to the nitrocellulose using a Trans-Blot[®] Semi-Dry Transfer cell (BioRad) @ 15 V for 15 min. The nitrocellulose membrane was then carefully transferred into a large weighing boat containing 20 mL of 5 % (w/v) milk-PBS solution and blocked for 2 h at room temperature or at 4°C overnight with agitation. Any excess blocking solution was removed from the membrane via two washes with PBS. Next, the blocked membrane was incubated with 20 mL of 1 % (w/v) milk-PBST solution containing 2 µg/mL of CRP for 1 h at room temperature with gentle agitation. The CRP solution was then discarded and the membrane washed in 0.05 % (v/v) PBST (x3) and PBS (x3). Next, a 1/2000 dilution of Cλ-specific rabbit serum was prepared in 20 mL of 1 % (w/v) milk-PBST and again left incubate with the membrane at room temperature for 1 h with agitation. A 1/2000 dilution of a HRP-labelled anti-rabbit secondary mAb (Sigma) was then used for detection of the bound Cλ-specific serum antibodies. Following a 1 h incubation, the membrane was washed as before, followed by a brief wash with distilled water. Development of the specific complex was achieved via the addition of liquid TMB substrate and stopped by multiple washes with distilled water.

2.11 Generation and characterisation of a chicken anti-MPO scFv library

2.11.1 Immunisation and serum titre of MPO-immunised chickens

Two white Leghorn chickens aged 5-8 weeks were initially immunised with a final concentration of 75 µg/mL MPO, mixed in a 1:1 ratio with Freund's complete adjuvant. The mixture was vigorously shaken to ensure formation of a completely homogenous solution. A total volume of 1000 µL of this solution was injected over four separate subcutaneous sites of each chicken for immunisation. Subsequent injections were performed with 50 µg/ml MPO mixed in a 1:1 ratio with Freund's incomplete adjuvant. A bleed was taken from the chickens 10 days after each injection and the antibody titre against MPO determined. Once a high titre response was reached, the chickens were given a final boost and then sacrificed 6 days later. Two further immunogens, namely heart fatty acid binding protein (H-FABP) and C-reactive protein (CRP), were administered in an identical manner to the same two chickens. The

phylogenetic nature of the avian host allowed for the administration of this cocktail of mammalian proteins, simultaneously.

2.11.2 Extraction and isolation of total RNA from MPO-immunised chickens.

To ensure an uncontaminated environment (free from contaminant RNA) the inner surface of a Gelaire BSB 4 laminar unit was sprayed with both IMS and RNase ZAP. The spleen and bone marrow were removed from the chickens and all excess fat was trimmed from the spleen before being transferred into a 50 mL 'RNase-free' tube containing 30 mL of TRI[™] reagent. A homogenizer, previously autoclaved at 120°C for 15 min and baked O/N at 180°C was used to homogenize the spleen/bone marrow. The mixture was incubated for 5 min at room temperature to allow for the total dissociation of nucleoprotein complexes while maintaining the integrity of the RNA. The homogenized spleen/bone marrow was then centrifuged at 2,465 x g for 10 min at 4°C to pellet any excess cell debris and the supernatant transferred into a 50 mL polypropylene oakridge tube. Chloroform (6 mL) was then added to the tube containing the supernatant, thoroughly mixed through and then incubated for 15 min at room temperature. The resultant mixture was then centrifuged at 17,500 x g (Eppendorf centrifuge 5810R) for 15 min at 4°C. The centrifugation step produced 3 layers, a lower red phenol/chloroform phase, a protein interphase and a colourless liquid upper phase containing the RNA. The upper aqueous phase was carefully transferred (ensuring no lower layer contamination) into a 85 mL polycarbonate Oakridge tube and precipitated by addition of 15 mL of isopropanol. The RNA from both chickens was left to precipitate for 10 min at room temperature and then centrifuged at 17,500 x g for 25 min at 4°C, resulting in white RNA pellets. The isopropanol supernatant was carefully decanted and the pellets washed with 30 mL of 75% (v/v) ethanol by centrifugation at 17,500 x g for 10 min at 4°C. Finally, the pellets were allowed air dry in the laminar hood and then each resuspended in 500 µL of molecular grade water. The RNA preparations from both of the chickens were then quantified using the Nanodrop[™] ND-1000 and pooled in an equimolar ratio.

2.11.3 Reverse transcription of total RNA to cDNA.

Protocol was performed as described in section 2.9.3.

2.11.4 PCR primers for amplification of chicken scFv (pComb series)

V_λ Primers

CSCVK (sense)

5' GTG GCC CAG GCG GCC CTG ACT CAG CCG TCC TCG GTG TC 3'

CKJo-B (reverse)

5' GGA AGA TCT AGA GGA CTG ACC TAG GAC GGT CAG G 3'

V_H Primers

CSCVHo-F (sense), Short Linker

5' GGT CAG TCC TCT AGA TCT TCC GCC GTG ACG TTG GAC GAG 3'

CSCVHo-FL (sense), Long Linker

5' GGT CAG TCC TCT AGA TCT TCC GGC GGT GGT GGC AGC TCC GGT GGT GGC
GGT TCC GCC GTG ACG TTG GAC GAG 3'

CSCG-B (reverse)

5' CTG GCC GGC CTG GCC ACT AGT GGA GGA GAC GAT GAC TTC GGT CC 3'

Overlap Extension Primers

CSC-F (sense)

5' GAG GAG GAG GAG GAG GAG GTG GCC CAG GCG GCC CTG ACT CAG 3'

CSC-B (reverse)

5' GAG GAG GAG GAG GAG GAG GAG CTG GCC GGC CTG GCC ACT AGT GGA
GG 3'

2.11.5 Construction of chicken anti-MPO scFv library

Antibody production and selection was performed as described by Andris-Widhopf *et al.*, (2000).

2.11.6 Electro-transformation of scFv containing plasmid into XL-1 Blue *E. coli* cells.

Transformation of the ligated product was performed via electroporation into a commercially available strain of XL-1 Blue. The apparatus used was a Gene Pulser Xcell™ electroporation system with the parameters set to 25 μ F, 1.25 kV and the gene pulse controller at 200 Ω . The ligation mixture was split into 3 x 10 μ L aliquots. After thawing on ice, 100 μ L of the *E. coli* cells was added to each of the 3 x 10 μ L aliquots of ligation product, mixed by one gentle pipette up and down and then left on ice for a 30 s incubation. The mixture was then transferred to a chilled 0.2 cm electroporation cuvette, ensuring all the mixture settles on the bottom and then placed securely in the 'ShockPod'. A pulse was then passed through the cuvette, which was then immediately flushed with 1 mL of pre-warmed SOC medium using a sterile tip. A further 2 x 1 mL volumes of SOC media were used to flush the cuvettes. The time lapse between applying the pulse and transferring the cells to the growth media must be kept to an absolute minimum for optimal recovery of *E. coli* transformants. A transfer delay of even 1 min has been reported to cause as much as a 3-fold drop in transformation efficiency. The 3 mL of rescued ligation for the library was then incubated for 1 h at 250 rpm at 37°C. Following incubation, the 3 mL culture was plated out on 2 x TY agar plates supplemented with 100 μ g/mL carbenicillin and 2% (w/v) glucose. A negative control was also incorporated into the experiment by plating the XL-1 Blue cells containing no plasmid onto an identical carbenicillin/glucose agar plate. All agar plates were left grow O/N at 37°C and then scraped into 2 x TY medium containing 20% (v/v) glycerol for long term storage at -80°C.

2.11.7 Rescue of chicken anti-MPO scFv-displaying phage.

A 2 mL aliquot of the scraped library was inoculated into 400 mL of SB medium (30 μ g/mL carbenicillin and 10 μ g/mL tetracycline) for the chicken scFv library. Due to the high level of turbidity, the culture was left grow for approximately 1 h shaking at 37°C, after which more carbenicillin was added to a final concentration of 30 μ g/mL. The library was then rescued by the addition of 900 μ L of commercial M13K07 helper phage (Isis, Cat No. N0315S), left static at 37°C for 20 min and then transferred to a 37°C shaking incubator for 2 h at 250 rpm. Next, kanamycin was added, to a final concentration of 70 μ g/mL, before leaving the culture O/N at 37°C while shaking at 250 rpm.

2.11.8 Enrichment of library via biopanning against immobilised antigens.

Several wells of a 96-well ELISA plate (Maxisorp™, Nunc) coated O/N at 4°C with a set concentration MPO in PBS solution (See Table 3.4.8) were then blocked by filling with 3% (w/v) BSA-PBS and leaving at room temperature for 2 h. Meanwhile, the rescued phage-induced library was centrifuged at 15,000 x g in a GSM rotor for 20 min ('brake on' option selected) to pellet the bacterial cells. The phage supernatant was decanted into 250 mL sterile sorval tubes, to which 4 g of PEG and 3 g of NaCl was added for every 100 mL of phage. To ensure all the PEG and NaCl was dissolved, the sorval tubes were placed in a 37°C shaking incubator for 10 min at 200 rpm.

For precipitation of the phage, the sorval tubes were placed in ice and left in a cold room for 45 min. The PEG-precipitated phage was then harvested by centrifugation at 15,000 x g in a GSM rotor for 20 min ('brake off') and the media supernatant carefully decanted into a bucket of Virkon™ (Lennox, C222/0154/05). After removal of excess supernatant by inversion of the sorval tubes, the phage pellets were thoroughly resuspended in 2 mL of 1% (w/v) BSA-PBS and aliquoted into 2 mL micro-centrifuge tubes. The micro-centrifuge tubes were then centrifuged at 20,817 x g for 5 min at 4°C to pellet excess bacterial cells and the phage supernatants transferred into clean 1.5 mL micro-centrifuge tubes on ice (phage input). Meanwhile, the coated/blocked wells of the ELISA plate were washed 1 x PBST and 1 x PBS to remove excess BSA. Next, a specified aliquot (See Table 2.11.8) of the phage-BSA mixture was then added to the coated/blocked wells of the ELISA plate and left incubate at 37°C for 2 h. The wells were then decanted and washed several times with PBST and PBS (See Table 2.11.8) to remove weak-binding phage. To elute the bound phage an aliquot of 10 mg/mL trypsin in 1 x PBS (pH 7.4) was added to the washed wells, incubated static at 37°C for 20 min and finally agitated using an SRT1 roller mixer at room temperature for 10 min. The trypsin solution was vigorously pipetted up and down several times in the each of the wells to ensure all bound phage were eluted and then infected into 2 mL of XL1-Blue cells (OD₆₀₀ nm of ~0.5) for 15 min at room temperature. Next, 6 mL of pre-warmed SB media (containing 12 µL of 5 mg/mL tetracycline and 1.6 µL of carbenicillin) was added to a sterile 50 mL tube. The 2 mL of eluted phage was then added to the 6 mL of pre-warmed SB media and 4 µL was removed from this culture into 396 µL of SB medium for estimation of the output titre. The 8 mL phage infected culture was incubated at 37°C (250 rpm) for 1 h, after which 2.4 µL of carbenicillin was added to the culture and incubated at 37°C for a further 1 h. All 8 mL of the infected culture was then added to a 250 mL conical containing 92 mL of

pre-warmed SB medium (containing 184 μL of tetracycline and 46 μL of carbenicillin). For rescue of the library, 350 μL of commercial M13K07 helper phage was then added to the 100 mL culture. The helper phage was allowed infect the stationary culture at room temperature for 10 min and then incubated at 37°C (250 rpm) for 2 h. Finally, 140 μL of 50 mg/mL kanamycin was added to the culture which was left incubate at 37°C (250 rpm) O/N.

Output titre: The 1/100 dilution output titre (4 μL in 396 μL SB media) was then used to prepare output titre plates. Two 2 x TY agar plates (containing 100 $\mu\text{g}/\text{mL}$ carbenicillin) were plated with 100 μL of the 1 in 100 dilution of the culture). Two further 2 x TY agar plates (containing 100 $\mu\text{g}/\text{mL}$ carbenicillin) were plated with 10 μL of the 1/100 dilution of the culture). Plates were labelled pan output titre plates and incubated stationary at 37°C O/N.

Input titre: Dilutions of the input phage supernatant were prepared ($10^{-1} \rightarrow 10^{-8}$) using SB media. A 2 μL aliquot of each of the 10^{-7} , 10^{-8} , 10^{-9} phage dilutions were then infected into 3 separate sterile micro-centrifuge tubes containing 98 μL of XL1-Blue cells (OD600 nm of 1) for 15 min at room temperature. A 50 μL volume of each dilution were then plated onto 2 x TY agar plates (containing 100 $\mu\text{g}/\text{mL}$ carbenicillin) in duplicate. Plates were labelled pan input titre plates and incubated while stationary at 37°C O/N.

Table 2.11.8 Variable parameters of panning of chicken anti-MPO scFv library

	PAN 1	PAN 2	PAN 3	PAN 4
Culture vol.	400 mL	100 mL	100 mL	100 mL
CRP-coated	10 μg	5 μg	1 μg	1 μg
No. of wells	4	2	2	1
Input phage vol.	200 μL	100 μL	100 μL	50 μL
Washes	5 x PBST	10 x PBST	10 x PBST	10 x PBST
	5 x PBS	5 x PBS	5 x PBS	10 x PBS

2.11.9 Polyclonal phage ELISA.

Designated wells of a 96 well ELISA plate (Maxisorp™, Nunc) were coated with either H-FABP, CRP or MPO each at a concentration of 2 µg/mL in PBS and incubated O/N at 4°C. Each of the protein solutions were then decanted and the plate blocked with 3% (w/v) BSA in PBS for 1 h at 37°C. Some of the 3% (w/v) BSA solution was also added to several empty wells of the plate as a negative control to identify any background binding. The phage pools to be tested were diluted 1:1 with PBST containing 1% (w/v) BSA and a 100 µL aliquot of each added to designated wells of the coated/blocked ELISA plate. Following a 2 h incubation with the phage at 37°C, the plate was subjected to 3 washes with both PBST and PBS. Next 100 µL of 1/2000 dilution of an AP-conjugated anti-M13 antibody (GE Healthcare Life Sciences) in PBST containing 1% (w/v) BSA was added to each well and incubated for 1 h at 37°C. The specific complex was then detected by the addition of 100 µL of PNPP substrate and allowed to develop for 20 min at 37°C. Finally, the absorbance values were read at 405 nm on a Safire 2 plate reader (Tecan).

2.11.10 Infection of enriched phage pool into E. Coli Top 10 F' (non-suppressor strain) for soluble expression.

A 20 µL aliquot of the PEG-precipitated output phage from pan 4 was added to 2 mL of Top 10 F' cells (OD₆₀₀ nm of ~0.5) and incubated for 15 min at room temperature to promote infection. Next, 6 mL of pre-warmed SB media (containing 12 µL of 5 mg/mL tetracycline and 1.6 µL of carbenicillin) was dispensed into a sterile 50 mL tube. The 2 mL of infected Top 10 F' cells were then added to the 6 mL of pre-warmed SB media and 30 µL was removed from this culture into 270 µL of SB medium for titering to obtain single colonies for analysis. The remaining 8 mL phage infected culture was left incubate at 37°C (250 rpm) for 1 h, spun at 3,220 x g for 15 min and then resuspended in 500 µL of SB medium. The resuspended cells and titres were then plated on 2 x TY agar plates (containing 100 µg/mL carbenicillin) and incubated at 37°C O/N.

2.11.11 Direct and inhibition ELISA of soluble expressed scFv fragments.

Individual colonies (120 in total) were picked and inoculated into the inner 60 wells of a sterile 96 well plates containing 100 µL SB media with 100 µg/mL carbenicillin and grown

O/N at 200 rpm at 37°C (stock plates). The 2 x 96 well stock plates were then subcultured into fresh SB media (180 µL) containing 1 x 505 supplement (0.5% (v/v) glycerol, 0.05% (w/v) glucose final concentration), 1mM MgSO₄ and 100 µg/mL carbenicillin (subcultured plates). Glycerol was then added to the stock plates to a final concentration of 15% (v/v), which were then transferred to a -80°C freezer for long term storage. Meanwhile, the subcultured plates were incubated at 37°C and 200 rpm until cells appeared turbid (OD₆₀₀ nm of ~0.6). Expression was then induced by adding IPTG to a final concentration of 1mM and transferring to 30°C (180 rpm) O/N. Also, for each plate of clones, a 96 well plate (Maxisorp™, Nunc) was coated with 2 µg/mL MPO-PBS solution (100 µL per well) and incubated O/N at 4°C. The following day, the antigen-coated plate was blocked with a 3% (w/v) BSA-PBS solution (200 µL per well) for 1 h at 37°C. Meanwhile, the O/N plates of expressed clones were removed from 30°C and subjected to a freeze thaw protocol for the production of scFv-containing lysate. The protocol consisted of the plates being placed at -80°C until frozen and then thawing at 37°C, which was performed a total of 3 times. The plates were then centrifuged at 3,220 x g for 15 min to obtain the scFv-containing lysate supernatant. Each lysate supernatant was then added (100 µL per well) to its corresponding coated/blocked well and incubated at 37°C for 1 h. (Alternatively, an inhibition ELISA was performed, whereby the lysate was pre-incubated with several concentrations of the free antigen and then added to the corresponding coated/blocked well). Following incubation, the plates were washed using PBST (x3) and PBS (x3) to remove any unbound scFv. The scFv-bound MPO complex was detected using 100 µL per well of a 1/2000 dilution of an alkaline phosphatase (AP)-labelled anti-HA secondary mAb (Sigma, Cat. No. A5477). After a 1 h 37°C incubation with the secondary mAb, 100 µL per well of PNPP was added and incubated for 20 min at 37°C. The absorbance was then read at 405 nm on a Safire 2 plate reader (Tecan).

2.11.12 Immobilisation and reference cell surface capping for anti-MPO scFv analysis.

For capture-based analysis of the anti-MPO scFv clones, a monoclonal HA epitope tag (Affinity BioReagents, Cat. No. MA1-21314) was required for immobilisation onto FC2 of the CM5 chip surface. Initial preconcentration analysis was performed for identification of the optimal pH for immobilisation of the HA tag, as described in section 2.8.7. Immobilisation of the HA epitope tag to the CM dextran surface was performed at pH 4.0, following the protocol described in section 2.8.8. The only modification to the protocol was

the use of freshly prepared ethylenediamine (pH 8.5), as opposed to ethanolamine, as a capping agent. The reference flow cell to be used for the analysis (FC1) was also activated with EDC and NHS chemistry and then capped with ethylenediamine to reduce any potential non-specific binding of the MPO to the CM dextran surface.

2.11.13 Off-rate analysis of anti-MPO scFv clones.

Crude scFv-containing bacterial lysates (containing 12 mg/mL BSA and 12 mg/ml CM-dextran to reduce any potential non-specific binding to CM-dextran surface) were subsequently injected (10 μ L at a flow rate of 10 μ L/min) over FC1 and FC2 using reference subtraction of FC2-FC1. Next, MPO at a concentration of 3 nM was passed over the captured-scFv at a flow rate of 30 μ L/min. The association and dissociation times used were 3 and 10 min, respectively. Regeneration of the chip surface consisted of a 2 x 30 s injections of 20 mM NaOH.

2.11.14 Titration ELISA of purified avian anti-MPO B10B scFv.

A 96 well plate (Maxisorp™, Nunc) was coated with 1 μ g/mL MPO-PBS solution (100 μ L per well) and incubated O/N at 4°C. The following day, the antigen-coated plate was then blocked with 200 μ L per well of PBS (containing 2.5% (w/v) milk and 2.5% (w/v) BSA) and incubated for 1 h at 37°C. Any excess blocking solution was removed via a single wash with PBST followed by PBS. A 1/1000 dilution of the purified scFv stock was made in PBST (containing 0.5% (w/v) milk and 0.5% (w/v) BSA). Next, serial halving dilutions of this were prepared in the same buffer as far as 1/500,000,000. A 100 μ L aliquot of each of the dilutions were added in duplicate to the coated/blocked wells and incubated for 1 h at 37°C. Following incubation, the plates were washed using PBST (x3) and PBS (x3) to remove any unbound scFv. The scFv-bound MPO complex was detected using a 100 μ L per well of a 1/2000 dilution of an AP-labelled anti-HA secondary mAb (Sigma, Cat. No. A5477). After a 1 h 37°C incubation with the secondary mAb, 100 μ L per well of PNPP was added and incubated for 20 min at 37°C. The absorbance was then read at 405 nm on a Safire 2 plate reader (Tecan).

2.11.15 Novel assay for direct detection of captured MPO.

A 96 well plate (Maxisorp™, Nunc) was coated with 5 µg/mL of IMAC purified anti-MPO scFv in PBS (100 µL per well) and incubated O/N at 4°C. The following day, the scFv-coated plate was then blocked with 200 µL per well of PBS (containing 2.5% (w/v) milk and 2.5% (w/v) BSA) and incubated for 1 h at 37°C. Any excess blocking solution was removed with a wash with PBST followed by PBS. Serial halving dilutions of MPO were prepared in PBST (containing 0.5% (w/v) milk and 0.5% (w/v) BSA) ranging from 50000 to 97.5 ng/mL. A 100 µL aliquot of each of the dilutions were added in quadruplicate to the coated/blocked wells and incubated for 1 h at 37°C. Following incubation, the plates were washed using PBST (x3) and PBS (x3) to remove any unbound MPO. The scFv-bound MPO complex was detected by the addition of either TMB or OPD in duplicate to the wells and incubated for 20 min at 37°C. For quenching, 100 µL per well of 10% (v/v) HCl was added, after which the absorbance was read at 450 nm on a Safire 2 plate reader (Tecan).

2.11.16 Preliminary hybrid lateral flow/western blot assay for detection of MPO.

IMAC-purified avian MPO-specific scFv was diluted in PBS to a final concentration of 500 µg/mL. Next, HiFlow Plus HF07504 nitrocellulose membrane (Millipore) was sprayed with the diluted scFv at a flow-rate of 600 nL/s using the Linomat 5 system (CAMAG) across the width of the strip. Following a 15 min incubation at 37°C, the sprayed membrane was cut into 4 identical strips each containing embedded scFv. All 4 strips were then transferred into a large weighing boat containing 20 mL of 5 % (w/v) milk-PBS solution and blocked for 2 hs at room temperature or at 4°C overnight with agitation. Any excess blocking solution was removed from the membrane via two washes with PBS. Next, each of the strips were placed in 4 separate small weighing boats and incubated with 5 mL of 1 % (w/v) milk-PBST solution each spiked with varying concentrations of MPO. Following a 1 h incubation at 37°C, each of the MPO-spiked solutions were discarded and the membranes washed in PBST (x 2) and PBS (x 2). Development of each of the membrane strips was achieved via the addition of liquid TMB substrate and stopped by multiple washes with distilled water.

2.12 Immunoassays using novel platforms.

2.12.1 Lateral flow assay using purified avian B10B anti-MPO scFv.

A strip of HiFlow Plus HF07504 nitrocellulose membrane (Millipore) was cut to specific dimensions of 4 cm x 1 cm. An avian anti-MPO scFv purified via IMAC was diluted in 1% (w/v) trehalose – 50 mM sodium phosphate buffer, pH 7.5, (spotting buffer) to a final concentration of 500 µg/mL. The diluted scFv was then sprayed at a flow-rate of 400 nL/s using the Linomat 5 system (CAMAG) across the width of the strip (3 cm up the strip – test line). Also anti-rabbit IgG (HRP labelled) (Sigma) was diluted in the spotting solution to a concentration of 5 µg/mL and sprayed across the width of the strip (3.5cm up the strip – control line). The membrane is then left in a 37°C incubator for 20 min to ensure sufficient drying of both the scFv (test) and rabbit IgG (control) to the membrane surface. The sprayed nitrocellulose strip was set up to stand vertically with the bottom of the strip touching a strip of parafilm. A 200 µL aliquot of MPO-depleted human serum (HyTest Ltd., Cat. No. 8MPFS), spiked with a set concentration of MPO, was then applied to the parafilm. The MPO-spiked serum travels up the length of the strip via capillary action, assisted by wicking with Whatman paper at the end of the strip. A wash buffer solution consisting of 50 mM sodium phosphate pH 7.5 (0.05% (v/v) Tween 20) was then applied (200 µL volume) to the bottom of the strip. The Tween-20 (mild detergent) assists in the breakage of any hydrophobic bonds which may occur between the serum and the membrane, allowing movement of the serum and its components up the strip towards both the test and control lines. The MPO in the serum sample binds to the avian anti-MPO scFv saturated test line, with all other non-specific proteins etc. washed away. The bound MPO is then detected by the addition of TMB Liquid substrate (Sigma) to the bottom of the strip, which travels up via capillary action and reacts with the scFv captured-MPO forming a blue colour at the test line.

2.12.2 Fluorescent competition assay using the *Ámic Open Lateral Flow (OLF)* platform.

The capture antibodies were diluted in spotting solution (1% (w/v) trehalose, 50 mM NaPO₄ buffer, pH 7.5) to a final concentration of 0.4 mg/mL and deposited onto dextran functionalized slides in two rows across the channel. Each mixture was spotted under humid conditions (relative humidity 70%) with a sciFLEXARRAYER™ S3 (Scienion, Germany). A PLC 60 nozzle was used to spot the diluted capture antibodies. Each spot consisted of one

droplet (~25 nL). CRP (Scipac, UK) was spiked into CRP-depleted serum (Scipack, UK) at several concentrations (30, 10, 3.3, 1.1, 0.55 and 0 µg/mL). Alexa™ 647 labelled CRP was then added to each of the spiked samples to a final concentration of 100 ng/mL. A 15 µL volume of each of the CRP sample solutions was applied to the sample zone on the chip. Following migration of the entire sample droplet into the pillar array, a 15 µL volume of unspiked CRP-depleted serum was added to the rear of the sample zone as a washing step. The signal intensities were recorded in a prototype fluorescence scanner. All assays were performed in triplicate and total assay time was approximately 10 min.

2.12.3 Fluorescent sandwich-based assay on novel supercritical angular fluorescence (SAF) enhanced parabolic chip platform.

Purified rabbit anti-CRP pAb (section 2.8.2) was diluted in a 1% (w/v) trehalose-sodium phosphate solution (0.1M) at pH 7.5 to a final concentration of 200 µg/mL. The pAb solution was then accurately deposited onto each paraboloid platform using a non-contact sciFLEXARRAYER™ (Scienion AG, Germany) piezo dispensing system. Following a 1 h incubation in 70% humidity at room temperature, the spotted chips were blocked in a 5% (w/v) milk-PBS solution O/N at 4°C. Excess blocking solution from the incubation was removed by another washing step with PBS. Next, varying concentrations of CRP antigen diluted in either 1% (w/v) milk-PBST or CRP-depleted serum were pipetted onto each of the washed chip surfaces (330 per chip). The chips were incubated at room temperature for 1 h, constantly agitating the CRP-spiked sample on the chip surface using a pipette. Another wash step was performed comprising PBST (x3) and PBS (x3) to remove excess unbound CRP antigen. A 1/400 dilution of fluorescently labelled anti-CRP pAb (section 2.8.6) in 1% (w/v) milk-PBST was then pipetted onto the chip surface and left to incubate for a further 2 h. An identical wash step was then performed, followed by a wash with deionised water, to remove any excess salt. Finally, the washed chips were dried using compressed nitrogen and then read using a custom-built biochip reader.

2.12.4 Analysis of the re-engineered CRP-specific H2 avian scFv using the surface plasmon resonance (SPR)-based Spectral platform.

Prior to each experiment the poly(methyl methacrylate) or PMMA substrate of the Spectral device was cleaned with ultra-pure water and dried with a nitrogen stream. A cleaning step with argon plasma (Harrick Plasma) for 5 min was also performed to assure that no organic contaminants were present at the surface. The first baseline signal was extrapolated by passing degassed ultra-pure water through the flow channel and recording the resultant signal both with depolarized light and also no light (high frequency noise). This procedure was then repeated using degassed 1 x PBS buffer. The SPR signal was recorded for both solutions until the baseline levels stabilised. Next, the purified CRP-specific D9 scAb (section 3.3.6 to 3.3.8) was diluted in degassed PBS to a final concentration of 15 µg/mL. Immobilisation onto the gold surface was achieved by passing a 190 µL aliquot of the diluted scAb through the test channel at a flow rate of 40 µL/min (the flow of all solutions was kept constant at this flowrate). All solution injections were performed using a REGLO Digital peristaltic pump (ISMATEC, Glattbrugg, Switzerland). A dedicated temperature controller was used to maintain a set temperature of 20°C throughout the experiments. The new baseline level was identified again by passing degassed 1 x PBS through the scAb-immobilised test channel. Blocking of the test channel was achieved by passing through a 400 µL volume of a commercial blocking agent (Candor, Ref. 110-125). The latest baseline level was then calculated with 1 x PBS as before. CRP-depleted serum (Hyttest, ref. 8CFS) was then spiked with a specified set of concentrations of CRP, each of which was passed across the blocked/scAb immobilised test channel. Finally 1 x PBS was again used to determine the change in baseline level which correlated directly to the binding response.

Chapter 3

Results & Discussion

3.1 Generation and characterisation of rabbit anti-CRP polyclonal antibodies

3.1.1 Rabbit immune system

The rabbit immune system has been found to generate antibody diversity and optimise affinity by different mechanisms than those used by mice and other rodents. One attractive feature of the immune system of rabbits is the use of both gene conversion and somatic hypermutation to diversify rearranged heavy and light chain genes. Although, antibody diversity generated by VHDJH rearrangements in rabbits is much more restricted than in mice or humans, compensation is sought in the far superior diversity obtained from VKJK rearrangements in rabbits. For example, both mice and humans possess only one kappa light chain isotype, whereas rabbits have two (K1 and K2), including several highly diverse allelic variants of K1 (Popkov *et al.*, 2003). Further diversity to the immune repertoire may be contributed from the kappa light chain regions due to the unusual germline VK-encoded variability in the length of complementarity determining region 3 (LCDR3). Moreover, B lymphopoiesis has led to B cell recombination excision circles (BRECS), being found in bone marrow as early as twelve days into the gestation period of rabbits, indicating the occurrence of Ig gene rearrangement even at this early stage. Much interest has also been generated from the role that both gut-associated lymphoid tissues (GALT) and the intestinal flora play in development of the preimmune rabbit antibody repertoire (Mage *et al.*, 2006). IgM B cells have been shown to undergo further Ig repertoire diversification in both the appendix and other GALT tissues. This observation has been further supported by a study, showing poor responses to immunisations against several antigens in germ-free rabbits (Tlaskalova-Hogenova and Stepankova, 1980). This project involved the generation of both polyclonal and recombinant antibodies from female New Zealand white rabbits.

3.1.2 CRP as a target analyte

CRP is composed of five identical non-covalently linked polypeptide subunits (molecular weight of 23 kDa), each containing 206 amino acid residues (Thompson *et al.*, 1999) (See Figure 4.2). These monomeric subunits are arranged in a planar ring with pentameric symmetry. Each subunit has a concave face in which the ligand-binding site, containing two calcium atoms, is located. The conservation of the structure of CRP and of its calcium-dependent specific binding of ligands containing phosphocholine (PC) (Volanakis and Kaplan, 1971) and related substances, together with the failure thus far to detect any polymorphism or deficiency of CRP in man, argue strongly that CRP has an important

physiological role (Thompson *et al.*, 1999). This proteins slow evolution is also evident in its close homology to other species, where the 206 amino acid structure of CRP in mice and rabbits, shows a 70 – 80% sequence homology with human CRP (Urich, 1994).

The ability of CRP to dissociate into individual subunits (discussed in section 1.7) is another characteristic attribute of this analyte. These CRP isoforms, referred to as modified or monomeric CRP (mCRP), express several neo-epitopes and display properties distinct from those of native CRP (Potempa *et al.*, 1987; Zouki *et al.*, 2001; Khreiss *et al.*, 2004b). Therefore, the common use of EDTA-containing tubes for hospital blood sampling may prove problematic, due to the potential chelation of CRP in the sample. Another potential obstacle associated with antibody-based CRP detection is cross-reactivity to homologous proteins. CRP is a member of the pentraxin family of cyclic oligomeric Ca^{++} -binding proteins, of which the homologous protein, Serum amyloid P (SAP), is also a member (Steel and Whitehead, 1994; Gewurz *et al.*, 1995). Structurally, SAP is a molecular homologue of CRP with approximately 70% amino acid sequence homology (Pepys and Baltz, 1983).

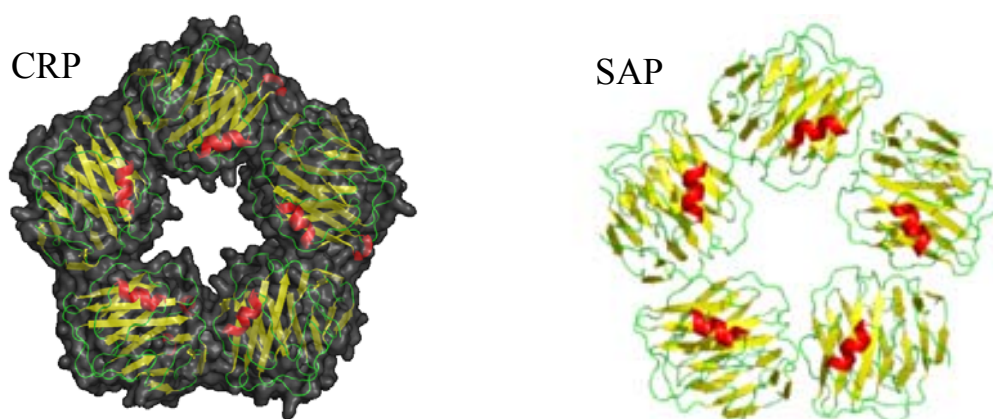


Figure 3.1.2 Cartoon models of CRP (ZD Net Healthcare, Accessed 18th January, 2009) and its homologous Serum Amyloid P (SAP) protein. Helices are highlighted in red, sheets in yellow and coils in green.

This protein may prove to be a major contaminant analyte in the identification of CRP levels, considering the high concentration of SAP found in normal human serum (30–40 $\mu\text{g}/\text{mL}$) (Lund and Olafsen, 1999). Consequently, cross-reactivity analysis against SAP remains an essential step in the screening of antibodies against CRP.

All of these features of CRP have led to its recognition as a valuable target molecule and resulted in its common use as a model analyte (Koskinen *et al.*, 2004; Peoples, Phillips *et al.*,

2007). CRP has also been selected as a relevant analyte in the Integrated Project founded by the European Community, entitled “Healthcare by biosensor measurements and networking (Care-Man),” for developing innovative analytical devices for fast molecular diagnostics (Bini *et al.*, 2008).

3.1.3 New Zealand white rabbits (XZB5 and XZCG) serum titres.

A serum titre was performed on both rabbits (XZB5 and XZCG) following an extensive immunisation regime (section 2.8.1) with antigen-grade CRP. Serum from the immunised rabbits was diluted (1/100 to 1/1,000,000 dilution) in PBS containing 1% (w/v) milk marvel and tested against CRP in a direct ELISA format. Both rabbits produced serum titres in excess of 1/100,000 against the CRP antigen, making both rabbits good candidates for extraction of CRP-specific polyclonal antibody. In addition, to the serum taken from the rabbits for production of polyclonal antibody, both the spleens and bone marrow were harvested for future construction of a recombinant antibody library.

3.1.4 Protein A purification of rabbit anti-CRP polyclonal antibody.

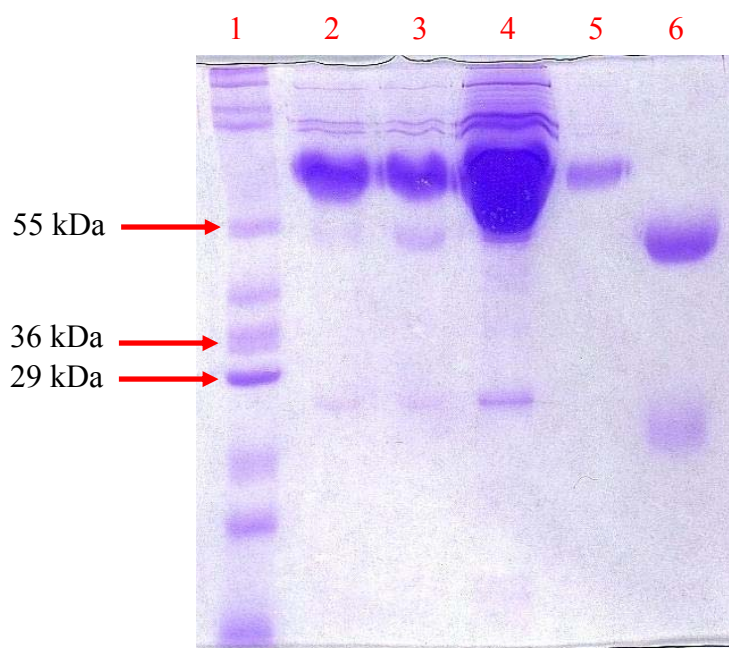


Figure 3.1.4 SDS-PAGE gel of fractions from Protein A purification of rabbit anti-CRP pAb. The fractions were loaded as flow-through 1 (Lane 2), wash 1 (Lane 3), ‘flow-through’ 2 (Lane 4), wash 2 (Lane 5) and finally the eluted purified pAb (Lane 6). A protein marker ladder (Sigma) was also loaded alongside the samples in lane 1 for estimation of the apparent molecular weights of the each of the protein samples.

Fractions from each stage of the protein A purification of the polyclonal antibody (pAb) (section 2.8.2) were kept for further analysis. SDS-PAGE was utilised to assess the efficiency of the purification protocol and subsequently identify the purity of the final eluted fraction of pAb. The fractions were resolved on a freshly prepared 10% (w/v) SDS-PAGE gel (Figure 3.1.4), stained and destained, as described in section 2.8.3. The two bands in lane 6 represent the heavy chain (~55 kDa) and the light chain (~25 kDa) of the polyclonal antibody, which showed a high level of purity.

3.1.5 Checkerboard ELISA to determine titre of purified rabbit anti-CRP polyclonal antibody.

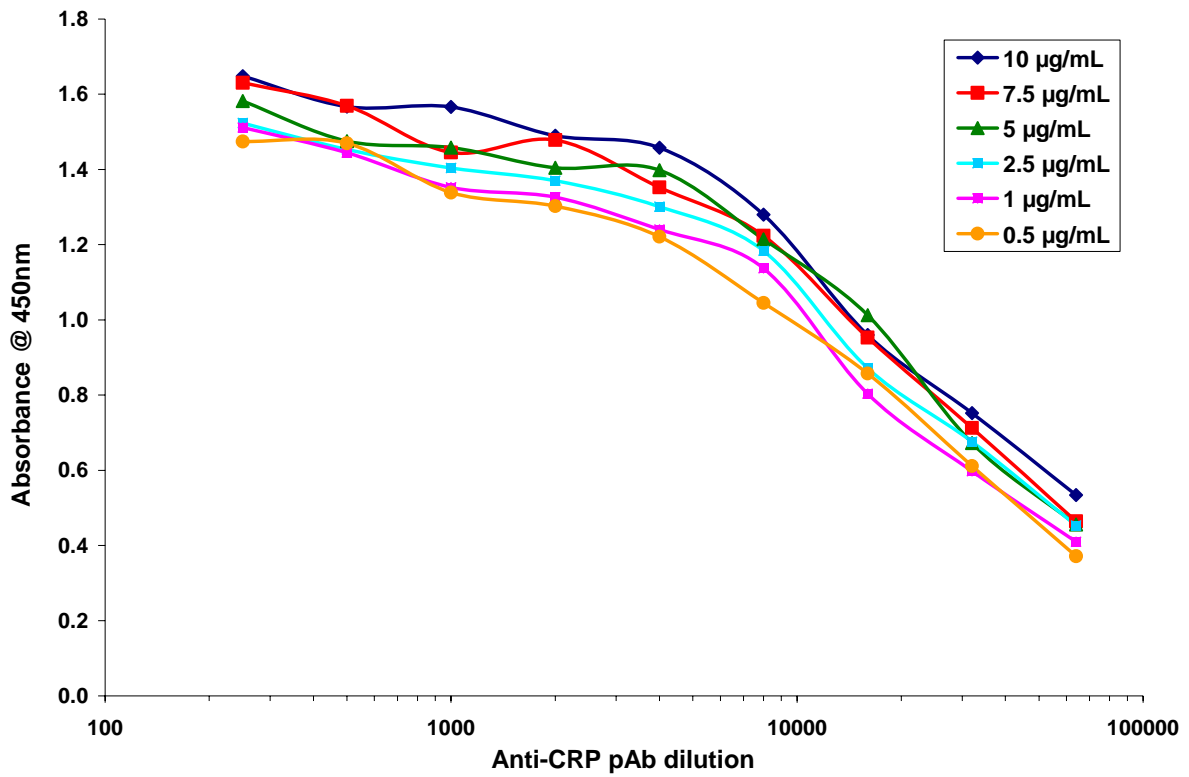


Figure 3.1.5 (a) Checkerboard ELISA using purified rabbit anti-CRP polyclonal antibody (pAb). CRP coating concentrations of 10, 7.5, 5.0, 2.5, 1.0, 0.5 µg/mL were all investigated in the ELISA. The purified rabbit pAb was then serially diluted (1/250, 1/500, 1/1000, 1/2000, 1/4000, 1/8000, 1/16000, 1/32000, 1/64000, 1/128,000) and the CRP-bound pAb complex detected using a HRP-labelled anti-rabbit pAb

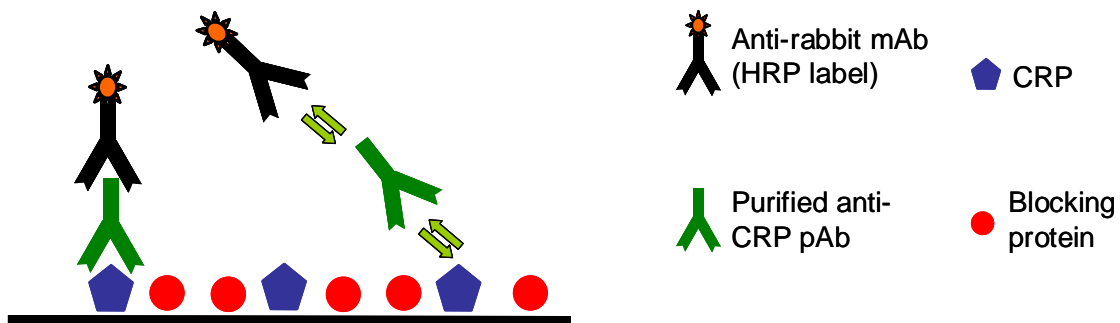


Figure 3.1.5 (b) Assay format used for checkerboard ELISA.

A simple checkerboard ELISA was performed (See format in Figure 3.1.5 b) on the purified rabbit anti-CRP polyclonal antibody (pAb), whereby both the concentrations of the coated CRP antigen and the anti-CRP pAb were varied (section 2.8.4). A good correlation between the polyclonal antibody and CRP may be observed in Figure 3.1.5 (a). Although good assay functionality was observed using this approach, the assay was limited by the many reagents (commercial secondary antibodies) required. To circumvent this, it was decided to directly label the purified pAb using a commercially available fluorescence-labelling kit (section 2.8.5). The fluorescently labelled pAb may then be incorporated into a more functional and direct assay.

3.1.6 Fluorescent sandwich ELISA using purified rabbit pAb labelled with DyLight 647.

The purified rabbit anti-CRP pAb was labelled using a commercially available mAb labelling kit (Pierce). The DyLight™ reagent contains an N-hydroxysuccinimide (NHS) ester, which is the most commonly used reactive group for labeling proteins. The NHS ester on the fluorescent label cross-links to primary amines forming a stable, covalent amide bond and releasing the NHS group. The optimisation of this fluorescent sandwich ELISA was undertaken in a two part assay (see section 2.8.6) using the same assay format (See Figure 3.1.6 a). The first part involved the determination of the optimal coating concentration of the purified rabbit anti-CRP pAb, whereby several coating concentrations were compared. The remainder of the assay involved the CRP antigen concentration being kept constant at 1 µg/mL and then varying the concentration of the labelled detection pAb.

Figure 3.1.6 (a) Assay format used for both fluorescent sandwich ELISAs.

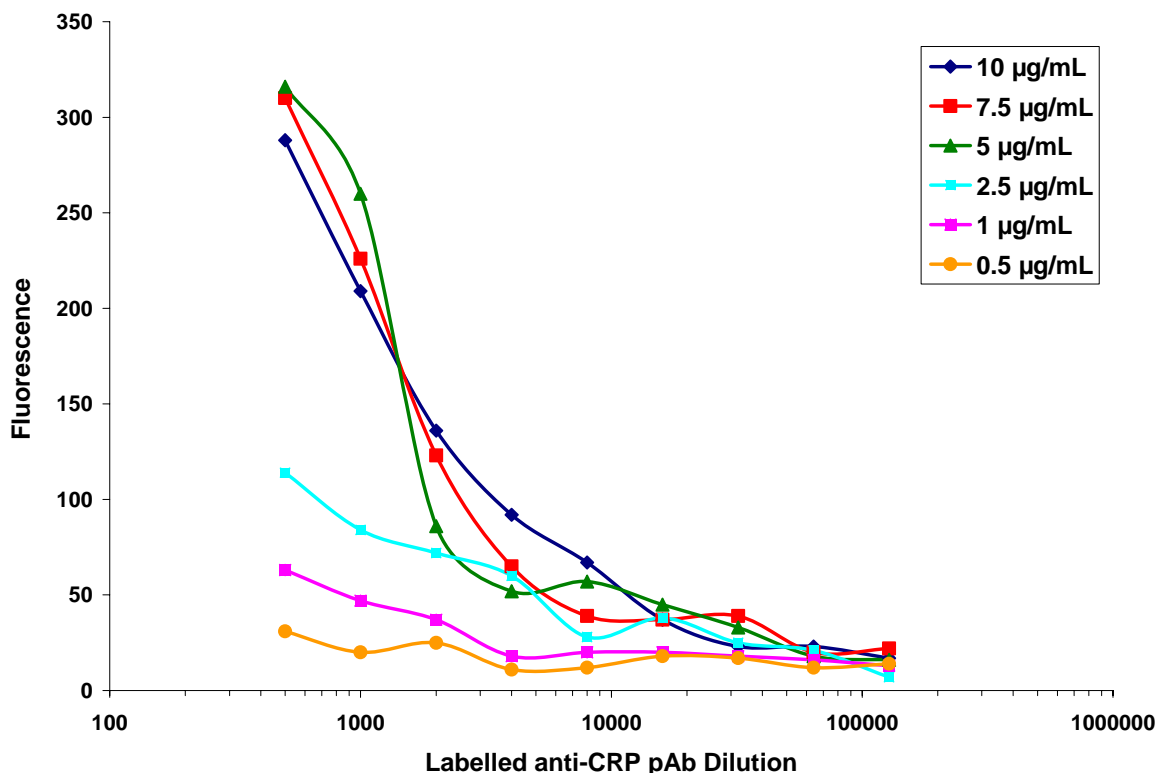


Figure 3.1.6 (b) Fluorescent sandwich ELISA using purified unlabelled rabbit anti-CRP pAb as capture antibody and fluorescently-labelled rabbit anti-CRP pAb as detection antibody. Several coating concentrations of purified CRP-specific pAb were used (10, 7.5, 5, 2.5, 1 and 0.5 µg/mL - legend). A set concentration of 1 µg/mL CRP was utilised in the assay. Finally, the pAb-captured CRP was detected with varying concentrations of fluorescently-labelled pAb (1/250, 1/500, 1/1000, 1/2000, 1/4000, 1/8000, 1/16000, 1/32000, 1/64000, 1/128000). The parameters used for measurement of the fluorescent signal, including the excitation and emission wavelengths are described in section 2.8.6.

Both the optimal pAb coating concentration and its corresponding fluorescently-labelled pAb concentration was then calculated from the plotted graph, shown in Figure 3.1.6 (b). The 5 µg/mL coating concentration of the purified pAb was chosen as the optimal concentration as the responses using the two higher concentrations of 7.5 and 10 µg/mL were almost identical. This suggested that sufficient saturation of the plate surface may be achieved using the 5 µg/mL coating concentration and, therefore, a higher concentration would be wasteful. This optimal coating concentration was then applied to part two of the assay optimisation (see section 2.8.6), which investigated the effect of varying the inner CRP concentration used in the assay.

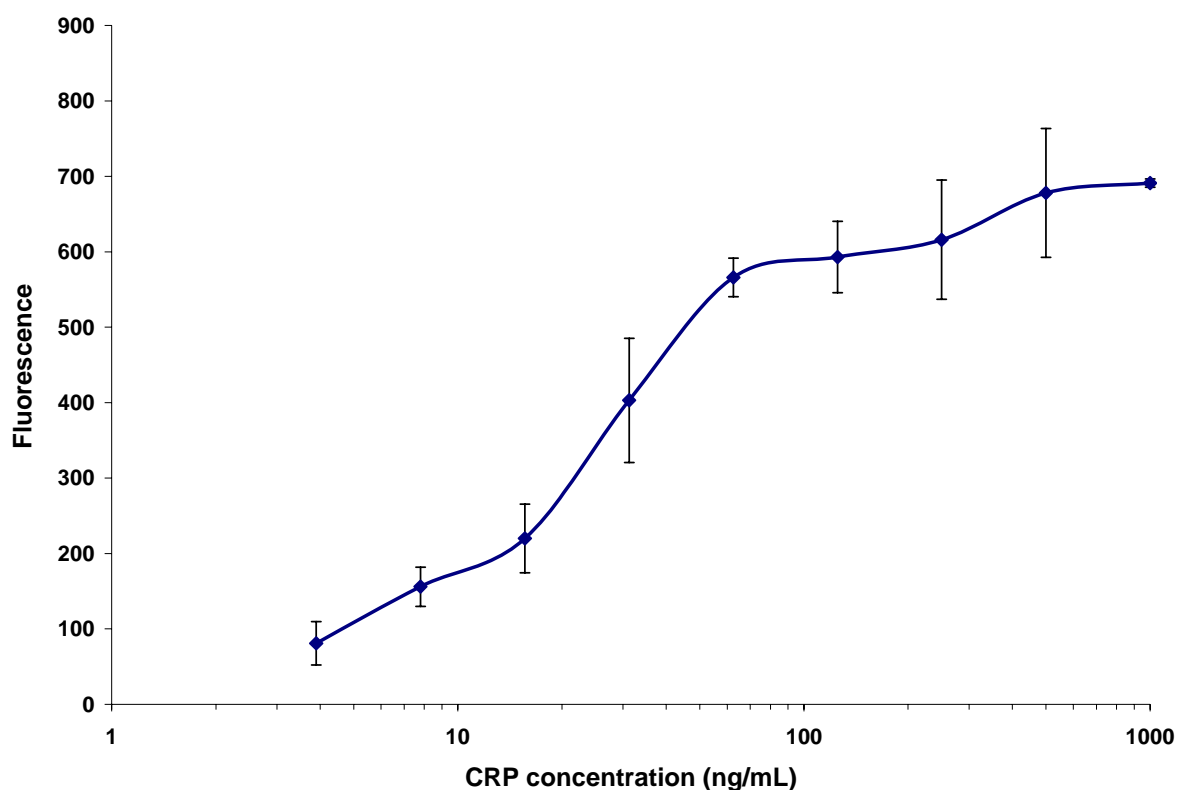


Figure 3.1.6 (c) shows the plotted averaged data from part two of the fluorescent sandwich ELISA optimization, performed in triplicate. An optimised coating concentration of 5 $\mu\text{g/mL}$ of purified CRP-specific pAb was used. The inner concentration of CRP was then varied from 1000, 500, 250, 125, 62.5, 31.25, 15.63, 7.8 to 3.9 ng/mL. The fluorescently-labelled detection pAb was also used at a set concentration (a 1/500 dilution). The mean response was plotted and the vertical error bars represent the SD over the 3 data points taken for each concentration ($n = 3$). Section 2.8.6 describes the parameters used for measurement of the fluorescent signal, including the excitation and emission wavelengths.

A good overall trend was observed for part 2 of the fluorescently labelled sandwich assay, however, performance of the assay involved several time-consuming steps. For instance, four separate incubation steps (coating, blocking, analyte, detection Ab) were required and the overall stability of fluorescent labels can cause significant assay variability. Therefore, it was decided to perform a more robust characterisation of the purified CRP-specific pAb using an automated SPR-based system.

3.1.7 'Real-time' characterisation of rabbit anti-CRP polyclonal antibody using Biacore.

Although ELISA is a robust immunoanalytical tool, it is very limited in its capacity for providing comprehensive information needed for antibody characterisation. Conversely, Biacore offers real-time, label-free analysis of binding interactions. A simple direct binding format was utilised for characterisation of the purified rabbit anti-CRP polyclonal antibody (pAb) on the Biacore 3000 system. Firstly, pre-concentration analysis (section 2.8.7) was performed on the purified rabbit anti-CRP pAb for identification of the optimal pH to employ for immobilisation onto the chip surface. The pAb was immobilised onto the surface of a CM5 sensorchip (GE Healthcare Life Sciences) using simple EDC-NHS coupling chemistry (see section 2.8.8). Next several concentrations of CRP antigen diluted in HBS buffer were passed across the chip surface. Each automated run incorporated a range of CRP concentrations, each concentration having 4 replicates. This run was performed 8 times in series, therefore yielding 32 data points for each concentration investigated. However, only replicates 2, 3 and 4 for each concentration were included in the data analysis, as replicate 1 consistently produced values for all 8 runs outside the data range. Figure 3.1.7 (a) shows a plot of the mean response values (RU) over each day of analysis.

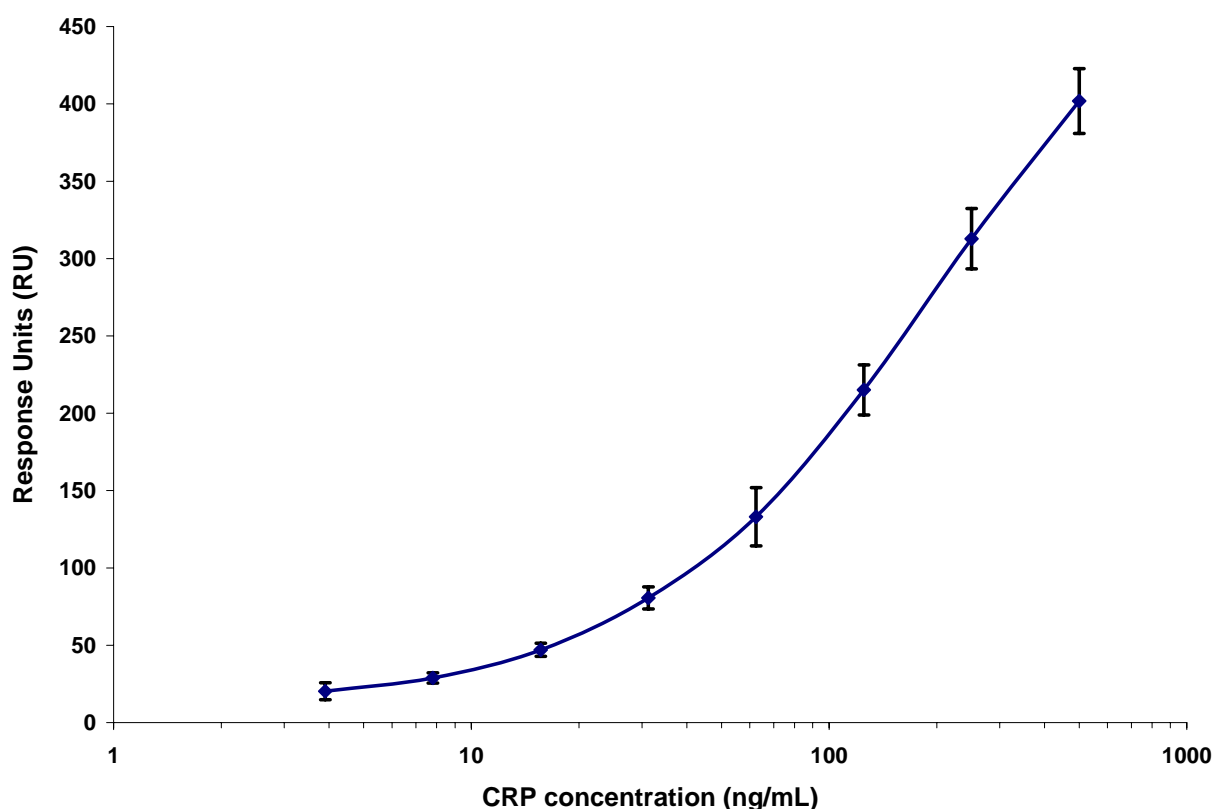


Figure 3.1.7 (a) shows a plot of the average CRP-binding response measured in response units (RU) on the Biacore 3000 system. A direct capture format was employed in the analysis involving a CM5 chip coated with purified rabbit anti-CRP pAb. Eight concentrations of CRP spiked into HBS buffer (500, 250, 125, 62.5, 31.3, 15.6, 7.8, 3.9 ng/mL) were passed across the pAb-immobilised chip surface. Also, a zero concentration made up of unspiked HBS buffer was run across the chip for subtraction analysis. The plotted results show the mean response \pm SD (vertical error bars), over each of the 3 days on which the assay was performed.

An excellent correlation between the CRP concentration and the binding response (RU) was observed. The standard error bars also further emphasized the high level of reproducibility within the assay. For a more comprehensive examination of the data, a 4-parameter equation calibration curve of the mean RU values was plotted against the standard CRP concentrations (ng/mL) on a logarithmic x-axis (Figure 3.17 b), using dedicated Biaevaluation software.

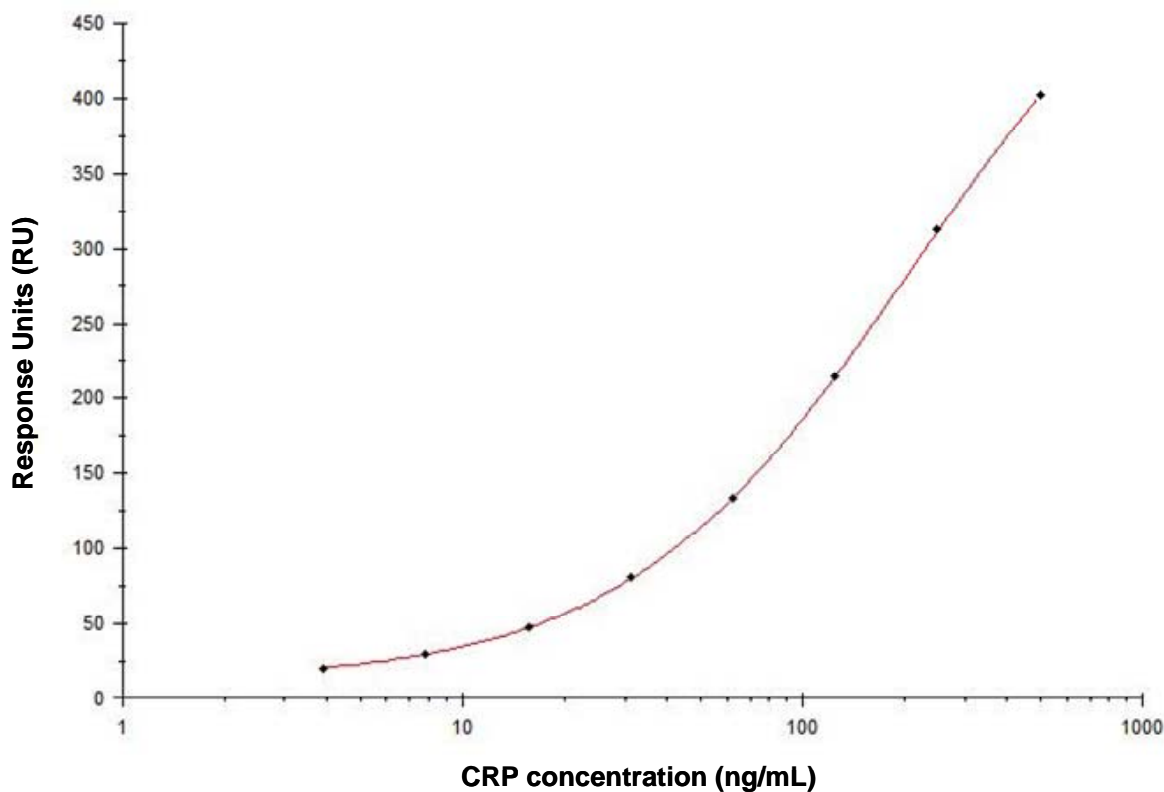


Figure 3.1.7 (b) shows a 4-parameter calibration curve generated from 9 identical direct capture assays on the Biacore 3000 system, involving purified rabbit anti-CRP pAb. The calibration curve was generated using dedicated Biaevaluation software.

The mean values for the standard CRP concentrations were then entered as ‘input values’ into the fitted equation and the resulting mean, back-calculated ‘output values’ found for each of the 9 data points of the assay. These output values represent how close the RU value is to its theoretical counterpart. The differences between the actual or ‘input’ concentrations and the ‘output’ concentrations extrapolated from the curve were used to calculate the % accuracy (Table 3.1.7), which determines a value for the precision of analytical measurement at different standard concentration points relative to the fitted 4-parameter plot. This value was calculated using the following equation:

$$\left(\left(\frac{\text{Output}}{\text{CRP}_{\text{conc.}}} - 1 \right) * 100 \right) + 100$$

Table 3.1.7 Response Units (RU) from direct binding assay of CRP antigen to CM5 chip immobilised with purified anti-CRP polyclonal antibody.

CRP conc. (ng/mL)	S.D. values	Biaevaluation Output value	% Accuracy value
0	4.73	Low	-
3.9	5.52	4.2	108.6
7.8	3.28	7.9	100.8
15.6	4.25	15.8	100.9
31.3	7.17	31.8	101.7
62.5	18.83	61.5	98.3
125	16.19	124.8	99.8
250	19.46	252.2	100.9
500	20.99	497.8	99.6

S.D. – Standard Deviations

Following observation of the accuracy values for each of the assay data points, it was clear that the assay has a high level of reproducibility. Generally, any accuracy value between 80 and 120 is acceptable (Wong *et al.*, 1997), therefore, the accuracy values for concentrations of 7.8 – 500 ng/mL show a high level of accuracy. The poorest accuracy value obtained from the statistical analysis was observed for the 3.9 ng/mL concentration (108.59), however, this accuracy value was still within the acceptable range. Furthermore, detection of CRP at this low range is not needed due to its relatively high basal concentration in the blood.

Both the limit of detection (LOD) and limit of quantitation (LOQ) values were also extrapolated from the 4-parameter calibration curve. An input value for the LOD and LOQ were calculated as follows:

- LOD – Zero value + 5 (Standard deviations)
- LOQ – Zero value + 10 (Standard deviations)

The 4-parameter equation was then used to extrapolate the LOD and LOQ values in ng/ml, which were 7.6 ng/mL and 18 ng/mL, respectively.

3.1.8 Discussion of results

The relatively rapid generation of polyclonal antibodies has led their frequent use in the field of diagnostics. It has been suggested that pAbs can be generated much more rapidly, at less expense and even with less technical skill than is required to produce mAbs (Lipman *et al.*, 2005). Once a sufficiently high serum titre response to the desired immunogen is achieved, a simple purification step (section 2.8.2) can yield large quantities of this useful reagent. Consequently, this bypasses the use of expensive molecular reagents and also the time-consuming process involved with construction of a recombinant antibody library. Polyclonal antibodies are a mixture of immunoglobulin molecules secreted against a specific antigen, each recognising a different epitope. The heterogenous nature of polyclonal antibody can hinder their specificity. This was indeed the case for the polyclonal antibody produced in this research, which showed cross-reactivity to SAP, a close homologue of CRP. The mixed population of polyclonal preparations, however, makes them ideal candidates as sensitive capture antibodies. Moreover, when combined with the specificity of a monoclonal antibody in a sandwich assay format, a potentially highly sensitive and specific test may be developed. The pAb generated in this research was successfully incorporated into both a fluorescent sandwich ELISA and also a direct capture assay on the Biacore 3000 system. Although the high sensitivity of the pAb is apparent on analysis of the fluorescent ELISA, a more accurate indication of the true sensitivity of the pAb was observed from the Biacore assay. The lowest concentration used in the assay was 3.9 ng/mL, however, the RU values observed for the zero concentration (control) were consistently lower than that for the 3.9 ng/mL concentration, suggesting a potential sensitivity even below the range of analyte concentrations investigated. One potential drawback associated with the use of pAb's, however, is the fact that they are limited in supply to the volume of serum taken from the sacrificed immune host. Conversely, the supply of recombinant antibodies can simply be replenished by culturing the specific clone harbouring the scFv-encoding DNA and purifying it from the expressed bacterial lysate (Ohara *et al.*, 2006). The use of recombinant phage display technology also allows for the production of monoclonal antibodies. The homogenous nature of monoclonal antibodies has led to their superiority in terms of specificity over polyclonal antibodies. Furthermore, one of the most defining characteristics of phage display is the direct link that exists between the phenotype and genotype of each of the clones in the recombinant library (Azzazy and

Highsmith, 2002; Paschke, 2006). This key feature facilitates the ability to refine almost any feature of the antibody such as their size, valency, affinity and even effector functions.

3.2 Generation and characterisation of mouse anti-CRP scFv library

3.2.1 Murine immune system

One of the first reports of the use of the murine immune system for monoclonal antibody production was accredited to Georges Köhler, César Milstein, and Niels Kaj Jerne in 1975 (Köhler and Milstein, 1975), who shared the Nobel Prize in Physiology or Medicine in 1984 for the ‘ground-breaking’ discovery of ‘hybridoma technology’ (discussed in section 1.8). These immortalised cell lines can produce an unlimited supply of a homogeneous, well-characterised antibody for use in a variety of applications, including in particular diagnosis and immunotherapy of pathological disorders. Subsequently, mice have become very popular for immunisation because of the ease of generation of murine monoclonal antibodies using hybridoma technology. However, this has extended into their application in the ever-growing field of recombinant antibody technology.

Use of the murine immune system for the construction of recombinant antibody libraries is well documented and has led to the production of high affinity recombinant antibodies to a vast array of specific antigens (Krebber *et al.*, 1997; Barbas *et al.*, 2001). Due to its small size, scFv fragments (See Figure 1.1) have been known to be more genetically stable than their larger Fab fragment counterpart (Hoogenboom *et al.*, 1998). Also, an extensive range of both PCR primers (particularly for Balb/c strain) and also methods for construction of mouse libraries have also been widely reported (Krebber *et al.*, 1997; Barbas *et al.*, 2001). Furthermore, the availability of a wide range of secondary reagents for the detection of mouse antibodies, have led to the murine immune system becoming a popular choice for antibody library construction.

3.2.2 Mouse serum titre.

Prior to sacrifice of the immunised mice, serum titres were performed to determine if a sufficient antibody response against the CRP antigen was generated. Serum from the immunised mouse was diluted (1/100 to 1/1,000,000 dilution) in PBS containing 1 % (w/v) milk marvel and tested against CRP in a direct ELISA format. A titre in excess of 1/100,000 against CRP was observed from the ELISA, indicating a high level of antibody generation, which indicates the presence of sufficient specific mRNA for creation of a recombinant antibody library against the specific antigen.

3.2.3 Mouse variable heavy and light chain optimisation in various buffer compositions.

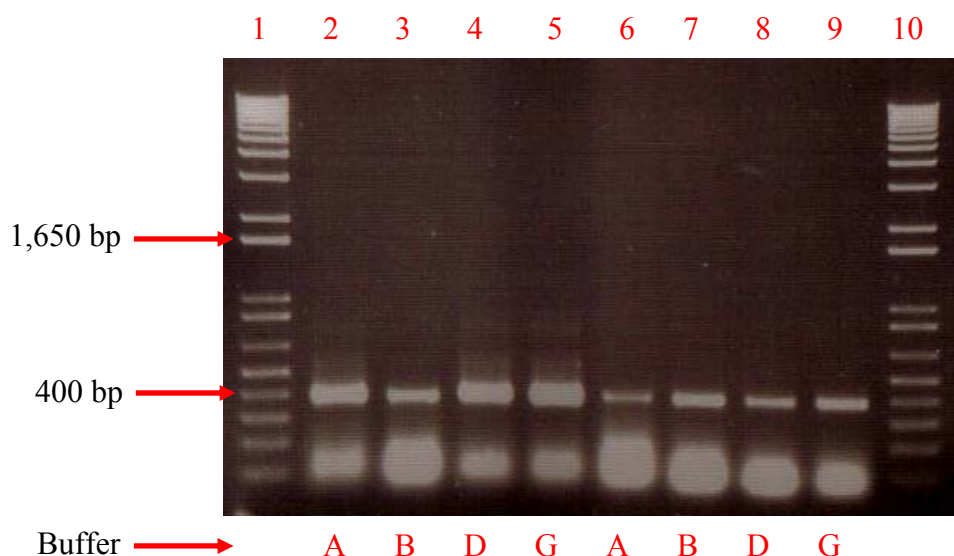


Figure 3.2.3 The optimisation of the variable heavy (VH) and variable light (VL) chain amplifications using the cDNA from a CRP-immunised Balb/c mouse. Lanes 1 and 10 contain a 1 kb Plus DNA molecular weight ladder (Invitrogen). The optimisation of the VH chains are represented in lanes 2-5 and the VL chains in lanes 6-9. The various buffer compositions were as follows: buffer A (7.5 mM MgCl₂, pH 8.5), buffer B (10 mM MgCl₂, pH 8.5), buffer D (17.5 mM MgCl₂, pH 8.5) and buffer G (12.5 mM MgCl₂, pH 9.5).

The V_H and V_L amplifications were resolved on a 1% (w/v) agarose gel and single bands at 386-440 bp (V_H chain) and 375-402 bp (V_L chain) were observed (See Figure 3.2.3). The results indicated that the most optimal buffer composition for the V_H and V_L chain amplifications were buffer G and buffer B, respectively. A large-scale PCR amplification was then performed, using the conditions described in section 3.1.5, for each of the variable chains in their respective buffers. Following purification of the V_H and V_L chains (see section 2.9.6), a SOE-PCR (section 2.9.7) was employed to fuse the two chains via a serine-glycine linker (G₄S)₄ resulting in the formation of the scFv fragment.

3.2.4 Mouse SOE-PCR of variable heavy and light chain.

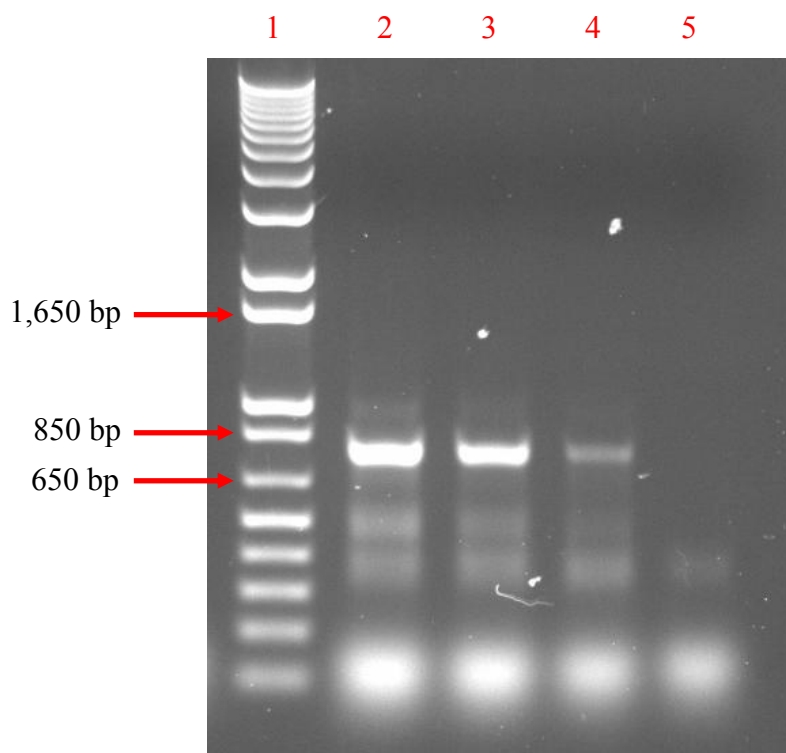


Figure 3.2.4 SOE-PCR using different DMSO concentrations to optimise the product yield. A 1 kb Plus DNA molecular weight marker was added to lane 1. Several DMSO concentrations were investigated i.e. 3, 5, 8 and 12% (v/v) as represented by lanes 2, 3, 4 and 5, respectively.

Both the purified VH and VL chain amplifications were incorporated in equimolar ratios into a SOE-PCR, producing a product size of ~800 bp. Some initial non-specific product was amplified. However, this was counteracted via the inclusion of DMSO into the PCR mixture. The resultant SOE products resolved on a 1% (w/v) agarose gel may be observed in Figure 3.2.4. The PCR mixture with a final DMSO concentration of 5% (v/v) proved to be the most optimal and was therefore used for the large-scale SOE-PCR of the scFv gene. Although a higher specific product yield was obtained using 3% (v/v) DMSO (lane 2), a reduced level of contaminant non-specific product was amplified using 5% (v/v) DMSO (lane 3).

3.2.5 Library construction and subsequent enrichment via biopanning.

The large-scale SOE product was concentrated via ethanol precipitation and quantified using the Nanodrop ND-1000™. Following quantification, the SOE product was then ligated into the pAK 100 vector (Krebber *et al.*, 1997) using the restriction enzyme *Sfi*I (see section 2.9.8). The successfully ligated product was then transformed into electrocompetent XL1-Blue cells by electroporation, using the protocol described in section 2.9.9. Several methods exist for the introduction of DNA into a bacterial host. One commonly used method is the chemical transformation or ‘heat shock’ technique, which may be employed when high efficiencies are not essential. In the case of diverse library building, however, a highly efficient method such as electroporation should be used. Electroporation is known to produce transformation efficiencies of 100 – 1000 times greater than those shown by chemically treated cells (Brown, 2000). The transformed mouse anti-CRP scFv library produced had a size of 2.94×10^6 cfu/mL. This library size may be considered relatively low, especially if the library was constructed from a non-immune/naïve B cell repertoire. However, in the case of immune libraries such as the one constructed in this work, the B cell repertoire used has the advantage of exposure to the required antigen. Consequently, there is a natural bias towards to required antigen and it has been reported that a library size of 5×10^7 should be sufficient for an immune library (Barbas *et al.*, 2001). Considering this library is approximately only 10 fold smaller than this figure, it was decided to proceed with the transformed library. The library was subject to phage display biopanning against immobilised CRP antigen, as described in sections 2.9.10 and 2.9.11.

Table 3.2.5 The phage input and output titres over the 4 rounds of biopanning of the mouse anti-CRP scFv library.

Biopanning round	Colony forming units/mL
Input 1	4.35×10^{12}
Output 1	2.65×10^9
Input 2	1.00×10^{13}
Output 2	8.65×10^9
Input 3	9.2×10^{12}
Output 3	6.0×10^7
Input 4	1.0×10^{13}
Challenge output remaining bound*	2.7×10^7
Challenge output dissociated*	5.4×10^5

* See section 2.9.11 for explanation

3.2.6 Mouse Polyclonal phage ELISA.

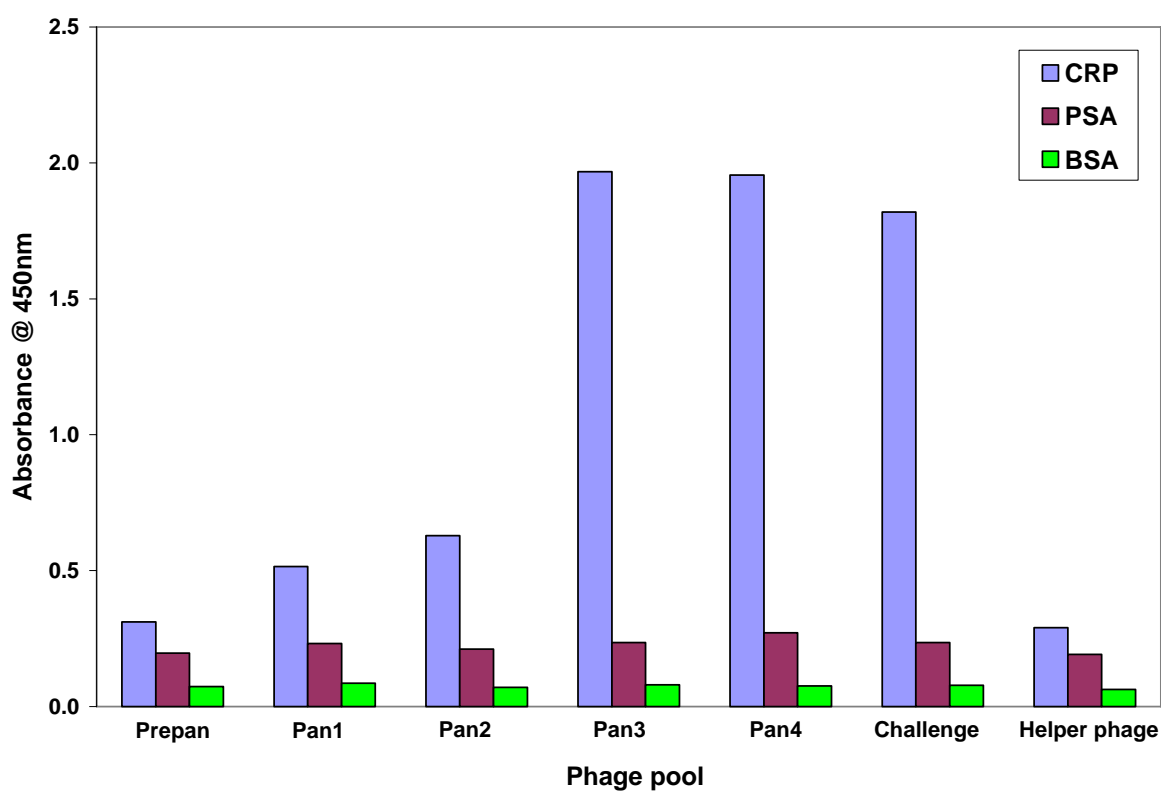


Figure 3.2.6 Polyclonal phage ELISA involving the phage pools of the unpanned library and the phage outputs from each of the successive rounds of panning. Each of the scFv-displaying phage pools were tested against the immunised CRP antigen, prostate specific antigen (PSA) and bovine serum albumin (BSA). M13K07 helper phage was also tested to identify any background non-specific binding.

The precipitated input phage from each round of panning were then incorporated into a polyclonal phage ELISA (section 2.9.12) to test for enrichment against the CRP antigen. PSA was included in the ELISA as parallel screening against PSA was being conducted in the lab during the same period, therefore, any potential cross-reactivity due to phage contamination may be identified. BSA was also tested as a negative control to observe the degree of non-specific ‘background’ binding. The ELISA also tested an antigen-challenged phage pool. The antigen challenge involved incubating 5 μ g of CRP on the washed immunotube for 10 min to remove any weakly binding phage-scFv fragments, which were infected as usual into mid-exponential phase XL-1 Blue cells. The scFv-displaying phage were detected using a HRP-conjugated mouse anti-M13 antibody (GE Healthcare Life Sciences) and the resultant

absorbance read at a wavelength of 450 nm following a 20 min incubation with TMB substrate. The sharp increase in absorbance from the second round onwards (Figure 3.2.6), suggested the presence of CRP-specific scFv-harboring phage within the panned library. Additionally, minimal or no binding was observed against both PSA and BSA.

3.2.7 Identification of scFv gene insert in panned murine scFv library.

A ‘colony-pick’ PCR (section 2.9.12) was then performed on 20 randomly selected individual colonies from the pan 4 output of the murine scFv library. The initial incubation of the colony at 94°C for 10 min results in the bacterial cell bursting, releasing the scFv-harboring plasmid DNA. The serine-glycine overlap extension primers then anneal to their respective sequences and amplify the scFv gene from the plasmid. The amplified scFv fragments were then analysed via gel electrophoresis on a 1% (w/v) agarose gel. Figure 3.2.7 shows the resultant scFv gene product (~ 800 bp) for 10 individual colonies from the pan 4 output of the murine scFv library.

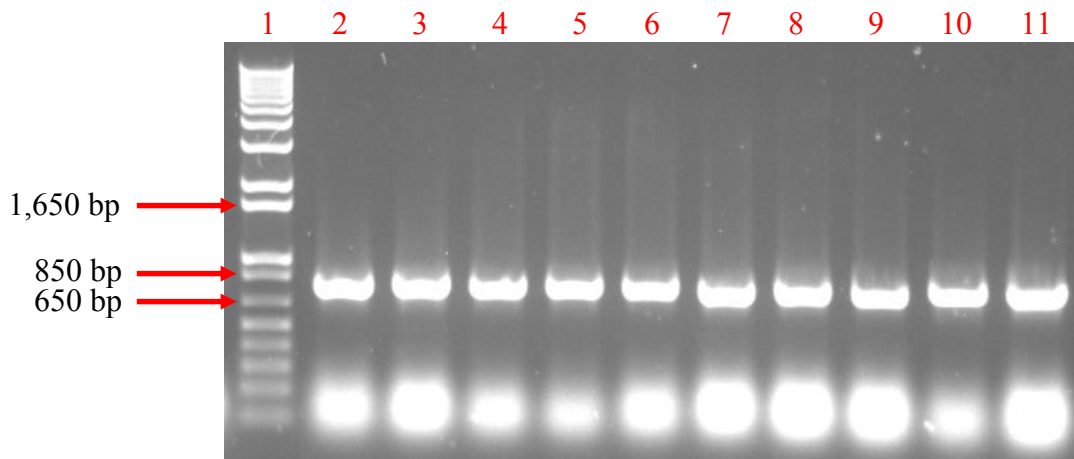


Figure 3.2.7 ‘Colony-pick’ PCR showing amplification of scFv gene inserts from 10 randomly selected clones from the murine library subjected to 4 rounds of bio-enrichment against CRP. A 1 kb Plus DNA molecular weight marker was added to lane 1. Lanes 1-10 represent the 10 successfully amplified scFv gene inserts.

3.2.8 Soluble expression and direct ELISA of mouse anti-CRP scFv clones.

Screening of the pan 4 output may be performed via monoclonal phage ELISA, however, due to the multivalent display on the phage, avidity effects may allow selection of antibodies with lower affinity (Kwasnikowski *et al.*, 2005). Therefore, the pan 4 output was subcloned into the expression vector pAK 400 (see section 2.9.13) and transformed into Top 10 F' *E. coli* cells for analysis via monoclonal soluble ELISA. A large number of single colonies (384) were then grown, solubly expressed and incorporated into a direct ELISA to identify scFv candidates for more 'in-depth' analysis (see section 2.9.14).

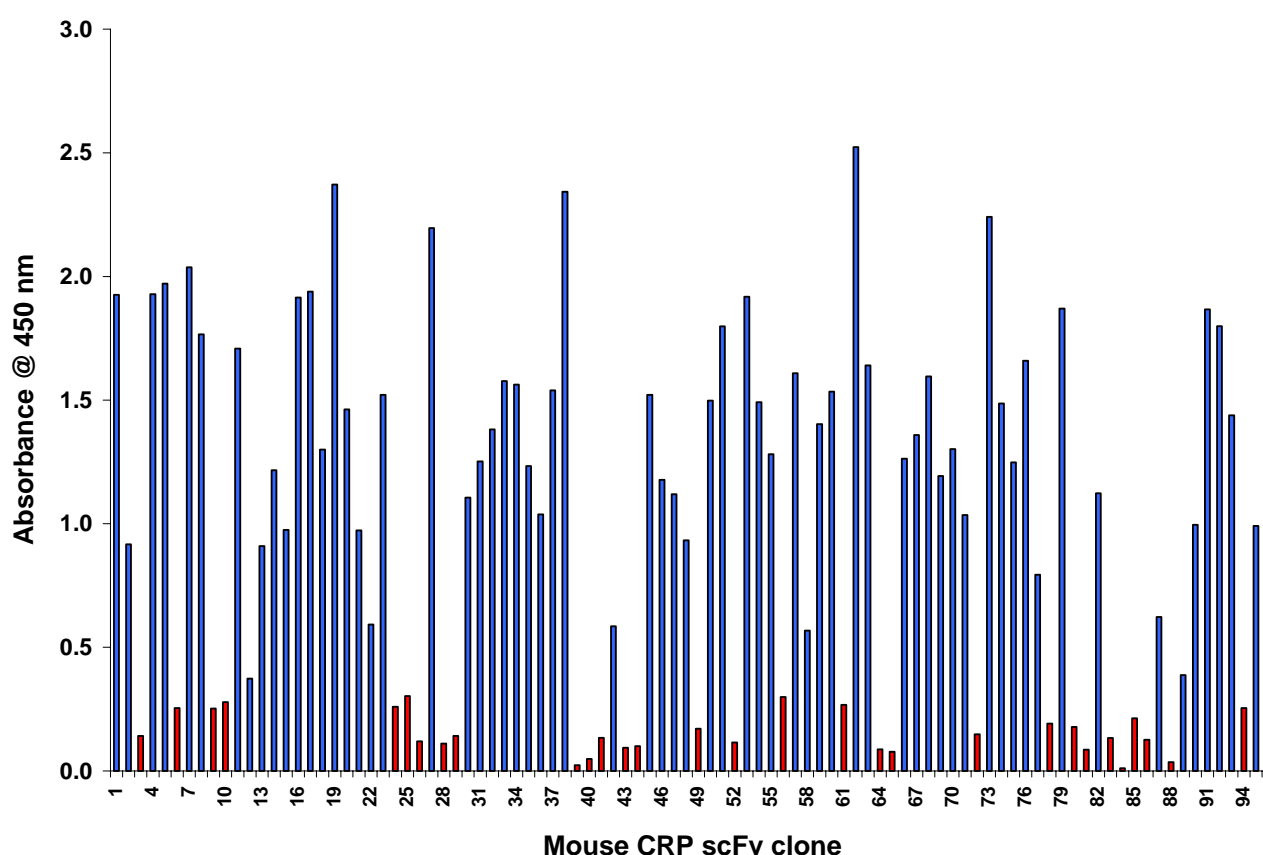


Figure 3.2.8 Direct ELISA using scFv-enriched lysate of 96 murine anti-CRP scFv clones. The bars highlighted in blue represent all the positive CRP-specific clones and the negative clones (response below the background level) are illustrated in red.

The scFv-enriched lysate was tested against both the target protein (CRP) and also BSA (negative control). Figure 3.2.8 represents absorbance values minus the background binding

values to BSA. Approximately, 250 clones specific for CRP were identified from the direct ELISA and taken forward for inhibition analysis (see section 2.9.14) to demonstrate their ability to bind CRP in solution.

3.2.9 Soluble inhibition ELISA of mouse anti-CRP scFv clones.

Initially, a crude inhibition ELISA format was performed on each of the expressed lysates of the 250 positive clones, identified from the the direct ELISA (previous section). This crude inhibition ELISA only utilised the higher free CRP concentrations (500 and 250 ng/mL), to identify clones showing any degree of depletion of CRP from solution (competitive clones). All of the competitive clones were then incorporated into a more comprehensive inhibition assay, investigating a large range of inhibiting CRP concentrations (Figure 3.2.9 a). These assays were used to extrapolate the degree of competitiveness of each of the clones tested.

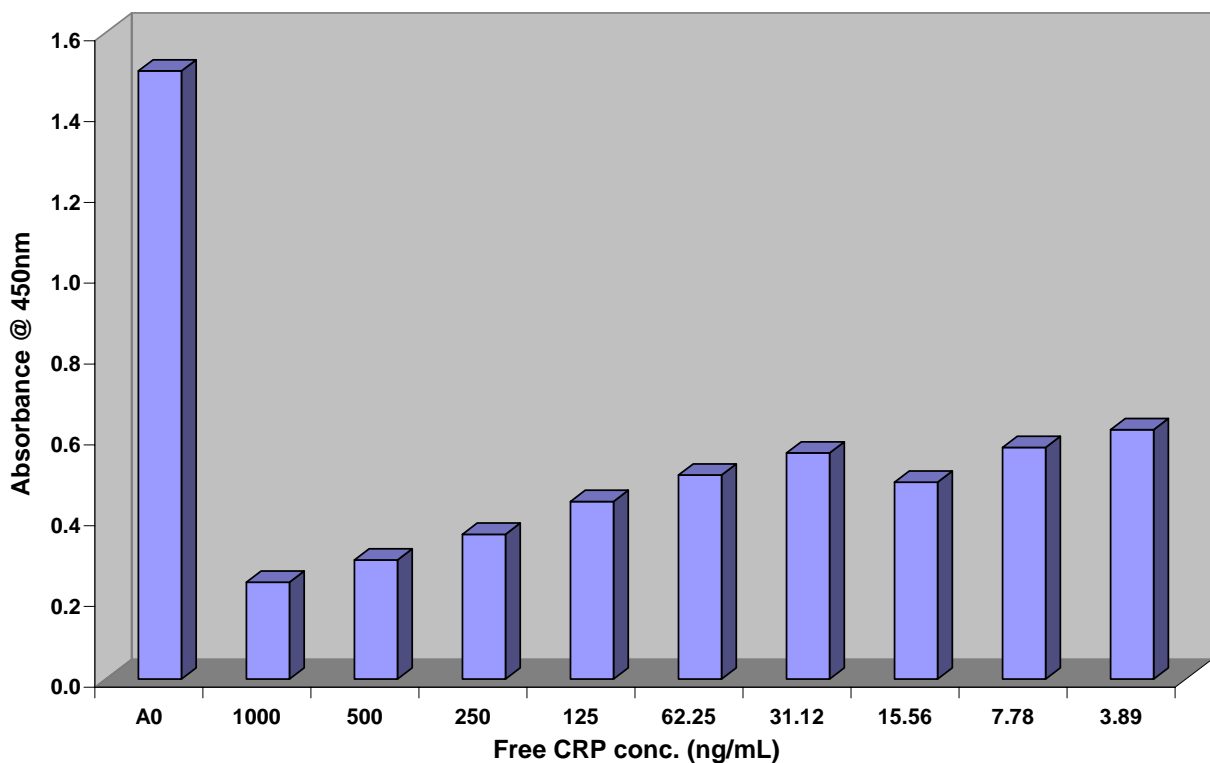


Figure 3.2.9 (a) An inhibition ELISA using the scFv-enriched lysate expressed from the murine anti-CRP scFv clone C11(2).

Figure 3.2.9 (a) illustrates typical inhibition ELISA data on crude lysate obtained from 5 mL cultures of the one of the best performing clones from inhibition analysis. The scFv-enriched lysate from clone C11(2) was pre-incubated with varying concentrations of CRP antigen (500, 250, 125, 62.5, 31.25, 15.625, 7.8, 3.9 ng/mL), which was then applied to a plate coated with CRP antigen (See Figure 3.2.9 b for assay format used). The scFv's ability to bind the free CRP in the pre-incubation is then determined by comparison of the absorbance response to the A0. The A0 consists of an aliquot of the same lysate without any prior incubation with free CRP. The scFv-captured CRP complex was detected using an anti-HIS (HRP-labelled) monoclonal antibody (mAb). It was observed that depletion of the free antigen is evident down to the low ng/mL range, as the absorbance level for the 3.9 ng/mL incubation is still clearly below that of the A0 control. Ten clones showing the most consistent and highest level of competition were taken forward for sequence analysis (section 3.2.10).

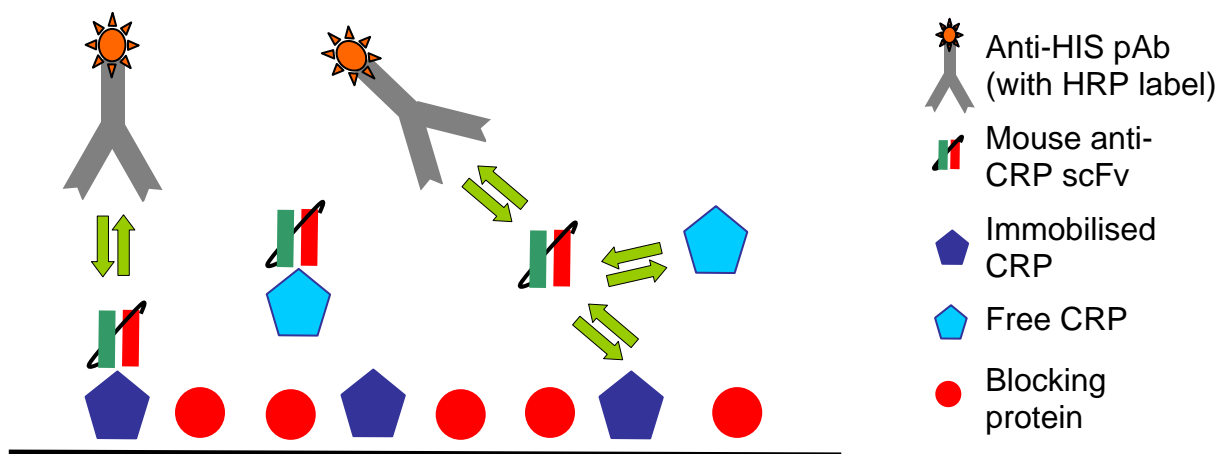


Figure 3.2.9 (b) Assay format used for inhibition ELISA.

3.2.10 Sequencing of 10 mouse anti-CRP scFv clones.

Clone	FLAG Tag	CDR - L1	CDR - L2	CDR - L3	Linker	HIS tag
H6 (3)	ADYKLIIV--METTQSPATLIVTPGDDRVSLSCRAASQSI	SDYLHWYQQRKSHESPRLLIKYASQSI	ISGIPSRFSGSGSGSDPFTLSINSVEPEVDVGVYCCQNGHSPFPTEFGGTRKLEIKRGGGGSGGGSGGGSGGGSEV			
H2 (3)	ADYKLIIV---ITQSPATLIVTPGDDRVSLSCRAASQSI	SDYLHWYQQRKSHESPRLLIKYASQSI	ISGIPSRFSGSGSGSDPFTLSINSVEPEVDVGVYCCQNGHSPFPTEFGGTRKLEIKRGGGGSGGGSGGGSGGGSEV			
E7 (2)	ADYKMETXMETTQSPATLIVTPGDDRVSLSCRAASQSI	SDYLHWYQQRKSHESPRLLIKYASQSI	ISGIPSRFSGSGSGSDPFTLSINSVEPEVDVGVYCCQNGHSPFPTEFGGTRKLEIKRGGGGSGGGSGGGSGGGSEV			
C8 (2)	ADYKLIIV--METTQSPATLIVTPGDDRVSLSCRAASQSI	SDYLHWYQQRKSHESPRLLIKYASQSI	ISGIPSRFSGSGSGSDPFTLSINSVEPEVDVGVYCCQNGHSPFPTEFGGTRKLEIKRGGGGSGGGSGGGSGGGSEV			
B9 (4)	ADYKLIIV--METTQSPATLIVTPGDDRVSLSCRAASQSI	SDYLHWYQQRKSHESPRLLIKYASQSI	ISGIPSRFSGSGSGSDPFTLSINSVEPEVDVGVYCCQNGHSPFPTEFGGTRKLEIKRGGGGSGGGSGGGSGGGSEV			
B8 (2)	ADYKLIIV--METTQSPATLIVTPGDDRVSLSCRAASQSI	SDYLHWYQQRKSHESPRLLIKYASQSI	ISGIPSRFSGSGSGSDPFTLSINSVEPEVDVGVYCCQNGHSPFPTEFGGTRKLEIKRGGGGSGGGSGGGSGGGSEV			
G10 (2)	ADYKLIIV--METTQSPATLIVTPGDDRVSLSCRAASQSI	SDYLHWYQQRKSHESPRLLIKYASQSI	ISGIPSRFSGSGSGSDPFTLSINSVEPEVDVGVYCCQNGHSPFPTEFGGTRKLEIKRGGGGSGGGSGGGSGGGSEV			
E11 (4)	ADYKLIIV--METTQSPATLIVTPGDDRVSLSCRAASQSI	SDYLHWYQQRKSHESPRLLIKYASQSI	ISGIPSRFSGSGSGSDPFTLSINSVEPEVDVGVYCCQNGHSPFPTEFGGTRKLEIKRGGGGSGGGSGGGSGGGSEV			
C5 (4)	ADYKLIIV--METTQSPATLIVTPGDDRVSLSCRAASQSI	SDYLHWYQQRKSHESPRLLIKYASQSI	ISGIPSRFSGSGSGSDPFTLSINSVEPEVDVGVYCCQNGHSPFPTEFGGTRKLEIKRGGGGSGGGSGGGSGGGSEV			
C11 (2)	ADYKLIIV--METTQSPATLIVTPGDDRVSLSCRAASQSI	SDYLHWYQQRKSHESPRLLIKYASQSI	ISGIPSRFSGSGSGSDPFTLSINSVEPEVDVGVYCCQNGHSPFPTEFGGTRKLEIKRGGGGSGGGSGGGSGGGSEV			
		CDR - H1	CDR - H2	CDR - H3		
H6 (3)	SEVQIQQSGPEPVKPGASVKMETSCKASGFTFTDYVIS--	WVKQRTGQGLEWIGIYIPVSDSTYYNENFKGKATLTADKSNNTAYMETQLSISLTSEDSAVYFCARSARLLRSDYDWGQGTTLITVSSAAGADHHHHH				
H2 (3)	SEVQIQQSGAELIVRPGSSVKIS--	CRASGYAFSSYMMETKAVKQRPGQGLVWIGIYIPGDDDTNNGRFRKRAVTLADKSSSTAYMETHLSSFTSEDSAVYFCVNRGNGHGMETDYMGGQGTVTWVSSAAGADHHHHH				
E7 (2)	SEVQIQQSGPEPVKPGASVKMETSCKASGFTFTDYVIS--	WVKQRTGQGLEWIGIYIPVSDSTYYNENFKGKATLTADKSNNTAYMETQLSISLTSEDSAVYFCARSARLLRSDYDWXGPGTTLITVSSAAGADHHHHH				
C8 (2)	SEVQIQQSGPEPVKPGASVKMETSCKASGFTFTDYVIS--	WVKQRTGQGLEWIGIYIPVSDSTYYNENFKGKATLTADKSNNTAYMETQLSISLTSEDSAVYFCARSARLLRSDYDWGQGTTLITVSSAAGADHHHHH				
B9 (4)	SEVQIQQSGPEPVKPGASVKMETSCKASGFTFTDYVIS--	WVKQRTGQGLEWIGIYIPVSDSTYYNENFKGKATLTADKSNNTAYMETQLSISLTSEDSAVYFCARSARLLRSDYDWGQGTTLITVSSAAGADHHHHH				
B8 (2)	SEVQIQQSGPEPVKPGASVKMETSCKASGFTFTDYVIS--	WVKQRTGQGLEWIGIYIPVSDSTYYNENFKGKATLTADKSNNTAYMETQLSISLTSEDSAVYFCARSARLLRSDYDWGQGTTLITVSSAAGADHHHHH				
G10 (2)	SEVQIQQSGPEPVKPGASVKMETSCKASGFTFTDYVIS--	WVKQRTGQGLEWIGIYIPVSDSTYYNENFKGKATLTADKSNNTAYMETQLSISLTSEDSAVYFCARSARLLRSDYDWGQGTTLITVSSAAGADHHHHH				
E11 (4)	SEVQIQQSGPEPVKPGASVKMETSCKASGFTFTDYVIS--	WVKQRTGQGLEWIGIYIPVSDSTYYNENFKGKATLTADKSNNTAYMETQLSISLTSEDSAVYFCARSARLLRSDYDWGQGTTLITVSSAAGADHHHHH				
C5 (4)	SEVQIQQSGPEPVKPGASVKMETSCKASGFTFTDYVIS--	WVKQRTGQGLEWIGIYIPVSDSTYYNENFKGKATLTADKSNNTAYMETQLSISLTSEDSAVYFCARSARLLRSDYDWGQGTTLITVSSAAGADHHHHH				
C11 (2)	SEVQIQQSGPEPVKPGASVKMETSCKASGFTFTDYVIS--	WVKQRTGQGLEWIGIYIPVSDSTYYNENFKGKATLTADKSNNTAYMETQLSISLTSEDSAVYFCARSARLLRSDYDWGQGTTLITVSSAAGADHHHHH				

Figure 3.2.10 Amino acid sequence alignment of functional variable domains of 10 murine anti-CRP scFv fragments. The three CDR regions for both the variable light (CDR-L) and variable heavy (CDR-H) regions are highlighted in blue. These blue regions determine the

specificity of the scFv for its target antigen. A glycine-serine linker (red) fuses the variable heavy and light regions together. This linker has sufficient flexibility to allow the two domains to assemble into a functional antigen-binding pocket. To aid in the purification and characterisation of the scFv fragments, both a poly-histidine tag (orange) and a FLAG tag (green) are incorporated into the structure.

The characterization process for each of the scFv clones in the pAK 400 vector (Krebber *et al.*, 1997) was severely hampered by the poor expression of the murine clones. The level of expression was so poor that a true IC50 value could not be established because of the inability to titre the lysates against plates coated with CRP antigen. Consequently, an IC50 value was estimated for inhibition analysis of each of the clones. Despite the fact that this approach still clearly identifies antigen depletion, the exact level or range of antigen depletion may not be reliable.

3.2.11 Biacore analysis of mouse anti-CRP scFv C11-2 in pAK400 format.

Several antibody-antigen assay formats may be employed on the Biacore system to obtain kinetic rate constants and binding affinities. For instance, a direct binding format may be used, involving the immobilization of purified CRP antigen on the sensor chip surface. Next, several concentrations of known concentration of purified scFv fragment may be passed across the CRP-immobilised surface. This approach may not be an accurate representation of the antibody-antigen interaction, however, as it is possible that the immobilization of the CRP to the surface may result in a non-native conformation. Furthermore, this approach requires purification of scFv from bacterial lysate and also the exact concentration of the purified scFv must be known. This direct binding format may be also be performed in reverse, whereby the purified scFv is immobilized onto the chip surface, followed by several concentrations of CRP antigen being passed across. In this case, there is no control over the scFv orientation on the sensor surface. Therefore, a large proportion of the scFv molecules will be non-functional, due to their binding epitopes being inaccessible. Consequently, it was decided to implement a capture-based assay format. Two potential capture tags may be used for detection of scFv fragments generated using the pAK system. Both a His and a FLAG tag are located in the C-terminal and N-terminals, respectively. During analysis of the scFv by both direct and inhibition ELISA (section 2.9.14), an anti-HIS (HRP-labelled) mAb was used for detection of the complex. Use of the His tag in such formats is acceptable, however, its non-

specific nature, restricts its application in more highly sensitive platforms such as Biacore. A study by Knappik and colleagues (Knappik and Pluckthun, 1994) found the commercially available anti-FLAG M1 antibody to be specific for the incorporated shortened FLAG tag sequence (Figure 3.2.10) of the pAK system.

Pre-concentration analysis followed by immobilization of the anti-FLAG M1 antibody were performed on a CM5 sensor chip (GE Healthcare), as described in sections 2.8.7 and 2.8.8, respectively. The mouse scFv clone C11-2 was cultured and expressed using an optimized expression medium (section 2.9.19) and the resultant lysate passed across the immobilized chip surface. No binding of the scFv to the anti-FLAG mAb immobilized surface was evident (Figure 3.2.11 a). An 'in-house' scFv with a fully-functional FLAG tag was also tested on the chip surface as a control and again no response was produced (results not shown).

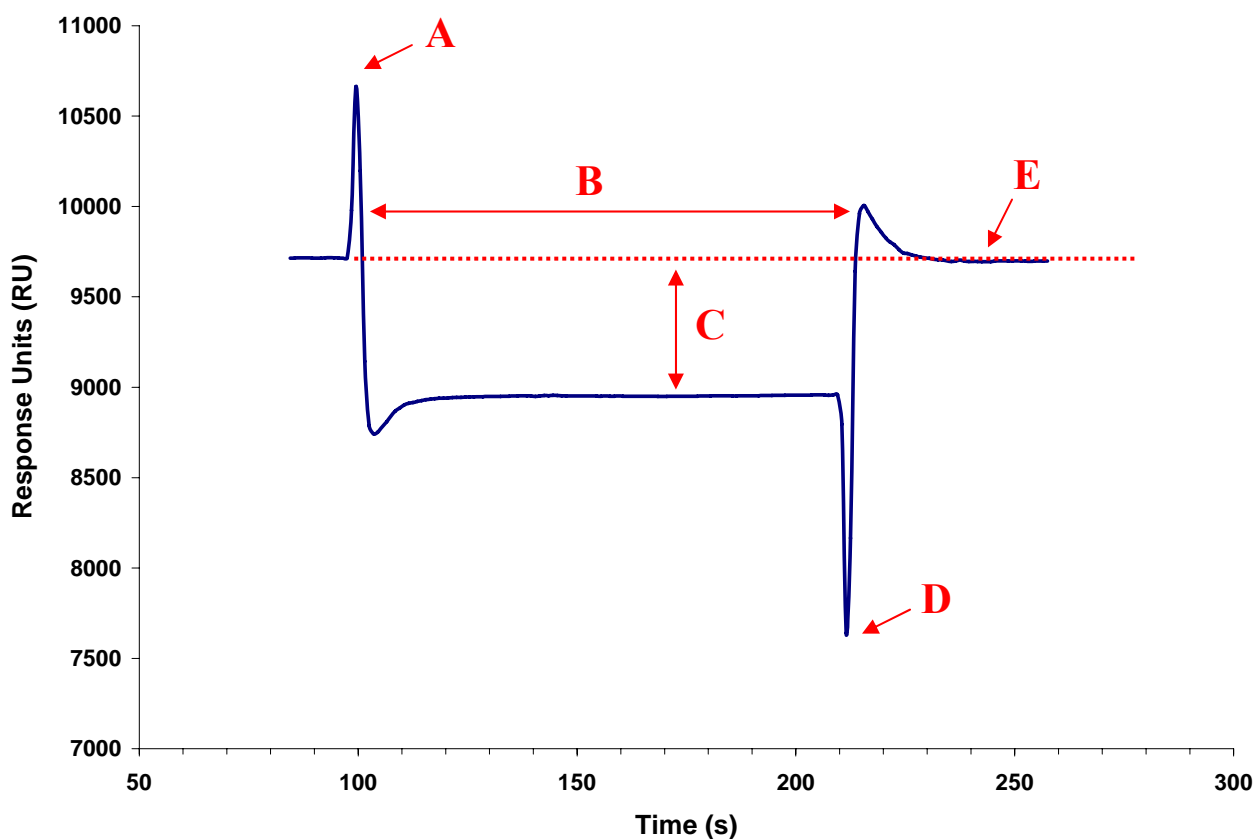


Figure 3.2.11 (a) Sensogram of C11-2 lysate (pAK 400 format) following passage across a CM5 chip immobilized with an anti-FLAG M1 mAb. The baseline level (anti-Flag mAb only) is represented by the red dotted line. The change from HBS buffer to scFv-rich lysate and vice-versa caused two drastic refractive index spikes, labelled as A and D, respectively. During passage of the lysate across the chip surface (B), an overall change in refractive index

(C) was observed. The final response (E) following completion of injection of the lysate was identical to the initial baseline level, indicating no binding.

As a further control, the same lysate was passed across another CM5 chip immobilized directly with CRP (Figure 3.2.11 b). Using an identical injection to that used with the anti-FLAG chip, a large binding response of approximately 380 RU's was observed. This eliminates the possibility of poor scFv expression being the cause of the lack of binding to the anti-FLAG chip. Moreover, this result would suggest that either the anti-FLAG mAb shows poor functionality or the N-terminal FLAG tag of the scFv is inaccessible.

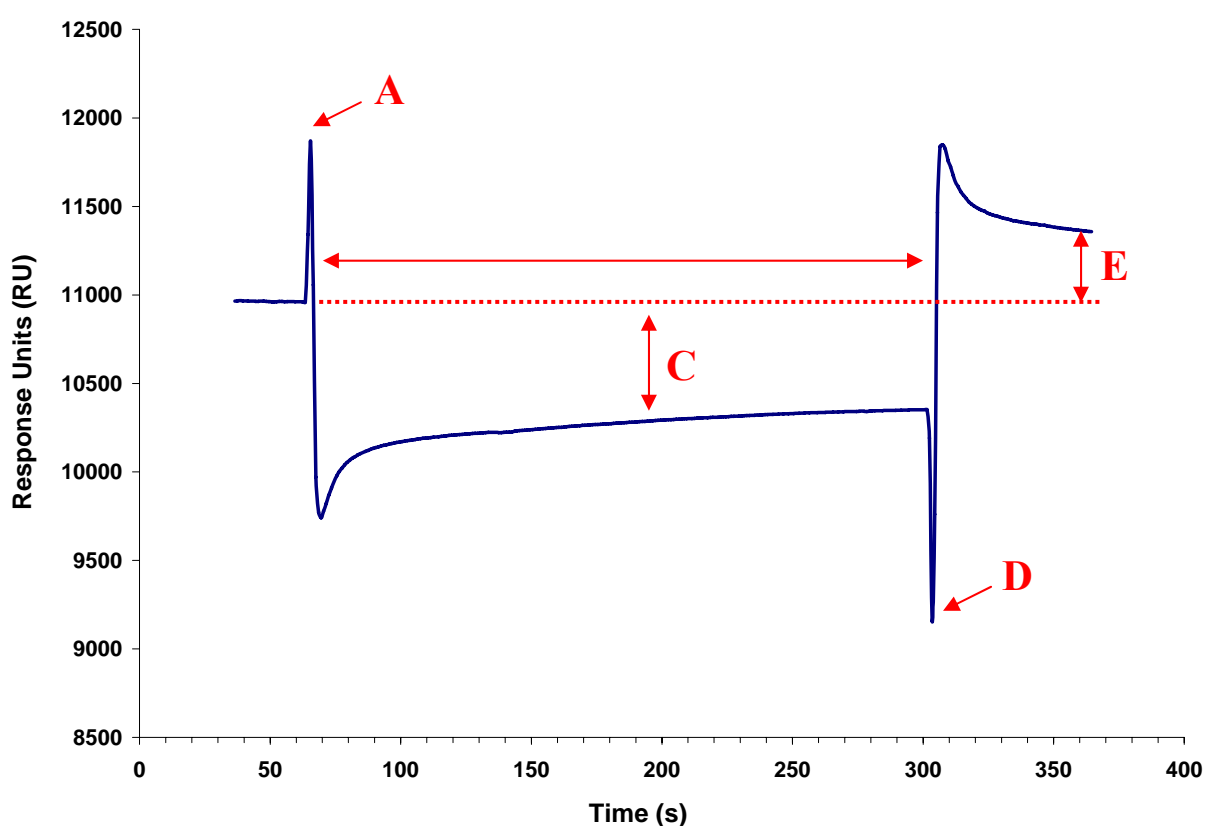


Figure 3.2.11 (b) Sensogram of C11-2 lysate (pAK 400 format) being passed across a CM5 chip immobilised with mCRP. The red dotted line represents the baseline level i.e. the CRP immobilised chip surface. The change from HBS buffer to lysate and vice-versa caused two drastic refractive index spikes, labelled as A and D, respectively. Additionally, during passage of the lysate across the CRP-immobilised chip surface (B), an overall change in refractive index (C) was observed. Finally, a change in the RU level (E) is shown following completion of the lysate injection.

3.2.12 Primer design and subcloning of C11-2 scFv via 'nested' PCR.

Both the non-specificity issues associated with his-tag capture and the flag tag inaccessibility of the pAK400 vector, have significantly reduced the capacity to produce reliable kinetic data on the C11-2 scFv clone in this format. To counteract this problem, it was decided to subclone the mouse anti-CRP C11-2 scFv into an alternative vector, namely the pComb3X vector (Barbas *et al.*, 2001). One of the main reasons behind the employment of this vector is its use of a highly specific hemagglutinin (HA) decapeptide tag. Use of the pComb3X system incorporates this affinity tag at the N-terminal of the scFv fragment, allowing for both more efficient screening and characterisation processes. In addition, it is possible that incorporation of the scFv into the pComb3X vector may lead to an improvement in its expression to further enhance the characterization process.

The *Sfi*I restriction sites were found to differ between the pAK and pComb systems as shown below:

<i>Sfi</i>I restriction site	
<i>pAK400 vector</i>	<i>pComb3X vector</i>
GGCCTCGGGGGCC	GGCCAGGCCGGCC

Therefore, to successfully subclone the C11-2 scFv into the pComb3X vector, this new *Sfi*I restriction site must be integrated into the scFv sequence. Firstly, the pComb series of murine primers (section 2.9.16) were analysed to identify the variable kappa (VK) sense primer showing the closest homology to that of the 5' end of the scFv light chain sequence. The sequence of the relevant VK forward primer (MSCVK5) is shown below:

5' GGG CCC AGG CGG CCG AGC TCG AYA TTG TRA TGA CMC AGT C 3'

Next, a variable heavy (VH) anti-sense primer was designed, which consisted of a generic sequence (shown below) common to the 5' end of all the VH reverse primers of the pComb series.

5' CCT GGC CGG CCT GGC CAC TAG TGA 3'

This was coupled with a sequence of bases common to the scFv variable heavy chain at the 3' end of a generic pAK sequence (shown below).

5' GAG GAG ACT GTG AGA GTG GTG CCT TC3'

The full sequence of the designed primer (SubRev) was as follows:

5' CCT GGC CGG CCT GGC CAC TAG TGA GAG GAG ACT GTG AGA GTG GTG
CCT TC 3'

The C11-2 clone was cultured and subjected to a plasmid extraction (section 2.9.13) to purify the pAK400 vector harbouring the scFv. Next, an *Sfi*I restriction digest was performed on the plasmid preparation to isolate the scFv insert (section 2.9.13) and then resolved via electrophoresis on a 1% (w/v) agarose gel. Following sufficient resolution, the scFv insert (~800 bp) was purified using a QIAquick™ gel extraction kit. This restricted scFv gene product was used as the template DNA for part 1 of a 'nested' type PCR reaction (section 2.9.17). This so-called 'nested' PCR was performed in two parts:

- Part 1 – C11-2 scFv in pAK format used as the template for PCR.
- Part 2 – PCR product from part 1 used as the template for PCR.

The use of a two part 'nested' PCR was required to enrich against the old pAK400 format of the scFv, thus reducing the potential for any contamination of this old pAK format in the final amplified product from part 2. To further ensure that the final product from part 2 was the scFv in the new pComb format, the minimum level of product from part 1 (~21 ng) was used as the template DNA.

An annealing temperature gradient was also incorporated into part 1 (section 2.9.17 a) of the 'nested' PCR. This was employed to identify the most optimal conditions for avoidance of contamination from any non-specific amplified products. The five different annealing temperatures investigated were 50.9, 52.9, 55.5, 58.4 and 59.8°C (Figure 3.2.12).

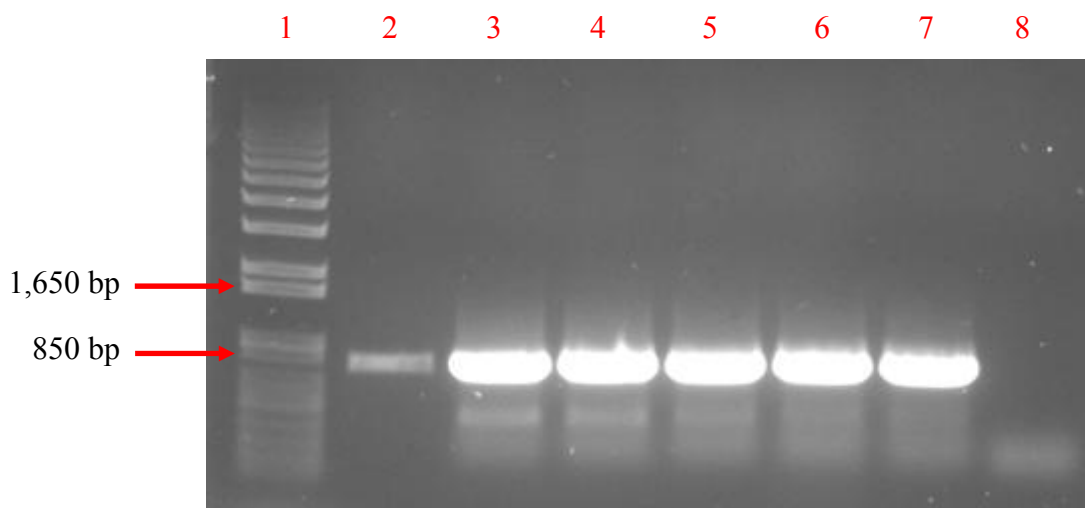


Figure 3.2.12 Optimisation of part 1 of the ‘nested’ PCR using various annealing temperatures. Lanes 3-7 represent the PCR products of the annealing temperatures of 50.9, 52.9, 55.5, 58.4 and 59.8°C, respectively. Lane 1 contains a 1 kb Plus DNA molecular weight ladder (Invitrogen). A small quantity of the scFv template used in the PCR was also resolved on the gel in lane 2. Finally, lane 8 shows a negative control, consisting of all the PCR components except the template DNA.

The PCR reaction using an annealing temperature of 59.8°C proved to be the most optimal, as the non-specific bands were least prevalent under these conditions. This reaction was scaled-up and resolved via electrophoresis on a 1% (w/v) agarose gel and gel-purified again using the QIAquick™ gel extraction kit. Part 2 (section 2.9.17 b) of the PCR then used this purified product as template for amplification of the final modified scFv gene. The amplified product was again resolved and gel-purified as before.

3.2.13 Identification of successfully subcloned scFv fragments via direct and inhibition ELISA.

The purified C11-2 scFv in the pComb format (product from part 2) was cloned into the pComb3X vector using *Sfi*I restriction enzyme as outlined in section 2.9.18. Prior to the ligation of the modified scFv gene, the digested pComb3X vector was treated with Antarctic Phosphatase™ enzyme to prevent self-ligation of the vector (see section 2.9.18). The ligated product was then electroporated into Top 10 F' cells for soluble expression (general method described in section 2.9.9).

Twenty single colonies from the transformation titre plates were then cultured, solubly expressed and incorporated into a direct ELISA (as per the general protocol described in section 2.9.14) to identify successfully subcloned scFv fragments. The expressed lysates of each of the clones were tested in duplicate against wells coated with 10 $\mu\text{g}/\text{mL}$ of CRP in PBS. Detection of the bound scFv using a HRP-labelled anti-HA mAb (Roche Applied Science) identified three potential scFv candidates (Figure 3.2.13 a).

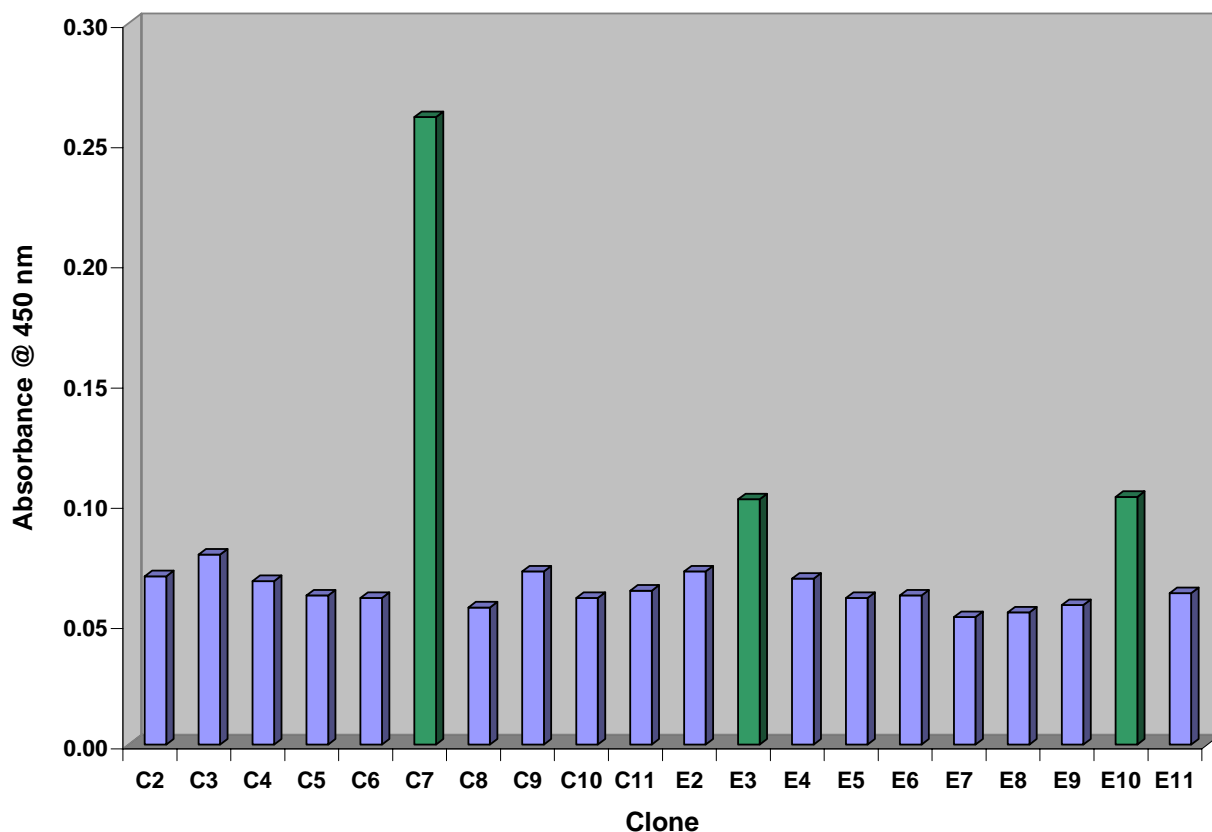


Figure 3.2.13 (a) Direct ELISA using scFv-enriched lysate from 20 candidate scFv clones. The bars highlighted in green represent potential scFv candidates in new pComb format and clones considered to be negative are illustrated in blue.

Some lysate from the C7 clone was titred and than then taken forward for use in a quick inhibition ELISA (Figure 3.2.13 b) to identify the scFv's ability to bind CRP from solution. Depletion of the CRP antigen was clearly evident from the inhibition analysis and, furthermore, the overall expression of the scFv in the pComb3X vector showed a minor improvement from that observed in the pAK400 vector.

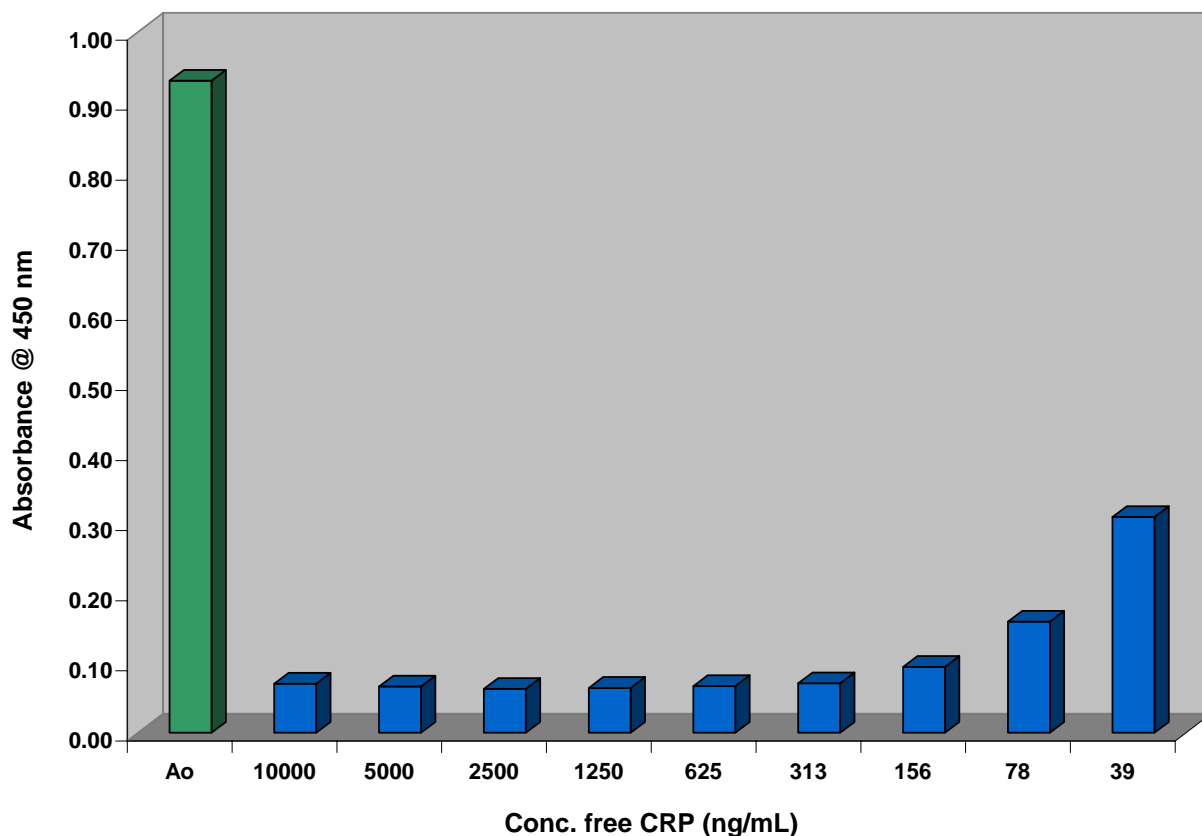


Figure 3.2.13 (b) An inhibition ELISA using the scFv-enriched lysate expressed from the murine anti-CRP scFv C11(2) subcloned into the pComb3X vector. The binding response of the scFv-rich lysate with no inhibition of free CRP (Ao) is shown in green. The bars in blue represent the same lysate incubated with varying concentrations of CRP antigen.

3.2.14 Sequence analysis of mouse anti-CRP scFv C11-2 subclone.

Both the sequences of the initial murine CRP-specific C11-2 scFv (pAK version) and its subsequent reformatted pComb version were compared to identify successful reformatting of the fragment into its new format. On analysis of the translated sequences of both clones (Figure 3.2.14), it was evident that the reformatted version was identical to its original format, except the flag tag was removed and also the highly-specific HA tag was incorporated alongside the already existing his tag.

C11-2 scFv (pAK format)

ADYKDIV **Met** TQSPATLSVTPGDRVSLSC **RASQSISDYLH**
WYQQKSHESPRLLIK **YASQIS** GIPSRFSGSGSGSDFTLS
INSVEPEDVGVYYC **QNGHSFPPT** FGGGTKLEIKR **GGGGS**
GGGSGGGSSGGGS EVQLQQSGPEPVKPGASVK **Met** S **C**
KASGFTFTDYVIS WVKQRTGQGLEWIG **EIYPVSDSTYYNE**
NF KGKATLTADKSSNTAY **Met** QLSSLTSEDSAVYFCAR **SA**
RLRSSYDY WGQGTTTLTVSSASGGD **HHHHHH**

C11-2 scFv (pComb format)

AAELDIV **Met** TQSPATLSVTPGDRVSLSC **RASQSISDYLH**W
YQQKSHESPRLLIK **YASQIS** GIPSRFSGSGSGSDFTLSIN
SVEPEDVGVYYC **QNGHSFPPT** FGGGTKLEIKR **GGGSGGG**
GGSGGGSSGGGS EVQLQQSGPEPVKPGASVK **Met** S **CKA**
SGFTFTDYVIS WVKQRTGQGLEWIG **EIYPVSDSTYYNENF**
KGKATLTADKSSNTAY **Met** QLSSLTSEDSAVYFCAR **SARLL**
RSSYDY WGE GTTLTVPLTSGQAGQ **HHHHHH** GAYPYDVP
DYAS

Figure 3.2.14 Sequences of the mouse anti-CRP C11-2 scFv clone in its original pAK format and its engineered pComb format. The three CDR regions for both the variable light (CDR-L) and variable heavy (CDR-H) regions are highlighted in blue and red, respectively. A glycine-serine linker (green) fuses the variable heavy and light regions together (green font). In the pAK format, a FLAG tag is shown in brown. A hexa-histidine tag (orange) is incorporated into both formats. Finally, a novel HA epitope tag (purple) is integrated into the scFv by the pComb system.

In all known species with an adaptive immune system, CDR-H3 is more diverse than any of the other five CDR regions (CDR-H1, CDR-H2, CDR-L1, CDR-L2, CDR-L3) that together form the outside border of the antigen-binding site (Kirkham and Schroeder, 1994; Padlan, 1994; Al-Lazikani *et al.*, 1997; Litman *et al.*, 1999). However, although the CDR-H3 region is generally associated with a high level of variability, the actual amino acid utilization is

typically non-random, whereby neutral hydrophilic amino acid residues such as tyrosine, glycine and serine have been shown to dominate (Ivanov *et al.*, 2002). On closer inspection of the amino acid sequence of the murine C11-2 scFv, such dominance of amino acids like tyrosine and serine is particularly evident. Tyrosine dominance in particular has been identified as a common feature associated with the murine CDR-H3 repertoire (Zemlin *et al.*, 2003). The use of tyrosine may confer structural diversity as it allows for many forms of inter- and intramolecular bonding (hydrogen bonding through its hydroxyl group, hydrophobic and electrostatic interactions via its aromatic ring).

3.2.15 Cross-reactivity analysis of mouse anti-CRP scFv C11-2 subclone via ELISA.

Another essential task in antibody characterisation is the analysis of cross-reactivity to homologous analytes. As discussed previously, SAP has been shown to have a high sequence homology to that of CRP. Any cross-reactivity of the scFv fragment to SAP, will lead to false positive results in patient blood testing. Therefore, the exclusion of cross-reactivity to such contaminant analytes is a key requirement in the field of diagnostics.

Expressed lysate from the C7 clone was incorporated into a direct ELISA (general protocol in section 2.9.14) against CRP, its homologous counterpart SAP and also BSA (background binding response). Both purified avian anti-CRP H2 scFv (see section 3.3.5) and rabbit anti-CRP pAb (see section 3.1.4) were also employed in the ELISA as negative and positive controls, respectively. HRP-labelled anti-HA mAb (Roche Applied Science) was used as a secondary antibody for detection of both the subcloned C11-2 scFv and the avian H2 scFv via the HA tag. The purified rabbit polyclonal antibody (positive control) was detected using a HRP-labelled anti-rabbit secondary antibody. Figure 3.2.15 (a) clearly illustrates the lack of any reactivity, of both the murine C11-2 scFv subclone and the avian H2 scFv, with SAP. Furthermore, the response to SAP was shown to be almost identical to that of the background binding levels (BSA), which again highlights the lack of any cross-reactivity to this homologous analyte.

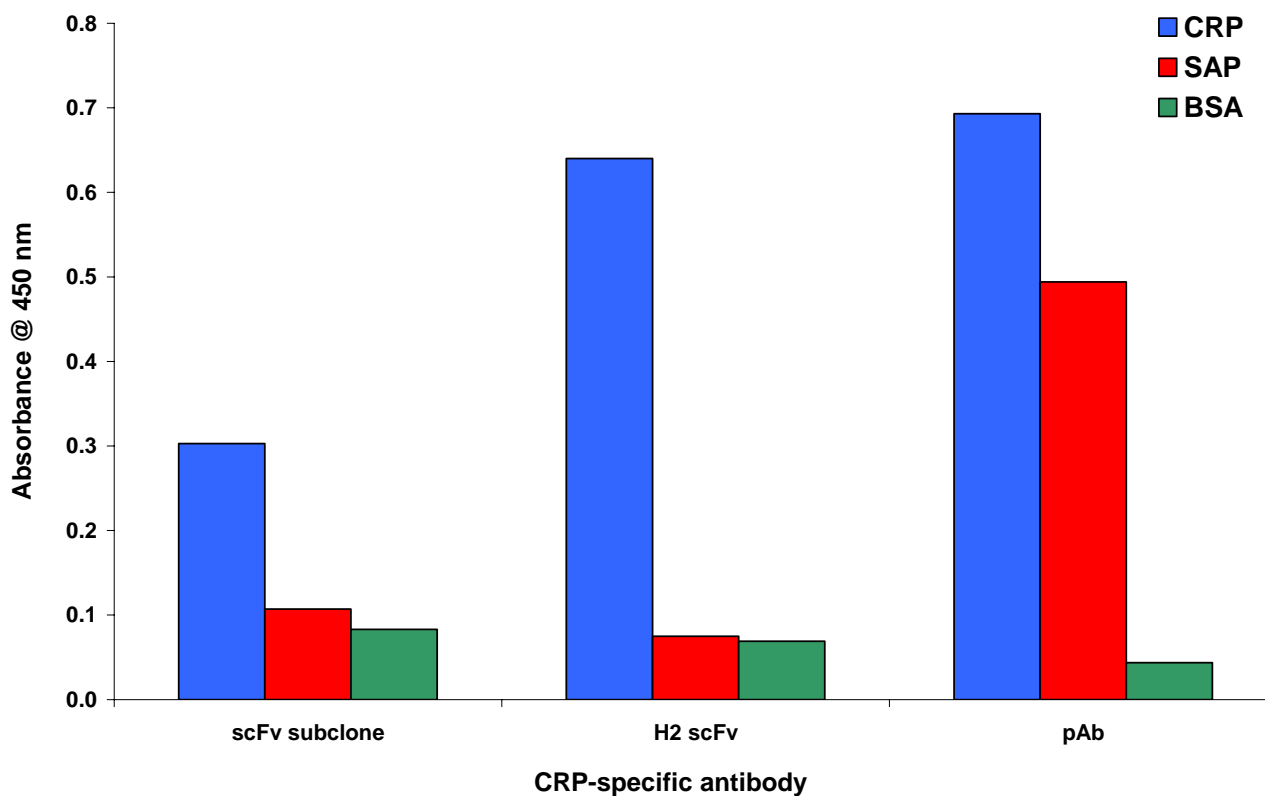


Figure 3.2.15 (a) Cross reactivity analysis of mouse C11-2 scFv subclone, avian H2 scFv and rabbit pAb via direct ELISA. The bars in blue, red and green represent the binding response in absorbance units to CRP, SAP and BSA (negative control), respectively.

Further verification of this result was conducted via analysis on the Biacore 3000 system. A capture-based approach was used involving an anti-HA mAb directly immobilised onto the CM5 chip (as per the general protocol described in section 2.8.8). Lysate from the expressed C11-2 scFv subclone was then passed across the immobilized chip-surface, resulting in subsequent capture of the scFv. Finally, CRP and SAP were both diluted in HBS buffer to a concentration of 1 $\mu\text{g}/\text{mL}$, passed across the scFv captured surface and their binding responses (RU value) monitored. Figure 3.2.15 (b) clearly identifies no binding of both the scFv subclone and the avian H2 scFv to the SAP analyte. CRP was also passed across the scFv-captured surface as a positive control to ensure functionality of the scFv used in the analysis.

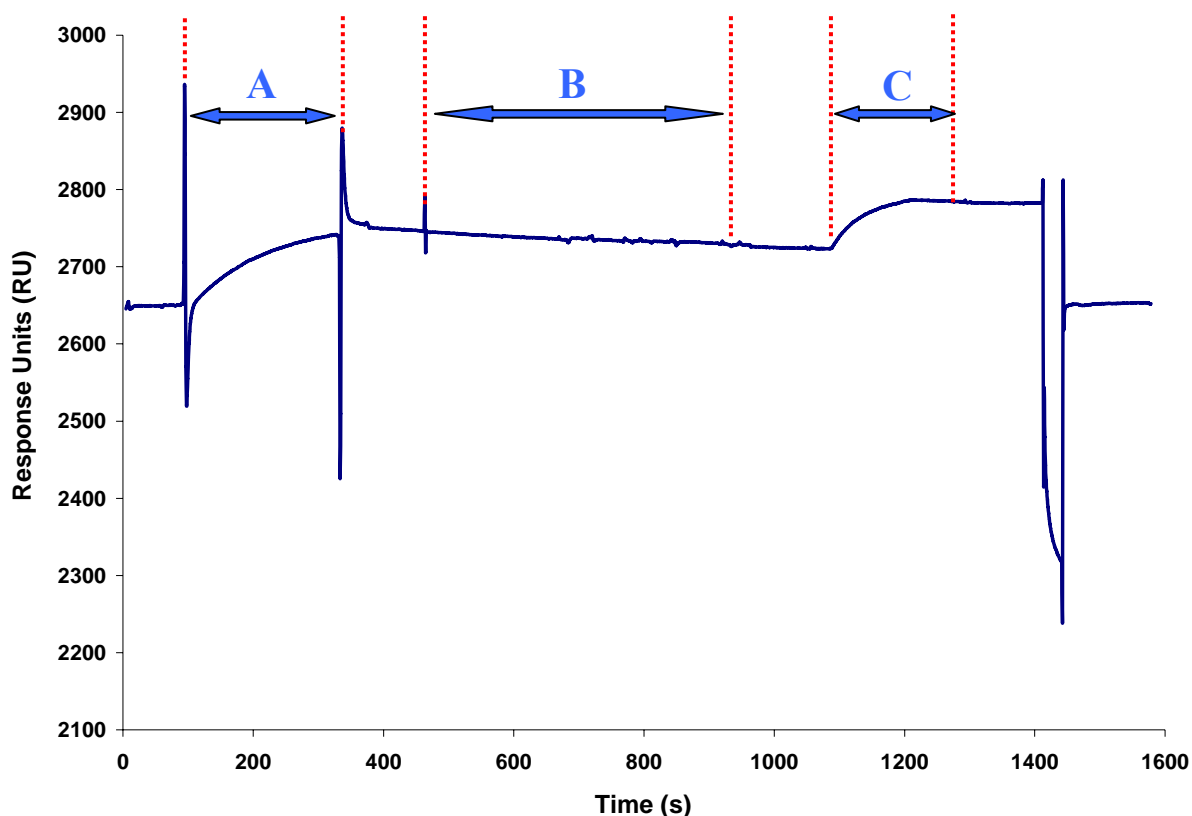


Figure 3.2.15 (b) Cross reactivity analysis of C11-2 scFv subclone lysate using an anti-HA capture method on the Biacore 3000. The sensogram represents the capture level of the C11-2 scFv subclone (A) on the anti-HA immobilized CM5 chip surface. Also, the subsequent binding responses of the captured scFv to both SAP (B) and CRP (C) are shown.

3.2.16 Kinetic analysis of C11-2 scFv subclone using the Biacore 3000 system.

The native pentameric form of CRP proves to be somewhat troublesome when a capture-based kinetic analysis format is employed. One of the simplest and yet most efficient models for obtaining high precision and reliable kinetic data is the 1:1 Langmuir equation. As the name suggests, a 1:1 ratio of ligand (scFv) to analyte (CRP) is required for implementation of this model. The use of native CRP in this format would result in a much more complex interaction of CRP with the captured scFv. Such is the complexity of the interaction that a simple 1:1 equation proves insufficient. Consequently, the monomeric sub-unit of CRP referred to as monomeric or modified CRP (mCRP) was employed in the ‘real-time’ analysis. The modified form of CRP was prepared using the method described by Kresl and colleagues (Kresl *et al.*, 1998) (see section 2.10.5). Furthermore, mCRP has been shown to directly facilitate endothelial cell adhesion molecule expression, leukocyte adhesion, and MCP-1 and

IL-8 production, indicating that mCRP rather than native CRP may contribute to the development of vascular inflammation (Khreiss *et al.*, 2004a). Therefore, antibodies with specificity for detection of both native CRP and its monomeric counterpart may prove to be key requirements in more accurate risk stratification.

Some preliminary Biacore analysis was first performed to ensure that the C11-2 scFv subclone does in fact bind the mCRP sub-unit. It is possible that the scFv fragment reacts with CRP at the linker regions responsible for combining the monomeric units into its native pentameric structure. Fresh C11-2 subclone lysate was prepared using an optimized expression protocol (section 2.9.19) and passed across the anti-HA immobilized chip. Both CRP and its monomeric sub-unit mCRP were then passed across the capture scFv at a concentration of 1 $\mu\text{g}/\text{mL}$ in HBS buffer. It is evident from Figure 3.2.16 (a) that the C11-2 scFv subclone binds both the native pentameric form and its monomeric sub-units.

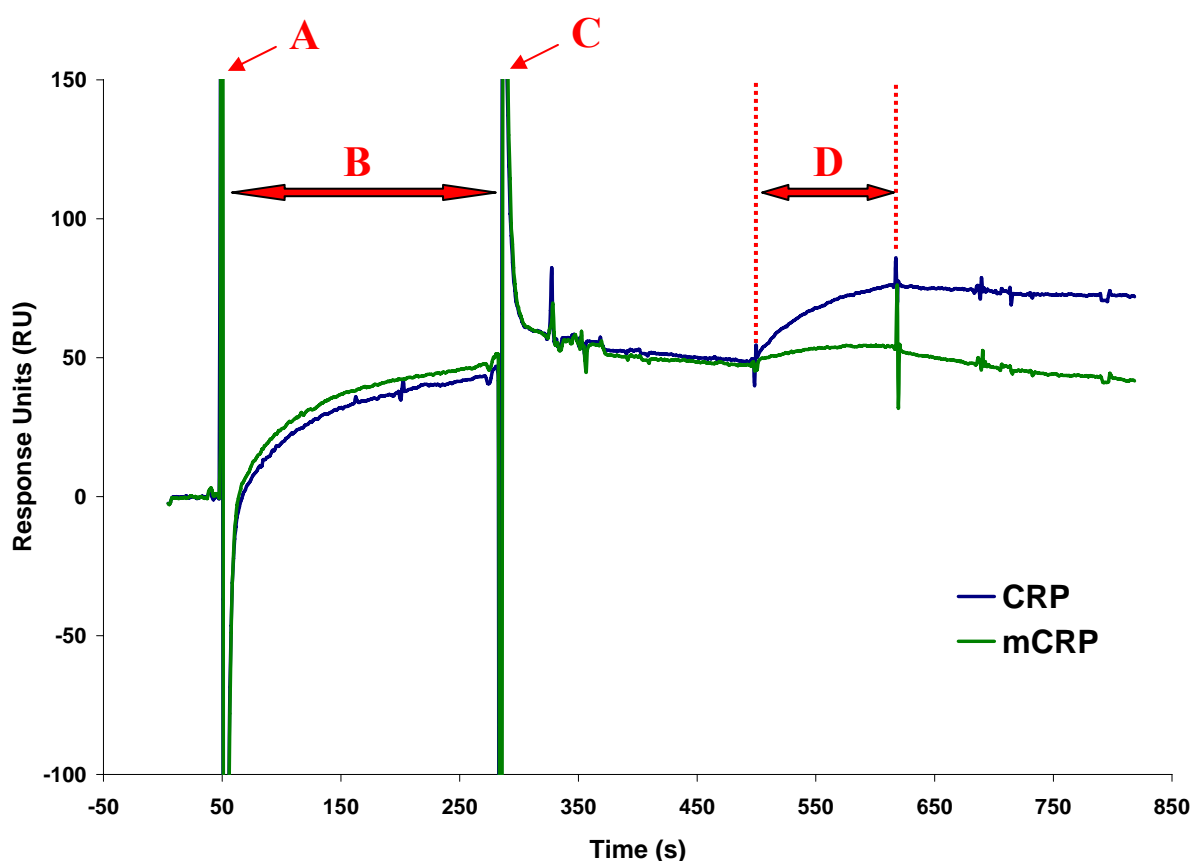


Figure 3.2.16 (a) Analysis of reactivity of the C11-2 scFv subclone with mCRP using an anti-HA capture method on the Biacore 3000. The sensogram illustrates the level of C11-2 scFv subclone captured (A) by the anti-HA mAb immobilized surface, followed by the binding responses of either CRP or mCRP (B). As discussed earlier, the change from HBS

buffer to scFv-rich lysate and vice-versa caused two drastic refractive index spikes, labelled as A and C, respectively.

The employment of a capture-based format for kinetic analysis allows for the use of crude scFv-containing bacterial lysates (section 2.9.19). Capture of the scFv was performed using a 3 min injection of the crude lysate across the anti-HA chip surface at a flow rate of 10 $\mu\text{L}/\text{min}$, followed by a stabilization period of 3 min. Next, mCRP was spiked into HBS at concentrations of 200, 100, 50, 25, 12.5, 6.3, 3.1 nM and passed across the captured scFv at a flow rate of 30 $\mu\text{L}/\text{min}$. This high flow rate was employed to remove any potential interference from mass transfer effects. The 12.5 nM concentration was run in duplicate and a zero concentration included, enabling double referencing. Association and dissociation phases were monitored for 3 and 10 min, respectively. Sensograms for each of the mCRP concentrations were fit globally to a 1:1 interaction model using Biacore 3000 dedicated software. A good fit (Figure 3.2.16 b) was observed for the kinetic run using the Langmuir equation. This 1:1 interaction model was subsequently used to extrapolate the relevant kinetic constants and binding affinities of the scFv for mCRP (Table 3.2.16). The overall accuracy of the kinetic analysis was further justified by a considerably low Chi^2 output value of 0.123.

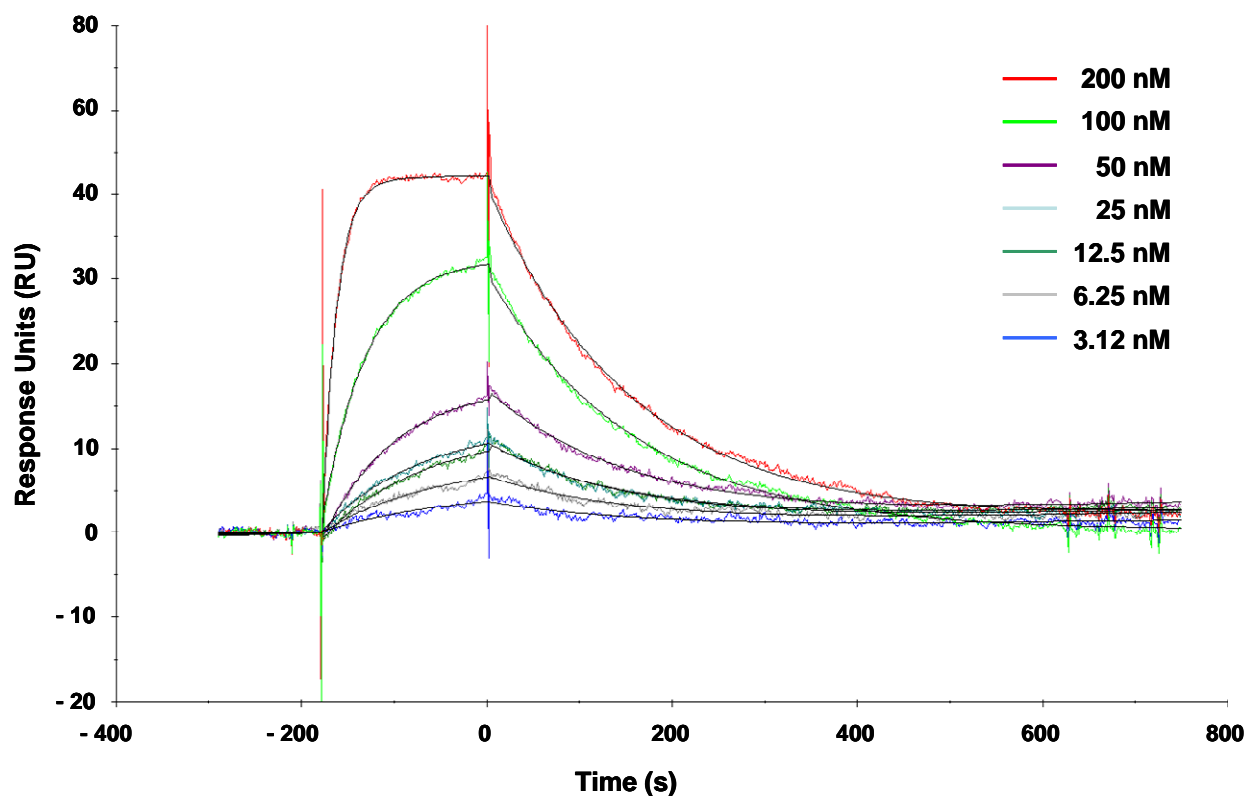


Figure 3.2.16 (b) Kinetic analysis fit of the mouse C11-2 scFv subclone using the Biacore 3000 system. Shown is the local fit of a 1:1 interaction model (with drifting baseline) to the response data obtained from the Biacore 3000 with multiple analyte concentrations. The black lines represent the local fit to the response data shown as coloured lines.

Table 3.2.16 Kinetic constants and binding affinity calculated for the C11-2 scFv subclone

Kinetic parameter	k_a ($M^{-1} s^{-1}$)	k_d (s^{-1})	KD (M)
Value	2.97×10^5	6.24×10^{-3}	2.1×10^{-8}

3.2.17 Discussion of results

Following analysis of the sequences of the ten murine anti-CRP scFv clones (Figure 3.2.10), it is clear that a single scFv sequence pattern dominates the pool of clones. The top nine scFv sequences all contain this dominant sequence pattern, with only minor base pair differences occurring in the framework regions. However, the H2-3 scFv sequence (3.2.10) deviates substantially from this dominant sequence pattern, showing extensive modifications to the

CDR regions in both the heavy and light chains. This phenomenon of a final dominant antibody sequence was previously reported. One such study by Kashyap and colleagues (Kashyap *et al.*, 2008) encountered this result, referring to it as the “jackpot solution”. Both the natural progression of affinity maturation and selected synthetic antibody libraries (Rajpal *et al.*, 2005; Lerner, 2006) can yield this repeating dominant antibody sequence to a specific antigen. Consequently, the presence of these so-called “jackpot libraries” validates the panning procedure and its level of stringency.

Although, the murine immune repertoire provides us with a relatively simple and readily available system for the generation of recombinant antibodies, its use is accompanied by several disadvantages. Due to mice being such a close relative of humans, the generation of antibodies against conserved epitopes of the antigen of interest is less likely to occur compared to when more phylogenetically distant species are used e.g chickens (section 3.3.1). Furthermore, the CDR-H3 region has been shown to be a major contributing factor toward the affinity of antibodies (Tonegawa, 1983; Chothia *et al.*, 1989; Wilson and Stanfield, 1994; Schroeder *et al.*, 1998; Deng and Notkins, 2000; Eisenhardt *et al.*, 2007) and diversity within this region may be restricted by shorter lengths of this region within the murine repertoire compared to those of chickens. In addition, to capture a good representation of the murine immune repertoire, an excessively large number of primer combinations must be employed. The incorporation of all the appropriate heavy and light chain variable regions into the library, would involve the amplification of a total of 166 separate primer combinations. Due to this method being both time-consuming and impractical, a master mix was prepared for both the forward and reverse primers for both the variable heavy and light primers. While this modified approach leads to a much simpler and rapid construction of the scFv library, there is the potential for the loss of some diversity from the immune repertoire. For instance, certain primer combinations may amplify efficiently, whereas, other combinations may need extensive optimisation. This occurrence may lead to bias towards abundant genes over more conserved genes, which may be integral to the development of a highly specific scFv library. Following construction of the mouse library and its subsequent enrichment against the antigen of interest (in this case CRP), several obstacles were encountered during both screening and characterisation of the scFv candidates from the library. For example, initial high-throughput screening of the scFv clones using crude lysate proved problematic due to the very poor levels of scFv expression, even following sub-cloning of the enriched scFv fragments into the supplied vector (pAK 400) for optimised expression. This poor expression level is another negative feature associated with the

employment of the murine genetic system (Mavrangelos *et al.*, 2001). The lack of any highly-specific affinity tags within the pAK system also limits the screening capacity of the clones. Both a histidine and FLAG tag were incorporated into the vectors, however, both tags proved to be either non-specific or inaccessible during characterisation via either ELISA or Biacore. Subsequently, the best-performing murine scFv (C11-2) was subcloned into the pComb3X vector. An appealing characteristic of the pComb vector is the incorporation of the hemagglutinin (HA) decapeptide tag at the 3' end of the HIS tag for capture of the recombinant antibodies produced, allowing for a more efficient screening and characterisation process. It also incorporates a 6x histidine (HIS) tag enabling universal protein purification. The HA-tag proved to be extremely useful for both detection of the scFv via ELISA and also capture of scFv during Biacore analysis. Subsequently, use of this highly-specific affinity tag facilitated the determination of reliable kinetic data on the C11-2 scFv fragment.

Although, some good potential scFv candidates with specificity towards CRP were produced from this murine library, several problems such as those mentioned were encountered throughout construction, screening and characterisation of the murine library. Consequently, it was decided to investigate alternative hosts and vector systems (see section 3.3) for the generation of scFv fragments specific for CRP.

3.3 Generation and characterisation of a chicken anti-CRP scFv library

3.3.1 Avian immune system

The avian immune system was the subject of considerable focus over the years and is now regarded as an extremely simple and efficient model for the generation of highly specific recombinant antibody fragments. The large phylogenetic distance from humans is one of the primary advantages of the avian genus. Therefore, the avian immune system can often produce a more vigorous antibody response to highly conserved mammalian antigens, whereas in the case of closely related species such as rabbits or mice (Song *et al.*, 1985; Michael *et al.*, 1998; Andris-Widhopf *et al.*, 2000), a much more limited immune response may be observed due to immunological tolerance. This characteristic of the avian immune system can also provide a greater opportunity to generate antibodies to certain epitopes that may be dominant in mammalian immune responses (Andris-Widhopf *et al.*, 2000). Furthermore, birds generate their immunoglobulin repertoire from single VH and VL germ line sequences (McCormack *et al.*, 1993), making antibody library construction relatively simple. This phenomenon can also lead to a reduction in the loss of rare transcripts because of variability in priming efficiency (previously discussed in section 3.2.17). Due to the existence of only a single set of germlines, the molecular mechanisms by which chickens achieve their immunoglobulin diversity are sought via gene conversion, as well as the common mammalian hypermutation pathway (McCormack *et al.*, 1993). Further diversity may also be provided in the greater length of the CDR3 residues compared to those exhibited by mice, which was confirmed in findings from this research. Another factor contributing to both a more ethical and resourceful library construction, is the ability of the chicken to yield specific monoclonal antibodies to several antigens from the same immunised chicken (Hof *et al.*, 2008). In this particular project, the same male white leghorn chicken was immunised with CRP and the cardiac markers Fatty-Acid Binding protein (FABP) and Myeloperoxidase (MPO), simultaneously. The higher core body temperature of chickens (41°C) has also led to suggestions that avian-derived scFv fragments are more stable at both elevated temperatures and even wider pH ranges compared to other species (Chiou, 2002; Narat, 2003). Finally, the use of recombinant antibodies generated from the avian immune system, prevents any potential assay interference from both heterophile and human anti-mouse antibody (HAMA) contaminants.

3.3.2 Construction, screening and selection of avian anti-CRP scFv library

All data associated with the immunisation strategy, library construction, selection and screening of the avian anti-CRP scFv library was previously published by (Hearty *et al.*, 2006; Leonard *et al.*, 2007). A summary of the methodology employed for construction, selection and screening of the library may be found in section 2.10.1.

Following an intensive screening and selection strategy, four scFv clones were chosen (F6, F8, G5 and H2) from the library, based on their affinities for the CRP antigen. This section will focus on characterisation of these four avian anti-CRP scFv antibodies.

3.3.3 Cross-reactivity analysis of avian anti-CRP scFv antibodies

A vital component of immunoassay development involves determination of the specificity of the scFv fragments for the antigen of interest i.e. for CRP. Therefore, it is essential to test for the most likely cross-reactants in clinical samples that may lead to invalid test results. The protein showing the highest level of homology to CRP is SAP (discussed in section 3.1.2). Its homologous structure makes it an essential analyte to be incorporated into the characterisation of the specificity of anti-CRP scFv fragments.

It was decided to perform an antibody capture-based method for the determination of CRP cross-reactivity by ELISA (section 2.10.2). The capture method exploited the pAb's ability to bind both CRP and SAP. The format involved a 96 well plate (Maxisorp™, Nunc), coated with the purified rabbit anti-CRP pAb, capturing either the CRP or SAP proteins. Crude lysate containing expressed scFv was then passed over the captured proteins. The binding complex was then detected using an HRP-labelled anti-HA mAb.

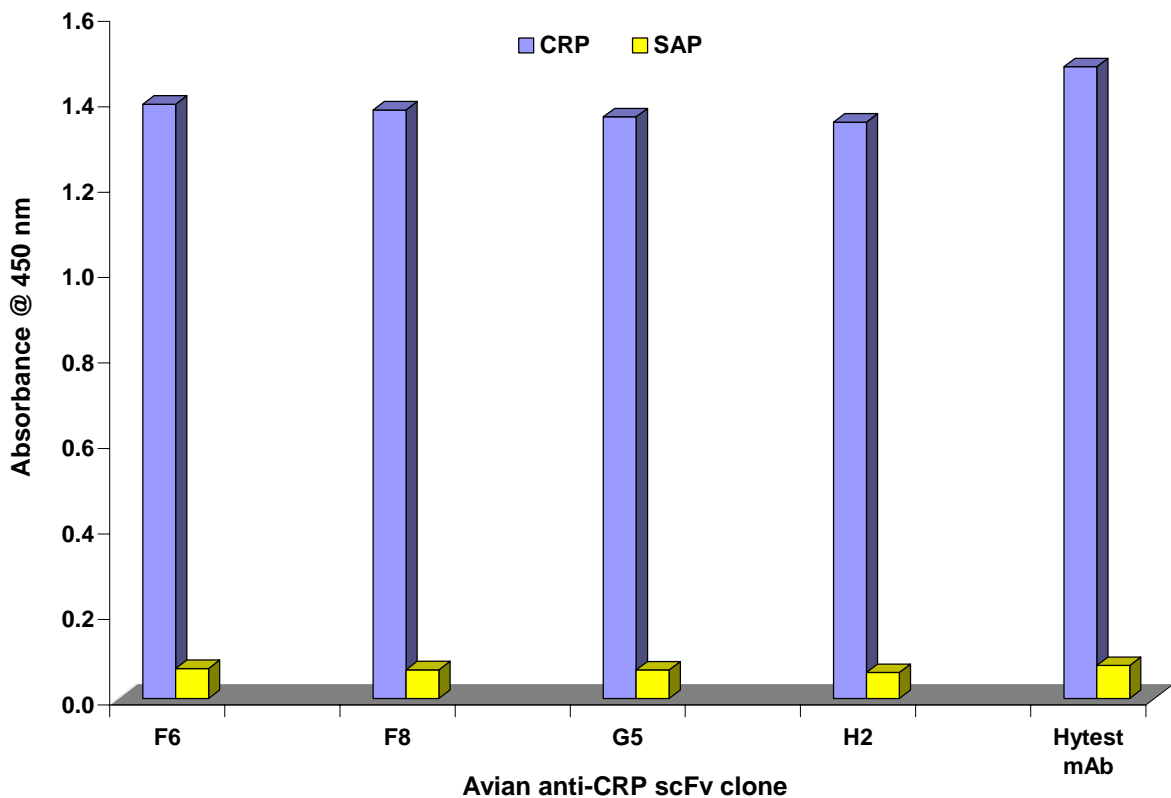


Figure 3.3.3 (a) Cross reactivity analysis of 4 avian scFv's and commercial mAb using direct ELISA. The bars in blue and yellow represent the binding response expressed as absorbance to CRP and SAP, respectively.

The plotted data from the cross-reactivity analysis can be seen in Figure 3.3.3 (a). It was clearly evident that all four of the avian anti-CRP scFv's showed no cross-reactivity to the homologous SAP protein. This was also the case for the HyTest anti-CRP mAb used as a positive control in the ELISA.

Further cross-reactivity analysis was performed using a Biacore SPR-based biosensor. A capture-based approach was again used involving an anti-HA mAb directly immobilised onto the CM5 chip surface (as per the general protocol described in section 2.8.8). Filtered lysate from the four avian clones was then passed across the anti-HA mAb, resulting in subsequent capture of the expressed scFv contained in the lysate. The final step involved passing either CRP or SAP (both at a concentration of 2 $\mu\text{g}/\text{mL}$) or HBS buffer across the captured mAb.

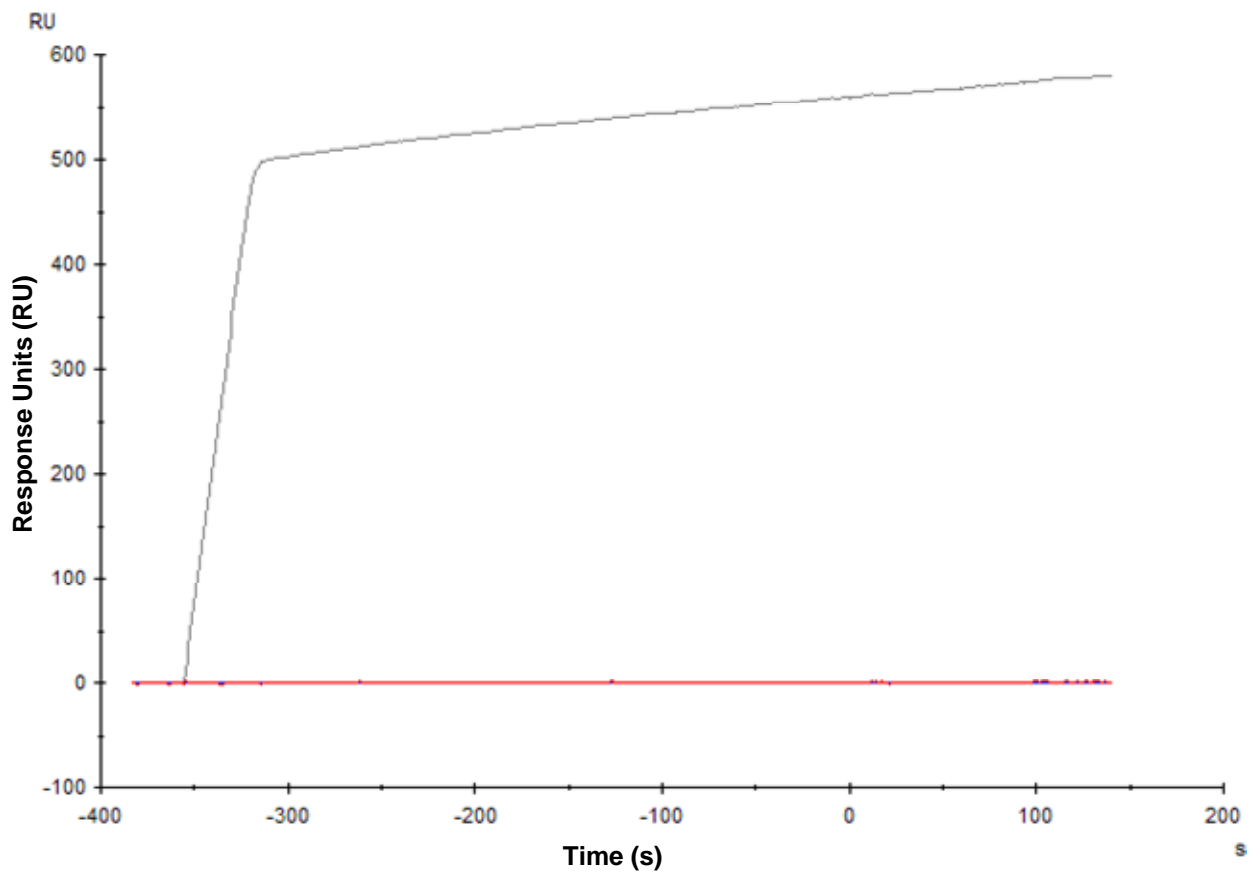


Figure 3.3.3 (b) Cross reactivity analysis of scFv-enriched H2 clone lysate using an anti-HA capture method on the Biacore 3000.

Figure 3.3.3 (b) shows one of the resultant sensorgrams of the avian clones (H2) tested. Again, as seen in the ELISA cross reactivity analysis, no binding of the SAP protein was observed (Red line). Significant binding responses to CRP (grey line) were produced (as high as 500 response units (RU)). Conversely, no significant binding to the SAP protein was evident, producing RU values equal to that of the background level of the HBS buffer (blue line) negative control. All 4 avian anti-CRP scFvs produced identical results to these, therefore, it was concluded that the 4 avian anti-CRP scFvs do not bind the SAP protein.

3.3.4 Kinetic analysis of avian anti-CRP scFv clones using the Biacore A100 system

As discussed in section 3.2.16, multivalent analytes such as CRP add complexity to protein–protein interactions, which cannot be fitted using a simple 1:1 Langmuir equation. Therefore, high precision kinetic analysis was again performed with purified modified monomeric CRP (mCRP). A capture-based assay format was employed for kinetic analysis of the scFvs (Figure 3.3.4 a). This format design enabled both high-throughput and high precision kinetic analysis to be performed on the CRP-specific scFvs.

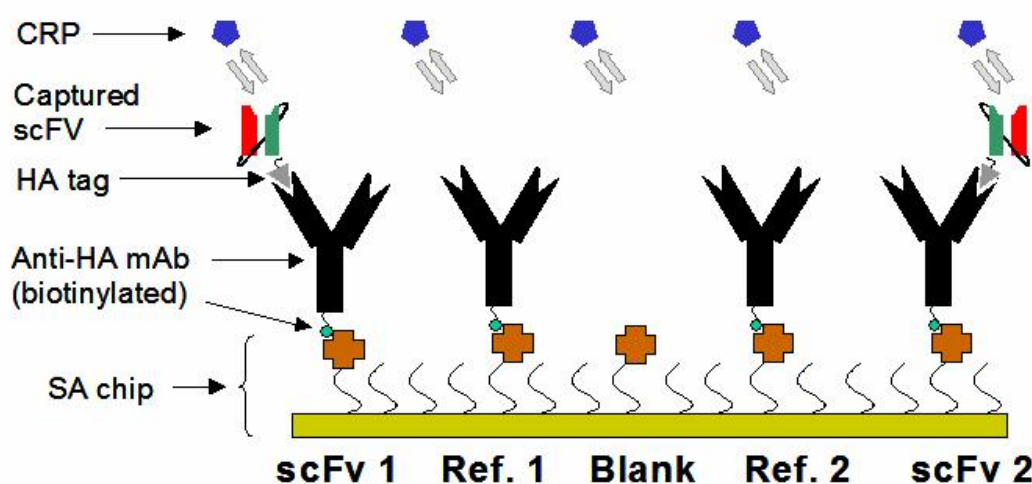


Figure 3.3.4 (a) Capture assay format used on the Biacore A100 instrument. Biotinylated anti-HA antibody was immobilised on spots 1, 2, 4 and 5 of a series S SA chip. The scFv antibody fragments were subsequently captured on spots 1 and 5 of each flowcell resulting in 8 scFv antibodies being analysed per cycle. Spots 2 and 4 were used as reference surfaces. Antigen was passed over each spot simultaneously for 2 min and the dissociation of antigen in buffer monitored for 10 min.

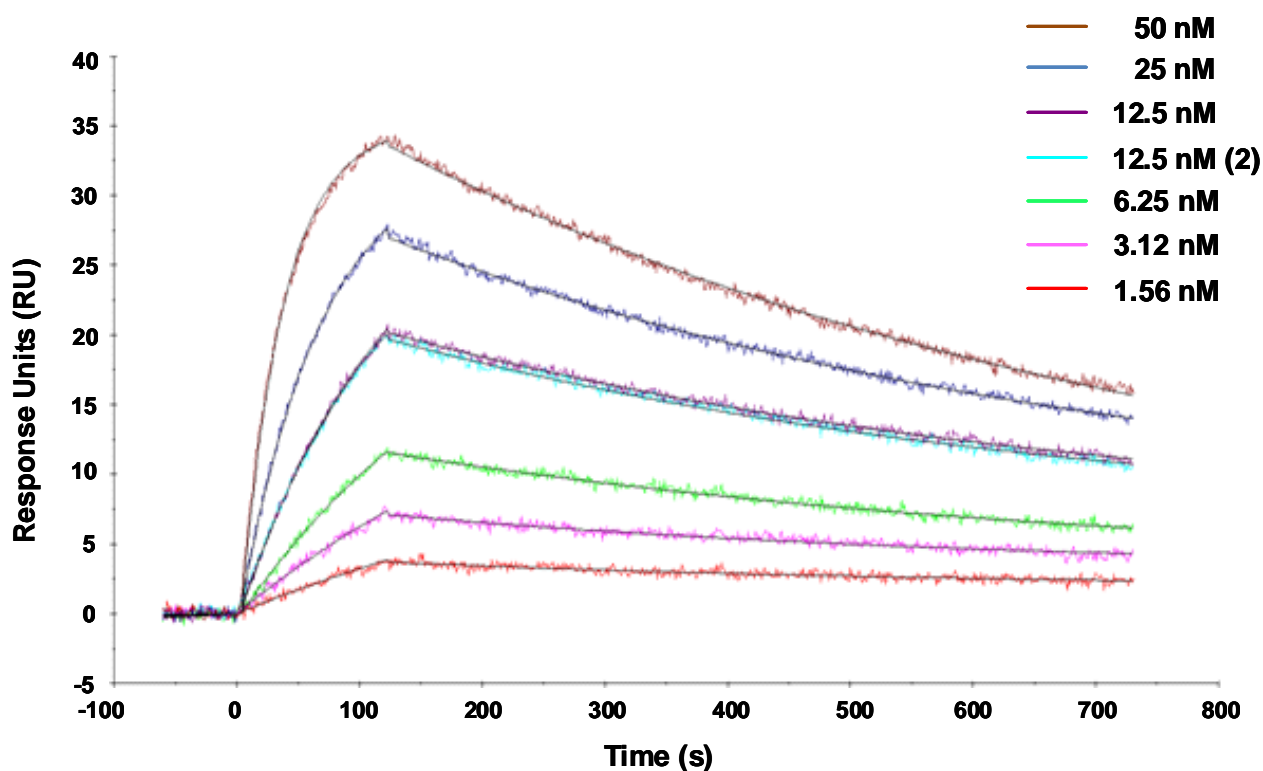


Figure 3.3.4 (b) Typical kinetic analysis fit of avian anti-CRP scFv clone (F8) using the Biacore A100 system. The global fit of a 1:1 interaction model to the response data obtained from the Biacore A100 for clone F8 with multiple analyte concentrations is shown. Monomeric CRP was injected across the captured scFv at 30 $\mu\text{L}/\text{min}$ for 2 min at 50, 25, 12.5 (duplicate), 6.25, 3.12 and 1.56 nM concentrations. The black lines represent the global fit to the response data shown as coloured lines.

Sensograms for each of the mCRP concentrations used in the kinetic analysis were fit globally to a 1:1 interaction model using Biacore 3000 dedicated software (Figure 3.3.4 b). The 1:1 Langmuir interaction model was subsequently used to extrapolate the relevant kinetic constants and binding affinities of the scFv for mCRP (Table 3.3.4).

Table 3.3.4 Summary of kinetic constants and binding affinities calculated for the four scFv antibody fragments that bound monomeric CRP

Clone	k_a ($M^{-1} s^{-1}$)	k_d (s^{-1})	KD (M)
F6	$8.90[1]^a \times 10^4$	$2.26[2]^b \times 10^{-3}$	2.54×10^{-8}
F8	$1.39[1] \times 10^5$	$1.41[1] \times 10^{-3}$	1.01×10^{-8}
G5	$1.75[1] \times 10^5$	$6.15[4] \times 10^{-4}$	3.52×10^{-9}
H2	$5.76[3] \times 10^5$	$2.03[2] \times 10^{-4}$	3.53×10^{-10}

^a The number in brackets represents the standard error in the last significant digit of k_a value from each experiment.

^b The number in brackets represents the standard error in the last significant digit of k_d value from each experiment.

3.3.5 Large-scale IMAC purification of anti-CRP scFv's

The use of crude lysate extract for preliminary characterisation of scFv fragments is acceptable; however, a high level of purity is required for the incorporation of these scFv fragments into sensitive novel assay platforms. Consequently, the four avian anti-CRP scFv clones (F6, F8, G5 and H2) were expressed in large-scale (section 2.10.3) and purified using IMAC purification (section 2.10.4). Figure 3.3.5 shows both the crude lysate and purified scFv fragment from all four expressed cultures of the avian anti-CRP scFv clones. The IMAC purification produced a highly pure sample of scFv fragment for all four of the avian clones, with no significant non-specific protein contamination.

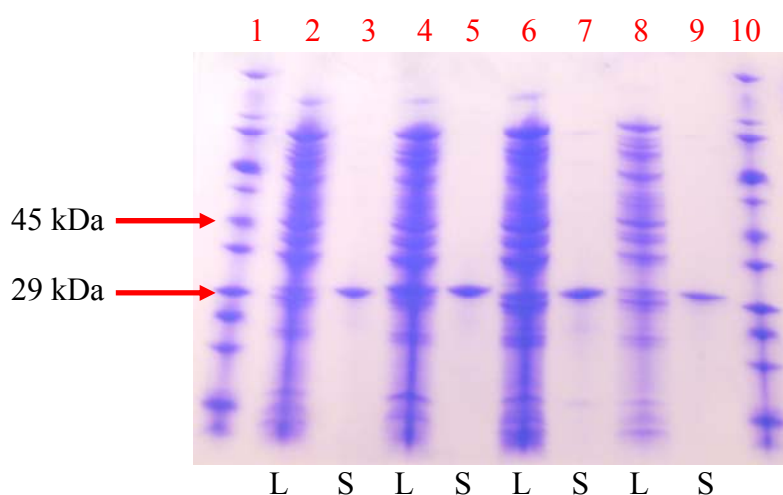


Figure 3.3.5 Crude scFv-enriched lysate (L) and purified scFv (S) for all 4 avian anti-CRP scFv antibodies. Each of the 4 analysed fragments are F6 (lane 2 and 3), F8 (lane 4 and 5), G5 (lane 6 and 7) and H2 (lane 8 and 9) resolved on an SDS gel. A protein marker ladder (Sigma) was loaded in lanes 1 and 10 for estimation of the apparent molecular weights of the components of each of the protein samples.

3.3.6 Engineering of avian CRP-specific H2 scFv for direct conjugation on the SPRSpectral® platform

A final goal of this research was the incorporation of these fully-characterised antibodies into a novel point-of-care (POC) biosensor platform. The scFv showing the highest affinity for CRP (H2 clone) was chosen for application in an SPR-based biosensor (see section 3.5.5). A classically used substrate for SPR-based analysis is a thin layer of gold on a high refractive index glass support (Homola *et al.*, 1999). Prior to its incorporation into this biosensor platform, it was decided to modify the H2 scFv fragment to allow for its direct conjugation onto the gold surface. To ensure that the engineered scFv fragment adopts a functional conformation on the gold surface, the terminal region of the scFv fragment was subjected to the genetic engineering process. One method in which direct conjugation of the antibody fragment to a gold surface may be achieved is via the incorporation of a terminal cysteine residue on the scFv fragment. A terminal cysteine residue would result in a free thiol group with reactive properties for the gold surface. The constant lambda ($C\lambda$) chains of chicken antibodies have been shown to possess a C-terminal cysteine residue used for linking the adjoining chain. Attaching a chicken $C\lambda$ chain onto the scFv fragment, will provide both the desired terminal cysteine residue for direct conjugation and also have a beneficial impact on

the stability of the recombinant antibody. This format of an scFv fused to a constant chain (kappa or lambda) is referred to as a scAb fragment (Figure 4.3.5 a) (McGregor *et al.*, 1994) and it was previously shown that this structure has superior expression, stability and serum half-life compared to scFv fragments (Maynard *et al.*, 2002).

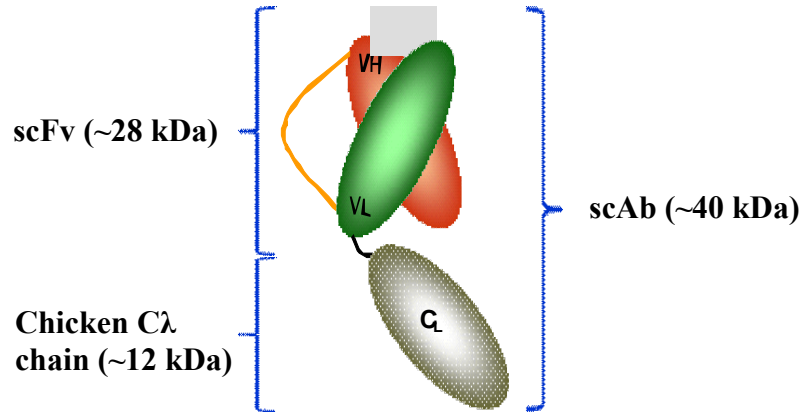


Figure 3.3.6 (a) Illustration of a scAb fragment, composed of an scFv fused to a constant chain (kappa or lambda).

The methodology used to convert the H2 scFv into this scAb format (containing reactive terminal cysteine) may be found in sections 2.10.6 to 2.10.10. Firstly, primers were designed and incorporated into a PCR for amplification of the Cλ chain from cDNA isolated from an immunised chicken (see section 2.10.6). The amplified chicken Cλ chain contains a naturally-occurring terminal cysteine residue and, therefore, the amplified chain will be referred to as Cλcys. Figure 3.3.6 (b) shows the amplified Cλcys product resolved via agarose gel electrophoresis.

Primer sequences used for amplification of the Cλcys chain:

Cλcys For

5' ATA AGA ATG CGG CCG CTC AGC CCA AGG T 3'

Cλcys Rev

3' CCG GCA ATG GCC GAC GTC GAC GCA CTC G 3'

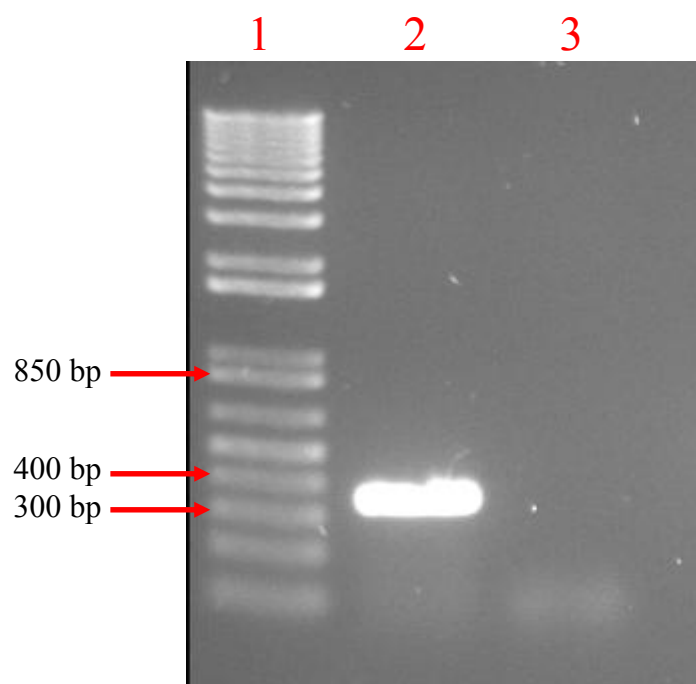


Figure 3.3.6 (b) PCR amplification of the C λ cys chain from chicken cDNA using ‘in-house’ designed primers (Lane 2). A 1 kb Plus DNA molecular weight marker was added to lane 1. Also, a negative control containing no template DNA is shown in lane 3.

Not1 and *Sal1* restriction sites were incorporated into the primers to allow for direct cloning of the C λ cys chain into the pMoPac 16 vector (Hayhurst *et al.*, 2003) (see Figure 3.3.6 c). This vector already contains a constant kappa (C κ) chain flanked by the *Not1* and *Sal1* restriction sites. Therefore, the existing C κ chain was replaced with the amplified C λ cys chain using the methods described in section 2.10.7 and then transformed into electrocompetent Top 10 F' cells for soluble expression.

The existing scFv gene harboured by the vector coded for an scFv fragment specific for prostate specific antigen (PSA). For confirmation of the successful incorporation of the C λ cys chain into the pMoPac 16 vector, sixty of the transformant clones were cultured and their expressed lysates tested in a direct ELISA format against PSA (see section 2.10.8). Figure 3.3.6 (d) illustrates the responses of the expressed lysates of the sixty individual PSA specific scAb clones (C λ cys chain).

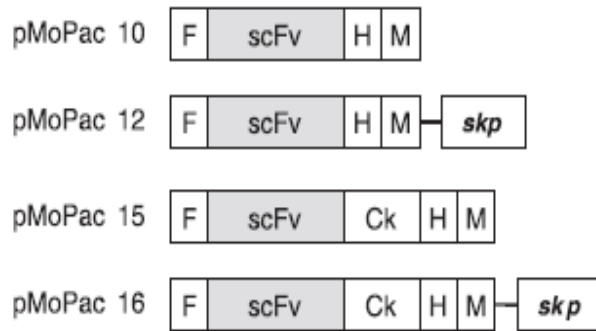


Figure 3.3.6 (c) Schematic diagram of the expression cassettes employed by the pMoPac series of vectors (Hayhurst *et al.*, 2003), a modification of the pAK series (see section 3.2.17). Abbreviations: F, FLAG tag; H, His6 tag; M, myc tag; Ck, human kappa light chain constant domain and Skp, seventeen kilo Dalton protein (periplasmic chaperone).

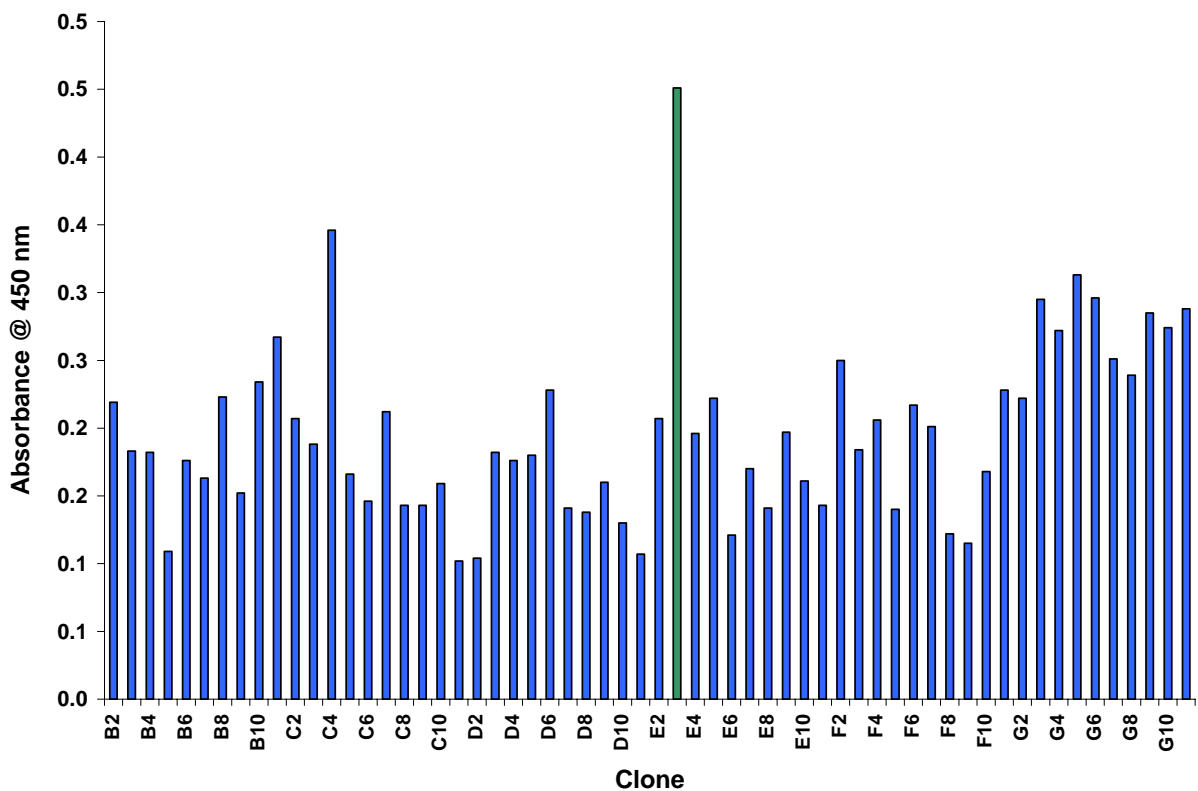


Figure 3.3.6 (d) Direct ELISA using scAb-enriched lysate from 60 PSA-specific scAb clones. The bar highlighted in green represented the E3 clone which displayed the highest level of expression.

On analysis of the ELISA results, E3 was found to be the clone showing the highest level of expression of scAb against PSA. The E3 clone was cultured and its plasmid harbouring the PSA-specific scAb purified using the Promega SV Miniprep™ kit.

The next step involved replacing the existing anti-PSA scFv gene with the avian anti-CRP H2 scFv gene, cloning into the pMoPac 16 vector (E3 clone) via flanking *Sfi*1 restriction sites. As discussed in section 3.2.12, the *Sfi*1 restriction sites of the pAK (parent vector of pMoPac vectors) and the pComb vector are different. Consequently, a further set of primers were used for modifying the flanking *Sfi*1 restriction sites of the H2 scFv gene from the pComb format to the pMoPac format.

Primer sequences used for cloning H2 scFv gene into the pMoPac 16 vector (E3 clone):

CSCpAK-For

5' GAG GAG GAG GAG GAG GAG GTG GCC CAG CCG GCC CTG ACT CAG 3'

CSCpAK-Rev

5' GAG GAG GAG GAG GAG GAG GAG CTG GCC CCC GAG GCC ACT AGT GGA
GG 3'

The specifically designed primers are a modified version of the SOE primers employed by the pComb system. Instead of the usual *Sfi*1 site utilised by the pComb system, a pAK-derived *Sfi*1 site was incorporated into the primers, to allow for direct cloning of the H2 scFv gene into the pMoPac 16 vector (E3 clone). In theory, the original H2 scFv format should not ligate into the pMoPac 16 vector due to the incompatibility of their respective *Sfi*1 sites. However, to avoid any potential background interference from the old pComb format of the H2 scFv gene, a 2 step 'nested-type' PCR was performed (see section 2.10.9). This will allow for enrichment of the new pMoPac format of the H2 scFv over the existing pComb format, as discussed in section 3.2.12. Several quantities of template H2 scFv were investigated (6, 12 and 18 ng) to identify the lowest quantity of template, which may be used for sufficient amplification of the required pAK format. Figure 3.3.6 (e) shows the amplified H2 scFv gene in its new pAK format, resolved via agarose gel electrophoresis.

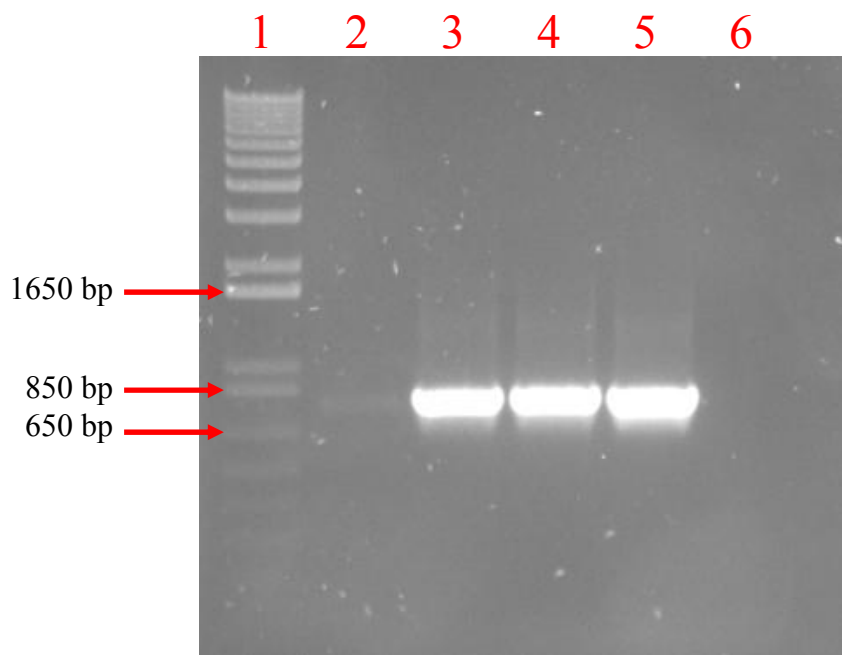


Figure 3.3.6 (e) PCR amplification of the H2 scFv gene using ‘in-house’ designed primers for incorporation of pAK format *Sfi*I sites. A 1 kb Plus DNA molecular weight marker was added to lane 1. Lanes 3 – 5 represent amplifications of the H2 scFv gene using various quantities of H2 scFv template (6, 12 and 18 ng, respectively). Lane 2 shows a 25 ng quantity of the PCR template used for the PCR. A negative control containing no template DNA is shown in lane 6.

The PCR using 6 ng of template was scaled-up and resolved via electrophoresis on a 1% agarose gel and gel purified again using the QIAquick™ gel extraction kit. Part 2 (section 2.10.9 b) of the ‘nested-type’ PCR then used this purified product as template for amplification of the final modified H2 scFv gene. Following purification, the final PCR product was cloned into the pMoPac vector (E3 clone) using *Sfi*I restriction enzyme, as outlined in section 2.10.10. The ligated product was then electroporated into Top 10 F' cells for soluble expression. Individual colonies from the transformation plates (60 in total) were then cultured, solubly expressed and incorporated into a direct ELISA. The format of the ELISA performed is identical to that described in section 2.10.8, except the antigen being tested against was CRP instead of PSA. The expressed lysates of each of the clones were tested in duplicate against wells coated with 5 µg/mL of CRP in PBS. Figure 3.3.6 (f) shows the absorbance levels for all 60 of the expressed CRP-specific scAb lysates.

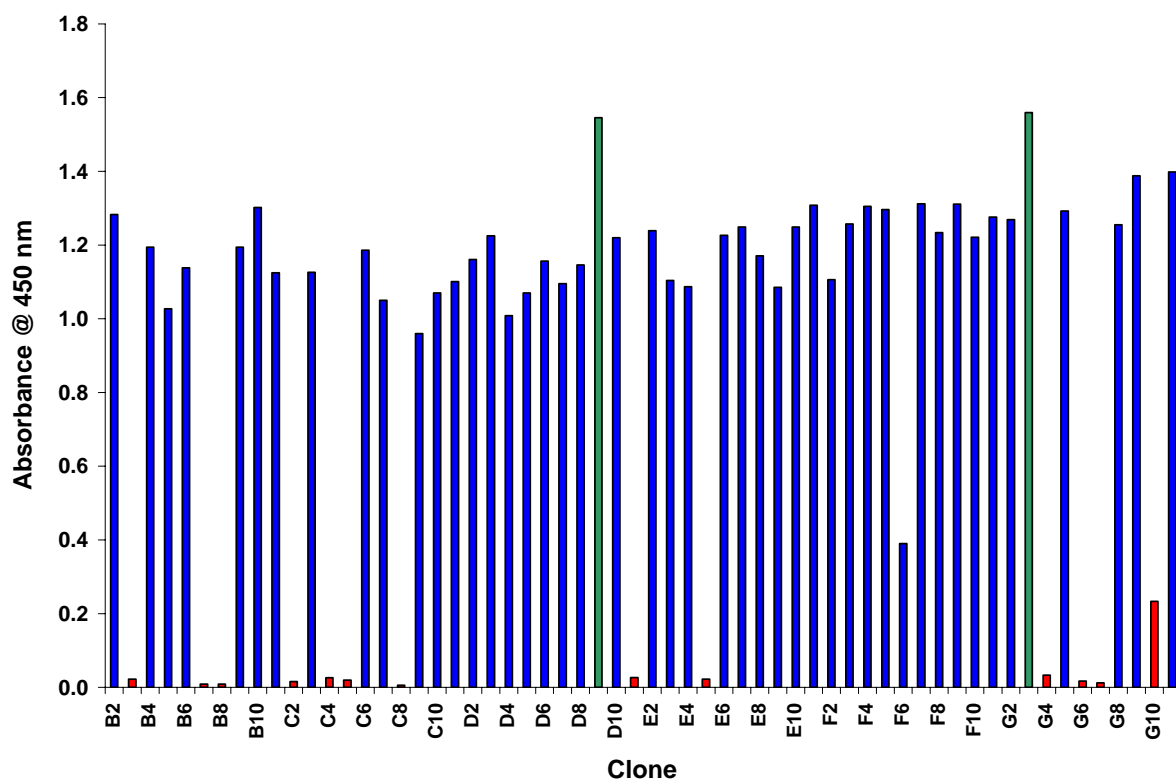


Figure 3.3.6 (f) Direct ELISA using scAb-enriched lysate from 60 CRP-specific scAb clones. The bars highlighted in blue represent potential positive candidates and clones considered to be negative are illustrated in red. Both bars highlighted in green were found to possess the highest level of expression of CRP-specific scAb.

On analysis of the ELISA results, D9 and G3 (highlighted in green) were identified as the clones showing the highest level of expression of the CRP-specific scAb. Due to the almost identical performance of both of the clones, only one of the clones was taken forward for large-scale expression and purification.

3.3.7 Large-scale expression and purification of the CRP-specific scAb fragment

For further characterization of the CRP-specific scAb clone and also its incorporation into a sensitive bioplatfrom, a purified sample of scAb fragment was essential. Therefore, a 1 litre culture of the D9 clone was subjected to large-scale expression and purification as outlined in sections 2.10.3 and 2.10.4. It was envisaged that the free thiol group from the terminal cysteine residue of the scAb fragment may lead to the formation of non-specific disulphide bonds. For this reason, a 15 mM concentration of β -mercaptoethanol was added to both the sonication and wash buffers of the IMAC purification. The β -mercaptoethanol will result in

the reduction of any non-specific disulphide bond formation throughout the purification process. Each of the sample preparations of the IMAC purification were resolved via SDS-PAGE (see section 2.8.3), which may be observed in Figure 3.3.7.

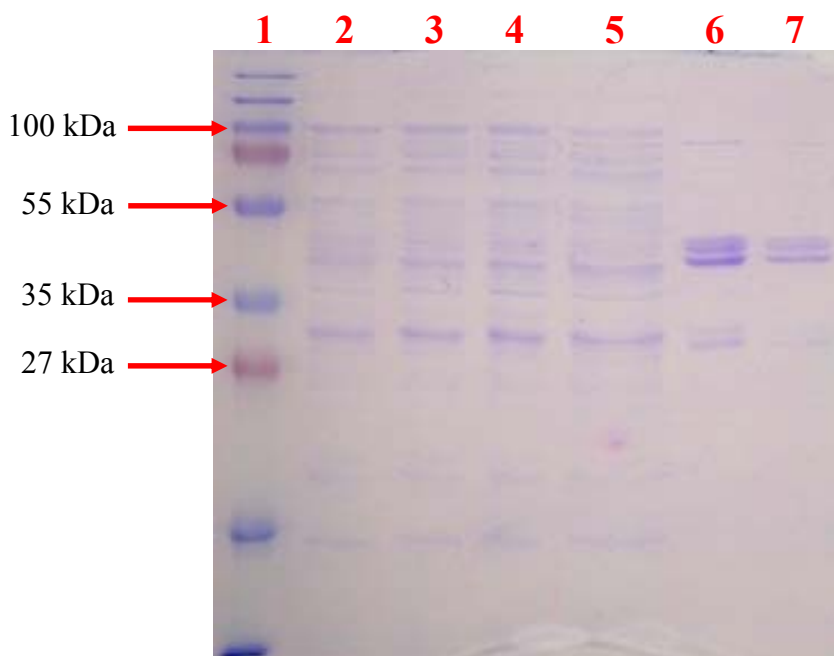


Figure 3.3.7 SDS-PAGE gel of each fractions of the IMAC purification of the CRP-specific D9 scAb fragment. The fractions were loaded as crude lysate (Lane 2), ‘flow-through’ 1 (Lane 3), ‘flow-through’ 2 (Lane 4), wash (Lane 5) and lanes 6-7 represent 4 µg and 2 µg quantity of the purified D9 scAb, respectively. A protein marker ladder (Fermentas) was also loaded in lane 1 for estimation of the apparent molecular weights of the each of the protein samples.

Analysis of the purified D9 scAb via SDS-PAGE identified several protein bands, indicating a lack of purity of the preparation. The approximate size of a scAb fragment is 40 kDa (Mabry *et al.*, 2005). However, instead of a single band at this point, three distinct protein bands were observed. In addition, two more unidentifiable bands were found at the ~30 kDa point. Finally, a band was also visible at the 80 kDa point, although this band was thought to represent a dimerized format of the scAb fragment. To elucidate the presence of these numerous bands in the purified scAb preparation, it was decided to perform a western blot on some of the purified scAb. The western blot will be used to ascertain which of the several bands show reactivity for CRP. Consequently, any bands showing no reactivity with CRP may be regarded as non-specific contaminant proteins.

3.3.8 Western blot analysis of the CRP-specific D9 scAb purified via IMAC

A 12.5% SDS-PAGE gel was prepared following the protocol in section 2.8.3. A protein ladder (Fermentas) and a 2 μ g aliquot of the purified D9 scAb were run in duplicate on the gel. The fully resolved gel was then split down the middle, resulting in two identical gels (A and B – see Figure 3.3.8 a). Gel A was subjected to the usual staining/destaining protocol, whereas gel B was transferred to nitrocellulose membrane and a western blot (see section 2.10.11). The western blot involved incubation of the scAb-containing membrane with a CRP solution. Detection of the scAb-CRP complex was achieved via incubation with diluted C λ -specific rabbit serum, followed by a commercial HRP-labelled anti-rabbit mAb. Both the SDS gel and its corresponding western blot are shown in Figure 3.3.8 (a).

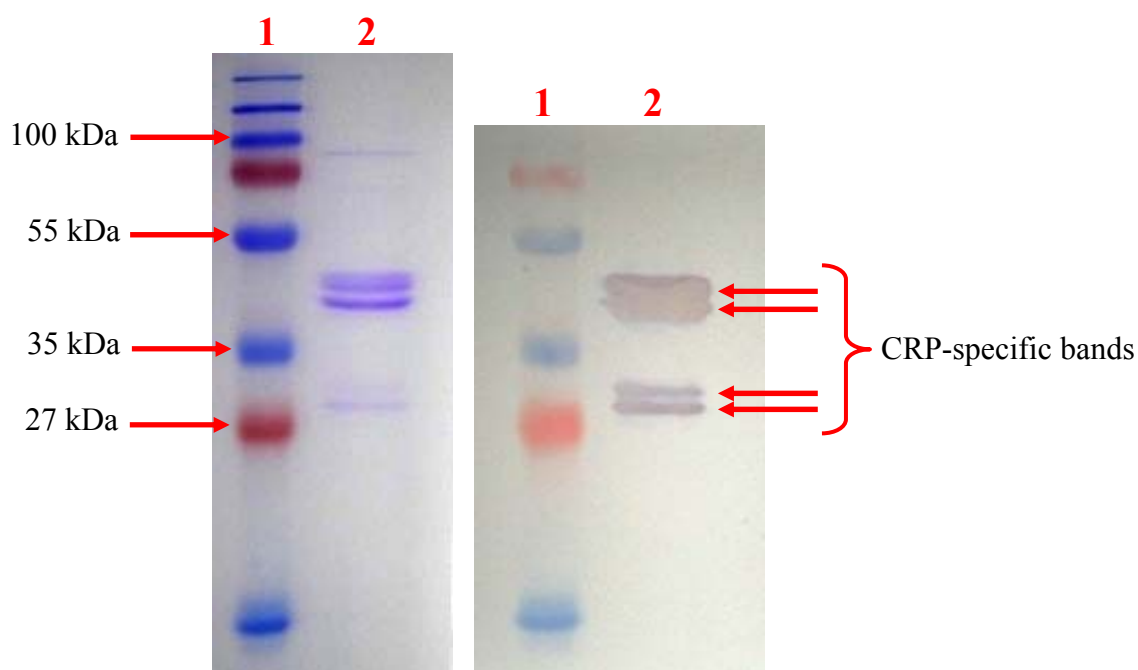


Figure 3.3.8 (a) Left - SDS-PAGE gel containing protein marker ladder (Fermentas) in lane 1 and purified D9 scAb in lane 2. Right - A developed nitrocellulose membrane of an identical gel showing protein marker ladder (Lane 1) and CRP-reacting bands of purified D9 scAb (Lane 2).

Following development of the nitrocellulose membrane with liquid TMB substrate, all three of the bands at the \sim 40 kDa mark and the two bands at the \sim 30 kDa mark were found to bind to CRP. It was thought that the two bands at the \sim 30 kDa mark may represent a contaminant scFv in the final purified scAb fraction. Although this seemed highly

improbable, it was decided to investigate this theory via western blot analysis. As before, a 12.5% SDS gel was prepared and loaded with both a protein marker ladder and a 2 µg sample of the purified D9 scAb in duplicate. A 2 µg sample of the purified H2 scFv (section 3.3.5), the scFv from which the scAb fragment was derived, was also loaded onto the gel as a positive control. Following sufficient resolution of the proteins, the gel was split into two and subjected to either a staining/destaining protocol or western blot. The western blot protocol described in section 2.10.11 was followed up to the blocking step and its subsequent wash. Next, the nitrocellulose membrane was incubated with a 1/2000 dilution of a mouse anti-HA (HRP-labelled) secondary mAb in 1 % Milk-PBST. Figure 3.3.8 (b) shows the resultant nitrocellulose membrane developed with TMB substrate.

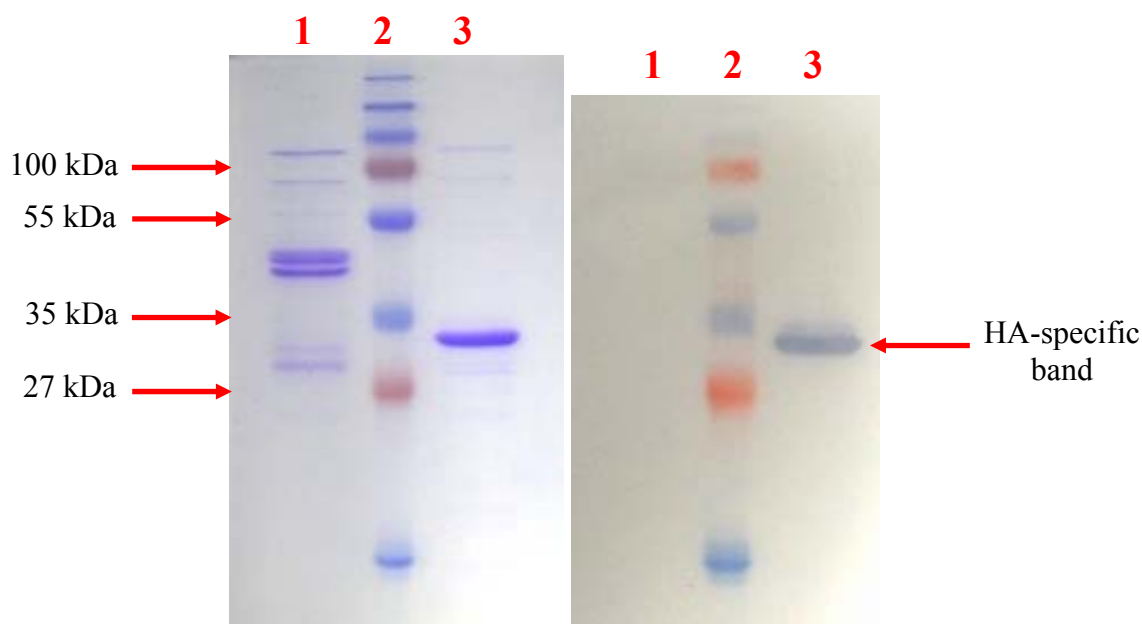


Figure 3.3.8 (b) Left - SDS-PAGE gel containing purified D9 scAb (Lane 1), protein marker ladder (Lane 2) and purified H2 scFv (Lane 3). Right – the corresponding nitrocellulose membrane probed with the HRP-labelled HA-specific mAb.

On first analysis of the gel, the sizes of the two bands under investigation in lane 1 (~ 30 kDa mark) were found to be inconsistent with that of the H2 scFv positive control in lane 3. Furthermore, neither of the two bands showed any reactivity with the HA epitope tag as opposed to the H2 scFv. It may be concluded that each of the protein bands represent scAb fragment, as each of the bands were shown to react with CRP antigen and also C λ -specific serum. No definitive conclusion, however, may be drawn with regards to the inconsistent migration patterns of the scAb fragment in the SDS gel. It may be conceivable that the free

thiol group of the terminal cysteine residue of the scAb fragment may be causing some interference in its migration through the SDS gel.

3.3.9 Discussion of results

An alternative system was employed for construction of the chicken scFv library, namely the pComb system (Barbas *et al.*, 2001). The use of chickens for the production of antibody libraries has already many advantages over other hosts such as mice (section 3.1), as discussed previously. However, the use of the pComb system in conjunction with this, led to several additional benefits. Construction of the scFv library using the pComb chicken scFv primers required minimal optimisation of all PCR reactions. Several phagemid systems, including pHEN (Hoogenboom *et al.*, 1991) and pCANTAB (Amersham Pharmacia Biotech), use the entire pIII as the fusion partner. In these systems, the phagemid-driven expression of the pIII fusion must first be shut down to allow superinfection by the helper phage, after which expression is induced to allow production of the fusion for phage display. Use of the pComb3X system, however, does not require this step due to the inclusion of a truncated pIII protein, comprised of the carboxy-terminal residues of the pIII. This truncated pIII can serve as the required fusion partner for the displayed protein by mediating incorporation of the fusion into the phage coat without producing immunity to helper phage infection. Also, soluble expression was achieved immediately after bio-panning, by simply infecting the phagemid into a non-suppressor strain (Top 10 F'), made possible by the presence of an amber codon between the 3' *Sfi*I restriction site and the 5' end of gene III. Propagation of phage in suppressor strains such as XL1-Blue allows production of gene III fusion proteins for phage display. However, if a male nonsuppressor strain such as Top 10 F' is infected with the phagemid phage, the stop codon will be read and soluble protein will be produced. Thus, the pComb3X facilitates the expression, detection, and purification of soluble protein following phage selection. This removes the time-consuming process of sub-cloning the enriched pool of scFv genes into a suitable expression vector for their subsequent screening and characterisation. Moreover, sub-cloning of the scFv genes into another vector may jeopardise the libraries diversity due to the potential loss of some of the more conserved and potentially superior scFv genes.

Considerably large yields of expressed scFv were obtained for each of the four fully-characterised scFv clones, with F8 being particularly good. A 500 mL bacterial culture of the clone produced approximately 15.5 mg of pure scFv using a simple IMAC protocol (section

2.10.4). Each of the recombinant fragments were also shown to recognise different epitopes of the CRP molecule. Both the pentameric (pCRP) and monomeric (mCRP) forms of CRP were detectable by pairing the G5 and F6 scFv fragments in a sandwich assay. Conversely, only the pentameric form was detected when H2 and F6 were combined in a sandwich assay format. Therefore, these four scFv fragments are capable of detecting both forms of this molecule, each of which play key roles in the development of life-threatening cardiovascular events. All four of the clones proved to be ideal candidates for model assay development due to their stable expression and high level of purity. However, to further enhance their applicability for a novel biosensor platform, it was decided to subject the highest affinity H2 clone to a novel engineering process. This novel engineering provided a re-formatted CRP-specific fragment (scAb), which may be directly conjugated to gold biosensor surfaces via the terminal thiol group. Therefore, the final characterisation of the re-engineered CRP-specific fragment involved incorporation into a commercial SPR-based device (See section 3.5.5). The novel format of the final engineered fragment allows for both direct conjugation to the gold surface and also ensures positioning of the fragment in a fully-functional confirmation. The combination of such novel strategies appreciably rationalises the task of generating and mining diverse panels of candidate antibodies for use in novel diagnostic biosensor formats and expedites the route from antibody production to functional biosensor assay development.

3.4 Generation and characterisation of a chicken anti-MPO scFv library

3.4.1 Multimarker detection

In the field of cardiac diagnostics, it has been shown that in certain instances, the cumulative information derived from a multimarker panel can be superior to traditional cTnI laboratory testing (Straface *et al.*, 2008). Considerable interest still remains in generating multimarker scores that use a composite of several biomarkers (measured in parallel) for the purpose of predicting disease risk and patient outcomes (de Lemos *et al.*, 2001; Newby *et al.*, 2001; Ng *et al.*, 2001; Sabatine *et al.*, 2002; Baldus *et al.*, 2003; James *et al.*, 2003; Bodí *et al.*, 2005; Heeschen *et al.*, 2005; Kip *et al.*, 2005). Therefore, the general consensus is that the future of cardiac diagnostics will involve a multimarker approach.

As previously mentioned in section 1.6, CRP has been consistently flagged as having great potential, particularly in the field of cardiac risk assessment. However, as a marker of disease activity and vascular inflammation, CRP detection has been affiliated with long-term risk stratification. Therefore, the implementation of a more comprehensive risk assessment strategy should also include a cardiac marker capable of identifying short-term risk cardiac patients. As was mentioned in section 1.7, MPO, being a marker of plaque instability and neutrophil activation may be prove to be a key marker for short term stratification. Furthermore, it has been suggested that both markers may even be complementary in the assessment of patient cardiac risk (Loria *et al.*, 2008). Consequently, this work also involved the generation of recombinant antibodies against MPO. This section will discuss the construction, screening and characterisation of an immune avian library against MPO.

3.4.2 Myeloperoxidase (MPO) as a target analyte

Native MPO (150 kDa) is a dimer consisting of two 15-kDa light chains and two variable-weight glycosylated heavy chains bound to a prosthetic heme group (Figure 3.4.2). Three isoforms of MPO have been identified (MPO A, MPO B, and MPO C), differing in the size of their heavy chains. Each contains a calcium binding site with 7 ligands, forming a pentagonal pyramid conformation. One of these ligands is the carbonyl group of Asp 96. Calcium-binding is important for the structure of the active site due to the close proximity of Asp 96 to the catalytic His 95 side chain.

In general, MPO is assumed to form a complex with anionic proteins such as albumin in serum, because it is a highly cationic protein with an isoelectric point higher than 10 (Tiruppathi *et al.*, 2004; Salavej *et al.*, 2006). Consequently, non-specific binding may prove

to be a significant obstacle in terms of antibody characterization against MPO, particularly in highly sensitive platforms such as Biacore.

Finally, the peroxidase nature of MPO may be exploited to allow for a more direct detection method. This may be achieved by employing a capture-based format, whereby the developed antibodies will be coated or immobilised onto the assay platform and the MPO-spiked sample passed across. Subsequently, the captured MPO can be used the detection enzyme of the assay and its concentration calculated via the addition of peroxidase-reactive substrates such as TMB or OPD. This ability to bypass secondary immunological detection agents may prove crucial in the development of a more rapid assay.

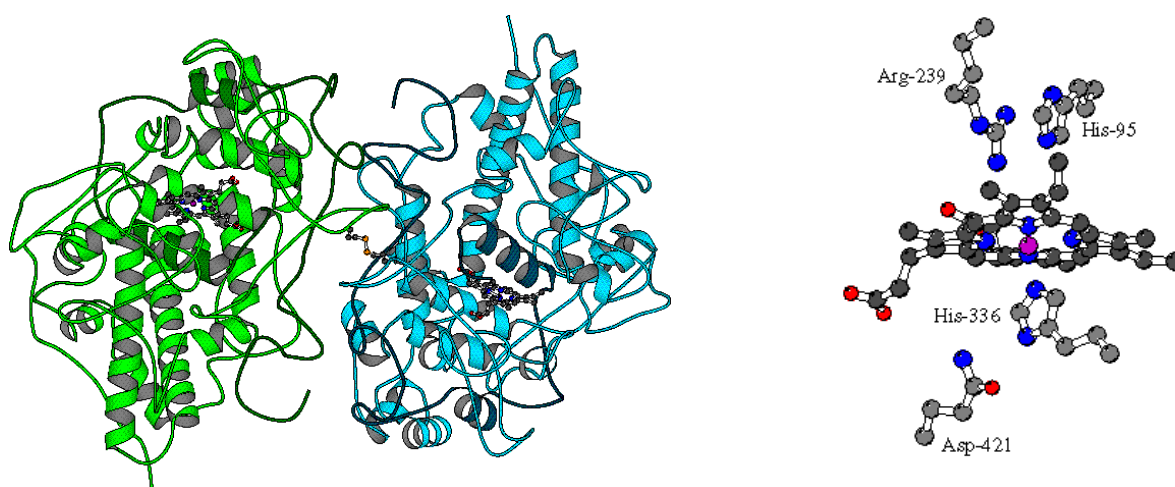


Figure 3.4.2 Ribbon representation of the MPO dimer structure (left) (Anonymous Last Accessed January, 2009). Chain A = dark green; chain C = light green; chain B = dark cyan; chain D = light cyan. An enlarged view of the incorporated inter-chain disulphide of MPO (CysC-153-CysD-153) is also shown (right).

3.4.3 Serum titre of MPO-immunised chickens

Following an extensive immunisation strategy (section 2.11.1), the responses of both chickens to the MPO immunogen were analysed via serum titre. Serum from the immunised chickens was diluted (1/100 to 1/1,000,000 dilution) in PBST (containing 0.5 % (w/v) milk marvel and 0.5% (w/v) BSA) and tested against MPO in a direct ELISA format. The antibody-MPO complex was detected using an AP-labelled anti-chicken antibody.

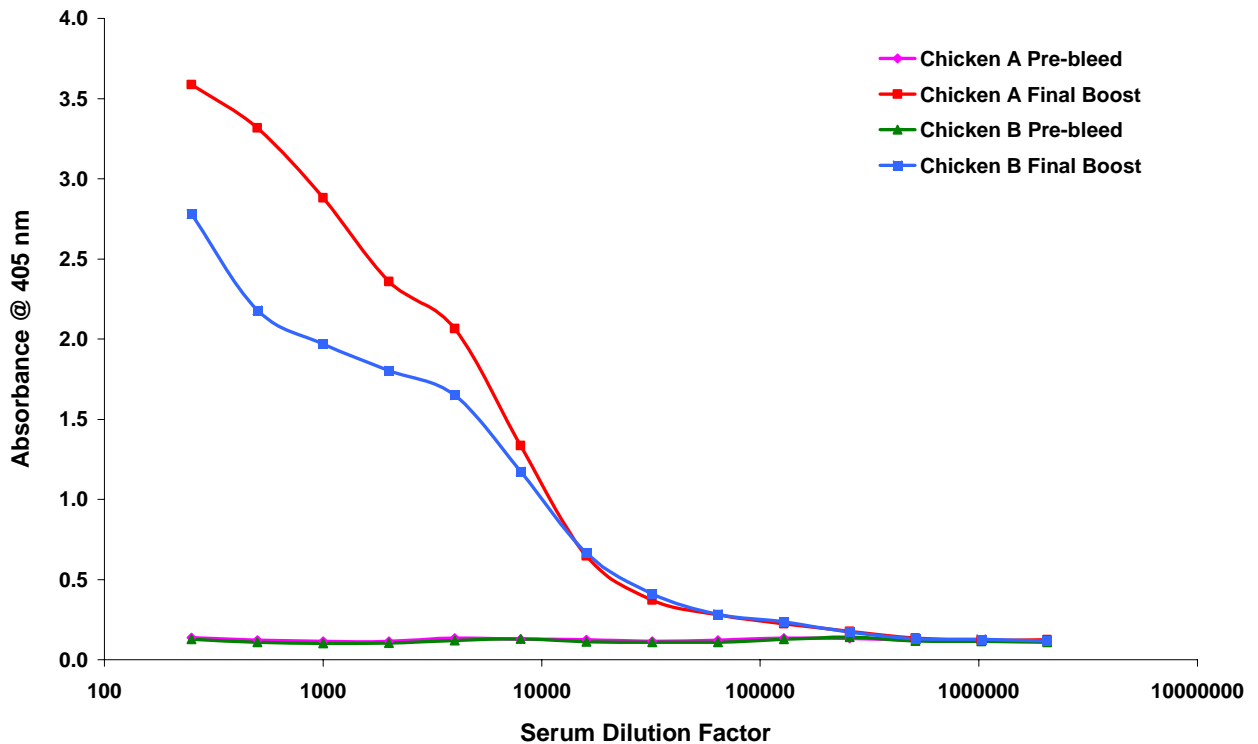


Figure 3.4.3 Titration curve illustrating the MPO-specific response of serum taken from the final bleeds (red and blue) for chickens A and B, respectively. A negative control, serum from a pre-bleed (green and pink) was also tested for both of the chickens.

Both chickens were found to produce serum titres in excess of 1/100,000 against the MPO antigen (Figure 3.4.3). These responses were deemed sufficiently high for the construction of a recombinant antibody library. As a control, serum taken from the chickens prior to any immunisations was also tested in the ELISA, to identify any non-specific binding of the serum matrix to MPO. However, a consistently low level of background binding was observed for all dilutions of the control serum.

3.4.4 RNA extraction and cDNA synthesis

High quality RNA was extracted from the spleen and bonemarrow of both chickens, as described in section 2.11.2, and then pooled in an equimolar ratio. The RNA pool was then transcribed to cDNA using a commercial RT-PCR kit (section 2.11.3). This cDNA was then used as the template for construction of the avian recombinant scFv library.

3.4.5 Library construction and subsequent enrichment via biopanning

Both construction and enrichment of the library was performed using the methodology as described by Andreas Widhopf and colleagues (Andris-Widhopf *et al.*, 2000). Briefly, both the variable light and heavy chains were individually amplified using the primers sets described in section 2.11.4. Construction of the subsequent scFv gene proceeded by fusing equimolar concentrations of the variable heavy and variable light chain using the pComb overlap primers (CSC-F and CSC-B). The fusion product may be produced using either a short serine-glycine linker (GGSSRSS) or a long linker (GGSSRSSSSGGGGSGGGG) depending on the overlap primers used. The long linker was utilised to favour formation of monomeric scFv fragments over diabody formation. Following quantification of the SOE-PCR reaction, the resultant scFv gene was cloned into the pComb3X vector using *SfiI* restriction enzyme. The successfully ligated product was then electroporated into commercial XL-1 Blue cells, resulting in a transformed library size of 7.5×10^7 colony forming units (cfu)/mL. The transformed avian library was then ‘rescued’ using M13K07 helper phage (section 2.11.7) and then enriched via four rounds of phage display biopanning against immobilised MPO antigen, as described in section 2.11.8. All of the variable panning parameters used throughout the panning process may be found in Table 2.11.8.

3.4.6 Polyclonal phage ELISA

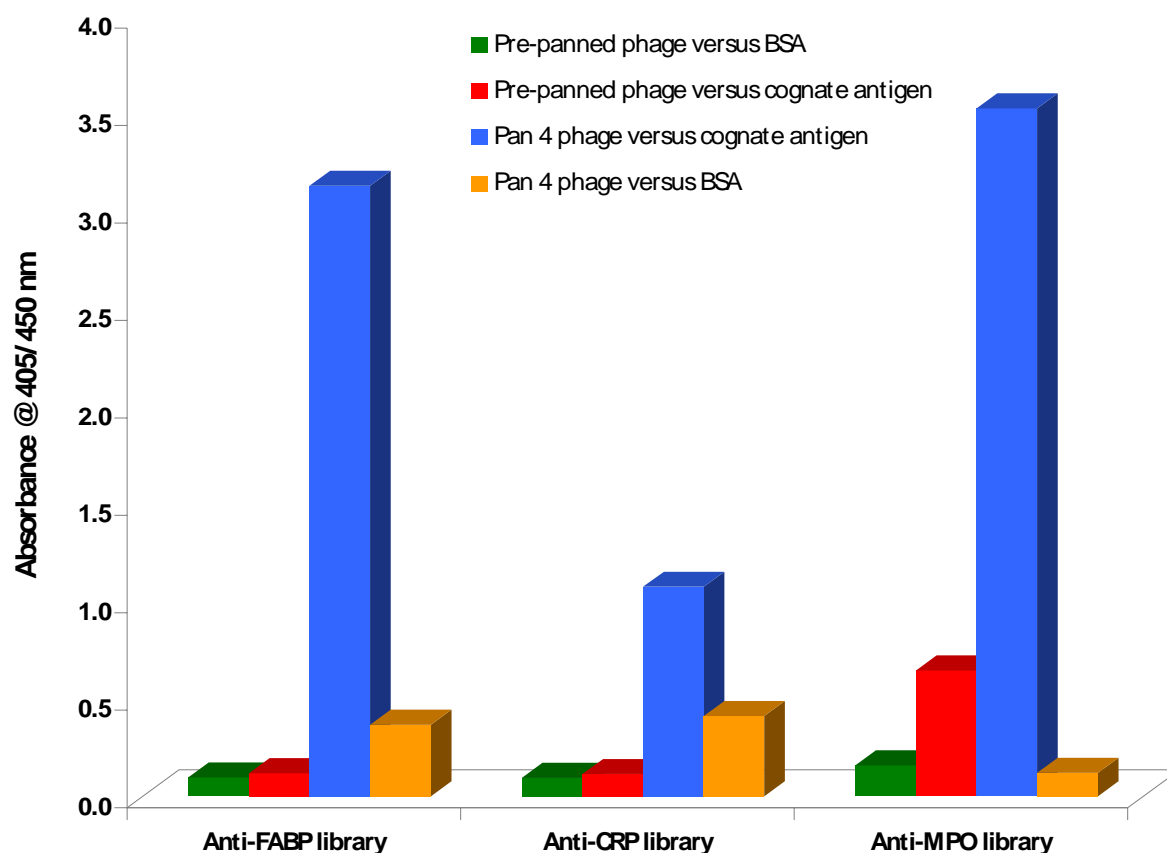


Figure 3.4.6 Polyclonal phage ELISA involving both the pre-panned and pan 4 phage pools from panning of the chicken scFv library. Both the pre-panned and pan 4 phage pools were tested in a direct ELISA format against their respective cognate antigens (CRP, FABP or MPO) and also against BSA (negative control).

Both the pre-panned and pan 4 phage pools were then incorporated into a polyclonal phage ELISA (Figure 3.4.6), as described in section 2.11.9. Due to the peroxidase nature of MPO, an AP-labelled secondary antibody was employed as opposed to the HRP-labelled secondary antibody used for detection of the CRP and FABP-specific phage. Therefore, following addition of the relevant substrates (PNPP for AP conjugate and TMB for HRP conjugate), the resultant absorbance values were read at either 405 nm or 450 nm, respectively. On analysis of the polyclonal phage ELISA, it is clearly evident that the final phage pool shows a significant level of enrichment towards MPO, which was also observed for the phage pools enriched against FABP and CRP. In each case, no non-specific binding of the phage against the BSA control protein was observed. This result clearly demonstrates the successful

employment of pooled immune chicken libraries for the generation of specific recombinant antibodies against multiple biomarker panels.

3.4.7 Soluble expression and direct ELISA of chicken anti-MPO scFv clones.

Based on analysis of the polyclonal phage ELISA, the phage output from round 4 was chosen for infection into Top 10 F' for soluble expression using protocol 2.11.10. The Top 10 F' bacterial strain is a non-suppressor strain that recognises the amber stop codon as a stop codon for production of soluble protein. The solubly-expressed enriched libraries were then analysed using expressed lysates of 120 single colonies in a direct soluble monoclonal ELISA (Figure 3.4.7) format, as described in section 2.11.11.

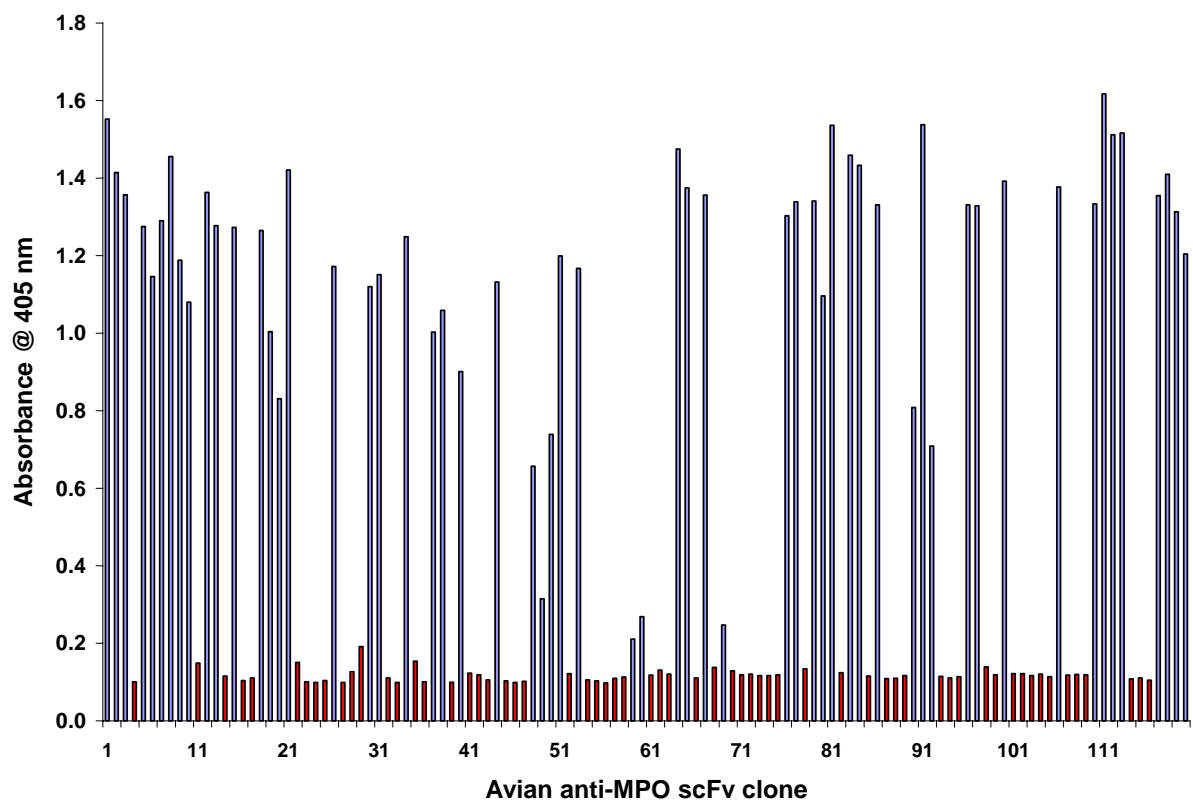


Figure 3.4.7 Direct soluble ELISA involving scFv-enriched lysate expressed from 120 chicken anti-MPO scFv clones from pan 4. The bars highlighted in blue represent all the positive MPO-specific clones and the negative clones (response below the background level) are illustrated in red.

The peroxidase nature of MPO required the use of an AP-labelled anti-HA mAb for detection of the MPO-scFv complex as opposed to the previously used HRP conjugate. Forty-four MPO-specific clones were identified, showing specificity to the MPO antigen, with no non-specific binding to bovine serum albumin. These positive clones (highlighted in blue) were taken forward for further analysis to determine solution-phase binding to MPO.

3.4.8 Preliminary Biacore analysis

The ELISA-based screening strategy employed for the murine anti-CRP scFv library (section 4.1) proved to be both considerably labour intensive and time-consuming (see sections 3.2.8 and 3.2.9). Additionally, this approach may lead to potential high affinity clones being overlooked due to poor expression. Therefore, an alternative more robust strategy was implemented for screening of the avian anti-MPO scFv library. A Biacore-based ‘ranking’ approach was decided upon, to ensure a more reliable and also high-throughput analysis of the positive clones.

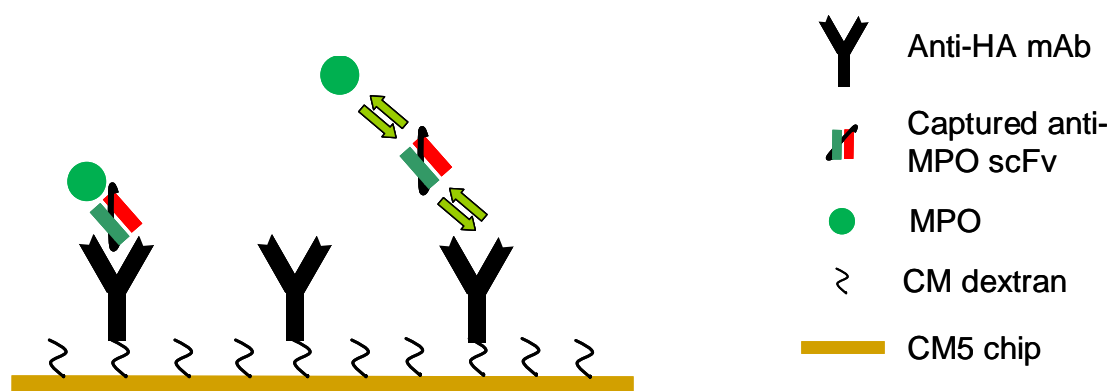


Figure 3.4.8 Capture assay format used on the Biacore 3000 instrument.

An off-rate ‘ranking’ approach was undertaken using the basic format illustrated in Figure 3.4.8. Initially, anti-HA mAb (section 2.11.12) was immobilised onto flow cell 2 (FC2) of a CM5 sensor chip (GE Healthcare) using the standard protocol described in section 2.8.8. Crude bacterial lysates were prepared for each of the positive clones using the techniques described in section 2.9.19. A 30 nM concentration of CRP proved optimal for ‘off-rate’ ranking of the avian anti-CRP scFv clones, therefore, this concentration was also investigated for the avian anti-MPO clones. However, a significant degree of non-specific binding of MPO to the FC 1 (unmodified CM-dextran reference flow cell) was identified. This was thought to be due to the highly cationic nature of MPO, resulting in non-specific binding to

the CM-dextran surface. To counteract this problem, a fresh CM5 chip was coated with anti-HA mAb described in section 2.11.12. Furthermore, the reference flow cell to be used in the analysis was activated using EDC/NHS chemistry and capped to reduce any potential non-specific binding. These modified immobilisation and surface-capping protocols involved the use of ethylenediamine (pH 8.5) as opposed to the traditional ethanolamine as a capping agent. It was envisaged that the strong basic nature of ethylenediamine would make it a more efficient capping agent for analysis of the highly cationic MPO protein.

3.4.9 Off-rate analysis of avian anti-MPO scFv clones

Each of the bacterial lysates were diluted in HBS buffer to ensure an scFv capture level of ~100 RU's. A 3 nM concentration of MPO was found to be optimal for the analysis, which showed insignificant binding to the reference flow cell. A reference control was also incorporated into the assay for each of the clones, whereby, HBS buffer was passed across each of the captured scFv clones. The conditions used in the 'off-rate' analysis assay may be found in section 2.11.13.

The 'off-rate' data for each of the clones was imported into the supplied BIAevaluation software package for analysis. Antibody/antigen complex stability (% left) was calculated for each of the clones by expressing the 'stability late' (calculated from the average response from 295 to 300 s after buffer injection) as a percentage of 'stability early' (calculated from the average response from the first 5 s after buffer injection), as illustrated in Figure 3.4.9.

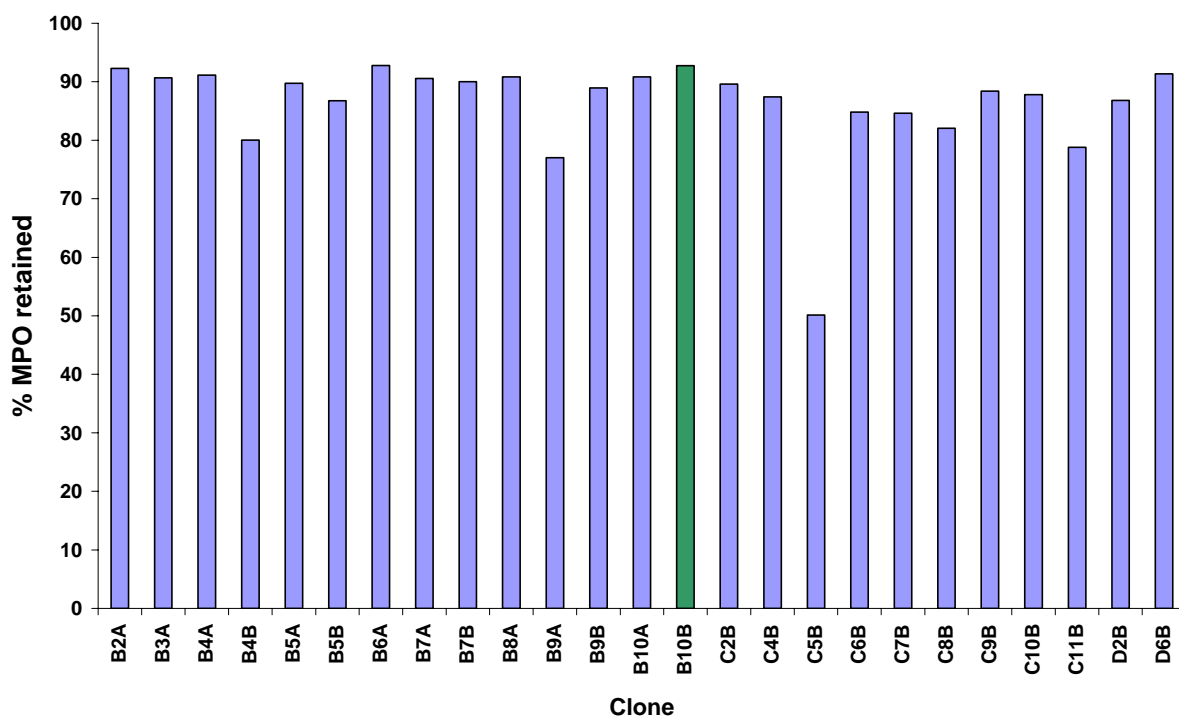


Figure 3.4.9 Analysis of the percentage antibody/antigen complex remaining after 5 min dissociation in buffer for 25 of the MPO-specific scFv clones.

Selection of the clone to be taken forward for sequencing and kinetic analysis was based on both the percentage of MPO retained and also the expression level. The clone showing the highest percentage of MPO retained was B10B, which was also found to have the highest level of expression (judged by dilution factor of lysate) of clones with over 85% MPO retained.

3.4.10 Sequence analysis of Avian B10B anti-MPO scFv clone

Following ‘off-rate’ ranking of the selected pool of MPO-specific scFv antibodies, the B10B scFv was selected for sequence analysis and more in-depth characterisation. The protein sequence of the B10B scFv is shown in Figure 3.4.10, with all of the key CDR regions, linkers and affinity tags highlighted.

IQEEFK **Met** KKT A I A I A V A L A G F A T V A Q A A L T Q P S S V S A N P G
 E T V K I T C **S G S S S G G Y G** W F Q Q K S P G S A P V T V I Y **R N N Q R P S**
 D I P S R F S G S K S G S T H T L T I T G V Q A E D E A V Y Y C **G T F D S S T S**
A G I F G A G T T L T V L G Q **S S R S S S G G G S S G G G S** A V T L D E S G
 G G L Q T P G G L S L V C K A S **G F S I S S Y G Met N** W V R Q A P G K G L E
 W V A **G I S S S G I T T G Y G S A V K G** R A T I S R D D G Q S T V R L Q L N N L
 R A E D T G T Y Y C A K **T I A D G W G Y V G S V D A** W G H G T E V I V S S T S
 G Q A G Q **H H H H H H** G A **Y P Y D V P D Y A S**

Figure 3.4.10 Sequence of the selected avian anti-MPO scFv clone. The three CDR regions for both the variable light (CDR-L) and variable heavy (CDR-H) regions are highlighted in blue and red, respectively. A glycine-serine linker (green) fuses the variable heavy and light regions together (green font). To aid in the purification and characterisation of the scFv fragments, both a hexa-histidine tag (orange) and a HA epitope tag (pink) are incorporated at the carboxyl terminus of the scFv fragment.

On analysis of the sequence data of the B10B scFv, the CDR regions for both the light (blue) and heavy chains (red) were found to be dominated by serine and glycine residues. Several studies have commented on the importance of these residues in providing suitable conformations within the CDR regions for high affinity binding (Wiesmann and Sidhu, 2004; Fellouse *et al.*, 2005; Fellouse *et al.*, 2006; Fellouse *et al.*, 2007). The small size of both serine and glycine, contribute to the overall flexibility of the CDR region, which has been shown to be a key feature in effective antigen recognition (Mian *et al.*, 1991; Padlan, 1994; Zemlin *et al.*, 2003). Furthermore, tyrosine residues were present in four of the six CDR regions, which have been suggested as playing an integral role in making favourable contacts with the antigen in the CDR regions (Birtalan *et al.*, 2008). The same study revealed that highly functional CDR-H3 loops could be derived from combinations of tyrosine, serine and glycine residues.

3.4.11 Large-scale IMAC purification of B10B anti-MPO scFv

Large-scale expression and purification of the B10B scFv was performed, as described in sections 2.10.3 and 2.10.4, respectively. Approximately 50 mg of purified scFv product was harvested from a 500 mL bacterial culture using an optimised IMAC protocol. The

production of 500 µg of pure scFv per ml of bacterial culture was deemed to be a significantly high yield.

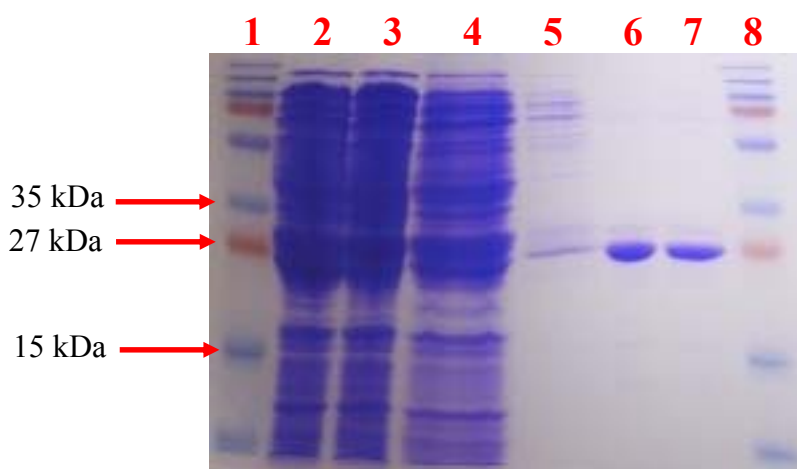


Figure 3.4.11 SDS-PAGE analysis of the various fractions of an IMAC purification of a MPO-specific scFv fragment. The fractions were loaded as crude lysate (Lane 2), ‘flow-through’ 1 (Lane 3), ‘flow-through’ 2 (Lane 4), wash (Lane 5), elution fraction (Lane 6) and buffer-exchanged fraction (Lane 7). A protein marker ladder (Fermentas) was also loaded alongside the samples in lane 1 and 8 for estimation of the apparent molecular weights of the each of the protein samples.

The final scFv fraction (Lane 7 in Figure 3.4.11) was found to have a high degree of purity with minimal contaminant proteins evident. Several formats such as ELISA, Biacore and lateral flow were used to further characterise this purified scFv preparation.

3.4.12 Titration and inhibition ELISA analysis of B10B anti-MPO scFv

Initial characterisation of the purified MPO-specific B10B scFv was performed via ELISA to determine its functionality in a basic assay format. It was decided to investigate the solution-based binding capacity of the purified B10B scFv in an inhibition-style ELISA format. Firstly, a titre ELISA (section 2.11.14) was performed to determine the optimal dilution of the purified B10B scFv to be used in the inhibition assay.

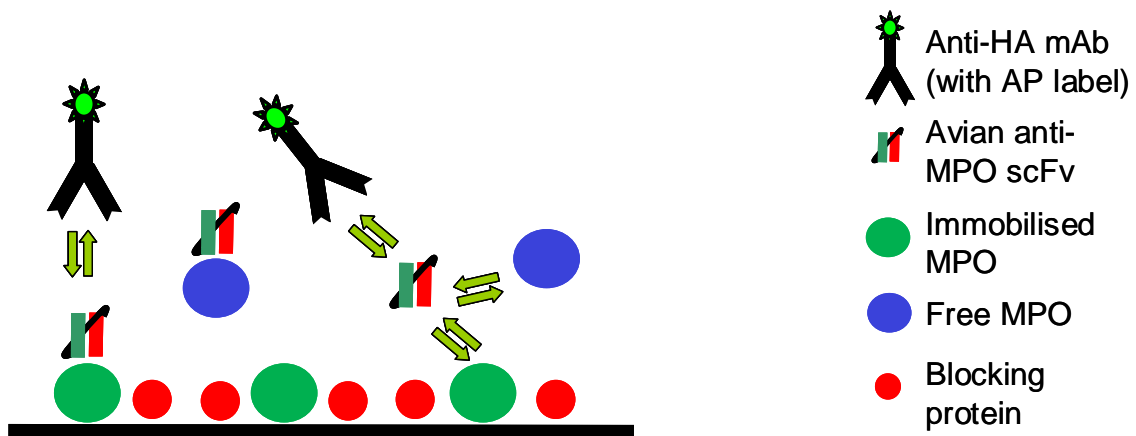


Figure 3.4.12 (b) Assay format used for inhibition ELISA.

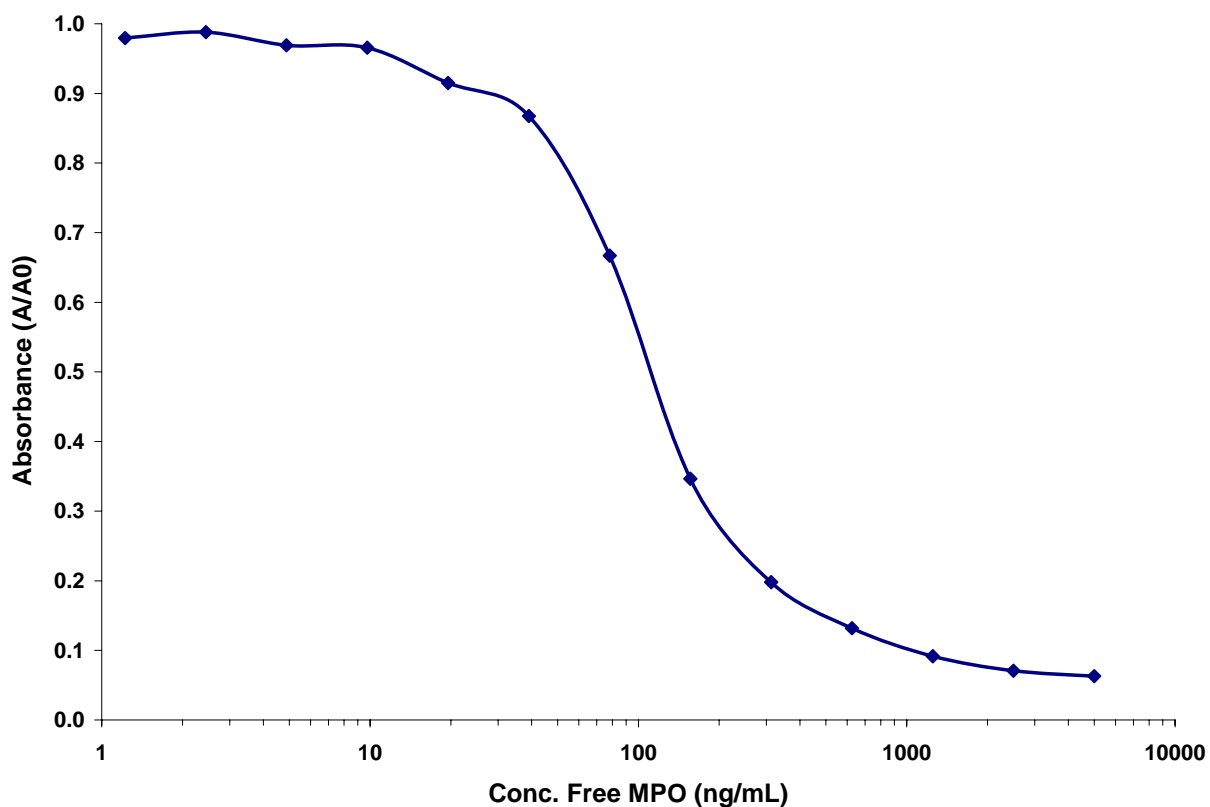


Figure 3.4.12 (c) Inhibition curve of purified avian anti-MPO scFv against several selected concentrations of MPO.

Detection of the free MPO was evident down to the low nanogram level (See Figure 3.4.12 c). An IC₅₀ is a useful value which may be extrapolated from an inhibition curve, which provides an indication of the affinity of the antibody under investigation. The IC₅₀ value (also known as the half maximal inhibitory concentration) refers to the concentration of free

MPO (ng/mL) required to give 50% inhibition of the binding of the scFv to the immobilised MPO. Therefore, the IC₅₀ value for the tested B10B scFv was approximately 90 – 100 ng/mL.

3.4.13 Kinetic analysis of B10B anti-MPO scFv clone

Crude 'scFv-rich' lysate may be employed to obtain kinetic data on a clone (as seen in section 3.2.16). Nevertheless, it was decided to use purified fractions of the MPO-specific B10B scFv due to the large yield of purified product obtained (section 3.4.10). A HA tag capture-based format was used for kinetic analysis of the B10B scFv. The anti-HA mab-immobilised CM5 chip used for kinetic analysis was prepared as described in section 2.11.12. Initially, serial dilutions of the purified B10B scFv were performed in HBS, ranging from 1/100 to 1/10,000,000. Each scFv dilution, starting with the most dilute, was passed across flow cells 1 and 2 of the CM5 chip and their subsequent capture levels monitored. A 1/200,000 dilution of the B10B scFv produced a capture level of approximately 100 RU's, following a 2 min injection at a flow-rate of 10 µl/min. This dilution translated into an scFv concentration of approximately 215 ng/mL, which was employed as the optimal scFv concentration to be used for kinetic analysis (Figure 3.4.13).

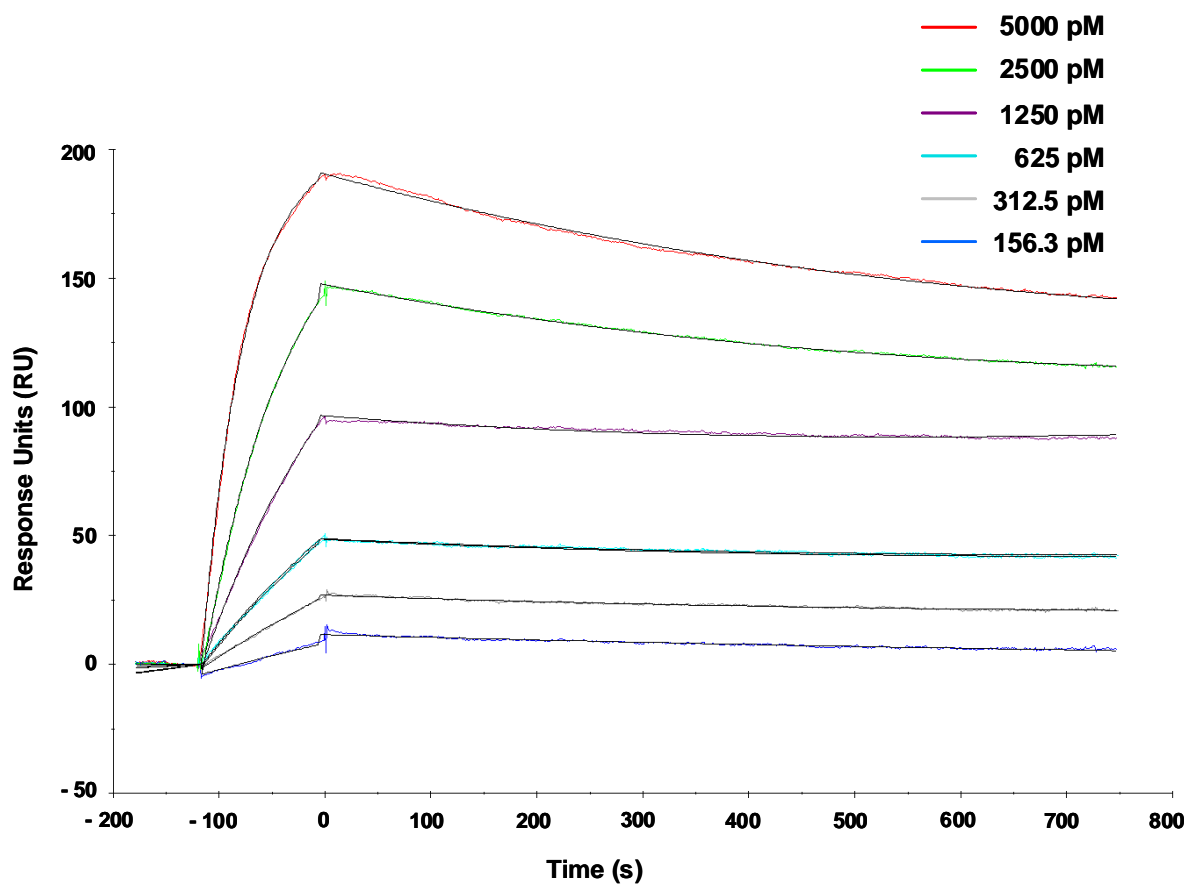


Figure 3.4.13 Kinetic analysis fit of the avian B10B anti-MPO scFv using the Biacore 3000 system. Shown is the local fit of a 1:1 interaction model (with drifting baseline) to the response data obtained from the Biacore 3000 with multiple analyte concentrations. The black lines represent the local fit, to the response data (shown as coloured lines). The six concentrations of MPO used in the analysis were 5000 (red), 2500 (green), 1250 (purple), 625 (turquoise), 312.5 (grey) and 156.3 pM (blue).

The kinetic run consisted of initial capture of the scFv, using a 2 min injection of the optimised dilution across the anti-HA chip surface at a flow rate of 10 $\mu\text{L}/\text{min}$, followed by a stabilization period of 3 min. Next, MPO was spiked into HBS at concentrations of 5000, 2500, 1250, 625, 312.5 and 156.3 pM and passed across the captured scFv at a flow rate of 30 $\mu\text{L}/\text{min}$. A duplicate of the 625 pM concentration of MPO was included, in addition to a zero concentration, enabling double referencing in the analysis. Association and dissociation phases were monitored for 2 and 10 min, respectively. Sensograms for each of the MPO concentrations were fit globally to a 1:1 interaction model using Biacore 3000 dedicated software. A good fit (Figure 3.4.13) was observed for the kinetic run using the Langmuir equation, producing a Chi^2 output value of 0.395. This 1:1 interaction model was subsequently used to extrapolate the relevant kinetic constants and binding affinities of the scFv for MPO (Table 3.4.13).

Table 3.4.13 Kinetic constants and binding affinity calculated for the B10B scFv

Kinetic parameter	k_a ($\text{M}^{-1} \text{s}^{-1}$)	k_d (s^{-1})	K_D (M)
Value	4.93×10^6	9.16×10^{-4}	1.86×10^{-10}

3.4.14 Direct detection of MPO with TMB/OPD

As discussed in section 3.4.2, the peroxidase nature of MPO was considered to be a very useful characteristic, which may be exploited in a diagnostic assay. Therefore, it was decided to investigate a potential use for the enzymatic properties of MPO in an immunological assay format, whereby MPO itself can be used as the detection enzyme in the assay format. The substrates TMB and OPD, commonly used for measurement of peroxidase activity, were identified as two potential candidates for use in the assay. To demonstrate ‘proof of principle’ a basic capture-based ELISA was performed, comparing the use of either TMB or OPD as a detection agent.

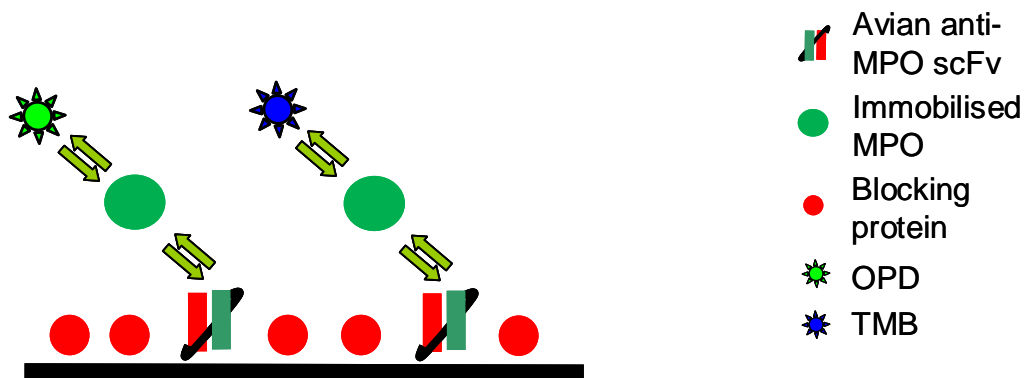


Figure 3.4.14 (a) Assay format used for direct detection of MPO with TMB/OPD.

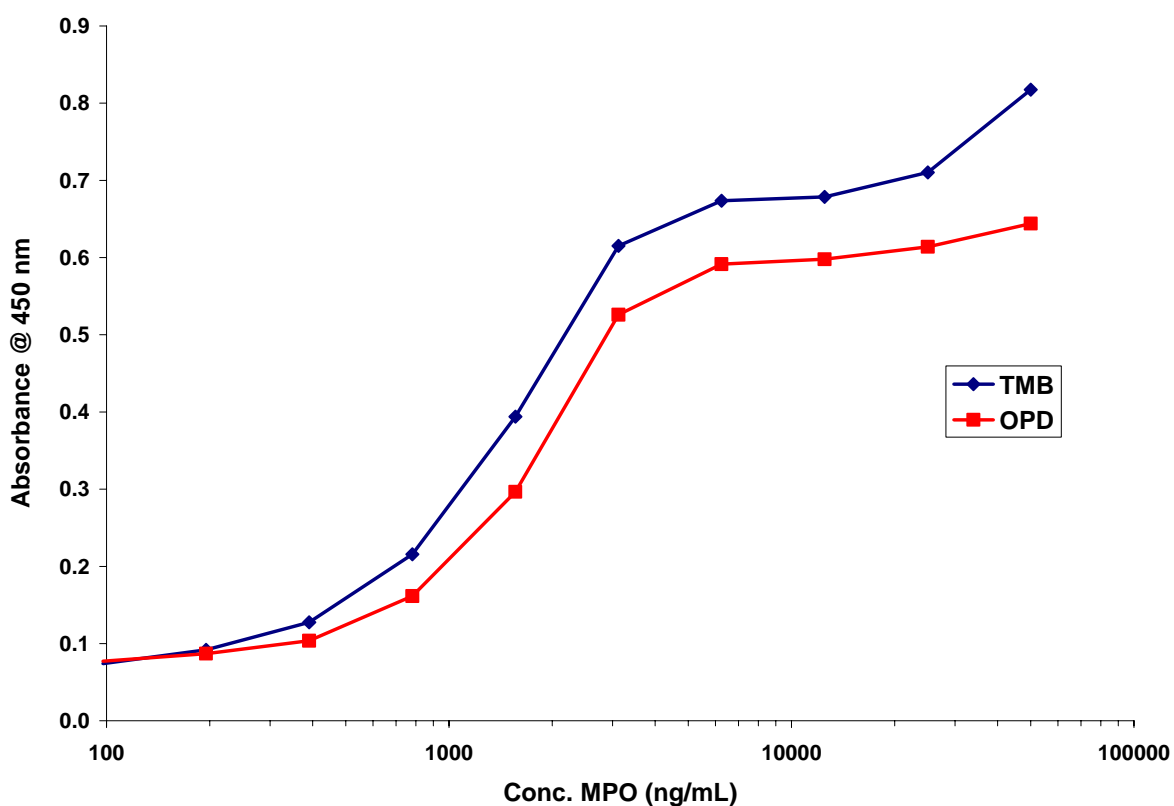


Figure 3.4.14 (b) Use of substrates TMB and OPD as direct detection agents of MPO in an ELISA-based assay.

The format of the ‘proof of principle’ assay is illustrated in Figure 3.4.14 (a) and a description of the assay itself may be found in section 2.11.15. On analysis of the assay data (Figure 3.4.14 b), a good correlation was observed between both of the substrates and the varying concentrations of MPO used. Although both substrates produced similar results

(detection of MPO down to the low ng/mL range), the TMB substrate was found to be slightly more sensitive and was, therefore, adopted for application in an alternative assay format.

3.4.15 Lateral flow assay development

It was decided to investigate this novel method for the rapid detection of MPO in an alternative more robust system. Although an ELISA-based approach proved successful for implementation of this novel assay format, several time-consuming steps such as hour long incubations and wash steps contribute to an overall poor assay turn-around-time (TAT). Conversely, the employment of a lateral flow immunoassay (LFIA) – based format will allow for a significant improvement in assay TAT. Initially, a preliminary hybrid-type lateral flow/western blot format (see section 2.11.16) was employed to ensure functionality of the assay on the LFIA nitrocellulose membrane. MPO was spiked into 1% (w/v) milk-PBST solutions at concentrations of 10000, 1000, 100 and 10 ng/mL. Instead of allowing the samples travel up the strip via capillary action (classic lateral flow), a less stringent approach was utilised involving full submersion of each of the strips in its corresponding spiked MPO sample. Similarly, liquid TMB substrate was applied to the test line area and allowed to develop (See Figure 3.4.15 a)

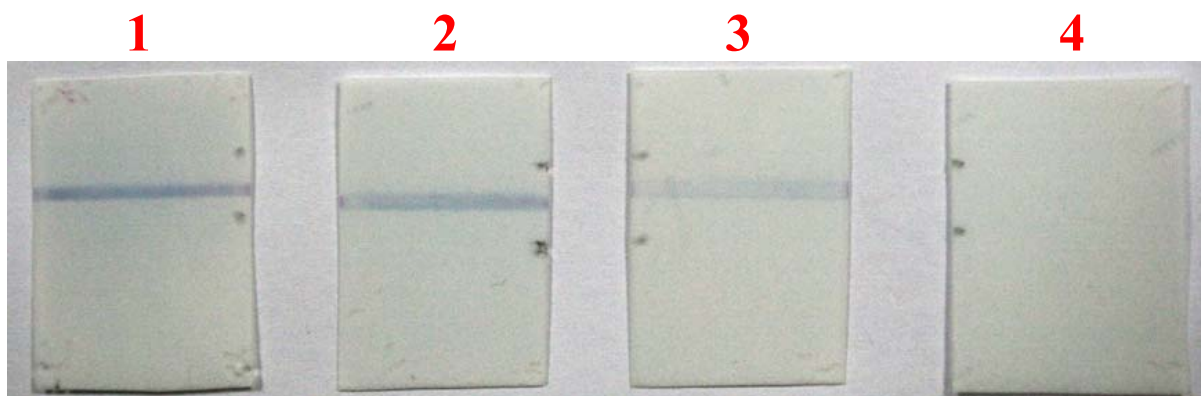


Figure 3.4.15 (a) Developed nitrocellulose membrane strips from the hybrid LFIA-western blot assay. Strips 1 – 4 represent detection of 10000, 1000, 100 and 10 ng/mL of MPO-spiked samples.

Detection of the scFv-captured MPO is clearly visible in the buffer samples spiked with 10000, 1000, and 100 ng/mL of MPO, however, the lowest concentration of MPO (10 ng/mL) was found to produce no visible band. The main focus of this hybrid assay was to identify whether or not this particular direct detection format could be applied to a

nitrocellulose membrane. Due to the successful application of this assay format on the nitrocellulose membrane, the next step involved performing the assay in an authentic LFIA.

The finalised protocol for the optimised LFIA may be found in section 3.12.1. An identical format to that shown in Figure 3.4.14 (a) was used for all subsequent LFIA experiments, except only TMB substrate was employed for detection of the test and control lines. In each assay the developed test line represents the scFv captured-MPO detected with TMB substrate and the control line shows the HRP-labelled Ab reacting with the TMB substrate. Prior to the identification of this finalised protocol, however, several preliminary LFIA experiments were performed involving optimisation of several components of the assay procedure such as spotting buffer, scFv spotting concentration, sample application and running/wash buffers used. One of these preliminary experiments examined the combination of various spotting buffers with various running buffers for use in the LFIA experiments (Figure 3.4.15 b).

Table 3.4.15 Various buffer combinations used for LFIA experiments

Label	Spotting Buffer	Running buffer
A	Borate (0.1% (w/v) BSA, 0.05% (v/v) Tween, 0.01% (v/v) Triton X)	Borate (0.05% (v/v) Tween)
B	Borate (0.1% (w/v) BSA, 0.05% (v/v) Tween, 0.01% (v/v) Triton X)	50mM sodium phosphate, pH 7.5 + 0.05% (v/v) Tween
C	Borate (0.1% (w/v) BSA, 0.05% (v/v) Tween, 0.01% (v/v) Triton X)	50mM sodium phosphate, pH 7.5
D	50mM sodium phosphate, pH 7.5 (1% (w/v) trehalose)	50mM sodium phosphate, pH 7.5 + 0.05% (v/v) Tween
E	50mM sodium phosphate, pH 7.5 (1% (w/v) trehalose)	50mM sodium phosphate, pH 7.5

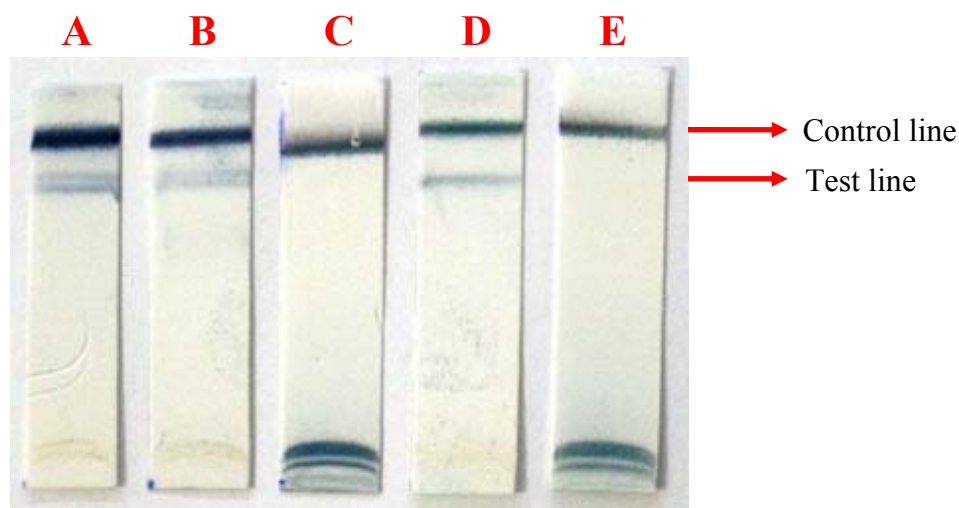


Figure 3.4.15 (b) Developed nitrocellulose membrane strips from LFIA optimisation experiments. Strips A – E represent various buffer combinations (Table 3.4.15) used for the LFIA experiments. Each of the strips was sprayed with a test line (purified MPO-specific scFv) and also a control line (HRP-labelled anti-rabbit antibody).

A selected scFv spotting concentration of 500 $\mu\text{g/mL}$ was applied for each strip. Additionally, a concentration of 1 $\mu\text{g/mL}$ of MPO was used for each of the five strips in this comparative experiment. On analysis of each of the developed LFIA strips, it was clear that combination D produced the most optimal conditions. In comparison to strips A and B, a clear defined test line band was observed for combination D (spotting buffer - 50mM sodium phosphate, pH 7.5, containing 1% (w/v) trehalose and running buffer - 50mM sodium phosphate, pH 7.5 + 0.05% (v/v) Tween). Furthermore, these experiments demonstrated the importance of the presence of 0.05 % (v/v) Tween in the running buffer solutions. It was discovered that the use of a buffer without Tween resulted in unsuccessful migration of the MPO protein up the strip. Instead the MPO stayed at the application area (bottom of the nitrocellulose membrane) where it was detected with the TMB substrate.

No ‘negative control’ had been incorporated for initial testing. Therefore, a further LFIA experiment was set up examining the detection of a range of MPO concentrations (1000, 500, 250, 125, 62.5 ng/mL). In addition, a ‘negative control’ was included in the experiment involving the application of running buffer to one of the strips containing no spiked MPO (Figure 3.4.15 c). Again, the scFv spotting concentration was set at 500 $\mu\text{g/mL}$ and buffer combination D was implemented for this assay.

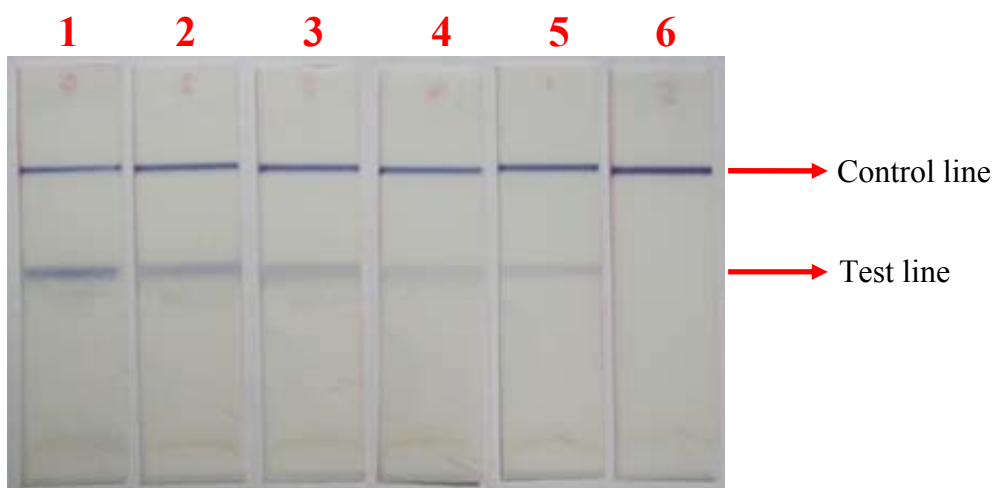


Figure 3.4.15 (c) Developed nitrocellulose membrane strips from LFIA optimisation experiments. Strips 1 - 6 represent the detection of 1000, 500, 250, 125, 62.5 and 0 ng/mL of MPO-spiked running buffer, respectively. Each of the strips was sprayed with a test line (purified MPO-specific scFv) and also a control line (HRP-labelled anti-rabbit antibody).

A good correlation was observed between the band strength and the concentration of MPO, where a clear pattern was evident. Moreover, no band was observed for the ‘negative control’ strip, which further validates the sensitivity and specificity of the LFIA. The final optimised LFIA experiment data, including a critical discussion of its potential use as a point-of-care (POC) assay may be found in section 3.5.4.

3.4.16 Discussion of results

Due to the impressive performance of the avian immune system in the generation of highly sensitive and specific CRP-specific scFv clones, it was decided to take advantage of this refined host for the generation of an MPO-specific scFv library. Avian hosts were combined with the use of the pComb system for construction of the MPO-specific library. As previously discussed, this system proved to be highly efficient in terms of both the ease of construction and subsequent characterisation of antibody libraries.

As described for the screening approach of the murine scFv library, an initial preliminary ELISA was performed for the identification of MPO-specific clones. However, due to differences in antibody expression and valency, the signal intensity of such assays cannot be reliably linked to antibody affinity (Steukers *et al.*, 2006). Furthermore, antibody concentration determinations are required prior to affinity constant determination. For this

reason, implementation of a complete ELISA-based screening strategy can prove to be both considerably labour-intensive and time-consuming. Therefore, for this library, an alternative more refined screening strategy was implemented, as opposed to the ELISA-based screening strategy employed for screening of the CRP-specific murine library (sections 3.2.8 and 3.2.9). A successful high-throughput screening (HTS) campaign involves ranking of promising candidates through a series of different screening assays that are both high-throughput and informative. The Biacore-based strategy employed for this library achieved both of these essential characteristics and enabled the identification of several high affinity MPO-specific scFv clones. Moreover, the off-rate approach enabled the identification of clones possessing high expression levels such as the B10B, which proved to be significantly advantageous for their purification and subsequent incorporation into the developed LFIA. Initially, obtaining reliable kinetic Biacore data on the MPO-specific B10B scFv proved somewhat troublesome due to the highly cationic nature of MPO. However, an optimised protocol was developed (section 2.11.12) for immobilisation of the Biacore CM5 chip. This enabled reliable kinetic data to be gathered on the scFv, without any interference from non-specific cationic interactions. An affinity of 1.86×10^{-10} M (186 pM) was extrapolated from the kinetic data of the B10B scFv, which was found to be well within the clinically relevant reference range. According to a key study by Baldus and colleagues (Baldus *et al.*, 2003), a threshold level of 350 ng/ml (2.33 nM) proved to be optimal in predicting cardiac risk in ACS patients. Thus, the isolated MPO-specific B10B scFv clone (affinity of 186 pM) has the ability to detect MPO well within such clinically relevant threshold levels.

The peroxidase nature of MPO provided a unique opportunity to develop a novel assay for its rapid detection. Initially, a proof-of-principle' ELISA was performed to determine the ability of TMB substrate to detect the B10B scFv-captured MPO, which proved successful. In terms of the combination of the use of TMB substrate with a capture-based immunoassay, a similar product is the InnoZyme™ Myeloperoxidase Activity Kit developed by Calbiochem. This kit is designed to measure human myeloperoxidase activity in cell lysates and biological samples and to screen enzyme inhibitors. This particular assay was employed by Baldus and colleagues (Baldus *et al.*, 2003) in the ground-breaking study investigating the ability of MPO serum levels to predict risk in ACS patients. The ELISA-based approach of this assay, however, means several time-consuming incubation and wash steps contribute to an overall poor TAT for the assay. For this reason, an alternative platform was decided upon for incorporation of the MPO-specific assay, namely LFIA. This robust LFIA technology provided a cheap and efficient method for developing a rapid, sensitive and specific assay for

the detection of MPO. The final optimised LFIA is discussed in more detail in section 3.5.1, including the advantages of having a one-step POC version of this assay available in the clinical arena.

3.5 Point-of-care platforms for detection of CRP and MPO

3.5.1 Point-of-care technology

Point-of-care (POC) tests are a simple, rapid and relatively inexpensive means for reducing hospital stay, complications and improving adherence to treatment (McDonnell *et al.*, 2009). The use of POC tests can lead to a reduction in test ordering, sample transport to laboratories and data reporting. Several high-throughput automated systems have enabled the introduction of a wide range of tests to be performed simply (no requirement for highly trained personal) and quickly (without the need for laboratory processing). Overall, there are mixed opinions regarding the issue of POC implementation. For instance, several POCT investigators have concluded that these POC analysers could serve as an alternative to lab analysers (Wu *et al.*, 2004; Ordonez-Llanos *et al.*, 2006). In contrast, other studies have questioned the accuracy of the technologies (Agewall, 2003; James *et al.*, 2004; Cramer *et al.*, 2007). Several studies have investigated the implementation of POCT devices in a clinical setting. For instance, a study by Rathore and colleagues (Rathore *et al.*, 2008) explored the application of the ‘Triage Cardiac Panel’ (Biosite) in a hospital A & E department. This panel consisted of the simultaneous detection of the three cardiac biomarkers of creatine kinase MB (CK-MB), myoglobin and cardiac troponin I (cTnI). The study concluded that the POCT device had the potential to significantly reduce hospital admissions of patients in the low to intermediate risk range. A clinicians experience of using a cardiac POCT device (developed by Roche) in a clinical setting (Alehagen and Janzon, 2008), whereby the device was compared to the performance of a clinical laboratory assay, concluded the POC device to be potentially useful in the clinical setting, with comparable results to the central lab system. A further study by Apple and colleagues (Apple *et al.*, 2006) demonstrated both the cost effectiveness and clinical efficacy of implementation of a POC assay by Dade Behring. Use of the POCT device led to a significant decrease in assay TAT compared to the central laboratory and also a 25% decrease in total charges, saving an estimated \$4,281 per patient admission.

The two main types of POC testing formats available in the clinical setting include small bench-top analysers and hand-held devices. Small bench-top analysers are basically a miniaturised version of the mainframe central lab equipment, except with essential modifications to prevent operator error and provide rapid, reproducible results. Hand-held devices are developed using state-of-the-art microfabrication techniques, which essentially integrate several key analytical steps i.e. sample clean-up, separation, analysis and data reporting. Devices for cardiac biomarker POC testing are predominantly based upon immunoassay methods. The current formats for these devices are principally 2-site

immunometric methods, lateral-flow technology (LFT) and flow-through immunoassay systems. However, rapid development in the field of antibody-based biosensors is predicted to lead to a new era in POCT design (Sluss, 2006). An example of this is the validation of a Resonant Acoustic Profiling™ (RAP™) (McBride and Cooper, 2008) system for quantification of CRP levels in serum samples. Although not a prototypical POCT, this system is label-free and shows good correlation with a commercial hs-CRP ELISA but with a much reduced sample analysis time.

3.5.2 Lateral flow immunoassay (LFIA)

A classic POC technique which continues to be successfully applied in many fields is LFIA. LFIA is designed as a robust and user-friendly immunochemical method suitable for specific semi-quantitative detection of analytes. This technique needs only low-cost instrumentation and enables significant reduction of the assay duration when set against ELISAs on microtitration plates. Such favourable characteristics have led to the application of LFIA technology across a wide range of areas (Henderson and Stewart, 2000; Aldus *et al.*, 2003; O'Keeffe *et al.*, 2003; Salomone *et al.*, 2004; Edwards and Baeumner, 2006; Koets *et al.*, 2006; Wang *et al.*, 2006; Kalogianni *et al.*, 2007; Wang *et al.*, 2007; Corstjens *et al.*, 2008; Posthuma-Trumpie *et al.*, 2009). The lack of any specialised storage conditions such as refrigeration, make this technology an ideal test format for biomedical purposes in third-world countries. Moreover, visual interpretation of the results is often satisfactory. Large batches of these devices may be prepared due to their extensive shelf-life, which in turn can lead to a reduction in variation between batches. Another appealing characteristic of LFIA's is their disposable single use design, which rules out the possibility of any contamination with previously tested samples.

As discussed in section 3.4.13, the intrinsic enzymatic activity of MPO provided a unique opportunity for its detection in a novel assay format. The exploitation of the peroxidase nature of MPO, eliminated the need for the standard sandwich-based format to be used. This removes additional steps in the assay such as the addition of a secondary conjugate antibody, reducing both assay TAT and also cost. Therefore, to ensure such beneficial characteristics were maintained in the final MPO-specific assay, it was decided to combine this novel assay format with the well-established technology of LFIA.

Following the optimisation of several parameters (section 3.14.4) of the MPO-specific LFIA, the detection of MPO from depleted human serum was investigated. The fully optimised

protocol for the LFIA may be found in section 2.12.1. As a comparison, several concentrations of MPO were spiked into both MPO-depleted human serum (HyTest) and also LFIA running buffer (50 mM sodium phosphate, pH 7.5, containing 0.05% (v/v) Tween). MPO was spiked into both the serum and buffer to concentrations of 500, 50 and 5 ng/mL. Additionally, control samples containing no spiked MPO were also prepared in both, to identify any non-specific background signal. Each of the serum- and buffer-spiked samples were prepared from an initial working-dilution of the MPO diluted in sterile filtered PBS. This approach was performed to avoid any potential variation between both sets of dilutions, which may become an issue when the dilutions are prepared from a concentrated stock of the analyte. Furthermore, the LFIA using both the serum and buffer methods were performed simultaneously to reduce any inter-assay variability. The developed LFIA strips (8 in total) using both methods are shown in Figure 3.5.2.

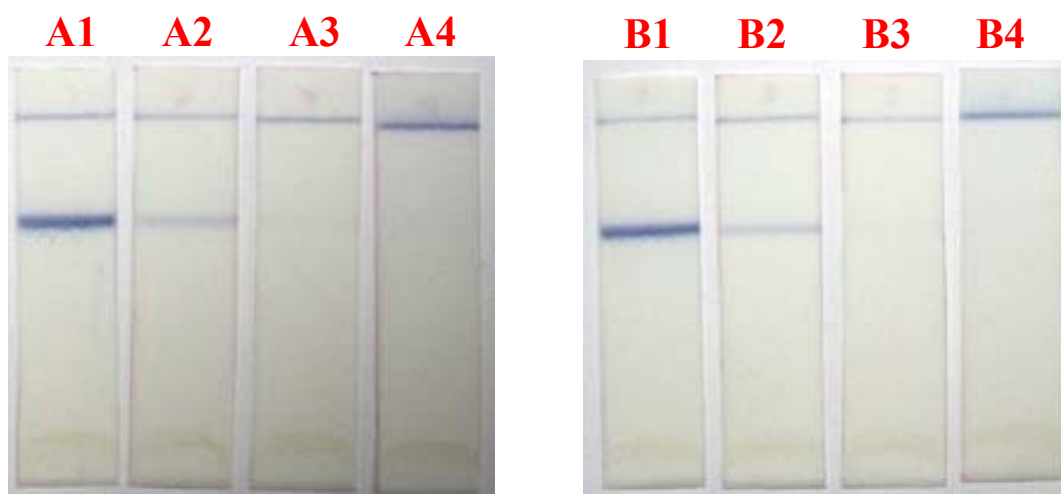


Figure 3.5.2 Developed LFIA strips from an the fully optimized assay, performed in both MPO-depleted human serum (A) and 50 mM sodium phosphate, pH 7.5, containing 0.05% (v/v) Tween (B). MPO was spiked to final concentrations of 500, 50, 5 and 0 ng/mL (1, 2, 3 and 4) for both methods.

Detection of both the 500 and 50 ng/ml (S1, S2 and B1, B2) concentrations of MPO-spiked serum are evident from Figure 3.5.5, where clear defined bands may be observed at the test line. A lighter yet distinct band was also observed by eye for the 5 ng/ml concentration of MPO tested, however, the camera was unable to clearly capture the relevant band. In any case, detection of MPO at this range is not required as clinical studies investigating the use of MPO as a risk predictor have identified concentrations as high as 350 ng/ml as being

clinically relevant threshold values (Baldus *et al.*, 2003). The key novel aspect of this LFIA is the combination of a highly specific and sensitive recombinant antibody fragment with the rapid reactivity of the TMB substrate with MPO. Furthermore, the incorporation of this system into a lateral flow strip, allows for the highly specific and sensitive detection of MPO, at a patients bedside, in approximately 20 min. Considering a prototype strip would contain both pre-sprayed test and control lines, the turn-around-time (TAT) mentioned, refers to the actual performance of the assay i.e 20 min.

As with any technology, LFIA has several limitations associated with its use. As was the case for the developed MPO-specific LFIA, a standard nitrocellulose material was employed. This mesh-like membrane is one of the most popular membranes used for LFIA devices (Henderson and Stewart, 2000; Paek *et al.*, 2000; Lönnberg and Carlsson, 2001; Oku *et al.*, 2001; Zhu *et al.*, 2002; Kim *et al.*, 2003; Leung *et al.*, 2003; O'Keeffe *et al.*, 2003; Jin *et al.*, 2005; Edwards and Baeumner, 2006; Zhang *et al.*, 2006; Kalogianni *et al.*, 2007) and is available in various pore sizes ranging from 0.05 to about 12 μm . However, these pores are not randomly distributed because of the manufacturing process and this can lead to inconsistent or poor flow rates. In addition, usually the nitrocellulose material to be used for production of the LFIA device can be stored at ambient temperature and humidity; however, at low humidity, handling of the material can be difficult owing to accumulation of static electricity (Posthuma-Trumpie *et al.*, 2009). Non-specific signal in nitrocellulose-based assays has also been highlighted as a significant problem for the diagnostic industry (Jones, 1999). In general, LFIA's are only capable of providing qualitative data, where the exact level of the detected analyte remains unknown. This characteristic is one of the main limitations associated with the use of LFIA in the field of diagnostics. One method used to circumvent this problem, is the incorporation of a dedicated fluorescent reader, which allows for quantitative data on the analyte to be obtained. An example of such a platform is the 4castchip™ developed by Åmic AB (Uppsala, Sweden). This open lateral flow (OLF) device was investigated for the development of a sandwich-based assay for the detection of CRP (next section).

3.5.3 Amic Open Lateral Flow (OLF) platform

In addition to its ability to provide quantitative information on an analyte, the 4castchip™ has several other beneficial attributes over standard lateral flow systems. This micro structured plastic device is composed of a highly ordered array of micro pillars (Figure 3.5.3 a). These custom designed micro pillars drive the flow of liquid in an open channel by capillary action, which generates wicking capabilities far superior to that of standard nitrocellulose-based LFIA. The flow of liquid through the chip is controlled by both the pillar geometry and the channel length, made possible via an extremely reproducible manufacturing technology. Such is the precision of this technology that every manufactured chip possesses an identical surface flow rate. Moreover, the chip surface also provides a biocompatible surface for the attachment of capture ligands at test and control lines. Therefore, the Amic device offers the capacity for multiple functionality, where the pillar-defined flow path can act as a sample application area, reaction surface and wick.

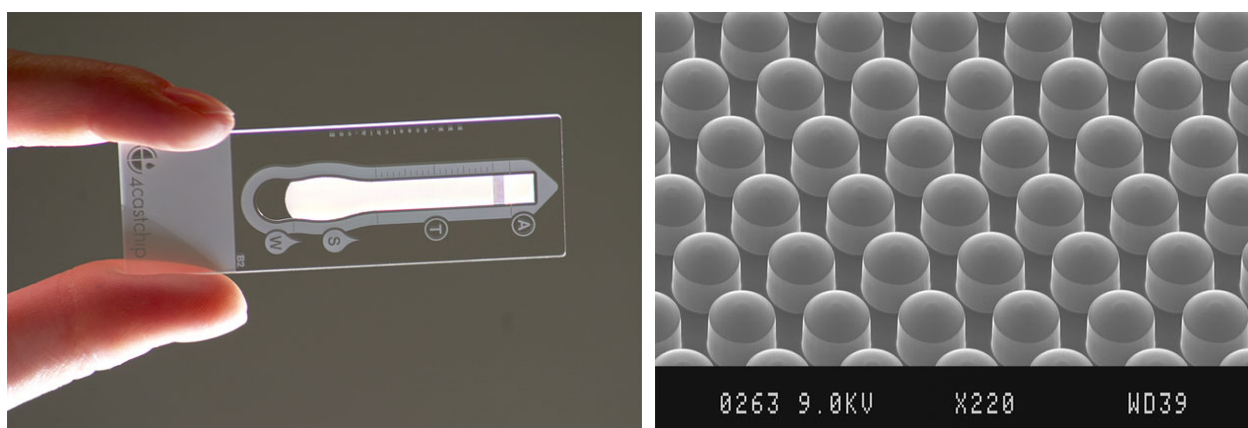


Figure 3.5.3 (a) The Open lateral flow 4 castchip™ (left) and a magnified image of the micro-pillar structures (right).

The aldehyde-functionalised surface chemistry of the 4castchip™ allows for simple coupling of capture molecules to the chip. Amine groups on the capture probes react by a simple one-step Schiff's base reaction to couple covalently to the chip surface. This novel surface chemistry also leads to a reduction in background signal from non-specific binding. Also, the hydrophilic nature of the surface is comparable with protein surfaces such as BSA which, unlike conventional lateral flow matrices, obviates the requirement for any blocking steps.

A competition-based approach was decided as the assay format for detection of CRP (See Figure 3.5.3 b). The ‘in-house’ CRP-specific antibodies chosen for the assay were the four scFv antibodies (F8, F8, G5 and H2) from the immune avian library (See sections 3.3.4 and 3.3.5). Two commercial anti-CRP mAb’s (M701289 and M7111422, Fitzgerald, MA) were also incorporated into this comparative assay. A negative control in the form of an anti-cTnI scFv was also used in the assay, to identify the background binding level. Finally, to ensure a realistic sample matrix, CRP-depleted serum was the medium employed in the assay (See section 2.12.2 for the full protocol).

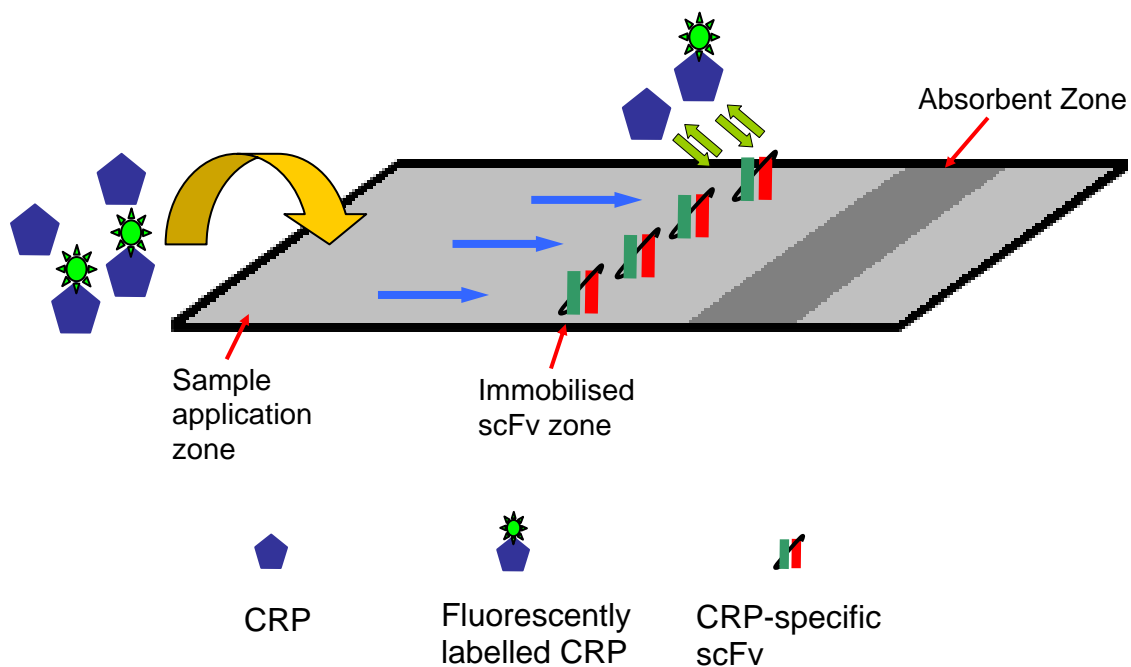


Figure 3.5.3 (b) Assay format for competitive CRP assay on an open lateral flow 4castchip™ chip. The ‘immobilised antibody zone’ of each chip was coupled with one of the six antibodies discussed. A defined mixture of unlabelled and labelled CRP was applied to the ‘sample application zone’, which travels up via capillary action towards the immobilised antibodies. The unlabelled CRP and the fluorescently-labelled CRP compete for binding to the immobilised antibodies.

The assay comprised each of the 6 capture antibodies (4 anti-CRP scFv, 2 anti-CRP mAb and 1 anti-cTnI scFv) being spotted onto individual chips. Next, CRP-depleted serum was spiked with seven concentrations of CRP antigen (30, 10, 3.3, 1.1, 0.55 and 0 µg/mL). CRP antigen labelled with a commercial fluorophore (Alexa 647) was added to each of the spiked samples

to a final concentration of 100 ng/mL and each mixture then applied to each of the chips in triplicate. The unlabelled CRP and the fluorescently-labelled CRP compete for binding to the strip containing the immobilised antibodies. The higher the spiked unlabelled CRP antigen concentration in the samples, the lower the quantity of bound labelled CRP antigen that binds to the immobilised antibody layer, hence, the lower the final fluorescent signal.

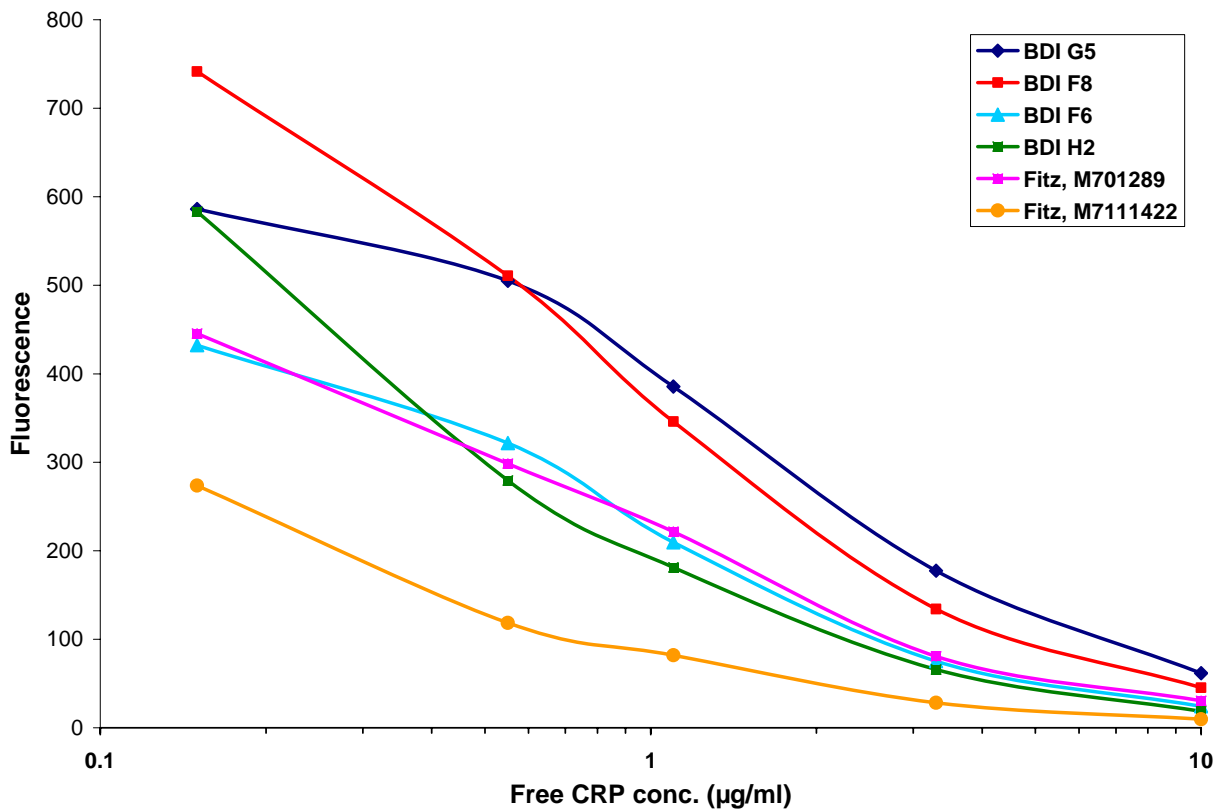


Figure 3.5.3 (c) Plotted competition ELISA data for all four purified avian anti-CRP scFv antibodies and two commercial CRP specific mAb's (Fitzgerald).

The plotted data for the competitive binding assay is shown in Figure 3.5.3 (c). Each of the plots shown were normalised to background using an unrelated anti-cardiac troponin I (cTnI) recombinant antibody. Comparable depletion of the labelled anti-CRP antigen was observed for each of the four avian anti-CRP scFv clones to that of the commercial Fitzgerald mAb's and also no cross reactivity was observed for the avian anti-cTnI scFv clone.

As previously discussed, the 4castchip™ offers a superior alternative to that of standard nitrocellulose-based LFIA's. However, the requirement for chips to be handled individually could be considered a drawback from a processing standpoint, by contrast with the ability of materials such as nitrocellulose to be processed in-line. Additionally, application of the test sample (spiked CRP-depleted serum in this case) to the 'sample application zone' must be highly regular, reproducible and carefully controlled to ensure assay consistency. Another potential cause of variation in this particular assay may be caused by the wash step (section 2.12.2) that must be performed to remove any non-specific material from the readout site (immobilised antibody zone).

3.5.4 Parabolic chip platform

One approach to circumvent the problem of 'wash step variation' is the employment of supercritical angular fluorescence (SAF) detection technology (Laib *et al.*, 2006). The use of SAF confines the fluorescence detection volume strictly to the close proximity of the biochip surface (surface confined fluorescence), whereas collecting below the critical angle allows gathering of the fluorescence emitted several microns deep inside the sample. Consequently, the signals from surface-bound and unbound diffusing fluorescent molecules can be obtained simultaneously (Verdes *et al.*, 2007). This removes the requirement for a wash step due to the devices ability to distinguish between the non-specific fluorescent signal in the bulk mixture from the specific fluorescent signal at the chip surface. In addition to a reduction in assay variation, the removal of wash steps may also lead to a significant decrease in the assay TAT. A common downfall of many diagnostic platforms is the poor signal to noise ratio associated with them. However, the ability of SAF technology to achieve highly specific surface excitation, leads to a more accurate and sensitive detection of analyte. An example of a biosensor employing SAF-based detection is the parabolic chip developed at the Biomedical diagnostic Institute (BDI) in Dublin City University (DCU), Ireland. Huge advances in injection moulding technology have led to the ability to mass produce novel lab-on-a-chip platforms (Tüdös *et al.*, 2001; Yakovleva *et al.*, 2002; Kim *et al.*, 2005; Situma *et al.*, 2006) possessing superior accuracies at sub-micron levels. This capability has led to the development of the lab-on-a-chip format such as the BDI proprietary parabolic chip. This novel biochip platform is composed of a low auto-fluorescence zeonex polymer (refractive

index 1.52). The biosensor chip (Figure 3.5.4 a) consists of a 3 x 3 annular aperture array, allowing for a total of nine biochemical surface reactions to be monitored in ‘real time’.

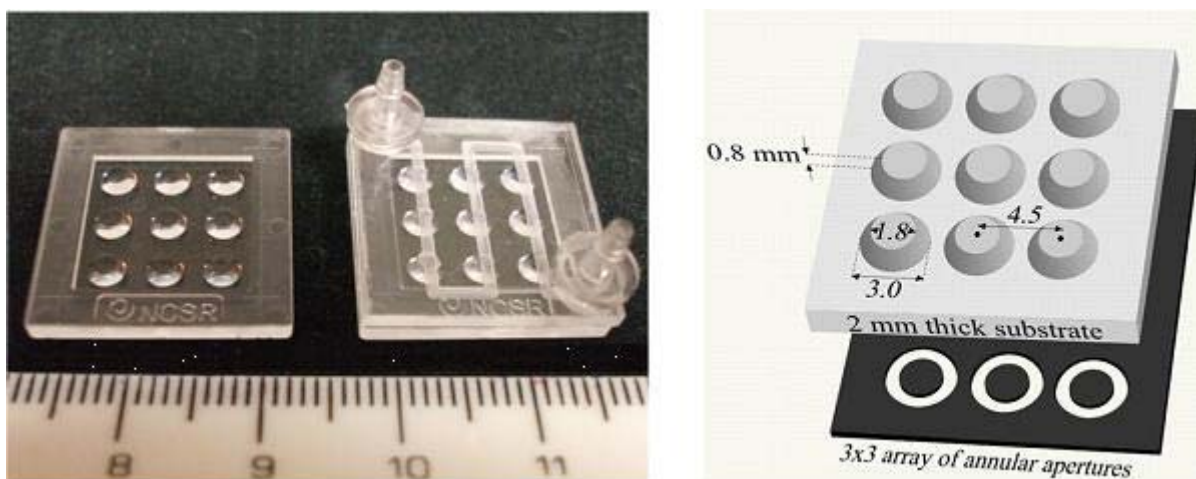


Figure 3.5.4 (a) Parabolic array format of biochip together with microfluidic channel for sample delivery (left). Annular aperture mask for blocking non-Total Internal Reflection Fluorescence (TIRF) excitation and non-SAF emission (right). TIRF excitation is the phenomenon of total internal reflection, which occurs at the interface between optically dense medium, such as glass, and optically less dense medium such as water or an aqueous solution. At large angles of incidence, the excitation beam reflects back into the glass and generates an evanescent wave at the water interface. The evanescent wave has a maximum intensity at the surface and exponentially decays with the distance from the interface. Only molecules that are at the TIRF surface are excited and fluoresce, while molecules in the bulk of solution, at distances larger than 100-200 nm are not excited and, respectively, do not fluoresce.

The enhancement of fluorescence capture, using this biosensor, is of the order of 100-fold. Following completion of the assay, a collimated excitation beam (Figure 3.5.4 b) is supercritically reflected off the edges of the paraboloid so that excitation of fluorophores on the polymer-liquid interface occurs due to an evanescent wave. Subsequently, light from surface-bound fluorophores is emitted preferentially into supercritical angles i.e. supercritical angle fluorescence (SAF). This emitted light is then collected again by the paraboloid edges and reflected into a ‘loss-free’ collimated beam towards a detector.

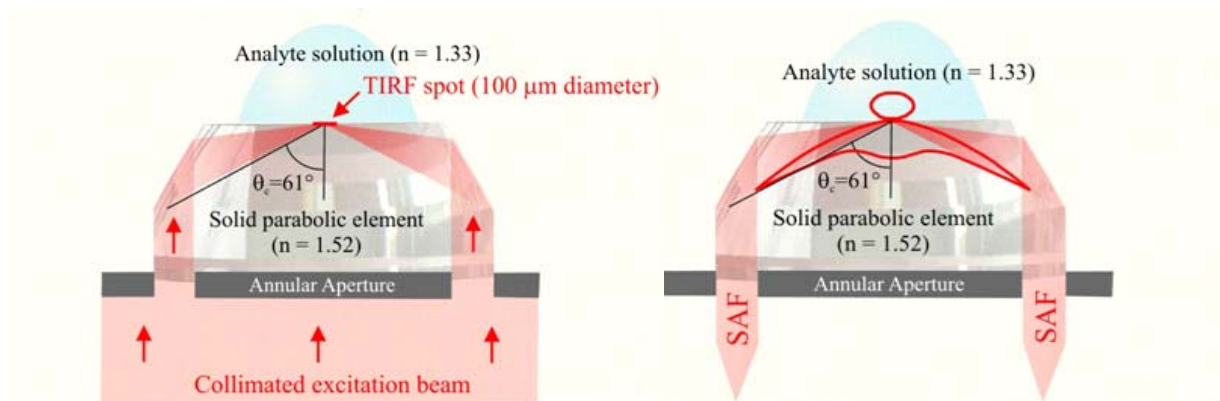


Figure 3.5.4 (b) Optically engineered biosensor platform (left) that focuses collimated light onto surface above critical angle to produce surface-confined TIRF excitation and the same platform exclusively collects SAF fluorescence above the critical angle (right).

The immobilisation of antibodies onto such polymer substrates requires the surface to be functionalised with groups capable of binding antibody structures. Amine and carboxyl groups within the antibody structure provide a site of attachment to the corresponding carboxyl group or amine groups located on the substrate. Following functionalisation of the chip surface using an aldehyde-activated dextran surface coating, the antibody-compatible surface is ready for deposition of the antibodies and commencement of the assay (section 2.12.3).

A fluorescent-based assay involving the detection of CRP from depleted human serum was performed on the parabolic chip platform. The fluorescent assay utilised a sandwich-based format involving an optimised concentration of capture antibody (purified anti-CRP pAb – section 3.1.4) deposition onto the functionalised paraboloids. Previously, several spotting concentrations of the capture pAb (ranging from 50 - 300 $\mu\text{g}/\text{mL}$) were investigated for determination of the most optimal coating concentration. Comparable results were observed for the capture Ab at concentrations of 200 $\mu\text{g}/\text{mL}$ and 300 $\mu\text{g}/\text{mL}$, indicating the possibility of a saturation effect occurring above 200 $\mu\text{g}/\text{mL}$. Therefore, to limit both pAb stacking and also the quantity of pAb used, a capture concentration of 200 $\mu\text{g}/\text{mL}$ was used in all subsequent experiments.

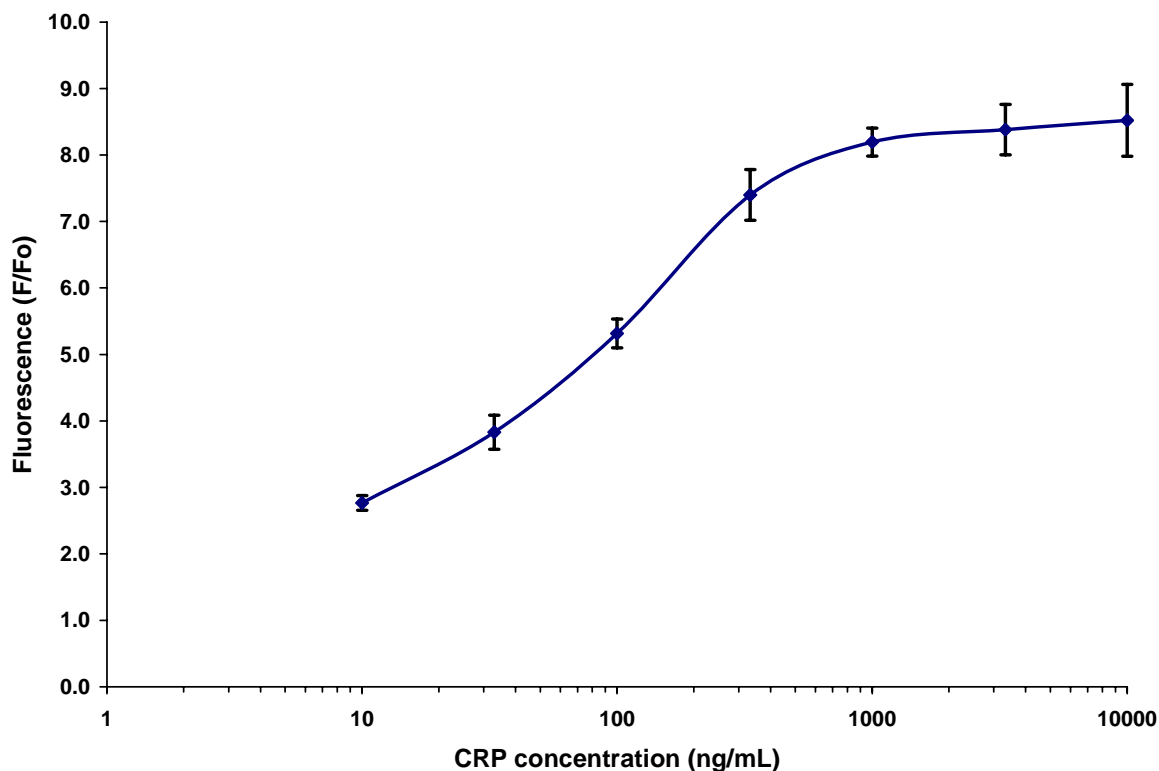


Figure 3.5.4 (c) Calibration curve for the determination of CRP levels from depleted human serum using a sandwich-based assay on a paraboloid chip. Purified unlabelled CRP-specific rabbit pAb was spotted on the parabolic chip surface (capture antibody). Various concentrations of CRP-spiked depleted human serum were tested for binding. Detection of the complex was achieved using fluorescently labelled rabbit anti-CRP pAb. The plotted results represent the mean response \pm SD (vertical error bars) over each of the 3 days during which the assay was performed.

Figure 3.5.4 (c) shows a plot of 9 separate assays (performed in triplicate over 3 days) involving CRP antigen spiked into CRP-depleted serum at 8 different concentrations (10, 3.3, 1.0, 0.33, 0.1, 0.033, 0.01, 0 μ g/mL). Detection of the CRP-pAb complex was accomplished using a fluorescently labelled sample of the same anti-CRP pAb deposited on the paraboloids. The pentameric nature of CRP enables the capture and detection pAb, employed by the assay, to be identical.

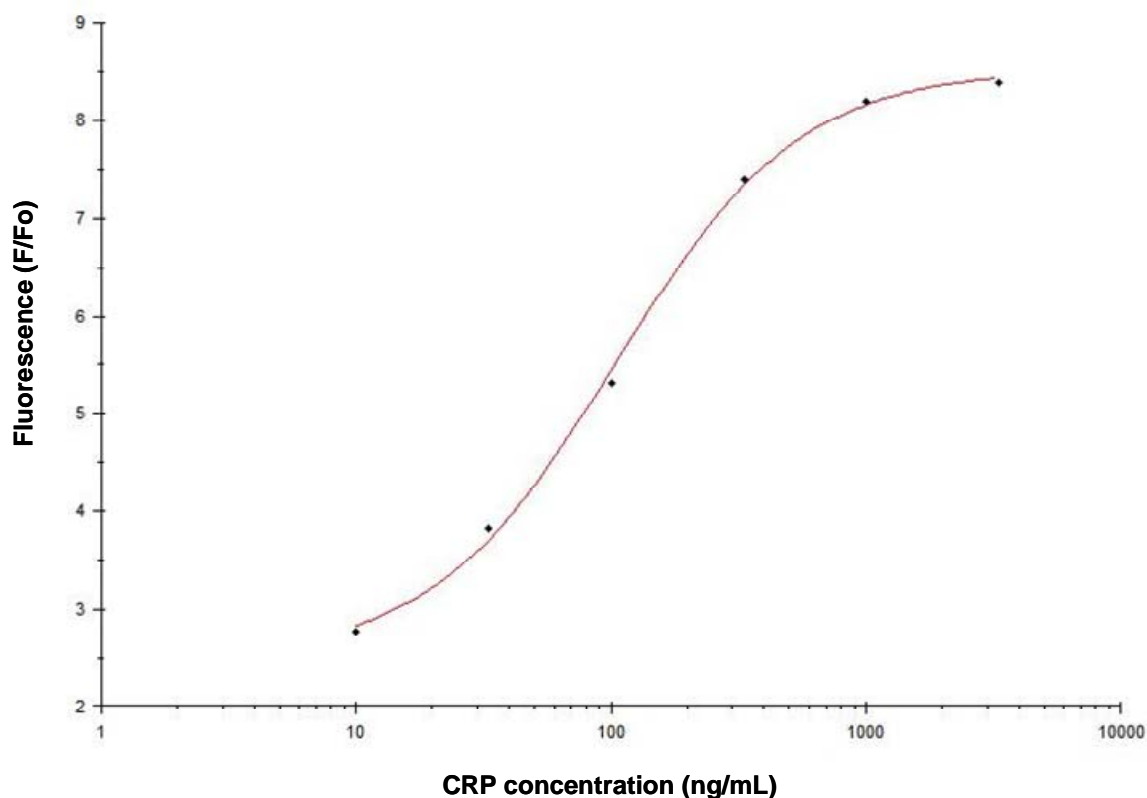


Figure 3.5.4 (d) Calibration curve for determination of CRP levels using a sandwich-based assay on the parabolic chip. See legend of previous Figure (Figure 3.5.4 c) for full description of the assay format. The calibration curve was generated using the Biacore Biaevaluation software package, as described in section 3.1.7.

The raw data was then subject to the same evaluation process as described for the Biacore pAb data in section 3.1.7. A 4-parameter equation was employed to generate a plot of the mean fluorescent values (F/F_0) against the spiked CRP concentrations (Figure 3.5.4 d). The resultant output values were then incorporated into an equation to determine the % accuracy values, which are shown in Table 3.5.4.

Table 3.5.4 Processed data from the fluorescent sandwich CRP assay on the parabolic chip platform using dedicated Biacore Biaevaluation software package (see section 3.1.7 for full description of data processing)

CRP conc. (ng/mL)	S.D. values	Biaevaluation Output value	% Accuracy value
10000	0.54	Low	-
3333	0.38	2191.7	65.8
1000	0.21	1112.9	111.3
333	0.38	353.2	106.1
100	0.22	93.7	93.7
33	0.26	36.7	111.1
10	0.11	8.5	84.6

S.D. – Standard Deviations

The output % recovery values in Table 3.5.4 demonstrated a good correlation within the assay. Therefore, this experiment has successfully demonstrated ‘proof of concept’ for this novel parabolic format for the detection of CRP. This particular platform offers many beneficial characteristics, particularly the incorporation of the SAF technology. As was discussed earlier, the use of such technology can remove the need for time-consuming wash steps. In the experiments shown, however, wash steps were performed prior to detection of the resultant fluorescent signal. This was due to further optimisation being required on the instruments ability to distinguish between the bulk and specific surface-bound signal on the chip. Although this platform is an exciting prospect for biosensors, the requirement for fluorescently-labelled antibody or analyte may be considered a major disadvantage. For instance, fluorescent labels can be vulnerable to degradation over time. Commonly used fluorescent labels have been shown to be susceptible to ozone damage and also photobleaching (Dar *et al.*, 2008). Several key issues must be addressed when choosing a fluorescent label that is compatible with the biological material being investigated. Firstly, the label must be conveniently excitable, without simultaneous excitation of the biological matrix. Secondly, that it possesses a high molar absorption coefficient at the excitation wavelength and a high fluorescence quantum yield (ratio of photons absorbed to photons

emitted through fluorescence). Thirdly, the label must be soluble in relevant buffers and also stable under relevant conditions used in the assays. Another important consideration includes the issue of steric and size-related effects of the label (Resch-Genger *et al.*, 2008). All of these issues can have a detrimental effect on the overall assay efficiency and reproducibility if not properly addressed. The use of label-free detection systems is one technique which has the ability to overcome such problematic issues. Label-free based detection systems have been associated with major benefits such as faster assay development times, greater accuracy, the ability to generate high information content data and finally less interference from labels (Cooper, 2006). Such characteristics have led to a revolution in the development of label-free based detection systems such as the SPR-based Biacore™ systems. The first application of this breakthrough technology was more than two decades ago, yet SPR remains a central tool for characterizing and quantifying biomolecular interactions. Since then, SPR sensor technology has been commercialised by several companies and has become a leading technology in the field of direct real-time observation of biomolecular interactions (Homola *et al.*, 1999). SPR sensors have made vast advances in terms of both development of the technology and its applications (Homola, 2008). The SPRSpectral® system, developed at the Institute Photonics and Electronics in the Czech Republic, is an example of a SPR-based POC device. This device was employed for the final characterisation of the re-engineered CRP-specific H2 avian scFv (section 3.3.6 – 3.3.8).

3.5.5 SPRSpectral® platform

Presently, a wide range of configurations of SPR biosensors have been applied to monitoring biomolecular interactions (Lukosz *et al.*, 1991; Brandenburg and Gombert, 1993; Buckle *et al.*, 1993; Cush *et al.*, 1993; Gauglitz *et al.*, 1993; Heideman *et al.*, 1993; Clerc and Lukosz, 1997; Schmitt *et al.*, 1997; Heideman and Lambeck, 1999; Ymeti *et al.*, 2005; Schmitt *et al.*, 2007). An example of some of the most popular configurations used can be found in Figure 3.5.5 (a). Although an extensive range exists, each of the devices is based upon the same principle. This principle involves the measurement of refractive index changes occurring in the field of an electromagnetic wave supported by the optical structure of a sensor.

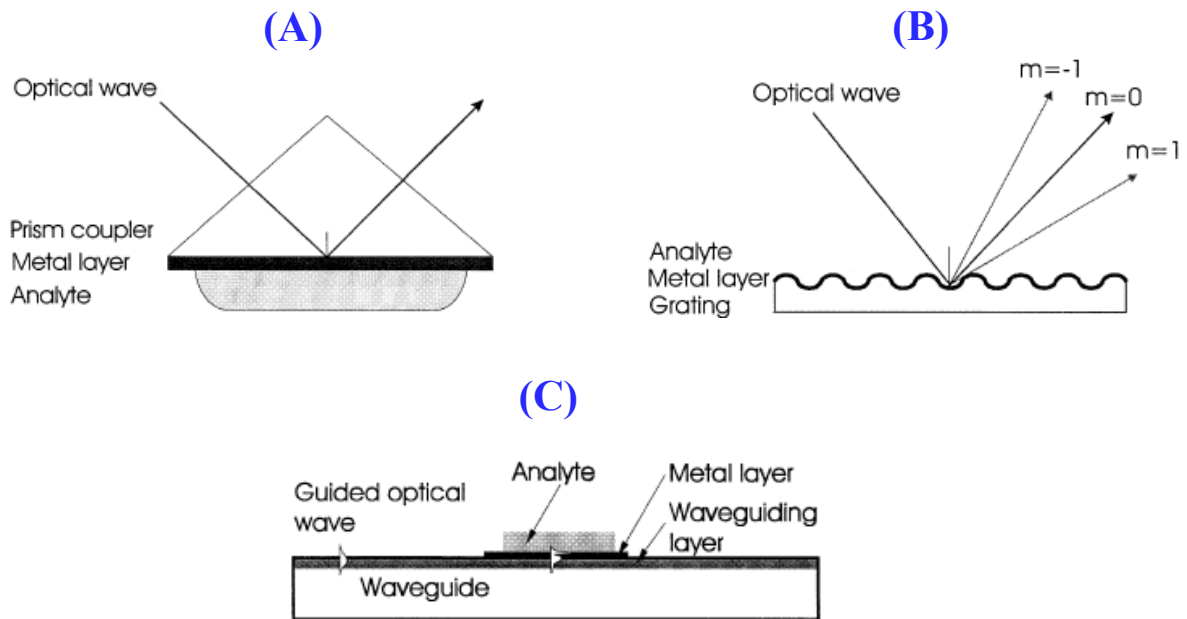


Figure 3.5.5 (a) Most widely used configurations for SPR sensors: (a) prism coupler-based SPR system - Attenuated Total Reflection (ATR) method; (b) grating coupler-based SPR system and (c) optical waveguide-based SPR system.

The SPRSpectral® system employed in this work falls under the category of a prism coupler-based configuration (A). The SPRSpectral® system uses a white light source with a spectral distribution ranging from 390 to 1070 nm. A Gaussian profile (bell-shape curve) is produced by the system with a maximum output at 680 nm. The actual SPR coupling occurs in the 700-800 nm range, with the angle between the light source and the sample remaining fixed. Analysis is performed in four independent test channels, each with an area of $2 \times 4 \text{ mm}^2$ and a height of 60 nm. The light emitted from each channel is collected on independent optic fibres and the resultant signals are converted for posterior analysis. The area between the gold film and the light beam is the PMMA substrate ($18 \times 32 \text{ mm}^2$) with is coupled to the prism using immersion oil (Plasmon IV immersion oil type A, Cargille). Cleaning of the system between experiments is performed according to the following sequence: 4 min with ultra-pure water, 1 min with 50mM NaOH, 4 min again with ultra-pure water and finally flushing of the system with compressed air.

As discussed in section 3.3.6 to 3.3.8, the highest affinity CRP-specific H2 scFv generated from the immunised avian library (section 3.3) was subjected to a novel re-engineering strategy. This re-engineering process involved the conversion of the H2 scFv fragment to a scAb fragment via fusion of the scFv to a chicken C λ chain. The resultant D9 scAb fragment may be directly conjugated to a gold surface via the unique cysteine residue at the terminal site of the fused chicken C λ chain. A free-thiol group provided by the terminal uncoupled cysteine residue reacts with the gold surface forming a relatively stable covalent bond. In addition to the fragments ability to achieve direct conjugation to a gold surface, the terminal location of the reactive site allows the fragment to assume a fully-functional conformation.

IMAC-purified D9 scAb (see Figure 3.3.8) was incorporated into a direct binding assay for CRP. To further validate the application of this assay in a clinical environment, depleted human serum was the sample matrix chosen for the assay (full protocol in section 2.12.4). Six concentrations of CRP were tested (200, 400, 600, 800, 1000 and 1200 ng/mL), as well as a zero concentration involving unspiked CRP-depleted serum. For each of the concentrations tested, a set concentration of the purified D9 scAb (15 μ g/mL) was immobilised onto the gold surface.

As was described in the full protocol in section 2.12.4, a new baseline was calculated following the addition of each of the experimental solutions (CRP-specific D9 scAb, blocking solution, CRP spiked serum/unspiked serum). Each of the new baseline levels were identified by passing degassed 1 x PBS across the modified test channels. In order to simplify the experiment, each of the solutions passed across the test channels were identified as a label shown below:

1. Baseline: ultra-pure water
2. Baseline: 1 x PBS
3. D9 scAb immobilisation
4. Baseline: 1 x PBS
5. Blocking reagent
6. Baseline: 1 x PBS
7. CRP spiked serum/unspiked serum
8. Baseline: PBS 1x

Therefore, quantification of the material absorbed on the surface was obtained from the calculations below:

Table 3.3.5 Calculations for quantification of material absorbed onto test channels

Step for quantification	Calculation
D9 scAb immobilisation	SPR signal (4.) minus SPR signal (2.)
Blocking solution	SPR signal (6.) minus SPR signal (4.)
CRP binding reponse	SPR signal (8.) minus SPR signal (6.)

Each of the concentrations tested were performed in triplicate and Figure 3.3.5 (b) shows the plotted average reponse for each of the six concentrations used minus the zero concentration.

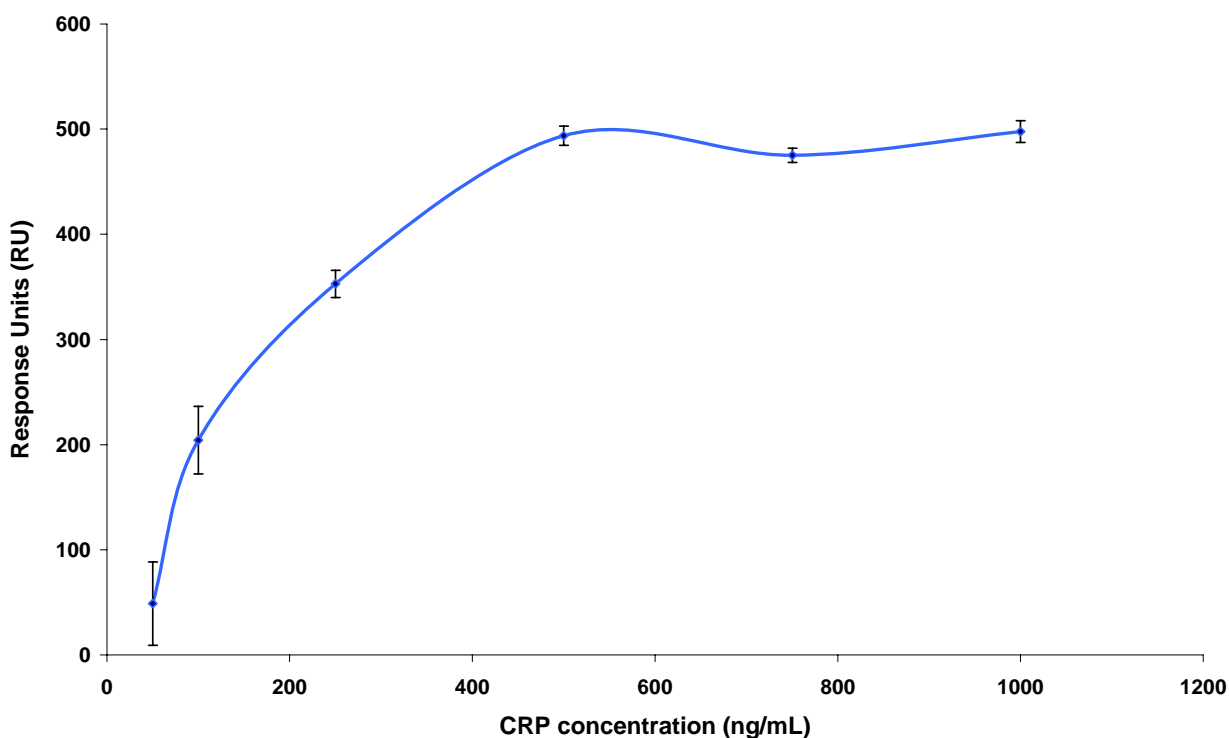


Figure 3.3.5 (b) Plotted data for a direct binding assay using a novel CRP-specific scAb fragment on the SPRSpectral® platform. The average responses for each of the six concentrations of CRP (200, 400, 600, 800, 1000 and 1200 ng/mL) performed in triplicate are shown. The plotted results represent the mean response \pm SD (vertical error bars), over the 3 data points taken for each concentration ($n = 3$).

Following analysis of the final plotted data of the CRP binding responses for each of the six spiked concentrations tested (Figure 3.3.5 b), a good correlation was evident with relatively minor standard deviations. One of the main advantages of the SPRSpectral® system was its enclosed flow-based format. Some of the previously discussed POC platforms, such as the OLF systems are lacking in this respect and, consequently, may suffer from problems such as sample evaporation. As previously mentioned, the antibody fragment employed in this assay was the product of a novel re-engineering strategy. Another major limiting feature of some biosensor technologies is the requirement for conjugation of the biomolecules such as antibodies to a gold surface. These conjugations can prove to be not only time-consuming, but also may also potentially degrade the biomolecule through the use of certain coupling chemistries. This novel fragment, however, may be directly conjugated to gold surfaces via its incorporated terminal cysteine residue, removing the need for potentially inefficient conjugation steps. The employment of such a strategy can, therefore, expedite the route from antibody generation to functional biosensor assay development.

3.3.6 Discussion of results

The main drawback associated with central lab testing (CLT) is their general poor TAT, which can lead to significant problems in the emergency unit setting. Consistent poor assay TAT can result in critical issues such as increases in unnecessary patient admissions and length-of-stay (Murray *et al.*, 1999; Lee-Lewandrowski *et al.*, 2003), inaccurate identification of critically ill patients and poor patient clinical outcome (McCord *et al.*, 2001; Ng *et al.*, 2001). The most recent guidelines from the American Heart Association (AHA) (Gibler *et al.*, 2005) regarding unstable angina/non-ST-segment elevation myocardial infarction (MI) in the emergency department (ED) states that a turnaround time for laboratory results should not exceed 1 h when central laboratory testing is used. However, a comprehensive survey by Novis and colleagues (Novis *et al.*, 2004) which assessed the TAT of over 11,000 cardiac biomarker tests in 159 institutions discovered that on average participants reported 90% of their order-to-report cardiac marker results in more than 90 min. Time-consuming tasks such as test ordering, sample transport to laboratories and data reporting may be avoided. Although, central lab testing is usually well validated, the much reduced human involvement accompanying POC testing (POCT) can lead to a significant decrease in both inter/intra assay variation and human error. This section demonstrated just some of the potential POC platforms which may be successfully applied in the clinical arena. Some of the platforms

discussed take advantage of key technologies such as novel surface chemistries, high precision microfluidics, SAF-based detection and label-free detection. It is felt that the application of such technologies to the clinical arena, can have a significant impact on the overall efficiency of cardiac diagnostics.

As previously discussed in section 1.6, CRP remains a key marker in the cardiac arena. However, in general apparently healthy individuals with a hs-CRP value >8 mg/L require the test to be repeated to rule out a recent response to undetected infection or tissue injury. Consequently, a large quantity of hs-CRP tests must be performed in most hospitals. Since CLT is the most commonly used approach, this can cause a massive backlog in central laboratories, which in turn can lead to poor TAT and even result in subsequent patient death. Therefore, the availability of a rapid, highly sensitive and specific test for hsCRP, such as those discussed, could potentially alleviate some of this backlog and significantly reduce TAT's. In the case of MPO, it has been demonstrated that a single measurement of this marker at hospital admission can predict the risk of major adverse cardiac events for both a 30-day and six month period (Balduis *et al.*, 2003; Brennan *et al.*, 2003). Therefore, a method for the rapid detection of MPO from human serum may prove extremely useful in the clinical setting. Currently, analysis of this cardiac biomarker in patients sera is performed via central laboratory testing (CLT), which has been the subject of much criticism. Presently, the CardioMPO™ assay developed by PrognostiX is the only FDA approved assay for determination of MPO in the clinical setting. The sandwich-based ELISA format, however, means that several time-consuming steps i.e. washes, incubations etc. must be performed via an adequately skilled central lab, resulting in a poor overall TAT. Conversely, the use of a point-of-care (POC) version of the LFIA assay presented in this work, would remove the need for skilled lab personnel, while also significantly reducing the TAT associated with central lab testing. Such a significant decrease in assay TAT would greatly improve the triage of cardiac patients and would allow for more time and resources to be focused on those patients identified as being at a greater risk of having a cardiac event.

Chapter 4

Conclusions

4.0 Conclusions

The principal objective of this research was the production, characterisation and application of antibodies for the detection of both CRP and MPO. In the case of CRP, an initial pool of polyclonal antibody was generated and purified from New Zealand white rabbits following an extensive immunization strategy. The resultant polyclonal antibody harvested from the rabbits proved to be a highly sensitive and useful reagent. This pAb was successfully incorporated into both a fluorescent sandwich ELISA and also a direct capture assay on the Biacore 3000 system. Although the high sensitivity of the pAb is apparent on analysis of the fluorescent ELISA, a more accurate indication of the true sensitivity of the pAb was provided by the Biacore assay. The polyclonal preparation was found to have a sensitivity in the low nanomolar range, making it an ideal candidate for use as a capture agent in an immunological assay. Consequently, the final characterisation of the polyclonal antibody involved its use as both a capture and detection agent in a sandwich-based fluorescent assay on a novel parabolic chip. The pentameric nature of CRP enabled the capture and detection pAb, employed by the assay, to be identical. Data evaluation packages were employed for the analysis of the overall performance of the polyclonal antibody in both the Biacore and parabolic chip platforms. A high level of accuracy and reproducibility was evident following analysis of both assays using statistical analysis packages. Use of the parabolic chip allowed for the major benefits of SAF technology to be harnessed. Implementation of such technologies allows for highly specific surface excitation to be achieved, therefore, leading to more accurate and sensitive detection of the analyte. Although, polyclonal antibody remains to be a highly utilised immunological agent, they have an obvious limitation in terms of their overall specificity. For instance, the polyclonal antibody preparation was found to react with not only the immunised CRP protein but also its homologue SAP. Alternatively, the homogenous nature of monoclonal antibodies has led to their superiority in terms of specificity over polyclonal antibodies.

For this reason, state-of-the-art recombinant antibody technology was harnessed for the generation of monoclonal antibody fragments to CRP. Both mice and chickens were investigated as immune hosts in the generation of CRP-specific scFv antibodies. Several problems were encountered throughout construction, screening and characterisation of the murine library (discussed in section 3.2.17). A major hindrance associated with the final characterisation of the murine clones was their poor expression levels. This was further exacerbated by the lack of any effective affinity tag of the pAK system used for construction

of the library. For this reason, the best performing murine scFv antibody (C11-2) was subcloned into an alternative vector (pComb3X). This system provided a highly specific HA affinity tag, which allowed for reliable kinetic data to be obtained using the Biacore system. A final affinity of 2.1×10^{-8} M was extrapolated from the kinetic data for the murine C11-2 scFv subclone. A high level of purity is required for the incorporation of these scFv fragments into sensitive novel assay platforms, as discussed in section 3.3.5. Unfortunately, in the case of the murine C11-2 subclone, the production of large quantities of purified scFv for incorporation into such devices was not feasible due to its extremely poor expression levels. Consequently, the avian immune system was investigated for the generation of scFv fragments specific for CRP. An alternative system was employed for construction of the chicken scFv library, namely the pComb system. Following an intensive screening and selection strategy, four scFv clones were chosen (F6, F8, G5 and H2) from the library, based on their affinities for the CRP antigen (2.54×10^{-8} M, 1.01×10^{-8} M, 3.52×10^{-9} M, 3.53×10^{-10} M, respectively). Large yields of expressed scFv were obtained for each of the four fully-characterised scFv clones, with F8 being particularly good. A 500 mL bacterial culture of the clone produced approximately 15.5 mg of pure scFv using a simple IMAC purification protocol. All four of the clones proved to be ideal candidates for model assay development due to their stable expression and high level of purity. Subsequently, each of the purified scFv fragments were incorporated into a competition-based assay on a novel OLF device (4castchip™). The 4castchip™ offered a superior alternative to that of standard nitrocellulose-based LFIA's and each of the recombinant fragments performances were comparable to that of two commercially available mAbs. Also, the highest affinity H2 scFv was subjected to a novel engineering process, allowing for its direct conjugation to gold biosensor surfaces via a terminal thiol group. Therefore, the final characterisation of the re-engineered CRP-specific fragment involved incorporation into the SPRSpectral® system. The re-engineered fragment was successfully applied in this commercial platform, efficiently detecting a range of concentrations of CRP, showing good overall reproducibility. Consequently, this platform was able to take advantage of the novel engineering process administered on the avian H2 scFv, which validates this novel strategy as an alternative approach to bioconjugation of antibodies to such platforms.

Due to the impressive performance of the avian immune system in the generation of highly sensitive and specific CRP-specific scFv clones, it was decided to take advantage of this refined host for the generation of an MPO-specific scFv library. Avian hosts were combined with the use of the pComb system for construction of the MPO-specific library. As

previously discussed, this system proved to be highly efficient in terms of both the ease of construction and subsequent characterisation of antibody libraries. Using an optimised 'off-rate' ranking strategy, B10B was identified as the highest affinity clone. Following kinetic data analysis on the scFv an affinity of 1.86×10^{-10} M (186 pM) was extrapolated. This value was found to be well within the clinically relevant reference range. The peroxidase nature of MPO provided a unique opportunity to develop a novel assay for its rapid detection. Initially, a 'proof-of-principle' ELISA was performed to determine the ability of TMB substrate to detect the B10B scFv-captured MPO, which proved successful. This was then successfully transferred to a novel LFIA format, which allowed for the highly specific and sensitive detection of MPO. Considering a prototype strip would contain both pre-sprayed test and control lines, the turn-around-time (TAT) for the assay could be as little as 20 min.

Spiked samples of depleted human serum were employed in each of the assay platforms, thus validating their performance in a clinically representative sample matrix. It is confidently anticipated that each of these systems will be successfully deployed in the clinical arena. Furthermore, some of the antibodies and platforms developed in this thesis are currently being evaluated by several companies with respect to their commercial potential. Recently, Biosurfit have exercised a licensing option on the developed CRP-specific scAb for use in their proprietary Lab-on-a-CD SPR-based platform. Also, Åmic (now part of Johnson and Johnson) are in the process of commercialising a cardiac test on their proprietary OLF platform, using the protocols partially optimised in this research. The work herein also demonstrates the first working assay performed on BDI-patented SAF technology on a parabolic substrate.

The primary location where some of the developed POC assays would be most beneficial would be in the coronary care unit (CCU) of hospitals, which specialises in the care of patients with heart attacks, unstable angina and various other cardiac conditions that require continuous monitoring. The POC format of the assay negates the need for skilled lab personnel, as nursing staff may perform the assay, following sufficient training on the correct use of the device. In fact, the previously mentioned study by Allehagen and colleagues (Allehagen and Janzon, 2008) investigated use of a POC device by nurses in the CCU, who found the assay easy to learn and the device simple to operate, without any impairment of the results obtained. Implementation of the device could, therefore, lead to a more efficient patient discharge system, which could lead to an increase in both effective use of bed capacity and minimise the need for patient admission to those with real problems.

Furthermore, a secondary location where use of the device may be required is in local GP practices, whereby discharged cardiac patients may be regularly monitored. This could significantly reduce the number of unnecessary patient admissions to hospitals, leading to a significant improvement in the use of scarce hospital resources. Inappropriate use of hospitals can result in lengthy discharge and admission cycles, emergency room (ED) over-crowding, higher ambulance diversion and potentially critical patients leaving without being seen. Therefore, delegation of some of the responsibility to GP practices could help to alleviate some of these potentially life-threatening situations.

5.0 Publications

5.0 Publications

Publications based on the work described in this thesis:

McDonnell, B., Hearty, S., Brahmhatt, S. and O’Kennedy, R. (2010) A high affinity recombinant antibody permits simple and sensitive one-step direct detection of Myeloperoxidase. *Anal. Biochem.* (In submission).

Crean (née Lynam), C., Gubala, V., Nooney, R., Hearty, S., **McDonnell, B.**, MacCraith, B., O’Kennedy, R. and Williams, D. E. (2010) Charge effects in bioconjugation reactions between dye-doped silica nanoparticles and proteins. (In submission).

Gubala, V., Lynam, C., Nooney, R., Hearty, S., **McDonnell, B.**, O’Kennedy, R., MacCraith, B., Williams, D. (2010). Improvement of sensitivity in immunoassays through the use of dendrimers as antibody linkers to fluorescent nanoparticles. *Anal. Bioanal. Chem.* (In submission).

Hill, D., **McDonnell, B.**, Hearty, S., Basabe-Desmonts, L., Blue, R., Ruckstuhl, T., Trnavsky, M., McAtamney, C., O’Kennedy, R. and MacCraith, B. D. (2010) Novel Disposable Biochip Platform Employing Supercritical Angle Fluorescence for Enhanced Fluorescence Collection. (In submission).

McDonnell, B., Hearty, S., Leonard, P. and O’Kennedy, R. (2009) Cardiac biomarkers and the case for point-of-care testing. *Clin. Biochem.*, **42**: 549-561.

Leonard, P., Säfsten, P., Hearty, S., **McDonnell, B.**, Finlay, W. and O’Kennedy, R. (2007). High throughput ranking of recombinant avian scFv antibody fragments from crude lysates using the Biacore A100. *J. Immunol. Methods.*, 323(2):172-179.

Poster - **McDonnell, B.**, Hearty, S., Leonard, P., Bakker, J., Merlin, J. and O’Kennedy, R. (2007) Diagnostic antibody production and model assay development for novel point-of-care devices. The 6th International Congress on Annual Recombinant Antibodies, Berlin, Germany.

Poster - **McDonnell, B.**, Hearty, S., Leonard, P., Gilmartin, N. and O'Kennedy, R. (2009) Expediting the route from antibody production to functional biosensor assay development. International Conference on Trends in Bioanalytical Sciences and Biosensors (ICTBSB), Dublin, Ireland.

Poster - **McDonnell, B.**, Hearty, S., Leonard, P., Bakker, J., Merlin, J. and O'Kennedy, R. (2007) Use of Recombinant Antibodies in Rapid Point-of-Care Diagnostics for Cardiac Markers. The Annual Meeting of the Irish Society for Immunology, Trinity College Dublin (TCD), Ireland.

Poster - Hearty, S., **McDonnell, B.**, Leonard, P., Ayyar, V., Gilmartin, N., Conroy, P.J., Desmots, L.B., Hill, D., MacCraith, B.D. and O'Kennedy R. (2008) Optimised isolation of recombinant antibodies for biosensor development. Eurotrode IX Conference, Dublin, Ireland.

Poster – Leonard, P., Säfsten, P., Hearty, S., **McDonnell, B.** and O'Kennedy, R. (2006) Rapid screening of scFv and Fab antibody fragments using Biacore A100. Antibody Engineering Conference, San Diego, USA.

Poster - Hill, D., Blue, R., Basabe-Desmots, L., Hearty, S., **McDonnell, B.**, McAtamney, C., O'Kennedy, R. and MacCraith, B. (2008) Detection of clinical biomarkers using a novel parabolic microchip diagnostic platform. Eurotrode IX Conference, Dublin, Ireland.

Presentation - Bakker, J., Kurzbuch, D., Ruckstuhl, T., Melin, J., Jönsson, C., Hearty, S., Leonard, P., **McDonnell, B.** and MacCraith B. (2008) Cardiac risk assessment with a supercritical angle fluorescence scanner. Eurotrode IX Conference, Dublin, Ireland.

Poster - Hill, D., Blue, R., Basabe-Desmots, L., Hearty, S., **McDonnell, B.**, McAtamney, C., Ruckstuhl, T., O'Kennedy, R. and MacCraith, B. (2008) Detection of clinical biomarkers using a novel parabolic microchip diagnostic platform. NSTI Nanotech, Boston, USA.

6.0 Bibliography

6.0 Bibliography

<http://metallo.scripps.edu/promise/1MHL.html> [Online]. [Accessed 9 January 2009].

Agewall, S. (2003). Evaluation of point-of-care test systems using the new definition of myocardial infarction. *Clin. Biochem.* **36** (1):27-30.

Agrawal, A. and Volanakis, J. E. (1994). Probing the C1q-binding site on human C-reactive protein by site-directed mutagenesis. *J. Immunol.* **152**: 5404–5410.

Aldus, C. F., Van Amerongen, A., Ariens, R. M. C. (2003). Principles of some novel rapid dipstick methods for detection and characterization of verotoxigenic Escherichia coli. *J. Appl. Microbiol.* **95** (2):380-389.

Alehagen, U. and Janzon, M. (2008). A clinician's experience of using the Cardiac Reader NT-proBNP point-of-care assay in a clinical setting. *Eur. J. Heart. Fail.* **10** (3):260-266.

Al-Lazikani, B., Lesk, A. M. and Chothia, C. (1997). Standard conformations for the canonical structures of immunoglobulins. *J. Mol. Biol.* **273** (4):927-948.

Allender, S., Scharbotough, P., Peto, V. (2008). European Cardiovascular disease statistics: 2008 edition. *London: British Heart Foundation.*

Alpert, J. S., Thygesen, K., Antman, E. and Bassand, J. P. (2000). Myocardial infarction redefined--a consensus document of The Joint European Society of Cardiology/American College of Cardiology Committee for the redefinition of myocardial infarction. *J. Am. Coll. Cardiol.* **36** (3):959-969.

Anderson, J. K., Stroud, R. M., Volanakis, J. E. (1978). Studies on the binding specificity of human C-reactive protein for phosphorylcholine. *Fed. Proc.* **37**: 1495.

Andris-Widhopf, J., Rader, C., Steinberger, P. (2000). Methods for the generation of chicken monoclonal antibody fragments by phage display. *J. Immunol. Methods.* **242** (1-2):159-181.

Apple, F. S., Chung, A. Y., Kogut, M. E. (2006). Decreased patient charges following implementation of point-of-care cardiac troponin monitoring in acute coronary syndrome patients in a community hospital cardiology unit. *Clin. Chim. Acta.* **370** (1-2):191-195.

Apple, F. S., Jesse, R. L., Newby, L. K. (2007). National Academy of Clinical Biochemistry and IFCC Committee for Standardization of Markers of Cardiac Damage Laboratory Medicine Practice Guidelines: analytical issues for biochemical markers of acute coronary syndromes. *Clin. Chem.* **53** (4):547-551.

Azzazy, H. M. E. and Highsmith, W. E. (2002). Phage display technology: clinical applications and recent innovations. *Clin. Biochem.* **35** (6):425-445.

Azzazy, H. M., Pelsers, M. M. and Christenson, R. H. (2006). Unbound free fatty acids and heart-type fatty acid-binding protein: diagnostic assays and clinical applications. *Clin. Chem.* **52** (1):19-29.

Baldus, S., Heeschen, C., Meinertz, T. (2003). Myeloperoxidase serum levels predict risk in patients with acute coronary syndromes. *Circulation.* **108** (12):1440-1445.

Barbas, C.F., Burton, D., Scott, J.K. (2001). *Phage display: a laboratory manual*. Cold Spring Harbor Laboratory Press, Cold Spring Harbor, NY.

Berry, J.D. and Popkov, M. (2005). Antibody Libraries from Immunized Repertoires. In: Sidhu, S.S, editors. *Phage Display in Biotechnology and Drug Discovery*. Series 3. CRC Press. *IN: Sidhu, S.S. (ed.) Phage Display in Biotechnology and Drug Discovery*. Series 3 ed. CRC Press.

Bharadwaj, D., Stein, M. -P., Volzer, M., Mold, C., DuClos, T. W. (1999). The major receptor for C-reactive protein on leukocytes is Fcγ receptor II. *J. Exp. Med.* **190**: 585-590.

Bini, A., Centi, S., Tombelli, S. (2008). Development of an optical RNA-based aptasensor for C-reactive protein. *Anal. Bioanal. Chem.* **390** (4):1077-1086.

Birtalan, S., Zhang, Y., Fellouse, F. A. (2008). The intrinsic contributions of tyrosine, serine, glycine and arginine to the affinity and specificity of antibodies. *J. Mol. Biol.* **377** (5):1518-1528.

- Black, S., Kushner, I. and Samols, D. (2004).** C-reactive Protein. *J. Biol. Chem.* **279** (47):48487-48490.
- Blake, G. J. and Ridker, P. M. (2003).** C-reactive protein and other inflammatory risk markers in acute coronary syndromes. *J. Am. Coll. Cardiol.* **41** (4 Suppl S):37S-42S.
- Bodí, V., Sanchis, J., Llàcer, À. (2005).** Multimarker risk strategy for predicting 1-month and 1-year major events in non-ST-elevation acute coronary syndromes. *Am. Heart. J.* **149** (2):268-274.
- Bradbury, A. R. and Marks, J. D. (2004).** Antibodies from phage antibody libraries. *J. Immunol. Methods.* **290** (1-2):29-49.
- Brandenburg, A. and Gombert, A. (1993).** Grating couplers as chemical sensors: a new optical configuration. *Sens. Actuat. B., Chem.* **17** (1):35-40.
- Braunwald, E., Antman, E. M., Beasley, J. W. (2002).** ACC/AHA 2002 guideline update for the management of patients with unstable angina and non-ST-segment elevation myocardial infarction--summary article: a report of the American College of Cardiology/American Heart Association task force on practice guidelines (Committee on the Management of Patients With Unstable Angina). *J. Am. Coll. Cardiol.* **40** (7):1366-1374.
- Brennan, M. L., Penn, M. S., Van Lente, F. (2003).** Prognostic value of myeloperoxidase in patients with chest pain. *N. Engl. J. Med.* **349** (17):1595-1604.
- Brown, T. (2000).** *Essential Molecular Biology: A Practical Approach.* Oxford University Press.
- Buckle, P. E., Davies, R. J., Kinning, T. (1993).** The resonant mirror: a novel optical sensor for direct sensing of biomolecular interactions Part II: applications. *Biosens. Bioelectron.* **8** (7-8):355-363.
- Calabro, P., Willerson, J. T. and Yeh, E. T. (2003).** Inflammatory cytokines stimulated C-reactive protein production by human coronary artery smooth muscle cells. *Circulation.* **108** (16):1930-1932.

- Char**, D. M., Israel, E. and Ladenson, J. (1998). Early laboratory indicators of acute myocardial infarction. *Emerg. Med. Clin. North. Am.* **16** (3):519-539, vii.
- Chiou**, V. (2002). Duck antibodies for IVD applications. *In vitro Diagnostic Technology*: 31-36.
- Chothia**, C., Lesk, A. M., Tramontano, A. (1989). Conformations of immunoglobulin hypervariable regions. *Nature*. **342**:877-883.
- Clerc**, D. and Lukosz, W. (1997). Direct immunosensing with an integrated-optical output grating coupler. *Sens. Actuat. B.Chem.* **40** (1):53-58.
- Cooper**, M. A. (2006). Optical biosensors: where next and how soon? *Drug discovery today*. **11** (23-24):1061-1067.
- Corstjens**, P. L. A. M., van Lieshout, L., Zuiderwijk, M. (2008). Up-converting phosphor technology-based lateral flow assay for detection of Schistosoma circulating anodic antigen in serum. *J. Clin. microbiol.* **46** (1):171-176.
- Cramer**, G. E., Kievit, P. C., Brouwer, M. A. (2007). Lack of concordance between a rapid bedside and conventional laboratory method of cardiac troponin testing: impact on risk stratification of patients suspected of acute coronary syndrome. *Clin. Chim. Acta.* **381** (2):164-166.
- Cush**, R., Cronin, J. M., Stewart, W. J. (1993). The resonant mirror: a novel optical biosensor for direct sensing of biomolecular interactions Part I: Principle of operation and associated instrumentation. *Biosens. Bioelectron.* **8** (7-8):347-354.
- Dar**, M., Giesler, T., Richardson, R. (2008). Development of a novel ozone- and photo-stable HyPer5 red fluorescent dye for array CGH and microarray gene expression analysis with consistent performance irrespective of environmental conditions. *BMC biotechnol.* **8**:86.
- de Lemos**, J. A., Morrow, D. A., Bentley, J. H. (2001). The prognostic value of B-type natriuretic peptide in patients with acute coronary syndromes. *New. Engl. J. Med.* **345** (14):1014.

- Deng**, Y. J. and Notkins, A. L. (2000). Molecular determinants of polyreactive antibody binding: HCDR3 and cyclic peptides. *Clin. Exp. Immunol.* **119** (1):69-76.
- Edwards**, K. A. and Baeumner, A. J. (2006). Optimization of DNA-tagged dye-encapsulating liposomes for lateral-flow assays based on sandwich hybridization. *Anal. Bioanal. Chem.* **386** (5):1335-1343.
- Eisenhardt**, S. U., Schwarz, M., Schallner, N. (2007). Generation of activation-specific human anti- α M β 2 single-chain antibodies as potential diagnostic tools and therapeutic agents. *Blood.* **109** (8):3521-3528.
- Fellouse**, F. A., Barthelemy, P. A., Kelley, R. F. and Sidhu, S. S. (2006). Tyrosine plays a dominant functional role in the paratope of a synthetic antibody derived from a four amino acid code. *J. Mol. Biol.* **357** (1):100-114.
- Fellouse**, F. A., Esaki, K., Birtalan, S. (2007). High-throughput generation of synthetic antibodies from highly functional minimalist phage-displayed libraries. *J. Mol. Biol.* **373** (4):924-940.
- Fellouse**, F. A., Li, B., Compaan, D. M. (2005). Molecular recognition by a binary code. *J. Mol. Biol.* **348** (5):1153-1162.
- Fellouse**, F. A., Wiesmann, C. and Sidhu, S. S. (2004). Synthetic antibodies from a four-amino-acid code: a dominant role for tyrosine in antigen recognition. *PNAS.* **101** (34):12467.
- Finlay**, W. J. J., deVore, N. C., Dobrovolskaia, E. N. (2005). Exploiting the avian immunoglobulin system to simplify the generation of recombinant antibodies to allergenic proteins. *Clin. Exper. Allergy.* **35** (8):1040-1048.
- Gauglitz**, G., Brecht, A., Kraus, G. and Nahm, W. (1993). Chemical and biochemical sensors based on interferometry at thin (multi-) layers. *Sens. Actuat. B. Chem.* **11**:21-27.
- Gewurz**, H., Zhang, X. H. and Lint, T. F. (1995). Structure and function of the pentraxins. *Curr. Opin. Immunol.* **7** (1):54-64.

- Gibler**, W. B., Cannon, C. P., Blomkalns, A. L. (2005). Practical Implementation of the Guidelines for Unstable Angina/Non–ST-Segment Elevation Myocardial Infarction in the Emergency Department. *Ann. Emerg. Med.* **46** (2):185-197.
- Hamm**, CW. (2001). Cardiac biomarkers for rapid evaluation of chest pain. *Circulation.* **104**:1454-1456.
- Hayhurst**, A., Happe, S., Mabry, R. (2003). Isolation and expression of recombinant antibody fragments to the biological warfare pathogen *Brucella melitensis*. *J. Immunol. Methods.* **276** (1-2):185-196.
- Hazen**, S. L. (2004). Myeloperoxidase and plaque vulnerability. *Arterioscler. Thromb. Vasc. Biol.* **24** (7):1143-1146.
- Hazen**, S. L. and Heinecke, J. W. (1997). 3-Chlorotyrosine, a specific marker of myeloperoxidase-catalyzed oxidation, is markedly elevated in low density lipoprotein isolated from human atherosclerotic intima. *J. Clin. Invest.* **99** (9):2075-2081.
- Hearty**, S., Leonard, P., Quinn, J. and O'Kennedy, R. (2006). Production, characterisation and potential application of a novel monoclonal antibody for rapid identification of virulent *Listeria monocytogenes*. *J. Microbiol. Methods.* **66** (2):294-312.
- Heeschen**, C., Dimmeler, S., Hamm, C. W. (2005). Pregnancy-associated plasma protein-A levels in patients with acute coronary syndromes: comparison with markers of systemic inflammation, platelet activation, and myocardial necrosis. *J. Am. Coll. Cardiol.* **45** (2):229-237.
- Heeschen**, C., Hamm, C. W., Bruemmer, J. and Simoons, M. L. (2000). Predictive value of C-reactive protein and troponin T in patients with unstable angina: a comparative analysis. CAPTURE Investigators. Chimeric c7E3 AntiPlatelet Therapy in Unstable angina REfractory to standard treatment trial. *J. Am. Coll. Cardiol.* **35** (6):1535-42.
- Heideman**, R. G., Kooyman, R. P. H. and Greve, J. (1993). Performance of a highly sensitive optical waveguide Mach-Zehnder interferometer immunosensor. *Sens. Actuat. B. Chem* **10** (3):209–217.

- Heideman**, R. G. and Lambeck, P. V. (1999). Remote opto-chemical sensing with extreme sensitivity: design, fabrication and performance of a pigtailed integrated optical phase-modulated Mach–Zehnder interferometer system. *Sens. Actuat. B. Chem.* **61** (1-3):100-127.
- Heinecke**, J. W., Li, W., Francis, G. A., Goldstein, J. A. (1993). Tyrosyl radical generated by myeloperoxidase catalyzes the oxidative cross-linking of proteins. *J. Clin. Invest.* **91**: 2866-2872.
- Henderson**, K. and Stewart, J. (2000). A dipstick immunoassay to rapidly measure serum oestrone sulfate concentrations in horses. *Reprod. Fertil. Dev.* **12** (4):183-190.
- Hof**, D., Hoeke, M. O. and Raats, J. M. (2008). Multiple-antigen immunization of chickens facilitates the generation of recombinant antibodies to autoantigens. *Clin. Exp. Immunol.* **151** (2):367-377.
- Homola**, J. (2008). Surface plasmon resonance sensors for detection of chemical and biological species. *Chem.Rev.* **108** (2):462-493.
- Homola**, J., Yee, S. S. and Gauglitz, G. (1999). Surface plasmon resonance sensors: review. *Sens. Actuat. B. Chem.* **54** (1-2):3-15.
- Hoogenboom**, H. R., de Bruïne, A. P., Hufton, S. E. (1998). Antibody phage display technology and its applications. *Immunotech.* **4** (1):1-20.
- Hoogenboom**, H. R., Griffiths, A. D., Johnson, K. S. (1991). Multi-subunit proteins on the surface of filamentous phage: methodologies for displaying antibody (Fab) heavy and light chains. *Nucleic. Acid. Res.* **19** (15):4133-4137.
- Ivanov**, I. I., Link, J. M., Ippolito, G. C. and Schroeder Jr, H. W. (2002). Constraints on hydrophobicity and sequence composition of HCDR3 are conserved across evolution. *The Antibodies.* **7**:43–67.
- James**, S. K., Lindahl, B., Siegbahn, A. (2003). N-terminal pro-brain natriuretic peptide and other risk markers for the separate prediction of mortality and subsequent myocardial infarction in patients with unstable coronary artery disease: a Global Utilization of Strategies To Open occluded arteries (GUSTO)-IV substudy. *Circulation.* **108** (3):275.

James, S. K., Lindahl, B., Armstrong, P. (2004). A rapid troponin I assay is not optimal for determination of troponin status and prediction of subsequent cardiac events at suspicion of unstable coronary syndromes. *Int. J. Cardiol.* **93** (2-3):113-120.

Jin, S., Chang, Z. Y., Ming, X. (2005). Fast Dipstick Dye Immunoassay for Detection of Immunoglobulin G (IgG) and IgM Antibodies of Human Toxoplasmosis. *Clin. Vaccine Immunol.* **12** (1):198.

Jones, K. D. (1999). Troubleshooting Protein Binding in Nitrocellulose Membranes, Part 1: Principles. *IVD Technology* **5**:32-41.

Kalogianni, D. P., Goura, S., Aletras, A. J. (2007). Dry reagent dipstick test combined with 23S rRNA PCR for molecular diagnosis of bacterial infection in arthroplasty. *Anal. Biochem.* **361** (2):169-175.

Kashyap, A. K., Steel, J., Oner, A. F. (2008). Combinatorial antibody libraries from survivors of the Turkish H5N1 avian influenza outbreak reveal virus neutralization strategies. *PNAS.* **105** (16):5986-5991.

Khreiss, T., Jozsef, L., Potempa, L. A. and Filep, J. G. (2004a). Conformational rearrangement in C-reactive protein is required for proinflammatory actions on human endothelial cells. *Circulation.* **109** (16):2016-2022.

Khreiss, T., Jozsef, L., Potempa, L. A. and Filep, J. G. (2004b). Conformational rearrangement in C-reactive protein is required for proinflammatory actions on human endothelial cells. *Circulation.* **109** (16):2016-2022.

Kim, J. E., Cho, J. H. and Paek, S. H. (2005). Functional membrane-implanted lab-on-a-chip for analysis of percent HDL cholesterol. *Anal. Chem. (Washington, DC).* **77** (24):7901-7907.

Kim, Y. M., Oh, S. W., Jeong, S. Y. (2003). Development of an ultrarapid one-step fluorescence immunochromatographic assay system for the quantification of microcystins. *Environ. Sci. Technol.* **37** (9):1899-1904.

- Kip**, K. E., Marroquin, O. C., Shaw, L. J. (2005). Global inflammation predicts cardiovascular risk in women: a report from the Women's Ischemia Syndrome Evaluation (WISE) study. *Am. Heart. J.* **150** (5):900-906.
- Kirkham**, P. M. and Schroeder, H. W., Jr. (1994). Antibody structure and the evolution of immunoglobulin V gene segments. *Semin. Immunol.* **6** (6):347-360.
- Knappik**, A. and Pluckthun, A. (1994). An improved affinity tag based on the FLAG peptide for the detection and purification of recombinant antibody fragments. *BioTechniques.* **17** (4):754-761.
- Koets**, M., Sander, I., Bogdanovic, J. (2006). A rapid lateral flow immunoassay for the detection of fungal alpha-amylase at the workplace. *J. Environ. Monitor.* **8** (9):942-946.
- Köhler**, G. and Milstein, C. (1975). Continuous cultures of fused cells secreting antibody of predefined specificity. *Nature.* **256**:495-497.
- Koskinen**, J. O., Vaarno, J., Meltola, N. J. (2004). Fluorescent nanoparticles as labels for immunometric assay of C-reactive protein using two-photon excitation assay technology. *Anal. Biochem.* **328** (2):210-218.
- Krebber**, A., Bornhauser, S., Burmester, J. (1997). Reliable cloning of functional antibody variable domains from hybridomas and spleen cell repertoires employing a reengineered phage display system. *J. Immunol. Methods.* **201** (1):35-55.
- Kresl**, J. J., Potempa, L. A. and Anderson, B. E. (1998). Conversion of native oligomeric to a modified monomeric form of human C-reactive protein. *Int. J. Biochem. Cell. Biol.* **30** (12):1415-1426.
- Kwasnikowski**, P., Kristensen, P. and Markiewicz, W. T. (2005). Multivalent display system on filamentous bacteriophage pVII minor coat protein. *J. Immunol. Methods.* **307** (1-2):135-143.
- Labarrere**, C. A. and Zaloga, G. P. (2004). C-reactive protein: from innocent bystander to pivotal mediator of atherosclerosis. *Am. J. Med.* **117** (7):499-507.

- Ladue**, J. S., Wroblewski, F. and Karmen, A. (1954). Serum glutamic oxaloacetic transaminase activity in human acute transmural myocardial infarction. *Science*. **120** (3117):497-499.
- Laib**, S., Krieg, A., Rankl, M. and Seeger, S. (2006). Supercritical angle fluorescence biosensor for the detection of molecular interactions on cellulose-modified glass surfaces. *Appl. Surf. Sci.* **252** (22):7788-7793.
- Lee-Lewandrowski**, E., Corboy, D., Lewandrowski, K. (2003). Implementation of a Point-of-Care Satellite Laboratory in the Emergency Department of an Academic Medical Center. *Arch. Pathol. Lab. Med.* **127** (4):456-460.
- Leonard**, P., Safsten, P., Hearty, S. (2007). High throughput ranking of recombinant avian scFv antibody fragments from crude lysates using the Biacore A100. *J. Immunol. Methods*. **323** (2):172-179.
- Lerner**, R. A. (2006). Manufacturing immunity to disease in a test tube: the magic bullet realized. *Angewandte Chemie (International ed.in English)*. **45** (48):8106-8125.
- Leung**, W., Chan, P., Bosgoed, F. (2003). One-step quantitative cortisol dipstick with proportional reading. *J. Immunol. Methods*. **281** (1-2):109-118.
- Libby**, P. (2002). Inflammation in atherosclerosis. *Nature*. **420** (6917):868-874.
- Lindahl**, B., Toss, H., Siegbahn, A. (2000). Markers of myocardial damage and inflammation in relation to long-term mortality in unstable coronary artery disease. FRISC Study Group. Fragmin during Instability in Coronary Artery Disease. *N. Engl. J. Med.* **343** (16):1139-1147.
- Lipman**, N. S., Jackson, L. R., Trudel, L. J. and Weis-Garcia, F. (2005). Monoclonal versus polyclonal antibodies: distinguishing characteristics, applications, and information resources. *ILAR JOURNAL*. **46** (3):258.
- Litman**, G. W., Anderson, M. K. and Rast, J. P. (1999). Evolution of antigen binding receptors. *Annu. Rev. Immunol.* **17** (1):109-147.

- Little**, M., Kipriyanov, S., Le Gall, F. and Moldenhauer, G. (2000). Of mice and men: hybridoma and recombinant antibodies. *Immunol. Today*. **21** (8):364-370.
- Lönnberg**, M. and Carlsson, J. (2001). Quantitative detection in the attomole range for immunochromatographic tests by means of a flatbed scanner. *Anal. Biochem.* **293** (2):224-231.
- Loria**, V., Dato, I., Graziani, F. and Biasucci, L. M. (2008). Myeloperoxidase: a new biomarker of inflammation in ischemic heart disease and acute coronary syndromes. *Mediators. Inflamm.* 135625
- Lukosz**, W., Clerc, D. and Nellen, P. M. (1991). Input and output grating couplers as integrated optical biosensors. *Sens. Actuat. A. Phys.* **25** (1-3):181-184.
- Lund**, V. and Olafsen, J. A. (1999). Changes in serum concentration of a serum amyloid P-like pentraxin in Atlantic salmon, *Salmo salar* L., during infection and inflammation. *Dev. Comp. Immunol.* **23** (1):61-70.
- Mabry**, R., Rani, M., Geiger, R. (2005). Passive protection against anthrax by using a high-affinity antitoxin antibody fragment lacking an Fc region. *Infect. Immun.* **73** (12):8362-8368.
- Mage**, R. G., Lanning, D. and Knight, K. L. (2006). B cell and antibody repertoire development in rabbits: the requirement of gut-associated lymphoid tissues. *Dev. Comp. Immunol.* **30** (1-2):137-153.
- Marnell**, L. L., Mold, C., Volzer, M. A., Burlingame, R. W., DuClos, T. W. (1995). C-reactive protein binds to Fc γ R1 in transfected COS cells. *J. Immunol.* **155**: 2185-2193.
- Mavrangelos**, C., Thiel, M., Adamson, P. J. (2001). Increased Yield and Activity of Soluble Single-Chain Antibody Fragments by Combining High-Level Expression and the Skp Periplasmic Chaperonin. *Protein. Express. Purif.* **23** (2):289-295.
- Maynard**, J. A., Maassen, C. B. M., Leppla, S. H. (2002). Protection against anthrax toxin by recombinant antibody fragments correlates with antigen affinity. *Nat. Biotechnol.* **20** (6):597-601.

McBride, J. D. and Cooper, M. A. (2008). A high sensitivity assay for the inflammatory marker C-reactive protein employing acoustic biosensing. *J. Nanobiotechnol.* **6**:5.

McCord, J., Nowak, R. M., McCullough, P. A. (2001). Ninety-Minute Exclusion of Acute Myocardial Infarction By Use of Quantitative Point-of-Care Testing of Myoglobin and Troponin I. *Circulation.* **104** (13):1483-1488.

McCormack, W. T., Tjoelker, L. W. and Thompson, C. B. (1993). Immunoglobulin gene diversification by gene conversion. *Prog. Nucleic. Acid. Res. Mol. Biol.* **45**:7-45.

McDonnell, B., Hearty, S., Leonard, P. and O'Kennedy, R. (2009). Cardiac biomarkers and the case for point-of-care testing. *Clin. Biochem.* **42** (7-8):549-561.

McGregor, D. P., Molloy, P. E., Cunningham, C. and Harris, W. J. (1994). Spontaneous assembly of bivalent single chain antibody fragments in *Escherichia coli*. *Mol. Immunol.* **31** (3):219-226.

Mian, I. S., Bradwell, A. R. and Olson, A. J. (1991). Structure, function and properties of antibody binding sites. *J. Mol. Biol.* **217** (1):133-151.

Michael, N., Accavitti, M. A., Masteller, E. and Thompson, C. B. (1998). The antigen-binding characteristics of mAbs derived from in vivo priming of avian B cells. *Proc. Natl. Acad. Sci. USA.* **95** (3):1166-1171.

Morrow, D. A. and de Lemos, J. A. (2007). Benchmarks for the Assessment of Novel Cardiovascular Biomarkers. *Circulation.* **115** (8):949.

Morrow, D. A., Sabatine, M. S., Brennan, M. L. (2008). Concurrent evaluation of novel cardiac biomarkers in acute coronary syndrome: myeloperoxidase and soluble CD40 ligand and the risk of recurrent ischaemic events in TACTICS-TIMI 18. *Eur. Heart.J.* **29** (9):1096-1102.

Morrow, D. A., Rifai, N., Antman, E. M. (1998). C-reactive protein is a potent predictor of mortality independently of and in combination with troponin T in acute coronary syndromes: a TIMI 11A substudy. Thrombolysis in Myocardial Infarction. *J. Am. Coll. Cardiol.* **31** (7):1460-1465.

- Murray**, R., Leroux, M., Sabga, E. (1999). Effect of point of care testing on length of stay in an adult emergency department. *J. Emerg. Med.* **17** (5):811-814.
- Narat**, M. (2003). Production of antibodies in chickens. *Food. Tech. Biotech.* **41**:259-267.
- Newby**, L. K., Storrow, A. B., Gibler, W. B. (2001). Bedside multimarker testing for risk stratification in chest pain units: The chest pain evaluation by creatine kinase-MB, myoglobin, and troponin I (CHECKMATE) study. *Circulation.* **103** (14):1832.
- Ng**, S. M., Krishnaswamy, P., Morissey, R. (2001). Ninety-minute accelerated critical pathway for chest pain evaluation. *Am. J. Cardiol.* **88**:611-617.
- Novis**, D. A., Jones, B. A., Dale, J. C. and Walsh, M. K. (2004). Biochemical markers of myocardial injury test turnaround time: A College of American Pathologists Q-Probes study of 7020 troponin and 4368 creatine kinase-MB determinations in 159 institutions. *Arch. Pathol. Lab. Med.*(1976). **128** (2):158-164.
- O'Brien**, P.M. and Aitken, R. (2002). Broadening the Impact of Antibody Phage Display Technology. *IN: O'Brien, P.M. and Aitken, R. (eds.) Antibody Phage Display: Methods and Protocols.*
- Ohara**, R., Knappik, A., Shimada, K. (2006). Antibodies for proteomic research: comparison of traditional immunization with recombinant antibody technology. *Proteomics.* **6** (9):2638.
- O'Keefe**, M., Crabbe, P., Salden, M. (2003). Preliminary evaluation of a lateral flow immunoassay device for screening urine samples for the presence of sulphamethazine. *J. Immunol. Methods.* **278** (1-2):117-126.
- Oku**, Y., Kamiya, K., Kamiya, H. (2001). Development of oligonucleotide lateral-flow immunoassay for multi-parameter detection. *J. Immunol. Methods.* **258** (1-2):73-84.
- Ordonez-Llanos**, J., Santalo-Bel, M., Merce-Muntanola, J. (2006). Risk stratification of chest pain patients by point-of-care cardiac troponin T and myoglobin measured in the emergency department. *Clin. Chim. Acta.* **365** (1-2):93-97.
- Padlan**, E. A. (1994). Anatomy of the antibody molecule. *Mol. Immunol.* **31** (3):169-217.

Paek, S. H., Lee, S. H., Cho, J. H. and Kim, Y. S. (2000). Development of rapid one-step immunochromatographic assay. *Methods*. **22** (1):53-60.

Paschke, M. (2006). Phage display systems and their applications. *Appl. Microbiol. Biotechnol.* **70** (1):2-11.

Pearson, T. A., Mensah, G. A., Hong, Y. and C., S. S., Jr. (2004). CDC/AHA Workshop on Markers of Inflammation and Cardiovascular Disease: Application to Clinical and Public Health Practice: overview. *Circulation*. **110** (25):e543-544.

Peoples, M. C., Phillips, T. M. and Karnes, H. T. (2007). Demonstration of a direct capture immunoaffinity separation for C-reactive protein using a capillary-based microfluidic device. *J. Pharm. Biomed. Anal.* **48** (2):376-382.

Pepys, M. B. and Baltz, M. L. (1983). Acute phase proteins with special reference to C-reactive protein and related proteins (pentaxins) and serum amyloid A protein. *Adv. Immunol.* **34**:141-212.

Pepys, M. B. and Berger, A. (2001). The renaissance of C reactive protein. *BMJ*. **322** (7277):4-5.

Popkov, M., Mage, R. G., Alexander, C. B. (2003). Rabbit immune repertoires as sources for therapeutic monoclonal antibodies: the impact of kappa allotype-correlated variation in cysteine content on antibody libraries selected by phage display. *J. Mol. Biol.* **325** (2):325-335.

Posthuma-Trumpie, G. A., Korf, J. and van Amerongen, A. (2009). Lateral flow (immuno) assay: its strengths, weaknesses, opportunities and threats. A literature survey. *Anal. Bioanal. Chem.* **393** (2):569-582.

Potempa, L. A., Siegel, J. N., Fiedel, B. A. (1987). Expression, detection and assay of a neoantigen(neo-CRP) associated with a free, human C-reactive protein subunit. *Mol. Immunol.* **24** (5):531-541.

Rajpal, A., Beyaz, N., Haber, L. (2005). A general method for greatly improving the affinity of antibodies by using combinatorial libraries. *PNAS*. **102** (24):8466-8471.

Rathore, S., Knowles, P., Mann, A. P. S. and Dodds, P. A. (2008). Is it safe to discharge patients from accident and emergency using a rapid point of care Triple Cardiac Marker test to rule out acute coronary syndrome in low to intermediate risk patients presenting with chest pain? *Eur. J. Intern. Med.* **19**:537-540.

Resch-Genger, U., Grabolle, M., Cavaliere-Jaricot, S. (2008). Quantum dots versus organic dyes as fluorescent labels. *Nature. Methods.* **5** (9):763-776.

Ridker, P. M. (2003). Rosuvastatin in the primary prevention of cardiovascular disease among patients with low levels of low-density lipoprotein cholesterol and elevated high-sensitivity C-reactive protein: rationale and design of the JUPITER trial. *Circulation.* **108** (19):2292-7.

Ridker, P. M., Buring, J. E., Rifai, N. and Cook, N. R. (2007). Development and validation of improved algorithms for the assessment of global cardiovascular risk in women: the Reynolds Risk Score. *J. Am. Med. Assoc.* **297** (6):611-619.

Ridker, P. M. and Cook, N. (2004). Clinical usefulness of very high and very low levels of C-reactive protein across the full range of Framingham Risk Scores. *Circulation.* **109** (16):1955-1959.

Ridker, P. M., Cushman, M., Stampfer, M. J. (1997). Inflammation, aspirin, and the risk of cardiovascular disease in apparently healthy men. *N. Engl. J. Med.* **336** (14):973-979.

Ridker, P. M., Hennekens, C. H., Buring, J. E. and Rifai, N. (2000). C-reactive protein and other markers of inflammation in the prediction of cardiovascular disease in women. *N. Engl. J. Med.* **342** (12):836-843.

Ridker, P. M., Rifai, N., Clearfield, M. (2001). Measurement of C-reactive protein for the targeting of statin therapy in the primary prevention of acute coronary events. *N. Engl. J. Med.* **344** (26):1959-1965.

Ridker, P. M., Rifai, N., Cook, N. R. (2005). Non-HDL cholesterol, apolipoproteins A-I and B100, standard lipid measures, lipid ratios, and CRP as risk factors for cardiovascular disease in women. *J. Am. Med. Assoc.* **294** (3):326-333.

- Ross, R.** (1999). Atherosclerosis-an inflammatory disease. *N. Engl. J. Med.* **340** (2):115-126.
- Sabatine, M. S., Morrow, D. A., de Lemos, J. A.** (2002). Multimarker approach to risk stratification in non-ST elevation acute coronary syndromes: simultaneous assessment of troponin I, C-reactive protein, and B-type natriuretic peptide. *Circulation.* **105** (15):1760-1763.
- Sakkinen, P., Abbott, R. D., Curb, J. D.** (2002). C-reactive protein and myocardial infarction. *J. Clin. Epidemiol.* **55** (5):445-451.
- Salavej, P., Spalteholz, H. and Arnhold, J.** (2006). Modification of amino acid residues in human serum albumin by myeloperoxidase. *Free. Radical. Biol. Med.* **40** (3):516-525.
- Salomone, A., Mongelli, M., Roggero, P. and Boscia, D.** (2004). Reliability of detection of Citrus tristeza virus by an immunochromatographic lateral flow assay in comparison with ELISA. *J. Plant. Pathol.* **86** (1):43-48.
- Schmitt, H. M., Brecht, A., Piehler, J. and Gauglitz, G.** (1997). An integrated system for optical biomolecular interaction analysis. *Biosens. Bioelectron.* **12** (8):809-816.
- Schmitt, K., Schirmer, B., Hoffmann, C.** (2007). Interferometric biosensor based on planar optical waveguide sensor chips for label-free detection of surface bound bioreactions. *Biosens. Bioelectron.* **22** (11):2591-2597.
- Schroeder, H. W., Ippolito, G. C. and Shiokawa, S.** (1998). Regulation of the antibody repertoire through control of HCDR3 diversity. *Vaccine.* **16** (14-15):1383-1390.
- Schull, M. J., Vermeulen, M. J. and Stukel, T. A.** (2006). The Risk of Missed Diagnosis of Acute Myocardial Infarction Associated With Emergency Department Volume. *Annals. Emerg. Med.* **48** (6):647-655.
- Shrive, A. K., Cheetham, G. M. T., Holden, D., Myles, D. A. A., Turnell, W. G., Volanakis, J. E., Pepys, M. B., Bloomer, A. C., Greenhough, T. J.** (1996) Three dimensional structure of human C-reactive protein. *Nat. Struct. Biol.* **3**: 346-354.
- Situma, C., Hashimoto, M. and Soper, S. A.** (2006). Merging microfluidics with microarray-based bioassays. *Biomol. Eng.* **23** (5):213-231.

- Sluss, P.** (2006). Cardiac Markers: Current technologies for their measurement at point of care. *Point-of-care: The journal of near-patient testing and technology*. **5** (1):38-46.
- Solomon, D. H., Stone, P. H., Glynn, R. J.** (2001). Use of risk stratification to identify patients with unstable angina likeliest to benefit from an invasive versus conservative management strategy. *J. Am. Coll. Cardiol.* **38** (4):969-976.
- Song, C. S., Yu, J. H., Bai, D. H.** (1985). Antibodies to the alpha-subunit of insulin receptor from eggs of immunized hens. *J. Immunol.* **135** (5):3354-3359.
- Steel, D. M. and Whitehead, A. S.** (1994). The major acute phase reactants: C-reactive protein, serum amyloid P component and serum amyloid A protein. *Immunol. Today (Amsterdam.Regular ed.)*. **15** (2):81-88.
- Steukers, M., Schaus, J. M., van Gool, R.** (2006). Rapid kinetic-based screening of human Fab fragments. *J. Immunol. Methods.* **310** (1-2):126-135.
- Straface, A. L., Myers, J. H., Kirchick, H. J. and Blick, K. E.** (2008). A rapid point-of-care cardiac marker testing strategy facilitates the rapid diagnosis and management of chest pain patients in the emergency department. *Am. J. Clin. Pathol.* **129** (5):788-795.
- Studier, F. W.** (2005). Protein production by auto-induction in high density shaking cultures. *Protein. Expr.Purif.* **41** (1):207-234.
- Sugiyama, S., Okada, Y., Sukhova, G. K.** (2001). Macrophage myeloperoxidase regulation by granulocyte macrophage colony-stimulating factor in human atherosclerosis and implications in acute coronary syndromes. *Am. J. Pathol.* **158** (3):879-891.
- Thompson, D., Pepys, M. B. and Wood, S. P.** (1999). The physiological structure of human C-reactive protein and its complex with phosphocholine. *Structure.* **7** (2):169-177.
- Tirupathi, C., Naqvi, T., Wu, Y.** (2004). Albumin mediates the transcytosis of myeloperoxidase by means of caveolae in endothelial cells. *PNAS.* **101** (20):7699-7704.
- Tlaskalova-Hogenova, H. and Stepankova, R.** (1980). Development of antibody formation in germ-free and conventionally reared rabbits: the role of intestinal lymphoid tissue in antibody formation to E. coli antigens. *Folia. Biol. (Praha).* **26** (2):81-93.

Tonegawa, S. (1983). Somatic generation of antibody diversity.

Tüdös, A. J., Besselink, G. A. J. and Schasfoort, R. B. M. (2001). Trends in miniaturized total analysis systems for point-of-care testing in clinical chemistry. *Lab on a Chip*. **1** (2):83-95.

Urich, K. (1994). Comparative animal biochemistry. *Springer publications*.

U.S. Department of Health and Human Services, Food and Drug Administration, Center for Devices and Radiological Health, Office of In Vitro Diagnostic Device Evaluation and Safety, Division of Chemistry and Toxicology Devices. (2005). Review Criteria for Assessment of C-Reactive Protein (CRP), High Sensitivity C-Reactive Protein (hsCRP) and Cardiac C-Reactive Protein (cCRP) Assays.

Verdes, D., Ruckstuhl, T. and Seeger, S. (2007). Parallel two-channel near-and far-field fluorescence microscopy. *J. Biomed. Opt.* **12** (3):034012.

Vita, J. A., Brennan, M. L., Gokce, N. (2004). Serum Myeloperoxidase Levels Independently Predict Endothelial Dysfunction in Humans. *Circulation*. **110** (9):1134-1139.

Volanakis, J. E. and Kaplan, M. H. (1971). Specificity of C-reactive protein for choline phosphate residues of pneumococcal C-polysaccharide. *Proc. Soc. Exp. Biol. Med. (New York, N.Y.)*. **136** (2):612-614.

Vukmir, R. B. (2004). Medical malpractice: managing the risk. *Medicine and law*. **23** (3):495-513.

Wang, S., Quan, Y., Lee, N. and Kennedy, I. R. (2006). Rapid determination of fumonisin B1 in food samples by enzyme-linked immunosorbent assay and colloidal gold immunoassay. *J. Agric. Food. Chem.* **54** (7):2491-2495.

Wang, X., Li, K., Shi, D. (2007). Development of an immunochromatographic lateral-flow test strip for rapid detection of sulfonamides in eggs and chicken muscles. *J. Agric. Food Chem.* **55** (6):2072-2078.

- White**, A. A., Wright, S. W., Blanco, R. (2004). Cause-and-effect analysis of risk management files to assess patient care in the emergency department. *Acad. Emerg. Med.* **11** (10):1035-1041.
- Wilson**, I. A. and Stanfield, R. L. (1994). Antibody-antigen interactions: new structures and new conformational changes. *Curr. Opin. Struct. Biol.* **4** (6):857-867.
- Wong**, R. L., Mytych, D., Jacobs, S. (1997). Validation parameters for a novel biosensor assay which simultaneously measures serum concentrations of a humanized monoclonal antibody and detects induced antibodies. *J. Immunol. Methods.* **209** (1):1-15.
- Wu**, A. H., Smith, A., Christenson, R. H. (2004). Evaluation of a point-of-care assay for cardiac markers for patients suspected of acute myocardial infarction. *Clin. Chim. Acta.* **346** (2):211-219.
- Yakovleva**, J., Davidsson, R., Lobanova, A. (2002). Microfluidic enzyme immunoassay using silicon microchip with immobilized antibodies and chemiluminescence detection. *Anal. Chem.* **74** (13):2994-3004.
- Yasojima**, K., Schwab, C., McGeer, E. G. and McGeer, P. L. (2001). Generation of C-reactive protein and complement components in atherosclerotic plaques. *Am. J. Pathol.* **158** (3):1039-1051.
- Ymeti**, A., Kanger, J. S., Greve, J. (2005). Integration of microfluidics with a four-channel integrated optical Young interferometer immunosensor. *Biosens. Bioelectron.* **20** (7):1417-1421.
- ZD Net Healthcare**. Available from: <<http://healthcare.zdnet.com/>>. [Accessed 18 January 2009].
- Zemlin**, M., Klinger, M., Link, J. (2003). Expressed murine and human CDR-H3 intervals of equal length exhibit distinct repertoires that differ in their amino acid composition and predicted range of structures. *J. Mol. Biol.* **334** (4):733-749.
- Zhang**, G. P., Guo, J. Q., Wang, X. N. (2006). Development and evaluation of an immunochromatographic strip for trichinellosis detection. *Vet. Parasitol.* **137** (3-4):286-293.

Zhang, R., Brennan, M. L., Fu, X. (2001). Association between myeloperoxidase levels and risk of coronary artery disease. *J. Am. Med. Assoc.* **286** (17):2136-2142.

Zhu, Y., He, W., Liang, Y. (2002). Development of a rapid, simple dipstick dye immunoassay for schistosomiasis diagnosis. *J. Immunol. Methods.* **266** (1-2):1-5.

Zouki, C., Haas, B., Chan, J. S. D. (2001). Loss of Pentameric Symmetry of C-Reactive Protein Is Associated with Promotion of Neutrophil-Endothelial Cell Adhesion 1. *J. Immunol.* **167** (9):5355-5361.

7.0 Appendix

7.0 Appendix

7.1 Vector maps

Several bacterial vectors were employed in this research to provide a means for efficient cloning, phage display and bacterial expression. The pComb3X vector was found to be the most robust vector for achieving each of these functions.

7.1.1 pComb3XSS vector

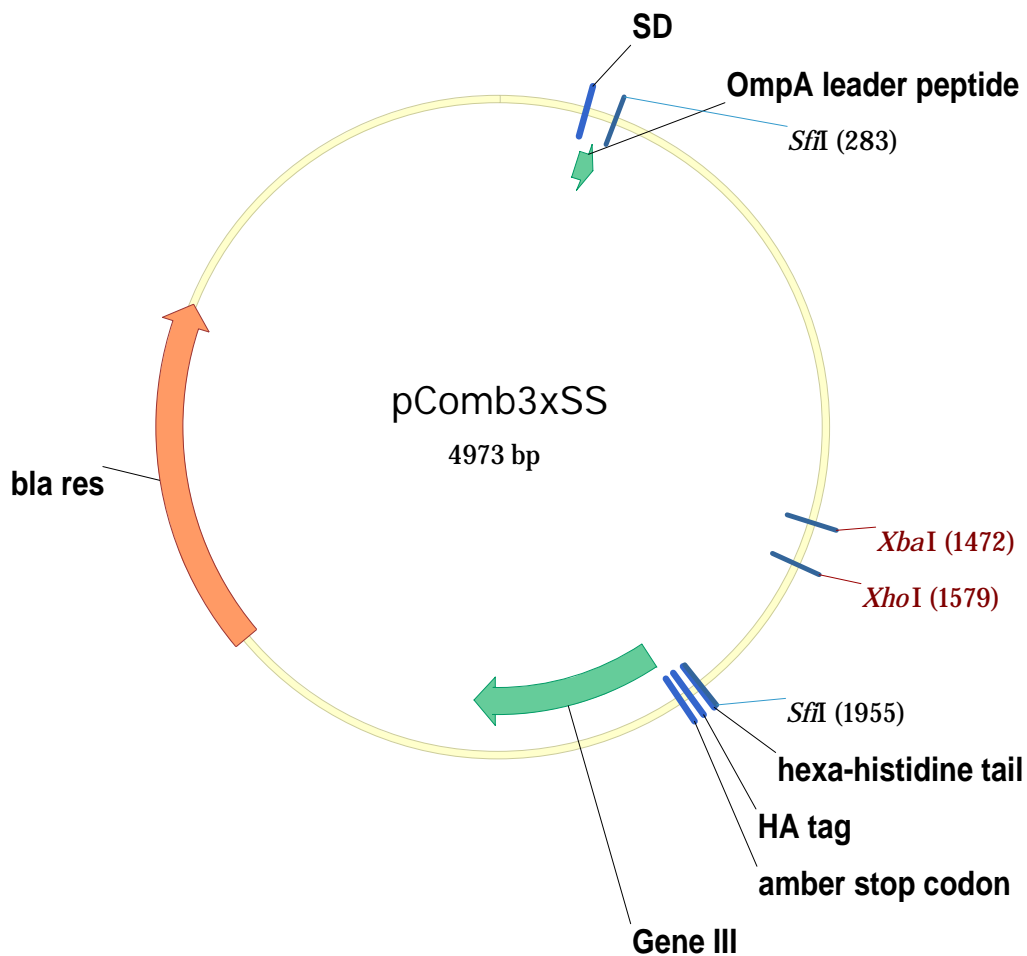


Figure 7.1.1 The pComb3 phagemid vectors are designed to express antibody fragments and other proteins on the surface of filamentous phage or to express them as soluble proteins. The antibody fragments are fused to the carboxy-terminal domain of the minor coat protein (coat protein III). An amber codon has been inserted between the 3' *Sfi*I restriction site and the 5' end of gene III. This allows for soluble protein expression in nonsuppressor strains of bacteria without excising the gene III fragment. A 6x histidine (HIS) tag has been inserted carboxy-terminal to the Fd fragment for universal protein purification. A hemagglutinin (HA)

decapeptide tag has been inserted at the 3' end of the HIS tag for universal detection using an anti-HA antibody. This vector allows the expression of Fab, scFv, diabody, or other proteins.

7.2 Process schematics

7.2.1 Phage panning/selection process

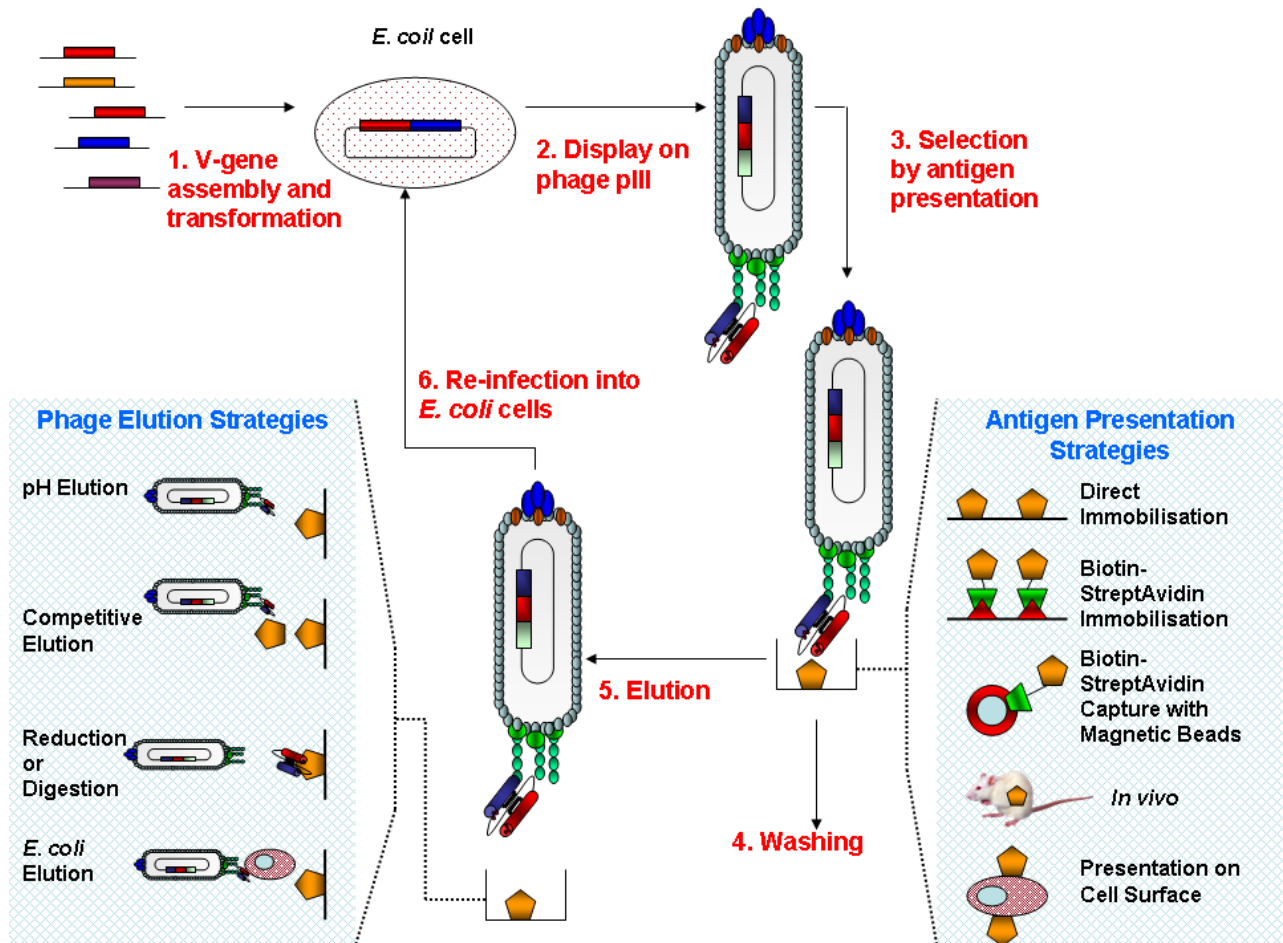


Figure 7.2.1 Phage selection strategy. Iterative selection shown here is a multistep process. V gene assembly by PCR allows cloning of the recombinant antibody (scFv is shown) library into *E. coli* cells. Subsequent rescue by helper phage allows for the propagation of the phage antibody library. Antigen presentation is a key consideration and there are many modes of antigen-phage antibody interaction. Serially increasing the stringency of washing after antigen presentation selects those phage displaying antibodies with highly specific binding properties. Elution strategies are also illustrated.

7.3 Tables

7.3.1 Biochemical markers of the acute coronary syndromes

Biochemical markers now play a fundamental role in the diagnosis, prognosis, monitoring and risk stratification of patients with acute coronary syndromes (ACS). The table below shows some of the most widely used cardiac biomarkers and their characteristics.

Marker	Structure	Implications	Utility
Myoglobin	18 kDa (single chain globular protein)	Early acute myocardial infarction	Re-infarction diagnosis
Creatine-kinase MB	85 kDa	Acute myocardial infarction	Re-infarction diagnosis
Myeloperoxidase	150 kDa (Dimeric enzyme)	Inflammation/plaque rupture	Short-term risk stratifier
C-reactive protein	125 kDa (pentameric form) 25 kDa (monomeric form)	Inflammation	Long-term risk stratifier
Brain natriuretic peptide	17 kDa	Ventricular overload/heart failure	Infarct sizing/prognosticator
Cardiac troponin I	23.5 kDa (subunit of a ternary regulatory protein)	Myocardial infarction	Benchmark for MI diagnosis